This file is part of the following work:

Ryan, Stephanie Margaret (2019) *Investigating the immunomodulatory properties of the hookworm recombinant secretome.* **PhD Thesis, James Cook University.**

Access to this file is available from:

https://doi.org/10.25903/zvcf%2D1p85

Stephanie Margaret Ryan

MSc. BSc. (Hons) Biomedical Science

Investigating the Immunomodulatory Properties of the Hookworm Recombinant Secretome

This thesis is presented for the degree of Doctor of Philosophy

College of Public Health, Medical and Veterinary Sciences

James Cook University

Submitted February 2019

Acknowledgments

Firstly, I would like to acknowledge Professor Rick Maizels and Dr Henry McSorley for believing in me and giving me my first opportunity that changed my life back in Edinburgh all those years ago. To this day and for the rest of my career I will be truly grateful. Secondly, I would like to thank Dr Katherine Smith, Ms Yvonne Harcus, Dr James Hewitson, Dr Lisa Reynolds, and Dr Kara Filbey and who truly taught me how to design and perform experiments, be a conscious lab citizen, conduct croissant / coffee fuelled lab meetings and publish quality collaborative science. A wonderful, joyful, and colourful group of incredibly clever people that ignited my belief in myself and our contribution to the field. Finally, Dr Lorna Proudfoot and Dr Eva Malone for believing in a very unconfident nervous Masters student and tutoring me to help me achieve my potential. Lecturers that truly care about teaching and their students are not as common as we all would like to believe and I am truly grateful for all the extra help they both gave me throughout my course. Without all of you lads and lassies, I would never have started to conduct research at the strange intersection of Parasitology and Immunology nor been given the building blocks that paved my way from Bonnie Scotland to Professor Alex Loukas in Australia.

Now the Aussies (and people of other nationalities residing in Australia), Professor Alex Loukas, my primary supervisor who spear headed this whole project and kindly gave me so much support. Secondly, Dr Paul Giacomin, I acknowledge the calm, critical and supportive way that you supervise and I believe it is a reflection of the calibre of the great teams that you stem from. Professor Kirill Alexandrov and Dr Wayne Johnston for collaborating with our team and training me at the Institute of Molecular Bioscience at the University of Queensland.

Dr Severine Navarro for fantastic training in so many experimental techniques. Dr Ramon Eichenberger for your kind words on tough days and all your help with illustrator. Professor Norelle Daly and Dr David Wilson for helping me with structural modelling and always being so friendly and supportive. Dr Matt Field and Dr Ashley Waardenberg, I acknowledge your invaluable bioinformatics expertise. Dr Adrian Esterman for his statistical analysis support. Mrs Linda Ryan (Jones) and Ms Martha Cooper who are not just great friends but the best lab partner and statistical queen/thesis editor, respectively, that I could have asked for; I am so lucky to have two such caring, clever, and kind women in my life. Mr Darren Pickering, Dr Mark Pearson, Dr Javier Sotillo, Dr Paramjit Bansal, Dr Claudia Cobos, Ms Rachael Ryan, Mr Luke Becker, Miss Geraldine Buitrago, Mr Phill Walsh, Mr Atik Susianto, and Mr Bjoernar Hauge, I would like to acknowledge as being key players in our lab and are our unsung heroes. Mr Mark Collins in the JCU Cairns Library, I am so appreciative for all your help formatting my thesis. I would also like to thank our US collaborators, the Mitreva Lab and Zhan Lab. Of course, I would like to give the biggest thank you of all to my family and friends, near and far, for all their support that helped me complete my PhD so far from home. Finally, I would like to acknowledge the mice that have contributed to this study, without which this project would not have been possible.

"Step into the fire of self-discovery. This fire will not burn you, it will only burn what you are not."

Mooji

Statement of the Contribution of Others

The work put forward for this thesis is original and I would like to state the contribution of others whether it be significant technical procedures, data analysis, experimental design or statistical assistance and any other original work reported or used in this thesis has been referenced throughout as per the James Cook University Codes of Conduct.

An electronic copy of this thesis has been submitted to the James Cook University Library in order for it to be available for future study and research in accordance with the Copyright Act 1968. Where appropriate, copyright permission was obtained from the copyright holder in order for this thesis to be reproduced.

The following institutions and people have helped and contributed to the work contained in this thesis.

	Top-up Scholarship Stipend Support	Prof Alex Loukas, JCU
	Research Costs	Fellowship from NHMRC (1117504)
		Program Grant (113295)
	Write-Up Grant	Doctoral Completion Grant, College of Public Health, Medical and Veterinary Science, James Cook University
Technical Support / Data Collection	Animal Unit Care	Mr Atik Susianto
		Mr Bjoernar Hauge
		Ms Jana Dwyer
	Animal Handling / FACS training	Dr Severine Navarro
		Dr Paul Giacomin
	Leishmania cell-free lysate production / training	Prof Kirill Alexandrov
		Dr Wayne Johnston
	DNA Plasmid Synthesis	Protein CT Biotechnologies

	Protein Expression	Mr Darren Pickering
		Ms Sally Troy
	Mouse Necropsy Assistance	Mrs Linda Ryan (Jones)
		Ms Geraldine Buitrago
	Mouse Histology Analysis	Dr Jen Whan
		Dr Paul Giacomin
Data Analysis	Flow Cytometry	Dr Paul Giacomin
		Dr Roland Ruscher
		Ms Jamie Brady
	PBMC Assay Design and Experimental Technical Training	Prof John Miles
		Ms Rachael Ryan
	Statistical Analysis	Dr Adrian Esterman
		Ms Martha Cooper
Administration		Mrs Julie Woodward
		Mrs Trilby Butcher
		Ms Mel Campbell

Published Works by the Author

Incorporated into the Thesis

Chapter 1. Harnessing helminth-driven immunoregulation in the search for novel anti-inflammatory modalities. *PLOS Pathogens*. Invited review – submitted and in review.

Ryan S, Eichenberger RM, Giacomin PR, and Loukas A.

Author Contributions: SR, AL, PG and RE wrote the review.

Collaboration in Published Projects:

Eichenberger RM, **Ryan S**, Jones L, Buitrago G, Polster R, Montes de Oca M, Zuvelek J, Giacomin PR, Dent LA, Engwerda CR, Field MA, Sotillo J, and Loukas A. Hookworm Secreted Extracellular Vesicles Interact With Host Cells and Prevent Inducible Colitis in Mice. *Frontiers in Immunology*. 2018;9:850.

Lau CL, Sheridan S, **Ryan S**, Roineau M, Andreosso A, Fuimaono S, Tufa J, and Graves PM. Detecting and confirming residual hotspots of lymphatic filariasis transmission in American Samoa 8 years after stopping mass drug administration. Churcher TS, ed. *PLoS Neglected Tropical Diseases*. 2017;11:9.

Navarro S, Pickering D, Ferreira I, Jones L, **Ryan S**, Troy S, Leech A, Hotez P, Zhan B, Laha T, Prentice R, Sparwasser T, Croese J, Engwerda C, Upham J, Julia V, Giacomin PR, and Loukas, A. Hookworm recombinant protein promotes regulatory T cell responses that suppress experimental asthma. *Science Translational Medicine,* 2017;8:362.

Unpublished Works by the Author Incorporated into the Thesis

Chapter 2, Chapter 3 and Chapter 4 contain data that is unpublished but will be submitted for publication after IP position has been protected.

Chapter 2, 3 and, 4: Hookworm recombinant secretome is replete with anti-inflammatory therapeutic proteins. **Ryan S**, Cooper M, Jones L, Buitrago G, Field M, Mitreva M, Johnston W, Alexandrov, K, Esterman A, Giacomin PR, and Loukas A. *Proposed submission to Nature*. 2019; Manuscript in Prep.

Author Contributions: AL and PG designed the study and wrote the paper with SR. SR, WJ, KA made the cell-free lysates. SR, MM, MF carried out the bioinformatics. SR, LJ and GB carried out the animal experiments. SR, AE and MC conducted statistical analysis. All authors analysed the results and approved the final version of the manuscript.

Abstract

Parasitic infections exact a costly and disproportionate disease burden on developing countries. However, evidence suggests that certain parasites, such as hookworms, offer substantial health benefits for diseases that result from a dysregulated immune response, typified by allergy and autoimmunity. Helminth therapy is gaining momentum and some studies detail the prospective efficacy of live parasitic helminth infection in improving the symptoms of both human and animal models of intestinal inflammation. However, there is not widespread acceptance in the medical community of such a radical therapeutic modality and the associated drawbacks and challenges. An increasing body of evidence suggests that a safer option is to harness the immunomodulatory properties of the hookworm's excretory-secretory (ES) complement. Subsequently, attention has fallen on the possibility of ascertaining immunomodulatory components secreted by helminths that might serve as more conventional biologics and offer an alternative to live helminth therapy. ES proteins protect against inflammation in several mouse models of colitis and other inflammatory diseases, but there are only few published examples of isolated bioactive helminth proteins to date. A new bioinformatic pipeline was devised and then employed to profile and identify candidate protective recombinant proteins from the *Ancylostoma caninum* ES proteome and transcriptome. In order to rapidly generate and screen large numbers of hookworm recombinant proteins for immunomodulatory activity *in vivo,* a *Leishmania* cell-free protein expression system was used to generate ~0.5 mL of each recombinant protein fused to GFP. One hundred and four (104) recombinant ES proteins in the form of crude ribosomal lysates were administered to mice (n = groups of five mice per protein lysate) to assess their anti-inflammatory properties in a model of acute colitis. Mice were assessed for histopathological, immunological and clinical features of disease in an acute

model of TNBS-induced colitis. Protection against colitis was conferred by individual hookworm recombinant proteins in the context of this model. After robust statistical filtering and ranking, twenty proteins were found to confer significant protection against various parameters of colitis. Select lead proteins were expressed in yeast and purified, and their anti-inflammatory activity was validated in: (1) two discrete models of colitis, and (2) human peripheral blood mononuclear cell cytokine profiling. This study has established a novel and rapid biologics discovery pipeline from bioinformatics to *in vivo* validation, and has identified a comprehensive library of hookworm derived immunotherapeutics. Proteins identified herein can be developed as an entirely novel approach to treating the global burden of inflammatory diseases.

Table of Contents

List of Tables

List of Figures

xviii

List of Abbreviations

αIL-12 = anti-interleukin-12

aa = amino acid

M2 = alternatively activated macrophages

AAC = advanced analytical centre

*Ac*ES = *Ancylostoma caninum* excretory-secretory products

Ac-FAR-2 = *Ancylostoma caninum* fatty acid retinol binding protein 2

Ac-NIF = *Ancylostoma caninum* neutrophil inhibitory factor

Ac-TIMP-1 = *Ancylostoma caninum* tissue metalloprotease inhibitor protein 1

AMP = antimicrobial peptides

AOX1 = alcohol oxidase

APC = antigen presenting cell

APC = allophycocyanin

ARC = Animal Resource Centre

AREG = amphiregulin

ASP = *Ancylostoma* secreted protein

ATG16L-1 = autophagy related 16-like-1

α-TNF = anti-tumour necrosis factor

Breg = regulatory B cells

CBA = cytometric bead array

CCR7 = chemokine receptor type 7

CD = Crohn's disease

cDNA = complementary DNA

CD103 = cluster domain 103 (integrin alpha E)

CD4+ = cluster domain 4 positive

cGMP = current good manufacturing practices

CRISP = cysteine-rich secretory proteins

CsA = cyclosporin A

CTLA-4 = cytotoxic T lymphocyte antigen 4

DALYs = disability adjusted life years

DC = dendritic cell

Dex = dexamethasone

DNA = deoxyribonucleic acid

DNBS = dinitrobenzene sulphate

DSI = disease severity index

DSS = dextran sulphate sodium salt

DTT = dithiothreitol

eGFP = enhanced green flurescent protein

ESP = excretory-secretory products

EST = expressed sequence tag

ECM-1 = extracellular matrix protein 1

EGFR = epidermal growth factor receptor

FAR = fatty acid and retinol binding proteins

FDR = false discovery rate

FITC-BSA = fluorescein-conjugated bovine serum albumin

FOXP3 = forkhead box marker P3

FP = forward primer

FT = flow through media

GI = gastrointestinal

GM-CSF = granulocyte macrophage - colony stimulating factor

GO = gene ontology

GOI = gene of interest

GWAS = genome wide association studies

H&E = haematoxylin and eosin

HA = human albumin

HES = *Heligmosomoides polygyrus* excretory-secretory products

IBD = inflammatory bowel disease

IBS = irritable bowel syndrome

IEC = intestinal epithelial cell

IFN-γ = interferon gamma

IgA = immunoglobulin A

IGV = integrative genomic viewer

ILC = innate lymphoid cell

IL-(n.) = interleukin (n.)

IL-(n.)R = IL-(n.) receptor

iNOS = inducible nitric oxide synthase

i.p. = intraperitoneal

i.r. = intra-rectal

IRGM = immunity-related GTPase family M

KO or -/- = gene knockout

L3 = free-living larvae

LAL = limulus amoebocyte lysate

LP = lamina propria

LPS = lipopolysaccharide

LTE = *Leishmania tarentolae* expression

MAPK = mitogen-activated protein kinases

MCB = master mix capture beads

MDB = master mix PE detection beads

MFI = mean fluorescence intensity

MHC = major histocompatibility complex

MLN = mesenteric lymph node

MMP = matrix metalloprotease

MCP-1 = monocyte chemoattractant protein-1

mRNA = messenger RNA

MWCO = molecular weight cut-off

MyD88 = myeloid differentiation primary response 88

NF-κB = nuclear factor kappa-light-chain-enhancer

NIF = neutrophil inhibitory factor

NK = natural killer

NMR = nuclear magnetic resonance

NOD-1 / 2 = nucleotide-binding oligomerisation domain containing 1/2

NOX = NADPH oxidase

NSAIDs = non-steroidal anti-inflammatory drugs

nt = nucleotide

ORF = open reading frames

PAMP = pathogen-associated molecular pattern

PBMC = peripheral blood mononuclear cell

PBS = phosphate buffered saline

PC = phosphorylcholine

PCR = polymerase chain reaction

PE = phycoerythrin

Pfam = protein families

PMA = phorbol 12- myristate 13-acetate

Pre = yeast supernatant media

PRP = plant pathogenesis protein

PRR = pattern-recognition receptors

RAG1$^{-/-}$ = recombinase activating gene-1-deficient

RBC = red blood cell

RBP = retinol-binding proteins

RELM-α = resistin-like molecule-alpha

RFU = relative fluorescence units

RNA = ribonucleic acid

RoI = reads of insert

RP = reverse primer

nr = non-redundant

rHA = recombinant human albumin

rIL-33 = recombinant IL-33

RPM = revolutions per minute

SAR = structure-activity relationship

SCFA = short chain fatty acid

SCP = sperm-coating-like extracellular proteins

SCP/TAPS = SCP/Tpx-1/Ag5/PR-1/Sc7 (SCP)

SITS = species independent translational RNA sequence

Std. Dev. = standard deviations

ShK = *Stichodactyla helianthus* toxin

SP = Signal peptides

SSH = suppression subtractive hydrisation

s.c.= subcutaneous

T-bet = T-box family transcription factor

Td = trypsinised / denatured

Td*Ac*-FAR-2 = trypsanised denatured fatty acid retinol binding protein 2

T_H = T helper

TLR = toll like receptor

TIMP = tissue inhibitor of metalloproteases

TGF-β = transforming growth factor beta

TNF = tumour necrosis factor

TNBS = 2,4,6-trinitro benzene sulfonic acid

TNP = trinitrophenyl

Treg = regulatory T cell

T_R1 = Type 1 regulatory

TSLP = thymic stromal lymphopoietin

TTR = transthyretin

UC = ulcerative colitis

UCEIS = ulcerative colitis endoscopic index of severity

UPR = unfolded protein response

UTR = untranslated regions

WT = wild type

YPD = yeast extract peptone dextrose

3D = three dimensional

Data Policy

The James Cook University Data Policy was followed in order to store the data produced from this research. All laboratory experiments and data was recorded in a handwritten laboratory book that was kept with the primary supervisor. All the electronic data files were uploaded to a shared dropbox with the primary supervisor.

James Cook University Library will receive an electronic copy of this thesis. The research findings from this thesis will be published as per the aforementioned publication plan after IP protection and will be available for access in the public domain.

Chapter 1

Introduction

1.1 Inflammatory Bowel Disease

Inflammatory bowel disease (IBD) is a collective term used to refer to a group of chronic gastrointestinal diseases, typified by Crohn's disease (CD) and ulcerative colitis (UC). CD and UC are defined by alternating cycles of intestinal inflammation flares, relapse and remission. Both pathologies result from chronic inflammation due to the disruption of gut homeostasis by an aberrant immune response mounted against harmless antigens[1]. CD is characterised by ubiquitously snake-like transmural lesions across the entire gastrointestinal (GI) tract that typically form deep abscesses or fistulas in the terminal ileum and colon (Figure 1-1 B)[2]. UC on the other hand regularly causes superficial ulcers that are limited to the colonic mucosa and originate at the colon and progress proximally (Figure 1-1 C)[3].

Figure 1-1.1 Colonoscopy images of the colon from a healthy individual (A) and patients with CD (B) and UC (C) respectively. Taken from[4].

UC patients are typically believed to display a non-classical T helper (T_H)-2 type response with elevated levels of interleukin (IL)-13, IL-5 but not IL-4, whereas CD patients are believed to display a T_H1 response with elevated levels of Tumour Necrosis Factor (TNF), Interferon Gamma (IFN-γ) and IL-12 summarised in Table 1-1. More recent advances have revealed that many cytokines overlap between both diseases, some of which include IL-6, IL-8 and IL-23, which makes these cytokines attractive options for targeting in IBD treatment[5].

Condition	Ulcerative Colitis	Crohn's Disease
Endoscopic manifestation	Colon specific	Non-specific GI tract
Annual European incidence rate	5.6 per 100,000 *	10.4 per 100,000
Annual Australian incidence rate	29.3 / 100,000 **	17.4 per 100,000
Immunological response	T_H2 cells	T_H1 / T_H17 cells
Inflammation depth	Mucosal	Transmural

Table 1-1 Summary of the differences between the two major forms of IBD, ulcerative colitis and Crohn's disease*[6], **[7].

1.1.1   Epidemiology

The incidence of IBD is approximately 0.5 % of all western populations[6]. The areas with the highest prevalence are North America (1.4 million people), Europe (2.5 million people), Australia and New Zealand (Figure 1-2)[8]. There does not appear to be sex distribution bias in IBD[9]. IBD onset peaks between twenty to forty years old, however, the age of new diagnoses is becoming younger and the incidence of CD has dramatically risen in European children between 2005 and 2007[10].
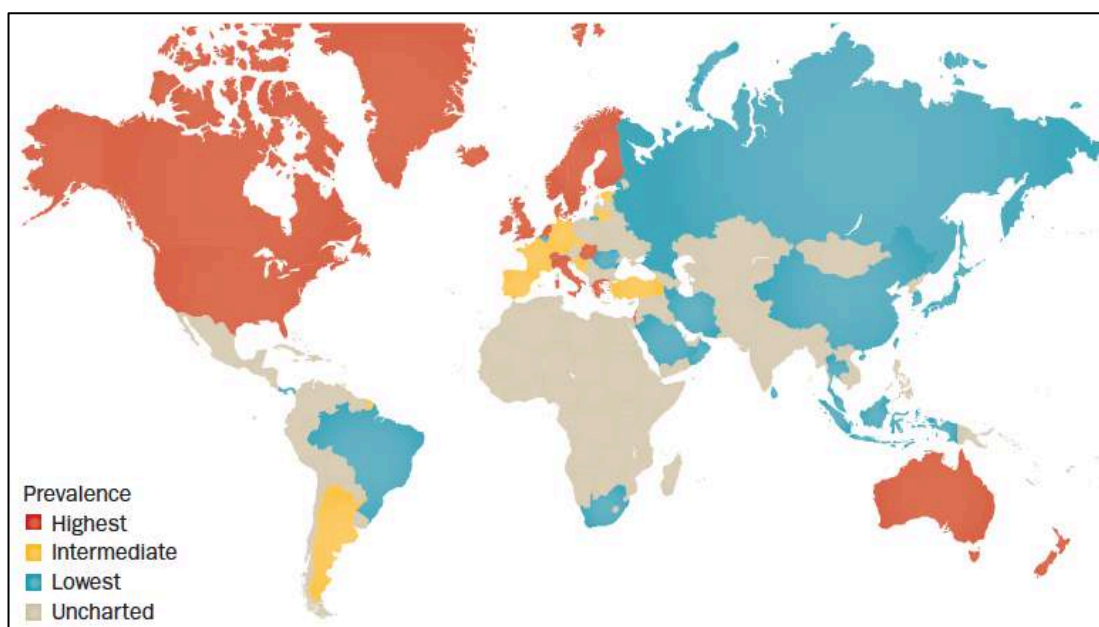
Figure 1-2 Map showing the global IBD distribution. Taken from[8].

The medical community has intermittently observed IBD since ancient historical times, but CD and UC were first outlined as individual diseases by Doctor Crohn in 1932 and Sir Samuel Wilks in 1859[10]. The medical community was slow to recognise IBD as a condition and there was a lack of a precise diagnostic criteria that resulted in inaccurate estimates of the prevalence prior to the mid-20th century[11]. Initially, UC was only

diagnosed and documented *post-mortem* but in 1969, colonoscopy was introduced which allowed the incidence to be more precisely determined[12], after which there was a steady and marked increase in the incidence and diagnosis of IBD worldwide[13]. Evans and Acheson (1965) first showed an increase in the number of new cases of UC from 4.7 to 9.7 new cases per 100,000 inhabitants in Oxford, England between 1951–1960[14]. Subsequent epidemiological studies have reported a continual increase in new cases per 100,000 inhabitants for both CD and UC[15],[16],[17],[18].

1.2 Diagnosis

Diagnosis of IBD is not clear-cut. In fact, the disease can go undiagnosed for years despite patients conveying a variety of symptoms including abdominal pain, faecal urgency, bloody diarrhoea, vomiting, fatigue and weight loss[19],[20]. IBD patients experience relapsing bouts of intestinal inflammation for many years, normally starting between the ages of twenty to thirty years old[21]. IBD is characterised by an increase in erosion and injury to the intestinal transmural layer, ulcerations, inflammatory cell infiltrate, crypt cell hyperplasia and production of mucous[14]. Physicians perform endoscopy to evaluate the extent of inflammation and collect stool samples to rule out foreign pathogens[22]. UC commences in the distal colon spreading proximally up the colon[23]. Only one in three UC patients present at this stage because usually symptoms are limited to intestinal discomfort[23]. UC patients report approximately eight flare-ups per annum which distinctly impairs their quality of life[23]. Two in three UC patients present when there is marked inflammation in the left-side of the colon or throughout the entire colon which is much more serious and can lead to them having part of their colon surgically removed[24]. Severe complications in chronic disease include fistulas, abscesses, strictures, acute bleeding, and increased risk and severity of colorectal cancer[25].

5

Physicians diagnose IBD and administer appropriate treatment and evaluate severity by using the Ulcerative Colitis Endoscopic Index of Severity (UCEIS) framework[26]. Colonoscopy is the gold standard diagnostic technique for both UC and CD[27]. The magnitude of inflammation is assessed by the Mayo Endoscopy Score, histology, radiology, faecal calprotectin, albumin, C-reactive protein levels and stool frequency[28]. Prognosis in the first decade is promising as most patients go into remission and there are low rates of colectomy and cancer[29]. Due to the patchy nature of inflammation in CD it is even harder to diagnose. Serology tests are used to distinguish CD from irritable bowel syndrome (IBS) as well as biopsies from both inflamed and non-inflamed sites for histological assessment[30]. Patients can also experience extra-intestinal symptoms such as uveitis and episcleritis of the eyes, peripheral arthropathy of the joints and erythema nodosum and pyoderma gangrenosum of the skin which further complicates accurate diagnosis[31]. Furthermore, the psychological issues experienced by IBD patients include depression and anxiety[23]. Finally, GWAS of both UC and CD has elucidated 163 associated risk loci and 110 overlaps between UC and CD, but unfortunately there is a lack of a distinct genetic markers to diagnose either form of IBD[32,33,7].

1.3 Aetiology

The definitive causes of IBD remain unidentified, however, it is generally accepted that the aetiological agents involved in the onset of IBD are the interplay between the mucosa and the composition of the gut microbiota, genetic susceptibility and environmental stimuli which include increased use of antibiotics and non-steroidal anti-inflammatory drugs (NSAIDs), vaccination, improved sanitation, and changes in diet (Figure 1-3)[34],[35].
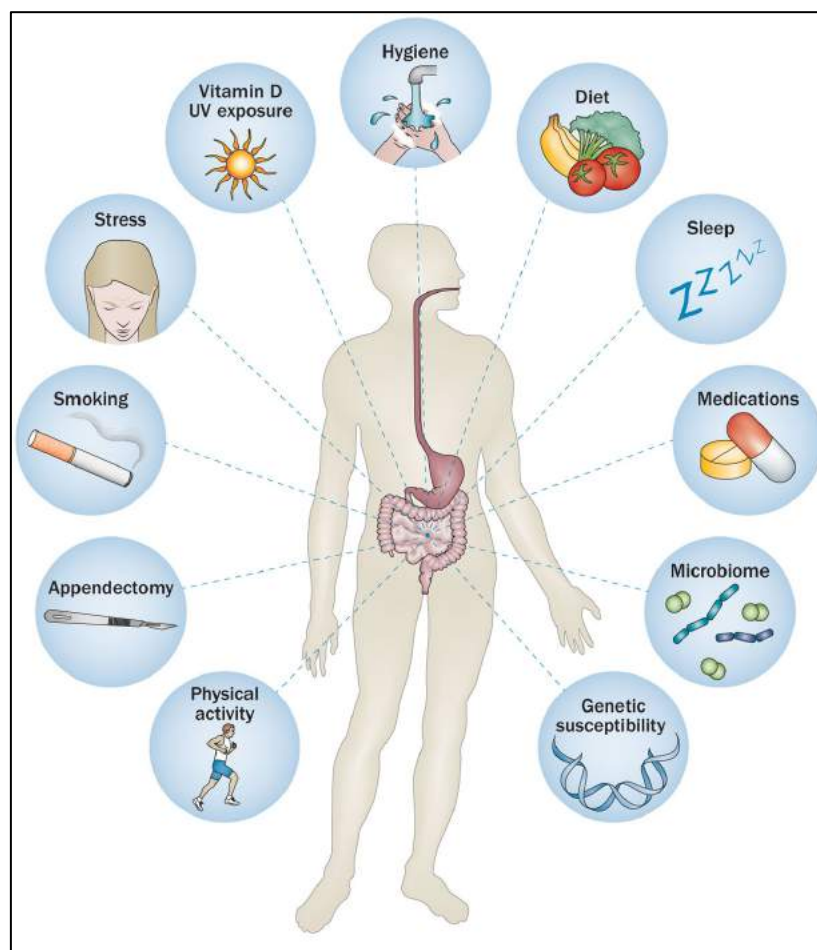
Figure 1-3 Aetiological factors of IBD that can contribute to the onset of disease. Taken from[36].

1.3.1 Aetiology: Environmental & Genetic Factors

Environmental stimuli and life style choices including smoking, stress, sleep, diet, pollutants and physical activity have been implicated in the onset of IBD, but the exact mechanisms by which these aetiological agents affect disease onset has yet to be elucidated[37]. Another accepted aetiological factor in the onset of IBD is genetic susceptibility. Given the rapid growth in the incidence of IBD, it is unlikely that genetic drift is a major factor and genome-wide association studies (GWAS) have clarified that polymorphisms in associated genes seem to be associated with particular populations[38].

CD is associated with gene polymorphisms involved in innate immunity, phagocytosis, autophagy and nucleotide-binding oligomerisation domain containing 2 (NOD-2) signalling[39]. On the other hand, UC is associated with variations in genes involved in mucosal barrier function such as extracellular matrix protein 1 (ECM-1), intestinal cell autophagy and the unfolded protein response (UPR) that disrupts goblet and Paneth cells[40]. Mutation of the gene for the IL-23 receptor (IL-23R) increases susceptibility to both diseases[39].

1.3.2 Aetiology: Epithelial Barrier

While genetics is an important factor in IBD, studies demonstrating that monozygotic twins only show 15 % and 27 % concordance for UC and CD, respectively, highlights the importance of other factors such as environmental stimuli and changes in the composition of the luminal flora of the gut mucosal system[41]. The gut's physical and biochemical barrier is composed of continuous specialised intestinal epithelial cells (IEC or enterocytes) connected through cellular junctions such as tight junctions, gap junctions and desmosomes. It also consists of antimicrobial peptides (AMP), immunoglobulin A

(IgA), mucous, saliva and pancreatic and gastric fluids[42]. Its major function is to segregate and moderate mucosal immune cells from commensal and pathogenic microorganisms as well as environmental and dietary antigens.

Dysfunction of the intestinal barrier via the tight junctions is suggested as an aetiological factor in IBD, where bacterial translocation across the epithelial barrier causes "leaky gut syndrome" and inflammation in the mucosa. In IBD, mucosal barrier dysregulation has been shown to occur by several means. Firstly, the cytoskeletal network can rearrange to disrupt the tight junctions and regulate the permeability of the barrier[42]. Secondly, tight junction malfunction is a consequence of the upregulated expression of the receptor for IL-13 (IL-13Rα2) as a result of bacterial glycolipids[43]. This cytokine cascade changes the IL-13-mediated Natural Killer (NK) T cell cytotoxicity towards tight junction cells, causing epithelial apoptosis and a loss of integrity of the intestinal barrier[43]. Thirdly, specialised microfold cells in peyers patches can acquire antigens from microorganisms and transport them into the lamina propria (Figure 1-4)[44]. Increased intestinal permeability and translocation of luminal contents permits bacteria, undigested food and waste products to traverse the lamina propria and causes chronic inflammation[45],[46],[1].
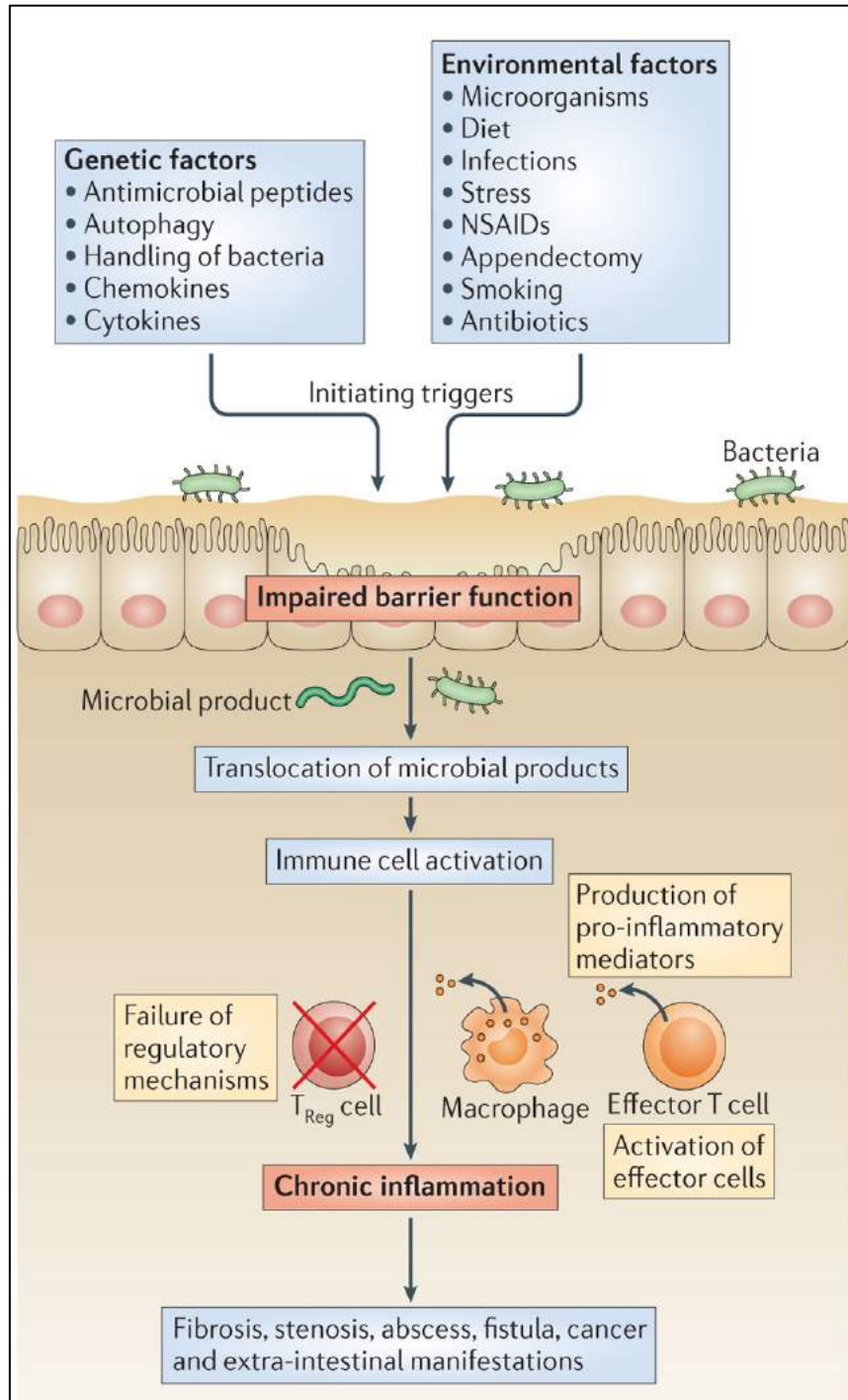
Figure 1-4 Aetiological factors result in translocation of microbial products and immune cell activation, resulting in chronic inflammation that characterises IBD pathology. Taken from[15].

After translocation to the lamina propria, bacteria and their products are taken up by antigen presenting cells (APCs) which include dendritic cells (DCs), macrophages and B cells[47]. Alternatively, translocation can occur by DCs squeezing their dendrites in between IECs to directly phagocytose luminal antigens[48]. Upon contact with bacteria, a network of haematopoietic cells including macrophages, monocytes, and granulocytes recognise pathogen-associated molecular patterns (PAMPs) that are conserved molecular constituents of the commensal or pathogenic bacteria[49],[50]. PAMPs interact with pattern-recognition receptors (PRR), such as scavenger and Toll-like receptors (TLR) found on the immune cell surface and intracellular receptors including NOD-1 / 2. Engagement of these receptors activates the associated downstream signalling pathways such as NF-κB (nuclear factor kappa-light-chain-enhancer of activated B cells). This promotes transcription and translation of immune-related genes that produce vast quantities of chemokines and cytokines and attracts granulocytes and leukocytes to the affected gut tissue[51],[52].

1.3.3   Aetiology: Dendritic Cells, Antigen Presentation and Adaptive Immune Cells

While the innate immune system is responsible for initiation of IBD, the adaptive immune system plays a significant role in chronic disease. Circulating APCs detect and engulf antigens to mature, migrate and process these antigens for presentation via the major histocompatibility complex (MHC) (Figure 1-5c)[53]. APCs that present an antigen on MHC-II engage with receptors on immature cluster domain 4 positive (CD4+) T cells that mature into effector T helper cells and activate the adaptive immune response (Figure 1-5b). In contrast, APCs that present an antigen on a MHC-I molecule engage with immature CD8+ T cells that mature into cytotoxic T cells.
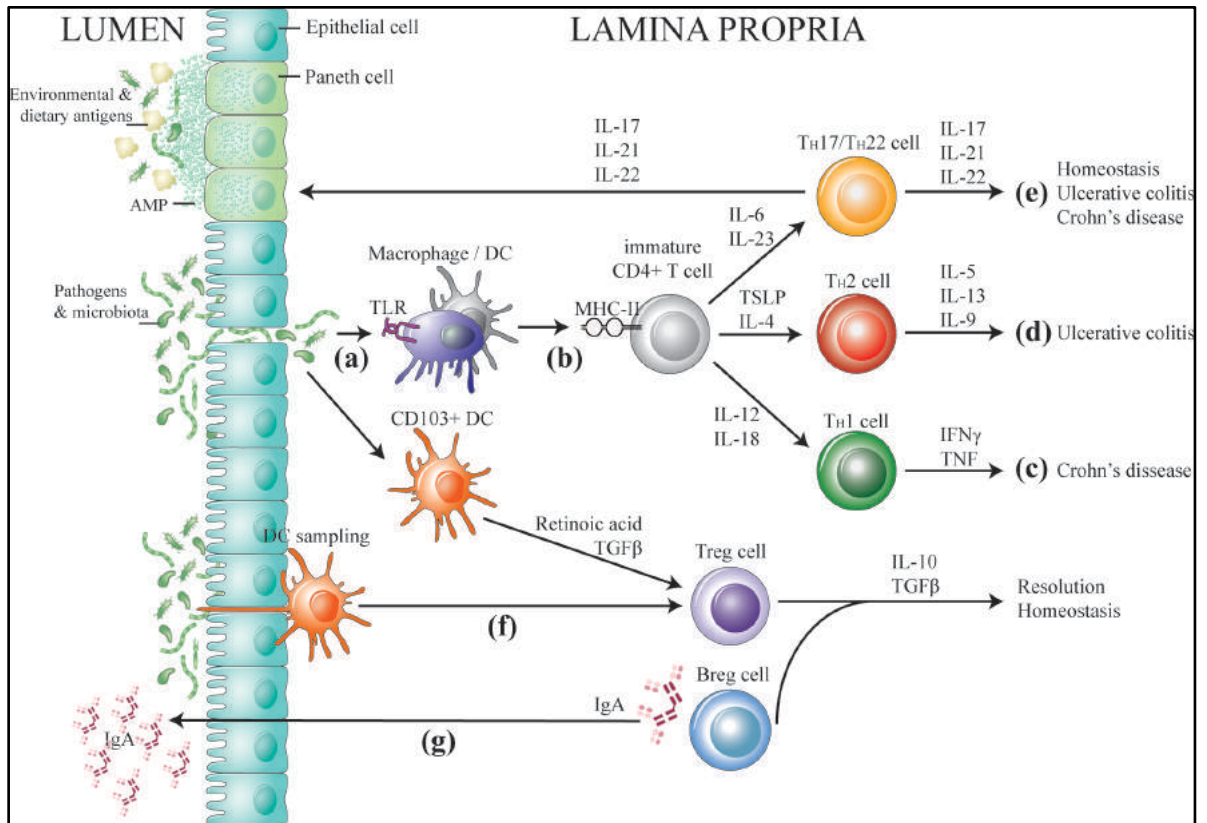
Figure 1-5 Gastrointestinal luminal microbiota sampling mechanisms and the adaptive immune responses in IBD. Adapted from[48].

Environmental and dietary antigens translocate across the epithelial barrier into the lumen where they are recognised by TLRs on macrophages or DCs. Antigen presentation on MHC-II under the influence of a milieu of cytokines leads to the differentiation and proliferation of immature CD4+ T cells into their three subsets which can lead to either CD or UC or homeostasis. T_H17 / T_H22 cells release IL-17, IL-21 and IL-22 which can stimulate Paneth cells to secrete defensins. DC sampling of luminal pathogens and microbiota results in the induction of the regulatory pathway and the production of IL-10 by regulatory T cells (Tregs). Finally, plasma B cells release antibodies which can bind to luminal pathogens.

CD is an inflammatory T_H1 mediated condition where macrophages release IL-6, IL-23 and TNF. This up-regulates expression of the T-box family transcription factor (T-bet) on CD4+ T cells which then produce pro-inflammatory mediators such as IFN-γ, IL-2 and TNF, thereby exacerbating inflammation (Figure 1-5c)[34]. In CD, the mediation of microbial recognition is disrupted, resulting in the inappropriate activation of innate inflammatory genes such as autophagy related 16-like-1 (ATG16L-1), immunity-related GTPase family M (IRGM) and NOD-2. This consequently results in inflammation[40],[54],[55].

In contrast, UC is a T_H2-mediated condition where an increased number of NK cells in the colon secrete IL-13, resulting in apoptosis, dysfunction of the epithelial barrier and epithelial cell cytotoxicity (Figure 1-5d)[6]. Activation of T_H17 / T_H22 effector cells plays a major role in both CD and UC through upregulation of IL-17A, IL-21 and IL-22 (Figure 1-5e)[50]. Dysfunction of the T_H17 / T_H22 effector cell pathways in IBD causes dysfunction of the intestinal mucosal barrier, specifically through Paneth cell autophagy, a cellular stress response and the release of antimicrobial materials that control the host-commensal balance[56].

B cells, a component of the adaptive immune system, produce antibodies, act as secondary APCs, and secrete cytokines and antibodies[57]. A subpopulation of B cells, known as regulatory B cells (Bregs), can maintain homeostasis and suppress inflammation by secreting immunoglobulin A (IgA) and producing IL-10 (Figure 1-5g)[58]. In a mouse model of chronic colitis, IL-10 producing Bregs regulated inflammation by suppressing activation of inflammatory cascades (Signal Transduction and Activation of Transcription 3 (STAT3) and IL-1β)[59]. Patients with CD, have low

numbers of IL-10 producing B cells, and it has been reported that this subset can ameliorate intestinal inflammation independent of Tregs[60].

1.3.4 Aetiology: Tolerance

In homeostasis, the engagement of innate immune pathways can activate either an inflammatory or homeostatic / tolerogenic transcriptional pathway depending on the ligand and tissue location[61]. The commensal bacteria that reside in the luminal gut mucosa are composed of a colossal assortment of external antigens. Even though the physical barrier of the gut mucosa prevents microbiota from infiltrating the lamina propria, it has become apparent that T cells frequently interact with the microbiome and educate the immune system, otherwise known as tolerance[62]. Central tolerance occurs in the primary lymphoid tissues and is crucial for the education of T and B cells to self-antigens[62]. Peripheral tolerance functions as a preventative measure for any T and B cells that circumvent negative selection in the primary lymphoid organs. Thus, they are subsequently caught in the peripheral organs such as the spleen and the lymph nodes[63]. Finally, tolerance can be acquired via exposure to foreign antigens that are experienced on a day-to-day basis[64]. Acquired tolerance to oral antigens including food, air borne antigens, and bacteria that are ingested or inhaled is paramount for the education of the immune system[65].

Dysregulation of the homeostasis of peripheral tolerance in the education of the immune system to external stimulus results in a disproportionate pro-inflammatory response, and has been observed in genetically susceptible populations[66,67,68,69]. It is essential for the innate and adaptive immune system to maintain peripheral tolerance because there is an estimated 100 trillion commensal bacteria inhabiting the intestine of an adult[70]. The

14

regulatory cell types involved in intestinal homeostasis include regulatory DCs, intestinal intraepithelial lymphocytes and B cells. Regulatory or tolerogenic DCs are located in in the intestinal mucosa and mesenteric lymph nodes and express integrin alpha E (CD103) (Figure 1-5f)[71]. Mucosal CD103+ DCs secrete TGF-β, retinoic acid and IL-2 and prevent immune-mediated pathology by promoting expansion of Treg cell populations and maintaining intestinal homeostasis.

In the thymus, IL-2 signalling causes naïve CD4+ T cells to differentiate into thymus-derived Tregs that express the transcription factor forkhead box marker P3 (FOXP3)[72]. Alternatively, CD4+ T cells differentiate into FOXP3+ peripherally-derived Tregs in the presence of retinoic acid and TGF-β and these cells display a CD4+ CD25+ FOXP3+ phenotype. Activated Tregs lead to resolution of inflammation in IBD by producing TGF-β, IL-10 and cytotoxic T lymphocyte antigen (CTLA)-4[73]. Therefore, a molecule that could induce Treg activation would be a potential therapeutic drug for IBD patients.

1.3.5 Aetiology: Innate Immune Cells

Eosinophils can home to the lamina propria in response to the chemokine eotaxin in IBD[74]. Eosinophils secrete various cytotoxic molecules such as TNF, IL-13, reactive oxygen species and matrix metalloproteases. While these molecules can hinder invading microorganisms, collateral damage to intestinal tissue results as a by-product of this process[75]. Eosinophilia has been implicated in paediatric UC and in experimental murine models of UC[76]. IL-5 has been shown to synergise with Granulocyte Macrophage Colony-Stimulating Factor (GM-CSF) and increases eosinopoiesis[76]. GM-CSF-activated eosinophils produce the inflammatory cytokines IL-13 and TNF which exacerbate IL-23-mediated chronic colitis. Powrie and colleagues have further implicated eosinophils

in IBD pathogenesis by demonstrating that depletion of eosinophils and blockade of IL-5 and / or GM-CSF ameliorates colitis[74].

On the other hand, eosinophils have also been shown to be beneficial and contribute to the repair process by regulating local macrophage responses[74]. The number of activated eosinophils was reported to be higher in UC patients in remission than patients in the active phase of the disease[77]. This eosinophil protective / destructive axis is enigmatic; eosinophilia does not always correlate with disease severity. Given that eosinophil degranulation is dependent on the cytokine milieu, it is plausible that the role of eosinophils is dependent on the presence of degranulation promoting cytokines[74]. Controlling eosinophil degranulation may have beneficial applications in IBD therapy.

Neutrophils, also called polymorphonuclear leukocytes, comprise 50 to 60 % of circulating leukocytes, and like eosinophils their contribution to gut homeostasis also remains ambiguous. The current dogma states that neutrophils are the primary responders at sites of inflammation, releasing inflammatory mediators and aiding in recruitment of additional immune cells[78]. The contribution of neutrophils to IBD is paradoxical as there are conflicting reports on whether they exacerbate or resolve inflammation[79,80,77]. An explicit role for neutrophils in IBD has not yet been delineated. However, what is clear is that the results vary based on the experimental model used[77]. Recently, neutrophils have been implicated in IL-23-T_H17-dependent colitis[80]. Neutrophil infiltration and oxidative stress occur in the colons of UC patients and their colonic epithelial cells have abnormally high alkaline phosphatase activity[79]. This highlights the need for further research to clarify the role of neutrophils in intestinal homeostasis and IBD therapy.

Innate lymphoid cells (ILC), of which there are 3 types (ILC1-3), are a heterogeneous innate immune cell group important in the initiation, management and resolution of intestinal inflammation[81]. This rare cell type does not have antigen specificity yet can swiftly secrete vast amounts of potent cytokines in response to alarmins and cytokines[81]. ILCs are implicated in IBD pathology because chronic ILC activation mediates IL-23-dependent innate intestinal pathology[36]. In CD patients, NK cells (ILC1s) produce IFN-γ, driving intestinal inflammation[82,83,84]. Furthermore, in a mouse model of IBD, inflammation is ameliorated by blocking IFN-γ[85]. ILC3-like cells promote intestinal inflammation by producing IL-17 in a T cell-independent mouse model of *Helicobacter hepaticus*-mediated colitis (Figure 1-6)[85]. Patients with chronic intestinal inflammation and mice with colitis-induced colon cancer have elevated numbers of pro-inflammatory ILC3s[86,87,88].

On the contrary, ILCs have also been implicated in resolution of inflammation. ILC2s promote tissue regeneration in response to stimulation by IL-10, IL-23, AMP and mucous[89,90]. In addition, ILC2s promote gut homeostasis by producing amphiregulin (AREG), a ligand of the epidermal growth factor (EGFR)[91]. Dysregulated expression of EGFR, its ligands and IL-33 have been detected in inflamed tissue from IBD patients and in mice with experimental colitis[92,93,94]. Therapeutic treatment with IL-33 or the transfer of ILC2s has been shown to diminish IBD severity by promoting an innate response dependent on AREG[95]. These reports highlight the importance of ILCs in the recovery of gut homeostasis.
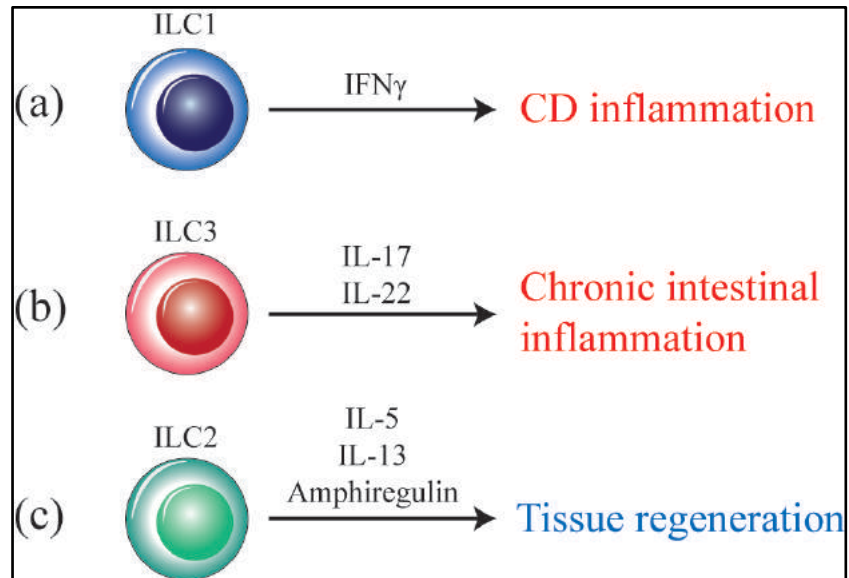
Figure 1-6 Innate lymphoid cells (ILCs) in IBD pathology. Adapted from[81]. Phenotypically distinct ILC populations are associated with the selective accumulation of inflammatory cytokine expression such as IL-17, IL-22, IFN-γ in response to IL-23, thereby mediating innate colitis.

1.4 Murine Models Addressing Inflammation in IBD Research

In order to develop new treatments for IBD the use of experimental rodent models has been essential to improve our understanding of the histopathological and clinical characteristics of human IBD. Presently, there are approximately thirty mouse and rat models of gastrointestinal inflammation[96].

There are three general categories that these models fall into, including:

1. Acute, abrasive, self-limiting colitis

2. Disturbance in T cell homeostasis resulting in chronic colitis and intestinal inflammation

3. Specific gene deletion resulting in spontaneous chronic inflammation.

In experimental models, colitis can be induced by a polarised T_H1 / T_H17 response (mimicking CD) or a T_H2 (mimicking UC) cell-mediated immune response[97]. Three widely recognised experimental models of colitis are; the TNBS-induced model, the DSS-induced model and the T cell transfer model[98]. There are integral caveats and principles to consider when using each experimental model of IBD:

- The effect of the genetic background of the experimental animal on the onset and severity of colitis

- The mediation by T cells of gastrointestinal inflammation

- The role of the microflora in the intestine in initiating and maintaining inflammation[99].

1.4.1 TNBS-Induced Model of Colitis

The trinitrobenzenesulfonic acid (TNBS) model is an example of T cell dependent acute transmural murine colitis induced by an exogenous molecule[100]. The general dosage is between 0.5 - 4.0 mg TNBS in 50 % ethanol, but this can vary depending on the age and strain of the mice used. C57BL/6 mice do not readily succumb to TNBS-induced colitis and will naturally regain weight lost. Meanwhile, BALB/c mice are susceptible to TNBS-induced weight loss[101].

Under mild anaesthetic, TNBS is administered with a solvent (ethanol) into the rectum; it then causes a disruption and perforation of the mucosal epithelial barrier[102]. The initial colitis-like symptoms observed are due to ethanol breaking down the mucous component of the epithelial lining (Figure 1-7). CD4+ T cells are then recruited to the gut during the chronic phase of inflammation. TNBS is a haptenising molecule which means that trinitrophenyl (TNP) attaches to components of the luminal microbiota and colonic proteins making them immunogenic and causing a delayed hypersensitivity reaction mediated by CD4+ T cells[102]. These haptenated proteins translocate across the epithelial barrier to the lamina propria and are recognised by DCs[102]. DCs present TNP, on their MHC-II to naïve T cells. TNP activates the naïve T cells to express the CD40 ligand (CD40L) signalling molecule. CD40L binds to its receptor on the DC and this causes the DC to release IL-12. IL-12 induces naïve T cells to differentiate to a T_H1 phenotype[103]. The T_H1 polarised cell releases TNF that positively feeds back to the DC to continue making IL-12[102]. The T_H1 cell also releases IFN-γ and TNF that acts on macrophages to stimulate them to produce TNF, IL-1β and IL-6[102]. These cytokines result in an influx of cells causing inflammation that gives rise to colitis.
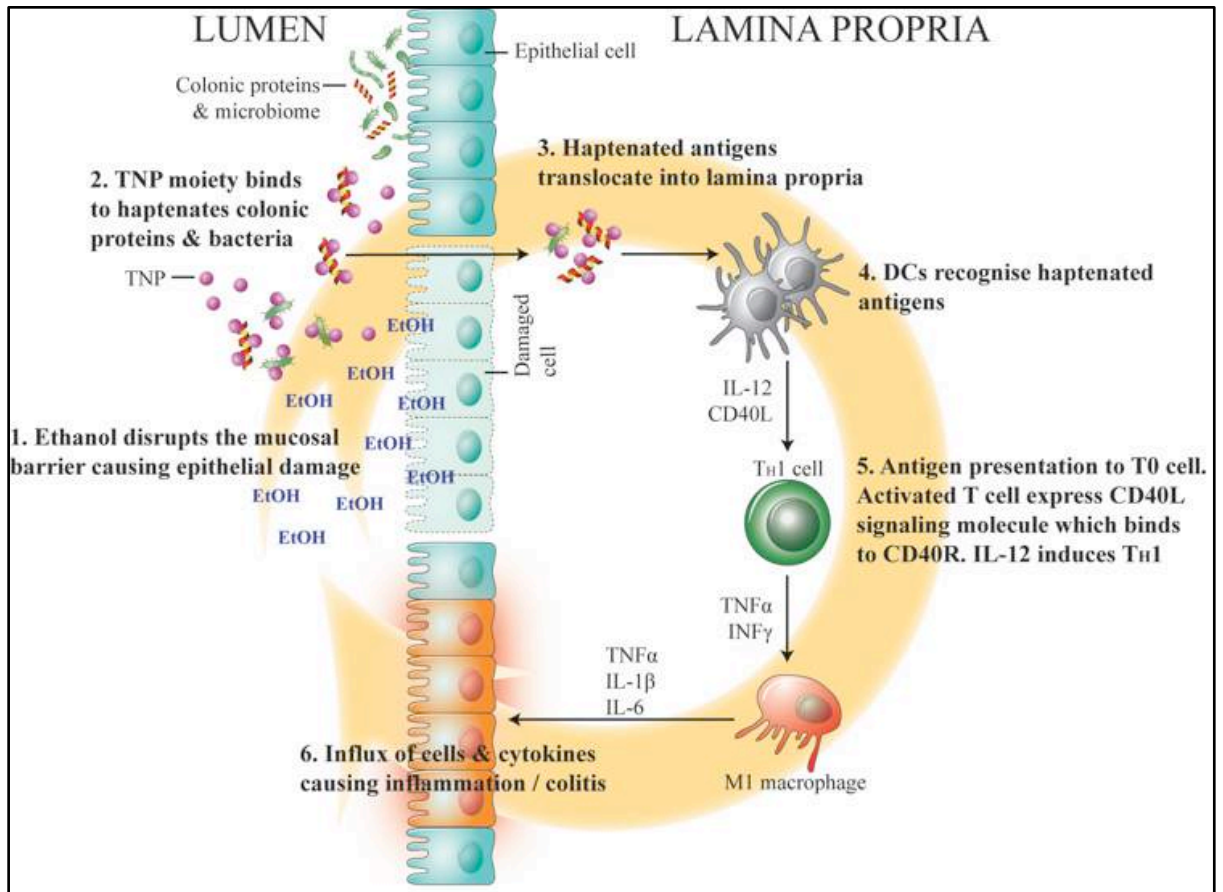
Figure 1-7 Diagram of pathology and the mechanism of induction of inflammation in TNBS-Induced Colitis. Ethanol administered into the rectum disrupts the mucosal barrier and causes epithelial damage (1). The TNP moiety in TNBS binds to and haptenates colonic proteins or bacteria making them immunogenic (2). Haptenated colonic proteins & bacterial antigens translocate to the lamina propria (3). DCs recognise haptenated colonic proteins and bacterial antigens (4) and present antigen to naïve T cells (T_H0) (5). Activated T cells express CD40L signalling molecule which binds to CD40R and under the influence of IL-12, cell differentiation and proliferation occurs. An influx of T_H1 cells, classically activated macrophages and pro-inflammatory cytokines gives rise to inflammation at the epithelial barrier that causes colitis.

1.4.2   DSS-Induced Model of Colitis

The dextran sulphate sodium (DSS)-induced colitis model is used widely because it is T cell independent and it closely mimics UC pathogenesis in humans[104]. DSS is a negatively charged, water-soluble, sulphated polysaccharide with anticoagulant characteristics that induces colitis[104]. A 3 to 5 % solution of DSS is administered in the drinking water of mice and their disease severity index (DSI), weight and blood content in faeces is monitored daily. It is hypothesised that DSS disturbs the gastrointestinal epithelial layer, enabling luminal contents to penetrate into the tissue underneath. It should also be noted that DSS-induced colitis is not dependent on adaptive immune cells[105]. If T cells are depleted, mice still develop colitis. Thus, this model is limited to studying the role of the innate immune response in intestinal inflammation[104].

DSS-treatment has been shown to up-regulate TLR-4 dependent myeloid differentiation factor 88 (MyD88) activation and subsequent NF-κβ-dependent gene transcription[105]. Human UC patients strongly up-regulate the lipopolysaccharide (LPS) PRR, TLR-4[106]. TLR-4 is a crucial part of the innate immune system and is extensively expressed on gastrointestinal epithelial cells to identify foreign molecular patterns[107]. TLR-4 regulates pro-inflammatory gene expression profiles by signalling through MyD88 which then translocates NF-κβ to the nucleus and / or mitogen-activated protein kinases (MAPK)[105]. The correlation between the up-regulation of TLR-4 in human UC and murine DSS-colitis supports its use as a model to delineate immunological mechanisms in colitis.

Another potential immunological pathway involved in the action of DSS-induced colitis is release of the alarmin IL-33. There are conflicting reports on the role of IL-33 in this model. Artis and colleagues demonstrated that ILC2s in the gut respond to IL-33 and

22

express AREG. When IL-33, exogenous AREG or ILC2s were administered to mice, intestinal inflammation was limited[91]. Other groups however report that DSS-induced colitis is exacerbated when recombinant IL-33 is administered[108]. Moreover, IL-33 induced a modified T_H2 response (increased levels of IL-5 and IL-13) and suppressed the T_H1 / T_H17 cell responses (reduced levels of IFN-γ and IL-17A)[108].

1.4.3   T Cell Transfer Model of Chronic Colitis

An elegant experimental model of chronic colitis is the T cell transfer model as it is the most similar to human disease in terms of pathology and gene expression changes[99]. In this model, naïve T cells (CD4+, CD45RB high) or T cells depleted of Tregs (CD4+ CD25-) from wild type (WT) mice are transferred into a recipient strain deficient in T and B cells[109]. After 5 to 8 weeks, gastrointestinal inflammation and colitis are observed[109]. T cells transferred into recombinase activating gene-1-deficient (RAG1$^{-/-}$) recipients show that inflammation is not confined specifically to the colon but is present across the small intestine, similar to that seen in CD[109]. Mice with active disease experience diarrhoea, weight loss, epithelial cell erosion, hyperplasia, transmural inflammation, leukocyte infiltration and crypt abscesses.

Colonic gene expression of the major three animal models of colitis has been analysed by oligonucleotide array in order to establish alterations in expression compared to control mice[99]. In mice with TNBS, DSS and CD45RB transfer colitis, 21, 387 and 582 genes were up-regulated more than two-fold, respectively, in the gastrointestinal mucosa compared to wild type mice[99]. The expression profiles were also compared to a database of genes that are known to be up-regulated in human IBD (Figure 1-8)[99]. The CD45RB

T cell transfer model was shown to most closely resemble human IBD in terms of the numbers and identities of genes that underwent differential expression.
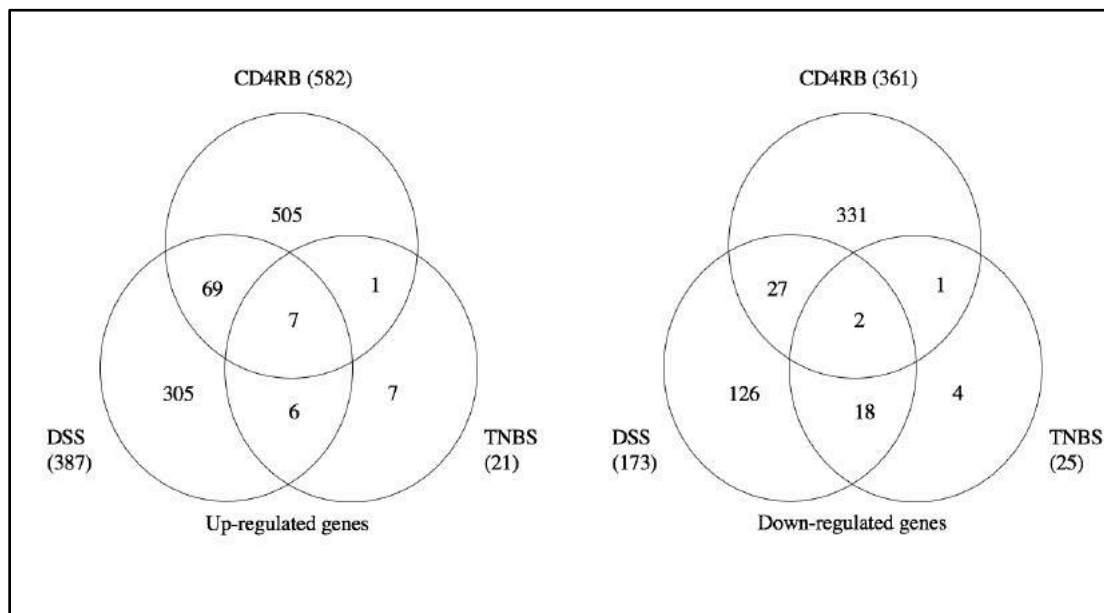
Figure 1-8 Venn diagrams of the unique and shared up-regulated & down-regulated genes in the three murine experimental models of colitis. Taken from[99].

1.4.4 Gene Deletion-Dependent Model of Spontaneous Chronic Inflammation

Additional mouse models of colitis include genetic knockouts that cannot generate regulatory cytokines (i.e. IL-2 and IL-10) and subsequently develop enterocolitis[110]. Notably, inflammation only occurs when mice are bred in non-sterile environments, and colitis does not occur in these disease-susceptible models when mice are bred in germ-free surroundings[111]. This research highlights the importance of antigen presentation in the immune response to mucosal microflora in the development of IBD[112]. Key components of the microflora, such as bacterial flagellin are currently being explored as a dominant antigen in CD[113].

The benefits of using animal model-based research / murine models of colitis include furthering the understanding of the scientific basis of disease pathology and treatment. Advances needs to be translated back to the clinic so they can improve the physician's ability to diagnose and treat patients with IBD.

1.5 Treatment

An internationally agreed definition for IBD remission and cure does not exist, however widely accepted clinical factors for remission are cessation of rectal bleeding and diarrhoea[114]. Treatment options are dependent on the severity of disease at presentation and whether treatment delivers symptomatic relief but does not alter the course of disease. The aim is to alleviate active symptoms, assist patients to enter remission and maintain remission longer[115]. If disease remission is maintained then patients continue on their current therapy.

The therapeutic armamentarium for IBD includes corticosteroids, aminosalicylates, antibiotics, immunomodulators and biologics (monoclonal antibodies) (Figure 1-9)[116]. Initial treatments limit bacterial infections, suppress inflammation and induce remission, and include the use of antibiotics, aspirin derivatives (aminosalicylates) and sulfasalazine (a derivative of mesalazine)[10]. Sulfasalazine is a compound that is poorly absorbed by the intestine, has a topical mechanism of action and is a mild suppressant of inflammatory cytokines and eicosanoids[10]. Remission typically lasts only two weeks before treatment re-administration is required[6]. The side effects of aminosalicylates include nausea, headaches, vomiting, fever, loss of appetite and a decreased white blood cell count[117]. If a patient is unresponsive, then therapy is stepped up to corticosteroids rectally and then orally (i.e. prednisone)[118]. Corticosteroids are effective in short-term treatment but due

to their immunosuppressive functions there are aggressive side effects such as osteoporosis, diabetes, hypertension, cataracts, glaucoma and weight gain, and therefore they cannot be taken long-term[115]. Thiopurine is a partially efficacious and safe immunosuppressive drug employed as a steroid-sparing therapy and widely used in the treatment of IBD to maintain remission[119]. However, if symptoms still persist and remission cannot be achieved then biologic agents are therapeutically employed.

The biologic agents that are presently accepted as effective IBD treatments fall into two categories; anti-integrin and anti-tumour necrosis factor (α-TNF) agents[120]. The three most commonly prescribed and efficacious α-TNF therapies for mucosal healing are infliximab, certolizumab pegol, and adalimumab[121],[122],[123]. These monoclonal antibodies (mAbs) bind to TNF and restrict inflammation by limiting pro-inflammatory cytokine expression which subsequently reduces apoptosis of enterocytes and Tregs, promotes apoptosis of pathogenic T cells and induces alternatively activated macrophages (M2) to induce wound healing[124]. The MUSIC and EXTEND trials assessed the efficacy of certolizumab pegol and adalimumab in CD, respectively[125],[126]. The rate of relapse six months after termination of α-TNF biologics is 38 % in UC and 44 % in CD and furthermore the risk of relapse increases to half of all patients after discontinuation for a year[127]. Evaluation of their relatively poor efficacy in preventing surgical interventions, safety, method / administration, cost-effectiveness and patient preference in the treatment of IBD is considered by practitioners before choosing a biologic as a first line treatment for IBD and highlights the need for new therapies[128]. Newer biologics that target the common p40 subunit shared by IL-12 and IL-23, such as ustekinumab have been used to improve T cell-mediated responses in double blinded clinical trials for treatment of CD[129],[130].

26

Inflammation in IBD causes tissue destruction and complications including abscesses, fistulas, fibrosis, cancer, and in these extreme cases surgical intervention is often required to resect inflamed sections of bowel[61],[131]. Surgery is considered curative in UC because it removes the entire inflamed area[132]. Approximately 33 % of UC patients and 66 % of CD patients need to undergo surgery under the current treatment program[133]. Surgical complications can lead to persistent pain, infertility, fistulas and bladder or sexual dysfunction. Furthermore, some post-surgery patients are dependent on the use of a colostomy bag, resulting in a drastically reduced quality of life[134]. Surgery is not curative in CD as the inflammation can continue further up the small intestine[133].
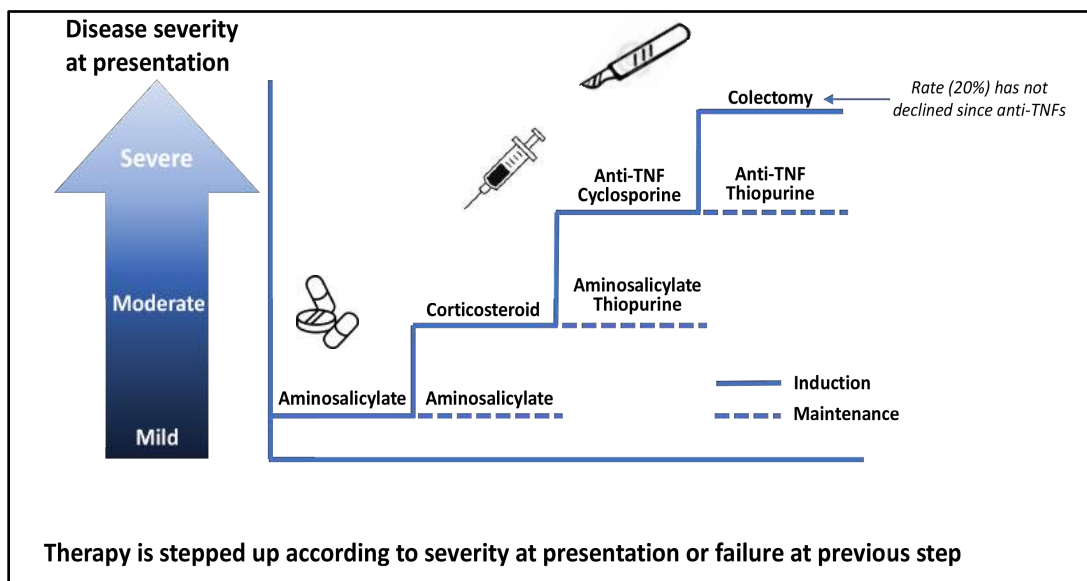
Figure 1-9   Schematic diagram displaying the progression of treatment options according to the severity of disease at presentation to a physician. Adapted from[135].

Alternative therapies for IBD include probiotics; *Escherichia coli* strain Nissle 1917 as a probiotic therapy was shown to be equally as effective as standard sulfasalazine to maintain remission in UC, but not CD[127],[6],[136]. Finally, there have also been several

studies focussed on the expression of matrix metalloproteases in the gastrointestinal mucosa of IBD patients as biomarkers of disease activity and also as a therapeutic target[137,138,138,139,140]. The lack of effective and viable treatment options highlighted here demonstrates the need for the discovery of novel therapeutic interventions.

1.6 Hygiene Hypothesis and IBD

The lack of effective treatment options for IBD is at least in part a result of the multitude of aetiological factors that contribute to the onset and relapsing nature of IBD, of which includes genetic susceptibility. CD is associated with gene polymorphisms involved in innate immunity, phagocytosis, autophagy and NOD-2 signalling[39]. UC is associated with variations in genes involved in mucosal barrier function such as ECM-1, intestinal cell autophagy and the UPR that disrupts goblet and Paneth cells[40]. The mutation of the gene for IL-23R increases susceptibility to both diseases[39]. However, there is a wealth of inflammatory disorders that are associated with genetic abnormalities in genes, and the incidence of inflammatory disorders is highest in economically developed nations such as North America, Europe and Australia (Figure 1-10).

A   B

Figure 1-10 Map displaying incidence of inflammatory disorders (A) and helminth infections (B). Taken from[9].

There is an interesting geographical correlation between the incidence of allergies and autoimmune diseases and helminth infections. Countries with a high incidence of inflammatory disorders tend to have no (or few) endemic helminth infections whereas countries with helminth infections have no to little inflammatory diseases. Infectious agents such as bacteria, viruses and parasites are pivotal in educating the immune system and only recently (in evolutionary terms) have been removed from industrialised countries. It is important to point out that this observation is more complex than accounting for the explosion in inflammatory disorders by just a reduction / eradication of infectious agents. A multitude of other factors need to considered such as diet, life-style, and genetic predispositions. Populations prone to parasitic infections have experienced parasite-driven genetic pressure. This is associated with changes in certain genes and now due to the eradication of these infectious agents, homeostasis has been thrown out of balance.

In industrialised nations, there has been a reduction in exposure to infectious pathogens due to vaccination, increased sanitation, improved hygienic standards and widespread

29

use of antibiotics[141]. The eradication of infectious agents from these communities, and helminths in particular, is inversely associated with an alarming increase in the incidence of non-infectious inflammatory diseases, notably disorders that are underpinned by immune and metabolic dysfunction[142]. While this association is clearly multifactorial, selective pressure placed on the human genome by ubiquitous helminth infection is thought to have driven various polymorphisms at loci associated with predispositions to inflammatory diseases[143]. A correlation has been found between populations from geographical locations with a high prevalence of parasites and genetic variability of immune related genes associated with IBD[144]. Genetic variation has occurred due to selective pressure from pathogens over millennia[144]. A total of 163 gene polymorphisms have been associated with predisposition to IBD, some of which correlate with both IBD predisposition and parasitic pressure within populations[145],[144]. Specifically, IL-1F5, IL-1F7, IL-1F10, IL-7R, IL-18RAP are differentially expressed in IBD patients and populations with heavy parasite burdens[36]. Furthermore, individuals with mutations in IL-10 and its receptor suffer from early-onset of IBD within the first months of life[19].

In the past 100 years there has been a pronounced increase in the incidence of immune disorders worldwide[142]. Minimal exposure to pathogens results in poor stimulation of the maturing immune system and an under-developed regulatory network, culminating in an increased prevalence of disorders that result from immune dysfunction[138],[146]. The hygiene hypothesis incorporates a combination of theories that try to explain the inverse relationship between the incidence of infectious diseases and the incidence of immune disorders. It has been proposed that minimal exposure to pathogens and the loss of microbe-driven immune signalling and regulation results in poor immune system stimulation and explains the pronounced increase in the incidence of autoimmunity and

allergic disorders since the 1950s[147],[148]. Support for this notion comes from both experimental animal and human immuno-epidemiology studies exploring atopy in communities undergoing anthelmintic therapy[149]. Several studies have highlighted how migration from developing to developed nations can increase the rate of IBD[150]. People who migrated from India to the UK were shown to develop IBD at the same rate as the local population, suggesting that the cause of IBD is related to environmental factors[150]. More strikingly, a study of migrants who moved from South Asia to Canada showed that their children were more susceptible to developing IBD than the resident paediatric population[109]. Moreover, a handful of clinical trials where iatrogenic helminth infection has been used to treat autoimmune diseases (or at least assess safety of infection in these subjects) have had mixed results but show enough promise to warrant further investigation.

Strachan first introduced the concept in his 'first child hypothesis', where children with no siblings had a higher incidence of atopic disorders[151]. This was hypothesised to be due to a lower incidence of early childhood infections attributable to a lack of transmission of pathogens by younger siblings[151]. This has been supported in animal studies where mice bred in a pathogen-free environment had a significantly increased incidence of inflammatory disorders[147].

Björkstén proposed another hypothesis called the "microbial deprivation hypothesis"[152]. This hypothesis suggests that the deprivation of exposure to non-pathogenic microbes during early life results in increased atopy[152]. The microbial deprivation hypothesis links in with the idea that the microbiome, to some extent, regulates inflammatory disease. McCoy *et al.,* (2015) reviewed data from animal models highlighting a link between the

composition of the microbiome and the increased susceptibility to inflammatory disease[140]. Specific bacterial species present in the gut microbiome of mice have been shown to heavily influence whether a response is inflammatory or homeostatic[147]. This is because certain bacteria have specific immunological properties; for example, the *Clostridium* species have been shown to induce colonic Tregs in mice[151]. Furthermore, it was shown in germ-free mice that post-natal maturation of the regulatory immune system is controlled by its interaction with microbes, of which a large number are within the intestinal microbiome[152]. These findings were confirmed in humans where changes in genetic and environmental factors, especially in the first year of life, reduced gut microbial diversity and caused the dysregulation of the human host's mucosal barrier[147].

1.7 Parasitic Helminth Therapy for Inflammatory Disorders

Parasitic helminths infect approximately two billion people worldwide, predominantly children in *rural* subtropical and tropical areas with inadequate sanitation[153]. Most infections are asymptomatic with a minimal risk of death, however, children with heavy worm burdens have an elevated risk of developing infection-related morbidities[153]. Moreover, during pregnancy, helminth infection is a risk for maternal mortality, premature delivery and diminished birth weight[154].

Parasitic helminths appear to have struck a fine balance with their hosts, refined by millennia of coevolution, to meet their needs for propagation and transmission while causing relatively little pathology given their size and the various niches occupied within the infected host[155]. Helminths have evolved a suite of mechanisms by which they penetrate and migrate through many different host organs and tissues relatively unhindered, often for many decades. Arguably the most masterful (and awe-inspiring

from a drug development perspective) trait of parasitic helminths is their exquisite ability to regulate host inflammatory responses. They do this by promoting wound healing and tissue repair and skewing distinct facets of immune processes to promote their own survival and longevity of infection, all the while ensuring that fitness, including immuno-competence, of the infected host is minimally affected[155].

The three major phylogenetic groups of helminths include nematodes (roundworms), cestodes (tapeworms) and trematodes (flukes). The most common human helminth infections are caused by the soil-transmitted intestinal nematodes including hookworms (*Necator americanus* and *Ancylostoma spp.*), whipworms (*Trichuris trichiura*), roundworms (*Ascaris lumbricoides*) and threadworms *(Strongyloides stercoralis)*. Of note, a growing body of literature suggests that members of these distinct phylogenetic groups protect mice against inducible colitis and other inflammatory diseases. Indeed, there is compelling evidence that these helminths possess the ability to interfere with multiple aspects of host immunity by inducing regulatory processes, thereby suppressing inflammatory pathways that drive the pathology associated with immune-mediated disease such as IBD[156]. The benefits of using live helminth infection to modulate the immune response in inflammatory diseases such as IBD, multiple sclerosis, asthma and atopy is often over-shadowed by its controversial drawbacks[157]. The "old friends theory" was proposed as an extension of the hygiene hypothesis to explain the inverse relationship between the incidence of parasitic infections and chronic IBD[158,159,160,67]. Evidence that helminths possess the ability to interfere with multiple aspects of host immunity by promoting regulatory responses whilst blocking the typical T_H1 / T_H17 and T_H2 responses and this has implications for the incidence and management of IBD[161].

There is evidence that helminth-driven induction of T_H2 / Treg responses leads to the direct secretion of immunomodulatory molecules, such as IL-4, IL-5 and IL-10, which decrease pro-inflammatory cytokine expression and promote epithelial barrier integrity by mucous production of goblet cells (Figure 1-10)[162]. However, there is mounting evidence that the anti-inflammatory activity of helminths is not exclusively intrinsic but instead partially due to the crosstalk between host commensal bacteria and gastrointestinal helminths. It is well documented that there is a symbiotic relationship between the host and specific gastrointestinal microbiota species and a detrimental relationship between a reduction in the diversity of the microbiota and the development of several inflammatory diseases[163]. Consistent with this, evidence of worm-induced alterations in the composition of the intestinal bacterial has been suggested as a mechanism in helminth-mediated suppression of inflammatory diseases[164]. Moreover, it has been shown that hookworm infection in humans can promote microbial changes by decreasing bacterial attachment and increasing bacterial diversity in the duodenal intestinal microbiome[165],[166]. Helminth-driven changes in bacterial communities increases production of short chain fatty acids (SCFA)[167]. This increase in bacterial-derived immuno-modulatory metabolites has been shown to attenuate allergic airway inflammation[167]. Together, these examples from the literature show that helminth infection in the gut can regulate local and systemic inflammatory responses and are mediated at least in part via the microbiome[163],[168].
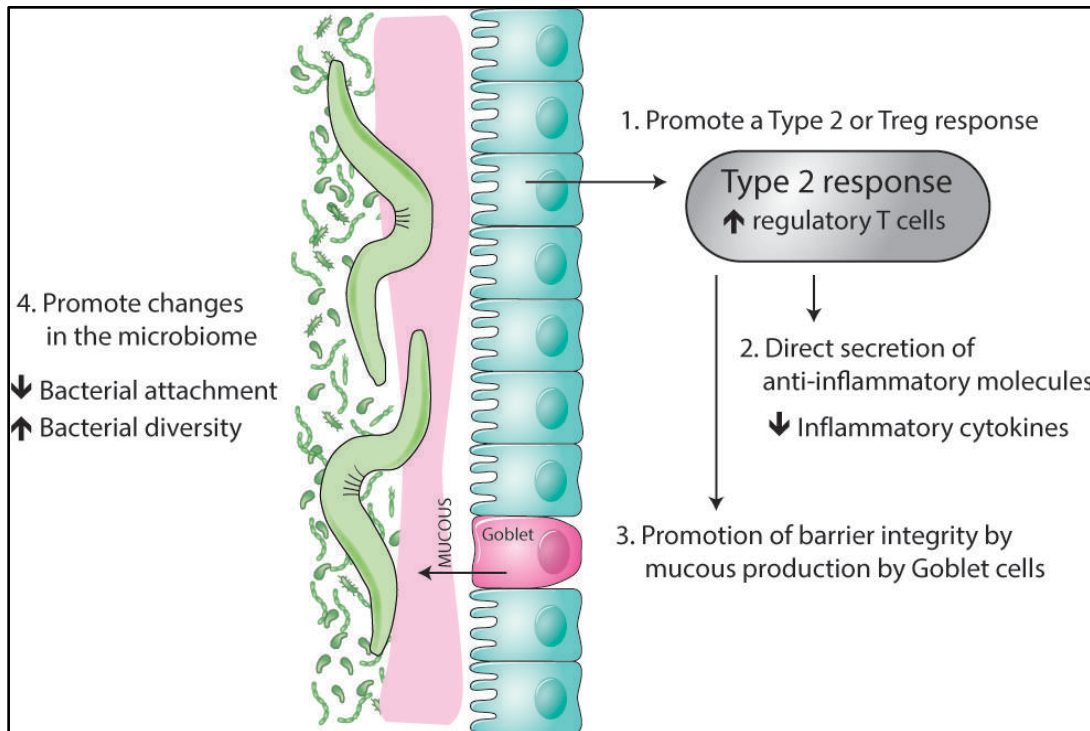
Figure 1-11 Helminth parasite therapy for autoimmune or allergic disease. The range of physiological parameters that helminths may induce in their host that could be hypothesised to alleviate disease include promoting changes in the microbiome, promoting a T$_H$2 or Treg response, improved barrier function by mucous production, and secretion of anti-inflammatory molecules to reduce pro-inflammatory cytokine secretion.

To date, two helminth species have been used in human clinical trials - the pig whipworm *Trichuris suis* and the human hookworm *N. americanus*. The therapeutic potential of *T. suis* was assessed in phase one trials in patients with IBD and multiple sclerosis[169],[170]. *T. suis* eggs were ingested and hatched to release larvae in the colon and caecum whereupon they survived in the gastrointestinal tract for one to two weeks. *T. suis* is not adapted to long-term survival in humans because of its species specificity for pigs, so frequent dosing of patients with eggs every fortnight was required to maintain intestinal worm

burdens[169]. In addition, while early trials with *T. suis* showed promise with reduced signs of disease observed, subsequent phase two trials failed to reach their clinical endpoints in both multiple sclerosis and IBD[169],[170]. Moreover, a clinical trial using *T. suis* to treat allergic rhinitis showed no therapeutic benefit[171].

N. americanus on the other hand has been shown to be well tolerated in human volunteers and in some settings, may be clinically beneficial in phase one trials for gastrointestinal diseases including CD[172] and coeliac disease[173]. Percutaneous administration of *N. americanus* third-stage larvae (L3) results in migration through the circulatory system to the lungs whereupon L3 exit the pulmonary vasculature and creep up the trachea to be swallowed and ultimately end up in the small intestine to establish chronic infections that can last several years[174]. Iatrogenic infection with *N. americanus* in adult human volunteers appears to be safe[175],[176], and in an open label study where CD patients were infected with *N. americanus*, infection was well tolerated and all patients who remained in the trial were in disease remission after one year, although it should be noted that some patients were being treated with steroidal and non-steroidal anti-inflammatories[172]. A particularly interesting outcome of the *N. americanus* trial in coeliac disease patients was that helminth infection resulted in decreased numbers of IFN-γ producing T cells in the gut accompanied by a corresponding increase in mucosal Treg numbers in response to escalating gluten challenge, which correlated with improved gluten tolerance and clinical symptoms[173].

1.8 Helminth Excretory-Secretory Products and Immune Regulation

A substantial body of literature from multiple animal models of inflammation, including autoimmune encephalomyelitis, type 1 diabetes mellitus and asthma, highlights the ability of many helminth species belonging to distinct phylogenetic groups to dampen the immune response and mitigate autoimmune / allergic pathologies[177]. Infection with the platyhelminth trematode *Schistosoma mansoni* suppressed inducible colitis in mice and dampened the inflammatory immune response[178]. Infection with the tapeworm *Hymenolepis diminuta* protected mice from DSS-induced colitis[179], and the soil-transmitted nematode roundworm *Trichinella spiralis* ameliorated dinitrobenzene sulphate (DNBS)-induced colitis in mice[177].

The ability of helminths to suppress the host immune system is due, in part to bioactive molecules, known as excretory-secretory products (ESP), that are excreted and secreted by oral openings or exposed surfaces of helminths (Figure 1-12)[180]. ESP contains a milieu of proteins, small molecules, extracellular vesicles, carbohydrates and lipids[177]. ESP molecules can regulate immune pathways that allow hookworms to live in the bloodstream, lymphatics or gastrointestinal tract for several decades where they are fully exposed to the host's immune system[181]. En route to their final destination, migrating helminths cause substantial tissue damage, but rather than inducing an inflammatory response, ESP instead can drive a response aimed at subduing and subverting the host's immune system so that they can establish a chronic infection without succuming to immune ejection.

ESP molecules have the ability orchestrate a multitude of pathways and evoke a modified T_H2 immune response to promote the longevity of the helminth infection[156]. The modified T_H2 response induced by helminths appears to be advantageous over a T_H1 response to prevent inflammation and secondary tissue damage[182]. The mechanisms that trigger the induction of the T_H2 response are largely unknown, however a fundamental role of the innate immune system, particularly programming of DCs by different stimuli, has been proposed to play a critical role[183].
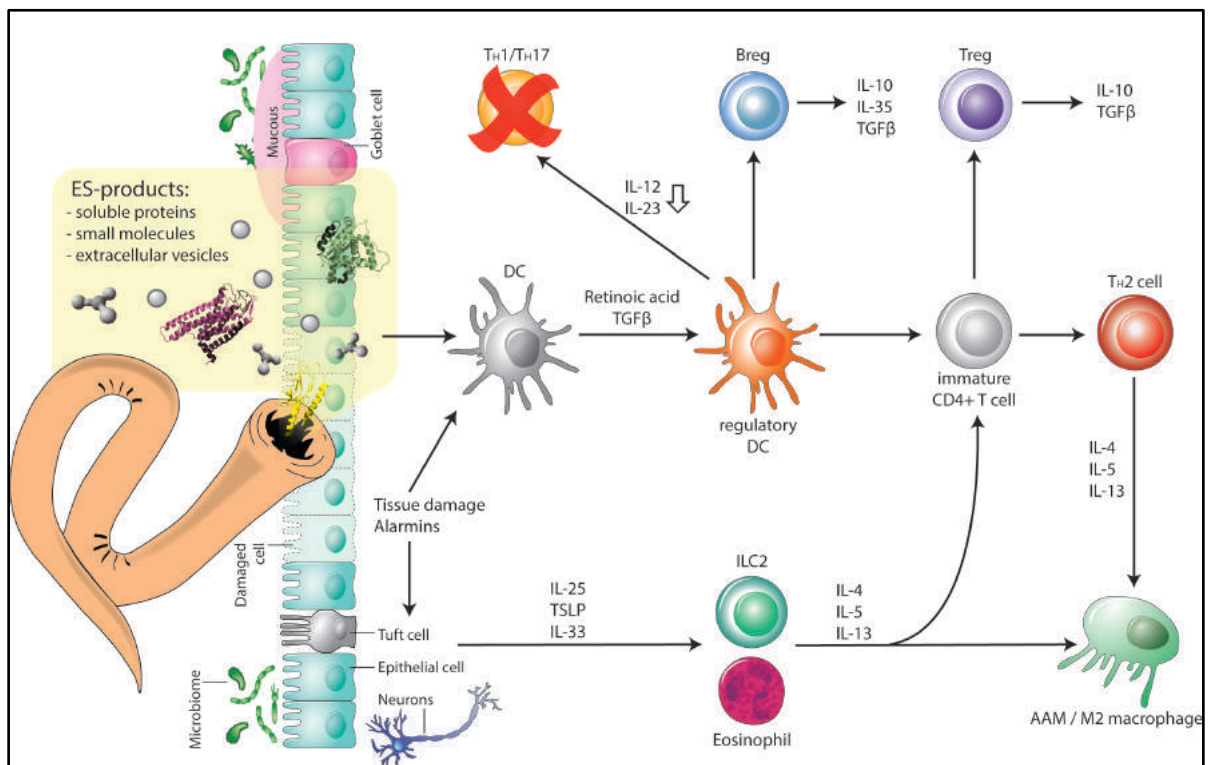
Figure 1-12 Effects of helminths and their ESP on the immune system. Adapted from[156]. Helminths are well known to be potent inducers of T_H2 immune responses but can suppress harmful (allergic) respones and extensive efforts have been made to examine the primary interface between helminths and their hosts. Both, ESP and helminth antigens stimulate receptors, signalling networks and interact with their local micro-environment to orchestrate the initiation of a modified T_H2 response.

The helminth-induced modified T_H2 response is different to the typical T_H2 response seen in allergy, which is defined by the secretion of T_H2 cytokines (IL-4) by activated CD4+ cells[184]. In a helminth-modified T_H2 response, cells secrete IL-13 to stimulate epithelial goblet cells and IL-9 / IL-13 to stimulate mast cells[180]. This is distinguised by the induction of T_H2 lymphocytes that secrete cytokines such as IL-4, IL-5, IL-9, IL-10, IL-13 and are accountable for eosinophil activation, macrophage inhibition and antibody production (Figure 1-12)[180]. These cytokines also induce B lymphocytes to secrete IgE, recruit eosinophils and M2 macrophages.

Chronic helminth-driven T_H2 responses become pathogenic due to excessive immunopathology and ensuing fibrosis[184]. Helminths regulate this response by inducing panoply of immunoregulatory pathways which include the induction regulatory cell populations and associated cytokines and ensures that the infected host does not succumb to excessive immunopathology yet remains functionally immunocompetent. One of the most prominent anti-inflammatory cell types induced by helminths is CD4+ CD25+ FOXP3+ Tregs. Helminth secretions induce immature T cells to become regulatory and express FOXP3 through the TGF-β pathway[185]. Tregs expressing FOXP3 have been shown to be a key evasion mechanism used by helminths to regulate the host's immune system during chronic infections[185]. In a chronic infection, Tregs suppress and dampen the T_H2 response by producing the anti-inflammatory cytokines TGF-β and IL-10 which in turn prevent T_H1 and T_H2 responses[186]. IL-10 has been shown to be important in maintaining chronic infections because it sustains the suppressive Treg function[186]. The gastrointestinal nematode parasite, *Heligmosomoides polygyrus,* and its ESP (HES) have been shown to directly induce Tregs *in vitro* from FOXP3-green fluorescent protein reporter mice[185]. It has also been shown that Tregs induced by HES can suppress allergic

airway disease in mice[187]. Therefore, dissection of the individual molecules that trigger the initiation of this response in the context of helminth protein immunotherapeutics opens up a novel area of drug discovery. Another characteristic feature of helminth-driven immune regulation is the stimulation of M2 macrophages. These cell are a characteristic feature of the polarized T_H2 responses and limit acute tissue damage[188]. At the site of helminth infection, or *in vitro* when exposed to IL-4, these macrophages produce arginase 1, resistin-like molecule alpha (RELM$α$) and Ym1[189]. The functional roles of M2 macrophages are becoming well defined and have been shown to induce effector responses that shape both the innate and adaptive immune system[190].

ESP is a complex mixture composed of vesicles, lipids, proteins, glycans, peptides and small organic molecules[191]. In terms of presenting a safer option for drug development than iatrogenic helminth infections, the use of ESP addresses some of the drawbacks and obstacles currently faced by the use of experimental helminth therapy for treating inflammatory diseases. Identification of novel helminth ESP molecules with anti-inflammatory activities involves delving into the constituents within ESP and teasing them apart to identify defined molecules for drug development. As previously discussed, live helminth therapy is gaining momentum in the medical community but the use of helminth-secreted proteins instead of live helminth infections potentially addresses some of the drawbacks of helminth therapy for inflammatory diseases.

Helminth secreted proteins have been shown to protect mice against inflammatory diseases, presenting a safer option for drug development than experimental human infection with live worms[192]. Dog hookworm, *Ancylostoma caninum* ESP (*Ac*ES) protected mice against TNBS-induced colitis[193] and DSS-induced colitis[194]. *Ac*ES has

40

been shown to prevent weight loss in DSS treated mice, decrease the macroscopic and histological inflammation scores and maintain gut architecture. ESP induced a mucosal T_H2 response and suppressed T_H1 / T_H17 responses in mice. *Ac*ES suppressed DSS-induced colitis by upregulating the secretion of IL-4 and IL-10 from CD4+ T cells. This protection was ablated by heat denaturation and protease digestion of *Ac*ES, an important finding that demonstrates that the protective components are proteins[194]. Levels of pro-inflammatory cytokines associated with pathology were reduced by *Ac*ES treatment in a dose-dependent manner in culture supernatants of stimulated mesenteric lymph node cells. The relative transcription of inducible nitric oxide synthase (iNOS), IL-6, IL-17A and IFN-γ was significantly decreased by *Ac*ES treatment in comparison to phosphate buffered saline (PBS). In contrast, the T_H2 cytokines IL-10 and IL-4 showed a significant increase in concentration in colon lysates when mice were treated with *Ac*ES[194].

1.9 Helminth Recombinant ES Proteins with Anti-Inflammatory Activities

There are many examples of recombinant proteins that have been identified in the last ten years from different helminth species. They have been described in detail in a table focussing on nematode secreted products and recombinant proteins[195].

Nematode	Parasite extract	Disease	Mechanism of action	Citation
Ancylostoma caninum	ES products	DSS-induced colitis	Induce IL4+IL10+CD4+ T cells	196
A. caninum	Soluble proteins	TNBS in Swiss mice		193
Ancylostoma ceylanicum	Somatic extract, ES	DSS colitis in BALB/c mice		197
Trichinella spiralis	Larval extract	DNBS in C57BL/6 mice		198
T. spiralis	ES	DSS colitis in C57BL/6		199

Nematode	Purified protein	Disease	Mechanism of action	Citation
Anisakis simplex	Recombinant MIF homologue	DSS colitis in C57/BL6 mice	Toll like receptor 2	200
Brugia malayi	Cytoplasmic asparginyl-tRNA synthase	T cell transfer model		201
Brugia malayi	CPI-2 or cystatin recombinant cystatin (rBmCys)	DSS colitis in BALB/c mice		202
Brugia malayi	rBmALT-2 recombinant abundant larval transcript 2	DSS-induced Colitis	Blocks antigen processing in mammalian cells	203
Toxascaris leonina	Galectin-9 homologues (Tl-gal)	DSS-induced colitis C57BL/6	Raised TGF-β and IL-10	204

Haemonchus contortus	Galectin Hco-gal-m			205
T. spiralis	53 kDA glycoprotein (rTsP53)		T_H2 immune deviation	206
A. caninum	AIPs tissue metalloproteases (nectrin domain)	Mouse model of asthma		207
Acanthocheilonema viteae	ES-62 glycoprotein	Mouse model of collagen induced arthritis	ES-62 targets IL-17 response	208

Table 2 Nematode secreted products and recombinant proteins used in animal models of disease to highlight their mechanism of action[161].

The *Ancylostoma caninum* transcriptome and *N. americanus* genome has been reported, facilitating the molecular identification and annotation of ES proteins, and to-date approximately 50 % of proteins have no known function[209],[210]. The *Ac*ES proteome was characterised and 105 proteins were identified using combined gel electrophoresis and off-gel peptide fractionation coupled with mass spectrometry[211]. The two most abundant proteins identified in *Ac*ES were structural homologues of the Tissue Inhibitor of Metalloprotease (TIMP) family, named *Ac*-TMP-1 and *Ac*-TMP-2. These proteins were later renamed *Ac*-AIP-1 and *Ac*-AIP-2 because despite possessing a netrin-like domain they do not appear to have TIMP-like activity (suppression of matrix metalloprotease catalytic activity)[212]. These proteins instead appear to have evolved a novel anti-inflammatory function. Recombinant *Ac*-AIP-1 suppressed expression of co-stimulatory molecules and increased DC activation[213]. Mechanistically, the function of *Ac*-AIP-1 and

Ac-AIP-2 still remain unclear but DCs exposed to *Ac*-AIP-1 when co-cultured with splenic T cells induced the differentiation into CD4+ and CD8+ CD25+ FOXP3+ Tregs and produced increased levels of IL-10[213]. In fact, genetic analysis of patients with colitis has shown specific mutations in the *il-10* gene, highlighting the pivotal role that this cytokine plays in the negative feedback required to preserve mucosal homeostasis[214]. Treatment of mice with recombinant *Ac*-AIP-1 protected mice against TNBS-induced weight loss, clinical disease and intestinal histopathology and significantly reduced expression of hallmark T_H1 / 17 cytokines that drive inflammation in human IBD[194]. Administration of *Ac*-AIP-2 to mice in a model of inducible asthma resulted in reduced disease indicators and clinical pathology and improved airway function via decreased expression of activation markers on CD103+ DCs. There was also an increased expression of retinoic acid and expanded Treg numbers in the mesenteric lymph nodes (MLN) of *Ac*-AIP-2 treated mice[194]. Moreover, adoptive transfer of MLN from *Ac*-AIP-2 treated mice to OVA-sensitized mice (that had not been previously treated with *Ac*-AIP-2) after removal of their own MLN resulted in protection against OVA-aerosol challenge, and highlighted a lymphoid tissue conditioning that resulted in long-term protection[207].

Helminths are likely to suppress inflammation by the secretion of multiple immunomodulatory components[207]. In similar fashion to the plasticity of the netrin / TIMP domain in hookworms, there is growing evidence that some cystatin superfamily members secreted by filarial nematodes have acquired novel roles that are independent of cysteine protease inhibition over the course of their evolution[215]. Historically, cystatins are reversible inhibitors of clan A cysteine proteases, that possess the canonical papain-like enzyme inhibitory activity as well as inhibit the catalytically distinct asparaginyl

endopeptidase activity. This dual function assists in inhibition of antigen processing in the MHC II pathway[215]. Not surprisingly, cystatins from various nematode and even trematode helminth species suppress secretion of inflammatory cytokines and promote IL-10 production by macrophages in particular[182]. Cystatin from the filarial nematode *Acanthocheilonema viteae* suppresses inducible colitis and asthma in mice [216] and displayed *ex vivo* bioactivity with human PBMCs from atopic patients with grass pollen allergy[217]. Moreover, oral delivery of *A. viteae* cystatin to mice via continual dosing of transgenic *Lactococcus lactis* prevented the onset of colitis in pigs[218]. Subsequent studies have shown that cystatins from both *Ascaris lumbricoides* and *Brugia malayi* can suppress DSS-induced colitis in mice[219],[202].

1.10 Eukaryotic Recombinant Protein Expression System: *Pichia pastoris*

Even though it is possible to isolate hookworm proteins from somatic extracts[220], it is generally impractical due primarily to the difficulty in obtaining sufficient material[174]. Therefore, to circumvent this problem hookworm proteins can be produced in recombinant expression systems in large quantities. Recombinant protein expression allows the study of purified proteins and site-directed mutants to understand their structure and activity. The information presented here is designed to deliver a concise justification of the decision to use the yeast protein expression system, *Pichia pastoris*. The importance of using a eukaryotic yeast expression system is paramount to ensuring that recombinant proteins, particularly secreted proteins, possess post-translational modifications and transit through the secretory pathway of a eukaryotic cell such that correct folding and disulphide bond pairing occurs.

Arguably, *E. coli* expression systems generate large quantities of recombinant proteins with ease and are inexpensive, rendering this quintessential system optimal for protein production in many ways. Approximately 50 % of all recombinant proteins produced in industry and 70 % in academic research utilise the *E. coli* expression system[221]. Notably, only 30 % of biopharmaceutical proteins are produced in *E. coli*, whereas 50 % are produced in mammalian cell-lines and 20 % in yeast[222].

Nevertheless, when eukaryotic proteins (notably secreted proteins) are made in prokaryotic host systems they are often produced in insoluble form through the formation of inclusion bodies, lack many important post-translational modifications such as glycosylation, and often contain high levels of endotoxins such as LPS[223]. The optimum / gold standard expression system to use for protein expression is a mammalian cell line because of the authenticity of glycosylation (for subsequent therapeutic use in mammalian species) and lack of LPS contamination, but unfortunately yields for foreign (non-mammalian) proteins are frequently lower than those obtained with other expression systems[224]. In response to this, eukaryotic microbes have been used for protein expression because they frequently produce high yields of functional secreted proteins. This is a result of the ability of yeast to grow an order of magnitude more rapidly than mammalian cell line counterparts. Moreover, protein production and method optimisation can be done more promptly and competently in yeast[225].

The two most widely used yeast expression systems are *Saccharomyces cerevisiae* and *P. pastoris*. The annotated genomes of *S. cerevisiae* and *P. pastoris* have been accessible since 1996 and 2009 respectively[226,227]. *P. pastoris* has a lower propensity to hyperglycosylate recombinant proteins which has made it the substantial workhorse for

biotechnology and preferential to *S. cerevisiae*[228],[229]. Challenging proteins successfully expressed in *P. pastoris* include ion channels and recombinant human G protein-coupled receptors[230].

Advantages	Disadvantages
Protein processing Efficient protein folding	Expensive culture media
Extensive post translational modification of proteins	
Easiness to manipulate	Use of methanol as an inducer has safety precautions as it is highly flammable
Endotoxin-free (important for *in vivo* applications)	
Good protein expression yields	
N-glycosylation is more similar to higher eukaryotes than with bacteria or *S. cerevisiae*	Glycosylation is still different to mammalian cells

Table 1-3 The common advantages and disadvantages of the yeast recombinant protein expression system.

The *P. pastoris* recombinant expression system utilises a specific vector designed for cytoplasmic gene expression called pPICZα. *P. pastoris* is a methylotropic yeast which means that it has a strong and tightly regulated gene that codes for alcohol oxidase (AOX1)[231]. As a result, *P. pastoris* is an inducible protein expression system that is under

the control of the addition of methanol. The strong, highly-inducible P_{AOX1} promoter sequence precedes the gene of interest, allowing for inducible expression of the desired protein[232]. Initially, growth on glucose represses the transcription of the AOX1 gene and once the reserve of carbon has been depleted and methanol is added the induction mechanism is activated. The benefit of this two-step process is that the growth and protein production phases are separated by the use of the inducible promoter. The biomass of yeast cells accumulates before protein expression and therefore there is less metabolic burden on the cells which subsequently results in a higher yield of protein produced[232].

The presence of a signal sequence (known as the α-mating factor) on the expressed protein is essential for secretion because it directs the recombinant protein to the secretory pathway[233]. Secreted proteins move across to the lumen of the endoplasmic reticulum where they are subjected to one or multiple post-translational modifications. These include the addition of disulphide bonds to cysteine pairs, protein folding into their native state, as well as *N*- and *O*- glycosylation. Glycosylation is of paramount importance as it is often essential for folding, function and protection against degradation because it affects solubility, charge, immunogenicity, correct cell targeting and the serum half-life of a protein. As previously mentioned, *P. pastoris* does have the propensity to hyperglycosylate recombinant proteins because it produces high mannose glycan structures that covalently attach to the secreted protein and cause adjoining proteins to aggregate together and not adopt their correct three dimensional (3D) structure[234]. Hyperglycosylation is a common problem experienced by users of yeast systems, however it can be circumvented by genetic engineering mutation strategies of troublesome glycosylation sites[233].

P. pastoris also secretes low levels of native proteins, but the secretion of the recombinant protein frequently dominates the protein biomass of the culture medium and is easily separated by affinity-tagged protein purification. There is a polyhistidine tag engineered into pPICZα that has the ability to bind to divalent cations (Ni^{2+}) and facilitates a one-step protein purification process[232]. The desired protein is purified from the culture medium by passing it over a metal binding resin and eluting it with in increasing gradient of imidazole[232].

In summary, *P. pastoris* can secrete large amounts of bioactive, properly folded and post-translationally processed recombinant proteins into the culture medium that can be readily purified. Considering the commercial aspects and clinical translatability of this PhD project, the use of a commercially scalable expression system such as *P. pastoris* was paramount to ensure that it was in-line with biopharmaceutical standards. Furthermore, *P. pastoris* has been used to successfully express large quantities of hookworm recombinant vaccine proteins using current good manufacturing practice (cGMP) for clinical trials, including *Na*-ASP-2, *Na*-GST-1 and *Na*-APR-1[235,236,237].

1.11 Cell-Based Versus Cell-Free Protein Expression Systems

The most common method to produce recombinant proteins is to use cell-based expression systems such as bacteria, yeast, insect, mammalian, or transgenic plants and animals. However, there are many drawbacks of common cell-based expression systems, particularly for high-throughput applications, that necessitate alternate cell-free expression systems[238], as summarised in Table 1-4.

Bacteria	Yeast	Insect and Mammalian cells	Transgenic plants and animals
Inadequate complex protein folding	Inappropriate post-translational modifications	Low protein yield	Lengthy developmental periods
Absence of some post-translational modifications	Cell disruption	Costly media	Convoluted handling
LPS endotoxins			Contamination issues

Table 1-4 Caveats of common cell-based protein expression systems.

Biomedical science is well and truly immersed in the post-genomic era as draft and complete genomes are becoming readily available, and thus there is an increasing need for high-throughput, straightforward and effective protein production systems[238]. The ability to extricate protein expression from the limitations of cell-based systems has given rise to a robust platform for high-throughput cell-free protein expression.
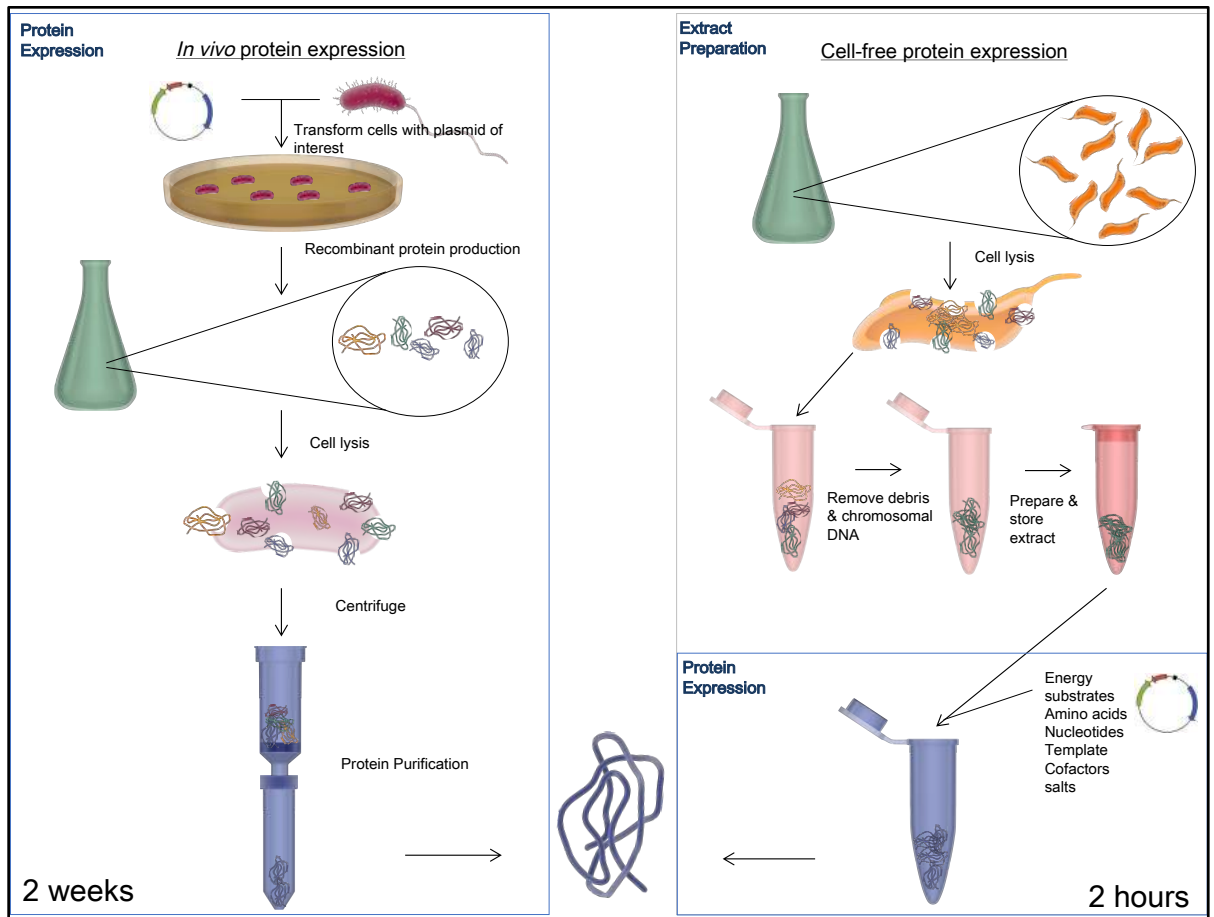
Figure 1-13 Comparison of cell-based and cell-free protein expression systems [239]. The figure highlights the differences, notably time constraints, of both forms of protein expression.

1.12 Cell-Free Coupled Transcription and Translation Systems

Cell-free systems were initially developed as a mechanism to convert sugar to carbon dioxide and ethanol by using yeast extract, and not for recombinant protein synthesis[240]. Subsequently, bacterial cell-free systems were used for decades to study transcription and translation of ribonucleic acid (RNA) and deoxyribose nucleic acid (DNA); this system was the basis of modern cell-free protein expression systems[241].

The central principle of all cell-free expression systems is that a crude extract known as a lysate is produced from cultured cells. Endogenous RNA and DNA are then removed and essential amino acids and energy constituents are added[242]. A coupled reaction occurs when template DNA is added to the supplemented lysate because simultaneous transcription and translation occurs, while a linked reaction occurs when purified mRNA is added[243].

The format of cell-free expression varies from standard batch reactions that are easily scalable, with short incubation times but generate limited protein yields[242], through to integrated dialysis systems which achieve higher protein yields[242]. Cell-free protein synthesis can be easily adapted to synthesise target proteins with radioisotope labels and chaperones[244],[245]. Mechanised high-throughput techniques for cell-free protein expression are being refined as the technology is evolving[246]. There is a diverse range of different cell-free expression systems as summarised in Table 1-4.

Prokaryotic cell-free systems	
Escherichia coli extracts[247]	
Archaeal extracts[248]	

Eukaryotic cell-free systems	
Yeast extracts[249]	
Plant extracts[250]	
	Tobacco BY-2 cell lysates[251]
Insect extracts[252]	
Mammalian extracts	Rabbit reticulocytes extracts[253]
	Cultured cell line extracts[254]
	CHO cell line[255]
	HEK293 cell line[256]
	HeLa cell line[257]

Table 1-5 Cell-free expression systems currently available.

1.13 Protein Expression in a *Leishmania tarentolae* Cell-Free Lysate System

Leishmania tarentolae is a single cell flagellated protozoan parasite that was first used in cell-free protein expression because it possesses complete eukaryotic protein folding and modification capacity[258]. *L. tarentolae* is not pathogenic to humans and its production and cultivation is inexpensive and uncomplicated[254]. An important benefit of *L.*

tarentolae is that it can be manipulated to exclusively translate only the gene of interest encoded by exogenous mRNA[254]. This is due to the addition of a single antisense oligonucleotide targeting the spliced leader sequence that inhibits all endogenous mRNA translation by binding to the 5'-terminus of all protein coding endogenous RNAs[259]. The protein expression vector for this system contains a species independent translational RNA sequence (SITS) that consists of a polymeric extension followed by three short stem hairpins that checks the start codon as well as assists the construction of the ribosomal subunit[260,259]. To date this cell-free system has exclusively been used to examine a finite number of proteins such as Rab GTPases, however it has great potential for broad scale protein production and therefore is a good candidate for high-throughput application[261].

1.14 Project Objectives Underpinning this Thesis

The hookworm genome presents as an untapped resource for pharmacopeia as many of the protective moieties within ESP are likely to be proteins because denaturation of ESP ablated its anti-inflammatory activity in DSS colitis[194,180]. Now, as a result of the proteomic characterisation of *Ac*ES, the publication of stage-specific transcriptomes, genomes of distinct hookworm species and the immunome of *N. americanus*, there is a plethora of new molecules to explore as novel therapeutic biologics[262,209,211,263,264,265,209].

1.14.1 Hypothesis

I hypothesise that anti-inflammatory proteins will be identified from the hookworm recombinant secretome and that these proteins will have potential for development of a novel platform of anti-inflammatory biologics for treating IBD and other diseases that result from a dysregulated immune system.

1.14.2 Aims

The first aim of this project was to use bioinformatics to selected relevant hookworm secreted protein candidates and produce a hookworm (*A. caninum*) recombinant secretome library using the *L. tarentolae* a cell-free lysate expression system. The second aim of the project was to screen the hookworm recombinant secretome in a mouse model of acute colitis to identify proteins with anti-inflammatory properties. The penultimate aim was to produce the most efficacious proteins in a cell-based protein expression system and validate their efficacy in both acute and chronic mouse models of colitis. The final aim was to explore the ability of the lead proteins to suppress inflammatory cytokine production by human PBMCs. Whilst PBMCs are not specifically cells from the gastrointestinal tract, they contain many of the cell types found in the gut and is therefore a good screening tool. Gastrointestinal-helminths are known to affect cytokine expression of cells from peripheral tissues and therefore this is the rationale for using these cells in the high throughput screening assay[207].

Chapter 2

Bioinformatic Analysis and Cell-Free Production of the *Ancylostoma caninum* Secretome

2.1 Introduction

Current IBD therapy can only alleviate active symptoms of the disease and assist patients to enter remission and maintain remission for longer[115]. This is because these treatment options only deliver symptomatic relief but do not alter the course of the disease. There is a serious lack of effective and viable treatment options and a real need for the discovery of novel therapeutic interventions. The hookworm genome presents as an untapped resource for anti-inflammatory molecule discovery. Work delineating the anti-inflammatory constituents of hookworm ESP has shown that many of the protective moieties are likely to be proteins because denaturation of ESP ablated its anti-inflammatory activity[194],[180]. Presently, as a result of the proteomic characterisation of ESP from the dog hookworm *A. caninum*, also known as *Ac*ES, a plethora of new molecules were revealed and can now be explored as potential therapeutics[262],[209],[211],[263],[264],[265],[209]. The therapeutic potential of *Ac*ES proteins is enormous but has yet to be explored in a high-throughput manner. Accordingly, in this project, previously published transcriptomic and proteomic data was used to shortlist candidate proteins to create a final list of *Ac*ES proteins that had the potential to be novel anti-inflammatory therapeutics for IBD.

The first study used to select protein-coding genes for the *A. caninum* secretome library was Mulvenna *et al.,* (2009)[211]. In this study, adult *Ac*ES material was separated with the use of a combination of one-dimensional SDS-PAGE and OFFGEL electrophoresis (Figure 2-1-1). Separation was followed by tandem mass spectrometry (MS/MS), which identified 105 *Ac*ES proteins. Using the MASCOT search engine v4.0, peptide spectra were matched *in silico* to predicted tryptic digest fragments of hookworm open reading

frames (ORF). Mulvenna *et al.*, (2009)[211] constructed a database containing all *A. caninum* DNA sequences present in GenBank™ at the time of the study (138,151 sequences) and used these sequences for MASCOT queries. Protein descriptions were assigned to expressed sequence tags (EST) of the MASCOT peptide hits using BLASTX when the reading frame hit was the same as the MASCOT hit[266]. Protein descriptions or gene ontology (GO) categories were assigned using Interproscan (version 17.0) with default parameters[267]. This work was performed in November 2007 when the NCBI non-redundant (nr) database only contained 130 *A. caninum* proteins that were predicted from cDNA sequences.

Accession	Mowse score	Unique Peps.	Cover (%)	TMW	MW delta	Sig	Glyc. Sites	Description
gi 21808632	112	1	12	19	125	N	N	Ferritin protein 2 [Caenorhabditis elegans]
gi 158018545	75	2	15	41	88	F	1	Aspartyl protease 6 [Caenorhabditis elegans]
gi 29124854	78	4	13	46	98	Y	N	Secreted protein 5 precursor [Ancylostoma caninum]
gi 158009159	57	1	12	49	51	F	2	Secreted protein 6 precursor [Ancylostoma caninum]
gi 158009795	58	1	6	49	51	F	N	Secreted protein 6 precursor [Ancylostoma caninum]
gi 158017414	55	1	11	56	44	F	N	Hyaluronidase [Xenopus laevis]
gi 156184190	92	1	9	27	48	F	1	Secreted protein 4 precursor [Ancylostoma ceylanicum]
gi 158018316	61	1	17	31	29	F	1	Neutrophil inhibitory factor [Ancylostoma caninum]
gi 56771777	93	3	8	46	3	F	N	Secreted protein 5 precursor [Ancylostoma ceyanicum]
gi 6450228	54	1	13	35	8	F	1	Galectin protein 5 [Caenorhabditis elegans]
gi 158007422	70	3	18	55	18	F	1	Secreted protein 4 precursor [Ancylostoma caninum]
gi 59254161	63	1	3	24	11	Y	N	Secreted protein ASP-2 [Ancylostoma ceylanicum]
gi 156183255	74	1	8	32	2	F	2	Hypothetical protein B0035.13 [Caenorhabditis elegans]
gi 157995016	58	1	8	41	-7	N	N	DNAse homolog F09G8.2 [Caenorhabditis elegans]
gi 15028472	268	7	38	20	10	N	N	Platelet inhibitor [Ancylostoma caninum]*
gi 158002424	52	1	4	25	12	F	N	Activation-associated secreted protein [Onchocerca volvulus]
gi 157988383	117	5	20	31	-7	Y	N	Lysozyme protein 8 [Caenorhabditis elegans]
gi 157991648	127	5	22	31	-7	Y	1	Lysozyme protein 8 [Caenorhabditis elegans]
gi 85672997	106	2	15	31	-7	F	1	Lysozyme protein 8 [Caenorhabditis elegans]
gi 158007955	62	2	15	42	18	F	N	C-type lectin (clec-63) [Caenorhabditis elegans]
gi 158009220	70	5	35	46	25	F	N	Secreted protein 5 precursor [Ancylostoma caninum]
gi 85673077	104	6	18	19	-5	F	N	Vitellogenin structural genes protein [Caenorhabditis elegans]
gi 22347361	151	9	40	16	-3	Y	1	Putative tissue metalloprotease inhibitor Aca14 [Ancylostoma caninum]
gi 59631715	75	2	8			N	N	ND
gi 14289448	207	9	39	16	-6	Y	1	tissue metalloprotease inhibitor [Ancylostoma caninum]
gi 16924887	45	2	20	14	-4	F	N	Transthyretin-like protein T07C4.5 [Caenorhabditis elegans]
gi 85672867	60	1	4	13	-3	N	1	Excretory-secretory protein 1 [Ancylostoma ceylanicum]
gi 158006869	63	2	17	19	-9	Y	N	Putative ES protein F7 [Ostertagia ostertagi]
gi 158011916	49	1	3	15	-5	F	N	Transthyretin-like protein 3 precursor [Radopholus similis]

Figure 2-1 SDS-PAGE of AcES Stained with coomassie brilliant blue. MS/MS was performed on excised gel pieces (horizontal black lines on gel) post-fractionation; the description column refers to the most significant NCBI Blast hit of each identified protein at the time of publication[266]. "Sig" refers the presence or absence of a signal peptide according to SignalP software. Taken from[211].

The second study used to select protein-coding genes for the *A. caninum* secretome library was Datu *et al.*, (2008)[265]. In this study, fluorescein-conjugated bovine serum albumin (FITC-BSA) was added to *A. caninum* free-living larvae (L3) that were activated

58

in vitro to mimic the transition from free-living to parasitic larvae stages. This process was visualised by observing the accumulation of FITC-BSA in the gut of actively feeding L3 (Figure 2-2).
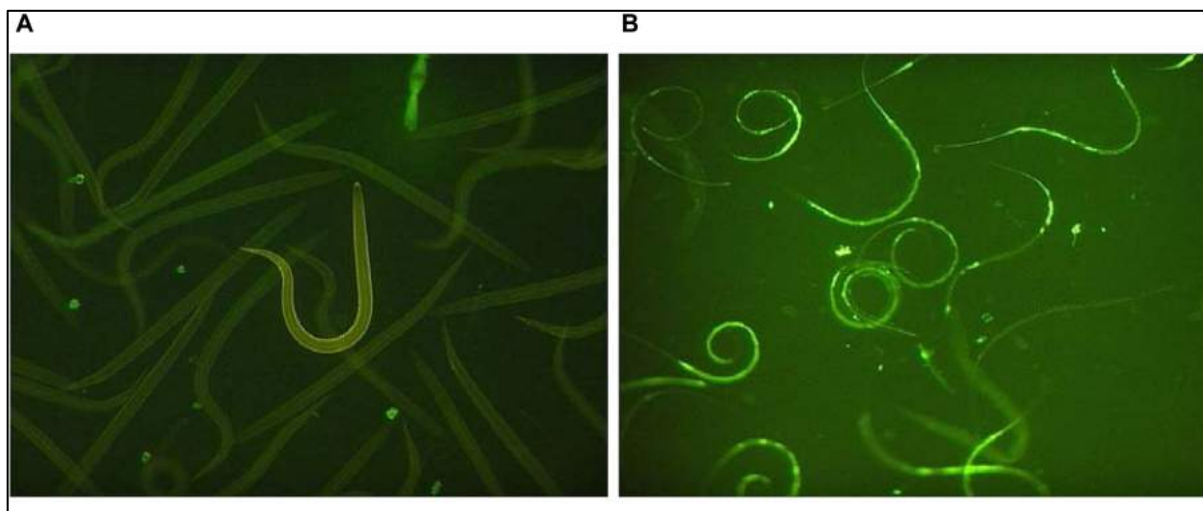
Figure 2-2 A. caninum L3 ingesting fluorescein-conjugated bovine serum albumin (FITC-BSA) following serum activation in vitro. A) Non-activated L3 do not ingest FITC-BSA, B) serum-stimulated L3 ingest the dye and exhibit fluorescence in the gut. Taken from[265].

Differentially transcribed mRNAs were identified by suppression subtractive hydrisation (SSH) after the L3 were serum activated and then analysed on a custom oligonucleotide microarray. These arrays were printed with SSH ESTs that were verified against publically available *A. caninum* ESTs in GenBank™ (2008) and WormBase ParaSite (www.wormbase.org) via BLASTx through NCBI and WU-BLAST[266]. Contigs were mapped to GO terms based on sequence similarity using the BLAST2GO platform which compared the contigs with sequences available in several databases including WormBase ParaSite and Uniprot[268].

To date, the ESP proteome of hookworm L3 has not been reported due to the difficulty in obtaining sufficient quantities of protein from hookworm L3 to be characterised by MS/MS. As such, I chose to source mRNAs encoding important ESP proteins from the Datu *et al.,* (2008)[265] study as a surrogate for secreted proteins given the emphasis on identification of genes involved in parasitism. This process identified protein-coding genes whose expression was significantly up-regulated upon penetration of the host by the infective larval stage of *A. caninum*, which I hypothesised are likely to be involved in host : parasite immunological interactions and therefore may have potential anti-inflammatory properties. Moreover, some of the most highly upregulated genes in this dataset have been linked to abundantly expressed L3 ESP proteins, including *Ac*-ASP-1[269], *Ac*-ASP-2[270], and *Ac*-MTP-1[271],[272].

This chapter outlines the experimental protocols and procedures used throughout the course of this section of the thesis in line with the research aims. In addition, this chapter presents the results and discusses the experimental strategy, statistical and bioinformatics workflows for the project. Research aims are described below.
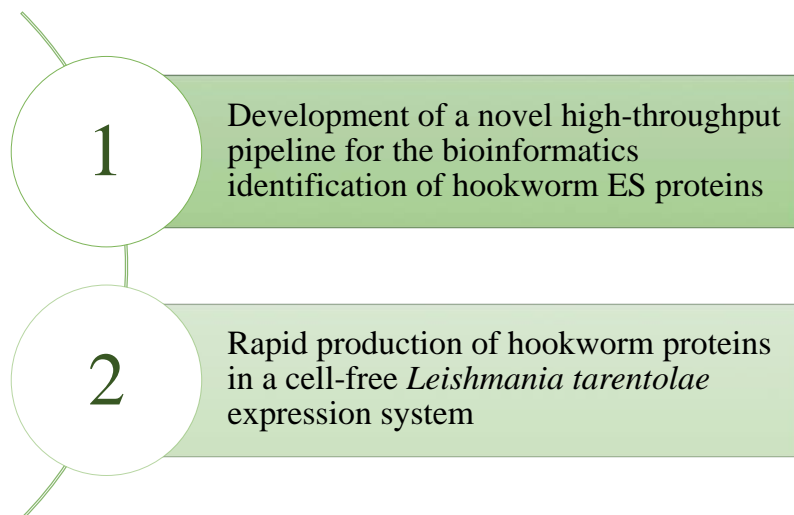
Figure 2-3 Research aims of chapter 2.

The basic schematic below was followed for the experimental workflow of chapter 2.
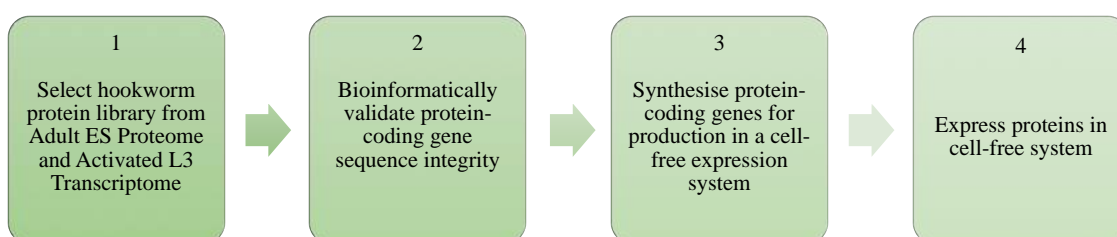
Figure 2-4 Schematic representation of the experimental workflow of chapter 2.

2.2 Materials and Methods

2.2.1 Bioinformatic Workflow for the Selection of Protein-Coding Genes Identified in Previous Studies

Scope: This procedure covers the generation of a list of protein-coding genes for cell-free expression constructed from two input datasets - the adult ES proteome and the activated L3 transcriptome - and the bioinformatic workflow employed to validate the sequence integrity (Figure 2-5).
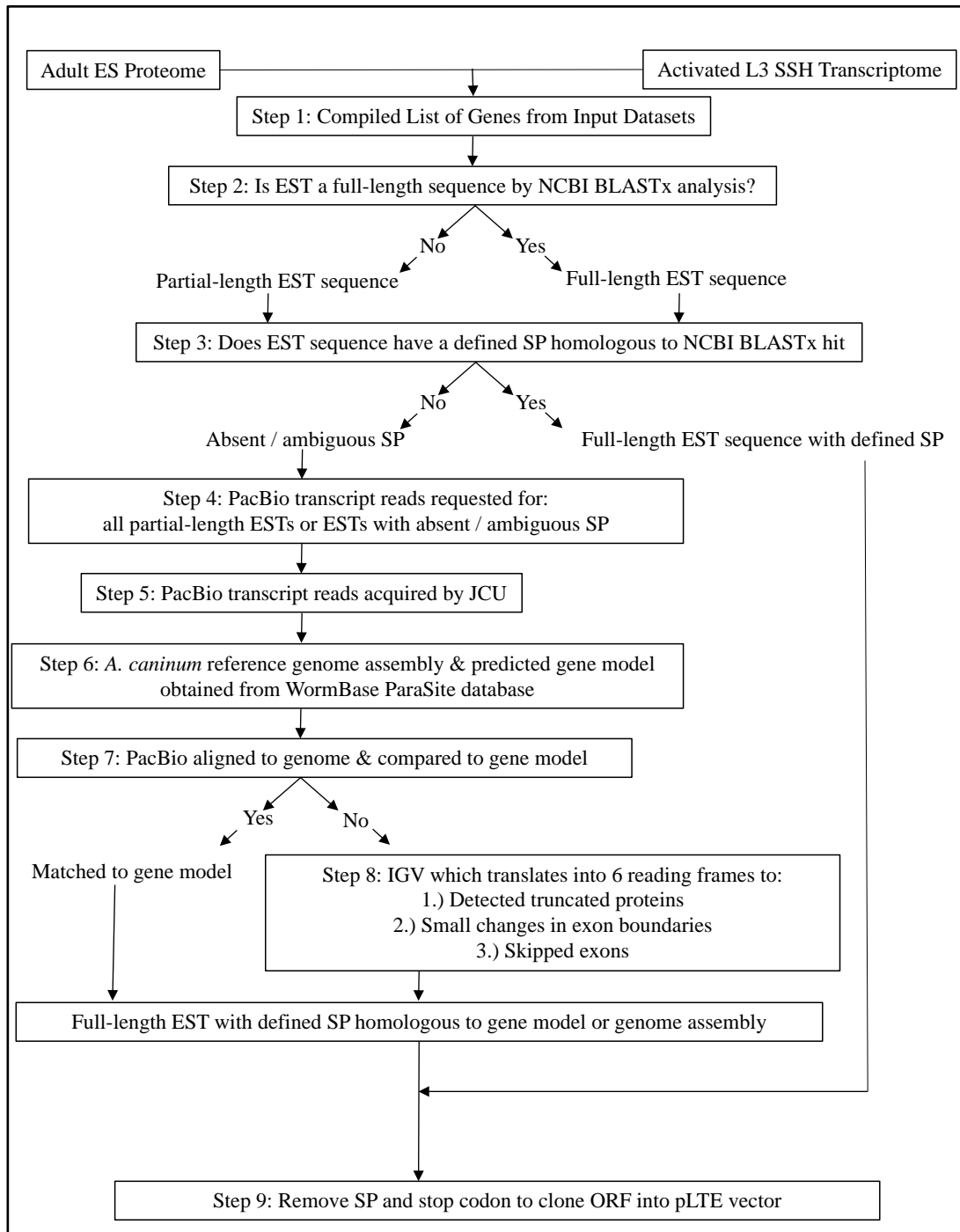
Figure 2-5 Bioinformatic workflow diagram. This workflow was used to compile the list of full-length AcES protein-coding genes from input datasets Mulvenna et al., (2009)[211] and Datu et al., (2008)[265]. The Integrative Genomic Viewer (IGV) was software used to visualise and compare large genomic or transcriptomic datasets against publicly available genomes[273]. PacBio refers to Pacific Biosciences long read sequencing

technology used to sequence the draft A. caninum genome (unpublished, Dr Makedonka Mitreva, Washington University at St Louis).

2.2.2 Molecular Cloning of ORF into Cell-Free Lysate Expression Plasmid

The ORF sequences that contained either *Kpn*I (ggtacc) or *Hind*III (aagctt) endonuclease restriction sites were analysed by New England Biolabs NEBcutter V2.0 tool with default parameters (http://nc2.neb.com/NEBcutter2/). ORF sequences that contained internal *Kpn*I and *Hind*III restriction sites were removed to facilitate cloning into the plasmid vector, pLTE eGFP (Figure 2-6). Protein-coding ORF sequences were sent to Protein CT Biotechnologies in China and genes were synthesised.
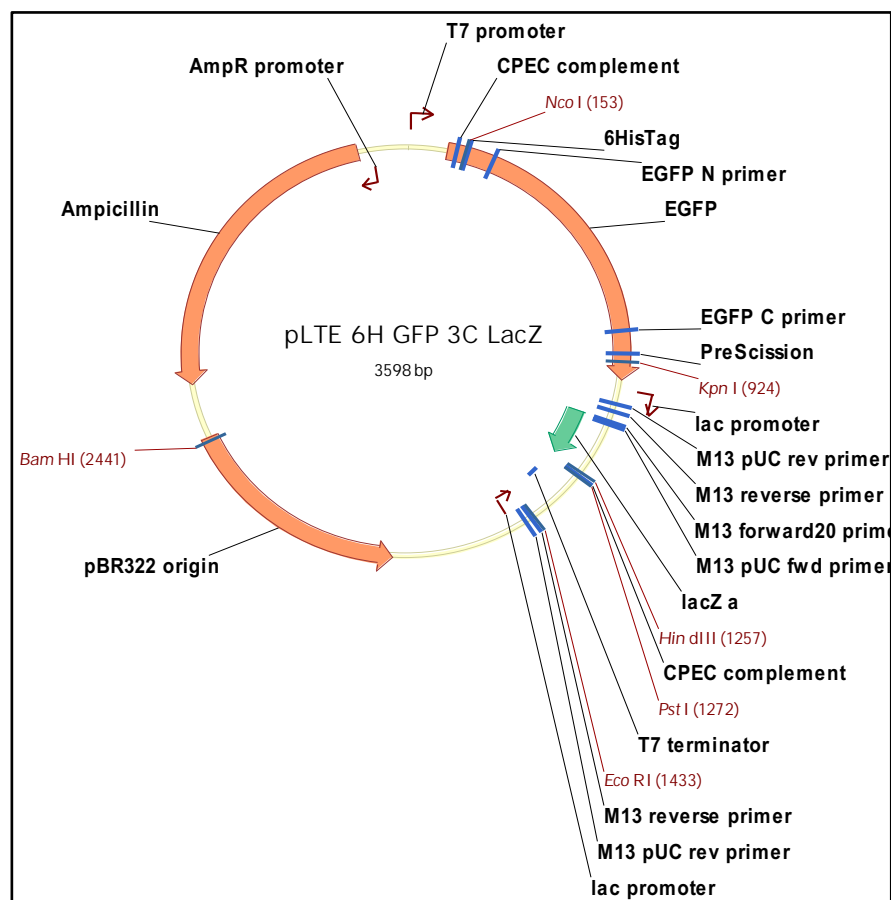
Figure 2-6 pLTE GFP 3C LacZ cell-free expression plasmid vector map.

Plasmid name:	05711 pLTE GFP 3C
Resistance:	Ampicillin
Tags:	N-terminal-GFP followed by PreScission protease site
Cloning strategy:	Remove signal peptide In-frame cloning restriction enzyme digest sites: *Kpn*I (924) and *Hind*III (1272) N-terminal GFP is separated from ORF by D3 protease cleavage site.

Table 2-1 Protein CT Biotechnologies cloning strategy of ORFs into the cell-free lysate plasmid 05711 pLTE GFP 3C.

2.2.3 Plasmid Propagation and Purification

The synthesised plasmid DNA vectors from 114 protein-coding ORF inserts were shipped from Protein CT Biotechnologies to James Cook University (JCU), Cairns, and transformed into calcium competent *E. coli* TOP10 cells by heat shocking. The plasmid was propagated by seeding the transformed cells onto LB / agar / ampicillin (50 μg/mL) plates and incubated overnight at 37 °C. Individual colonies were used to inoculate fresh LB / ampicillin (50 μg/mL) media and incubated overnight at 37 °C. The plasmid DNA was purified using QIAGEN® Plasmid Plus Mega kit (12981) as per the manufacturer's protocol and the concentration of the purified DNA (ng/μL) was ascertained using a Nanodrop™ 2000c Spectrophotometer (ThermoFisher Scientific™).

2.2.4 *Leishmania tarentolae* Expression (LTE) Protocol

Sufficient lysate (600 μL) for each recombinant protein was prepared to enable intraperitoneal (i.p.) injection of 100 μL LTE lysate to each of 5 mice. Lysate reactions were conducted in RNase / DNase-free 96-well culture plates. Four hundred and twenty (420) μL of lysate was added to 1 μg DNA (50 μg/mL), 1.5 μL RNAse OUT ribonuclease inhibitor (final concentration 0.25 %) (Invitrogen™ 10777019) and topped up to a final volume of 600 μL with Type 1 ultrapure H_2O.

The relative fluorescence units (RFU) produced by translation of eGFP-fused protein was continuously monitored for 2 hours on a POLARstar® Omega Plate Reader Spectrophotometer (BMG LABTECH) with a wavelength range of 485 nm excitation and 520 nm emission. The lysate reaction was centrifuged for 1 minute at 300 *g* and the pellet was discarded. Ten (10) μL of the supernatant was loaded onto a 12 % SDS-PAGE gel in an XCell SureLock™ Mini-Cell Electrophoresis System (ThermoFisher Scientific™) and subjected to 140 volts for 30 minutes using a PowerPac™ Basic Power Supply (BIO-RAD™). The fluorescence signal emitted by the eGFP-tagged recombinant protein band was visualised using a BIO-RAD™ VersaDoc Imaging System with the wavelength range of 485 nm excitation and 520 nm emission.

2.3 Results

2.3.1 Bioinformatic Workflow for the Selection of Protein-Coding Genes Identified in Previous Studies

The bioinformatics workflow summarised in Figure 2-5 was used to select and verify the protein-coding sequence integrity of 114 *Ac*ES protein-coding genes.

Dataset 1 Input: Adult ES Proteome - Mulvenna *et al.,* (2009)[211]

Protein-coding genes identified in dataset 1 were based on their predicted GO from the NCBI database (2007) (Table 2-2). The rationale behind selection of these proteins was previous evidence of immuno-regulatory properties or novel proteins of unknown function, and included protease inhibitors, proteases, lysozyme-like proteins, sperm-coating protein (SCP)-like extracellular proteins (also known as SCP/Tpx-1/Ag5/PR-1/Sc7 or SCP/TAPS), transthyretin (TTR)-like proteins, lectins and proteins of unknown function[194],[274],[275],[276],[277],[278]. Proteins with a predicted GO from NCBI database 2007 that indicated no clear role in suppressing inflammation were excluded from further analysis[279].

Gene Ontology	Accession number	Top BLASTX hit (bit score >30) 2007
Metalloprotease inhibitors	gi 22347361	Putative tissue metalloprotease inhibitor Aca14 (*A. caninum*)
Lysozyme-like	gi 157991648	Lysozyme protein 8 (*C. elegans*)
SCP/TAPS	gi 15028472	Platelet inhibitor (*A. caninum*)
ES proteins of unknown function	gi 85672966	Excretory-secretory protein (*Ancylostoma ceylanicum*)
Transthyretin-like proteins	gi 16924887	Transthyretin-like protein T07C4.5
Lectins	gi 158007955	C-type lectin family member (clec-63) (*C. elegans*)
Proteases	gi 14318583	Zinc metallopeptidase (*A. caninum*)
Miscellaneous	gi 158014078	Lipid-binding protein (*C. elegans*)

Table 2-2 The GO categories from dataset 1 included in the selection criteria for cell-free protein expression. An example protein from each category is provided[266].

Dataset 2 Input: Activated L3 SSH Transcriptome - Datu *et al.,* (2008)[265]

Protein-coding genes were identified at the mRNA level in dataset 2 based on upregulation at the mRNA level in serum-activated L3 (Table 2-3). The most highly expressed mRNAs were prioritised according to the Log2 signal intensity detected by SSH. The selection criteria excluded all mRNAs that were down-regulated upon serum stimulation.

Gene Ontology Category	Gene Name	GenBank™Accession numbers	Description
SCP/TAPS	Ac_SSH_C_0042_A	No accession number	PRP superfamily
Highly up-regulated in Activated AcL3	Ac_SSH_C_0032	BQ667276	Novel (SP)
Metalloproteases	Ac_SSH_C_015	AAK62032	*Ac*-MTP-1
Cysteine proteases	BQ125325	CAB03209	Hyp. protein m04g12.2
Aspartyl proteases	Ac_SSH_S0226	CAE66088	Hyp. protein cbg11305
Serine proteases	BE352528	AAH11328	Mast cell protease 7

Table 2-3 The GO categories from dataset 2 included in the selection criteria for cell-free protein expression. An example of a selected protein from each category is provided.

The NCBI reference database has been vastly improved and expanded due to advances in deep sequencing technologies and bioinformatic analyses since the Mulvenna *et al.,* (2009)[211] and Datu *et al.,* (2008)[265] studies were conducted. In these studies, protein-coding genes were predicted using bioinformatics software compared each read to gene models from other parasitic and free-living nematodes such as *B. malayi* and *Caenorhabditis elegans* respectively

(https://parasite.wormbase.org/Brugia_malayi_prjna10729/Info/Index/),

(https://www.pacb.com/auto_tags/c-elegans/).

Since these initial studies were conducted more than 1.5 million ESTs have been generated from different developmental stages of *A. caninum*[262]. I therefore conducted more up-to-date blast comparisons of the selected ESTs against current databases and this yielded more accurate predicted gene ontologies. One hundred and seventy-four protein-coding genes were selected in step 1 as per the bioinformatics workflow.

Secondly, the NCBI BLASTx tool, using default parameters of the nucleotide sequence database (nr/nt) was used to establish whether the 174 selected ESTs were indeed full-length (https://blast.ncbi.nlm.nih.gov/Blast.cgi?PAGE_TYPE=BlastSearch). The individual translated sequence queries were searched against the up-to-date protein databases to ascertain if sequences were full-length by comparison to the top BLAST hits. It was evident that some of the assembled nucleotide sequences appeared to be truncated at the 5' end or there was an observed reading frame shift and therefore the full-length protein-coding gene was not present; as a result, some of these proteins were flagged as partial-length EST sequences.

As per step 3 of the bioinformatics workflow process, each EST sequence was queried for the presence of a defined N-terminal signal peptide (SP) by comparison to homologous sequences in NCBI (2016). SPs direct a protein to be transported through the secretory pathway and outside the cell. However, in cell-free recombinant protein engineering SPs are redundant because there is no facility for directing sequences through the secretory pathway. Furthermore, SP's are hydrophobic, to facilitate translocation through membranes of the various organelles and the cell itself, and this is an undesirable attribute in recombinant protein expression where soluble proteins are required. The presence, location and cleavage site of an N-terminal SP was predicted for each query EST using SignalP 4.1 Server with default parameters (http://www.cbs.dtu.dk/services/SignalP/). Query EST sequences with close homologues that contained SPs proceeded to step 9. Any query EST sequence without an obvious SP proceeded to step 4.

As per step 4 in the bioinformatics workflow process, the partial-length transcripts (without a defined start or stop codon or with an ambiguous SP status) were mapped to PacBio Isoseq sequencing Reads of Insert (RoI). This data was acquired through a collaboration with Dr Makedonka Mitreva at Washington University School of Medicine in St. Louis, U.S.A. PacBio IsoSeq sequencing technology generates long sequencing reads that are up to 10 kilobyte with low systematic bias and a high consensus accuracy (https://www.pacb.com/products-and-services/)[280]. PacBio reads that mapped to the partial-length *A. caninum* ESTs were extracted. Query ESTs were mapped against the *A. caninum* reference assembly and gene models using HISAT2 (https://bio.tools/HISAT2). The transcript consensus sequences are available at http://nematode.net[262]. High quality PacBio reads were extracted from *A. caninum* transcript data and were mapped to the

71

same reference. Lists of the *A. caninum* PacBio RoI that mapped to those genes identified by the ESTs were built and the FASTQ data was extracted.

In step 5 of the bioinformatics workflow, PacBio reads for 11 of the 18 protein-coding genes of interest were obtained. The *A. caninum* reference genome assembly was obtained from WormBase ParaSite (version: WBPS11 – WS265– A_caninum_9.3.2.ec.cg.pg) and contained 25,339 contigs (step 6 of the bioinformatic workflow).

In step 7, the PacBio reads were aligned to the reference genome using STAR transcriptome aligner (STAR_2.5.2b) with default parameters (https://github.com/alexdobin/STAR)[281]. The predicted gene model was obtained from WormBase ParaSite (version: WBPS11 – WS265) which contained 30,198 predicted transcripts (https://parasite.wormbase.org/Ancylostoma_caninum_prjna72585/Info/Index/). IGV software (version 2.3.72)[273] was used to view the alignments and further translate the PacBio reads into all 6 reading frames which were subsequently compared to the predicted WormBase ParaSite gene model alignments (https://software.broadinstitute.org/software/igv/RelNotes2.3.x).

In step 8, in more than 50 % of cases the PacBio read transcript sequence did not match the gene model (Figure 2-7, Figure 2-8, Figure 2-9, Figure 2-10). IGV software images displayed are examples of discrepancies that were detected between the WormBase ParaSite predicted gene model and the actual PacBio read transcripts. These

discrepancies included the detection of truncated proteins that were shorter than the

transcript, small changes in exon boundaries, skipped exons and new exons.
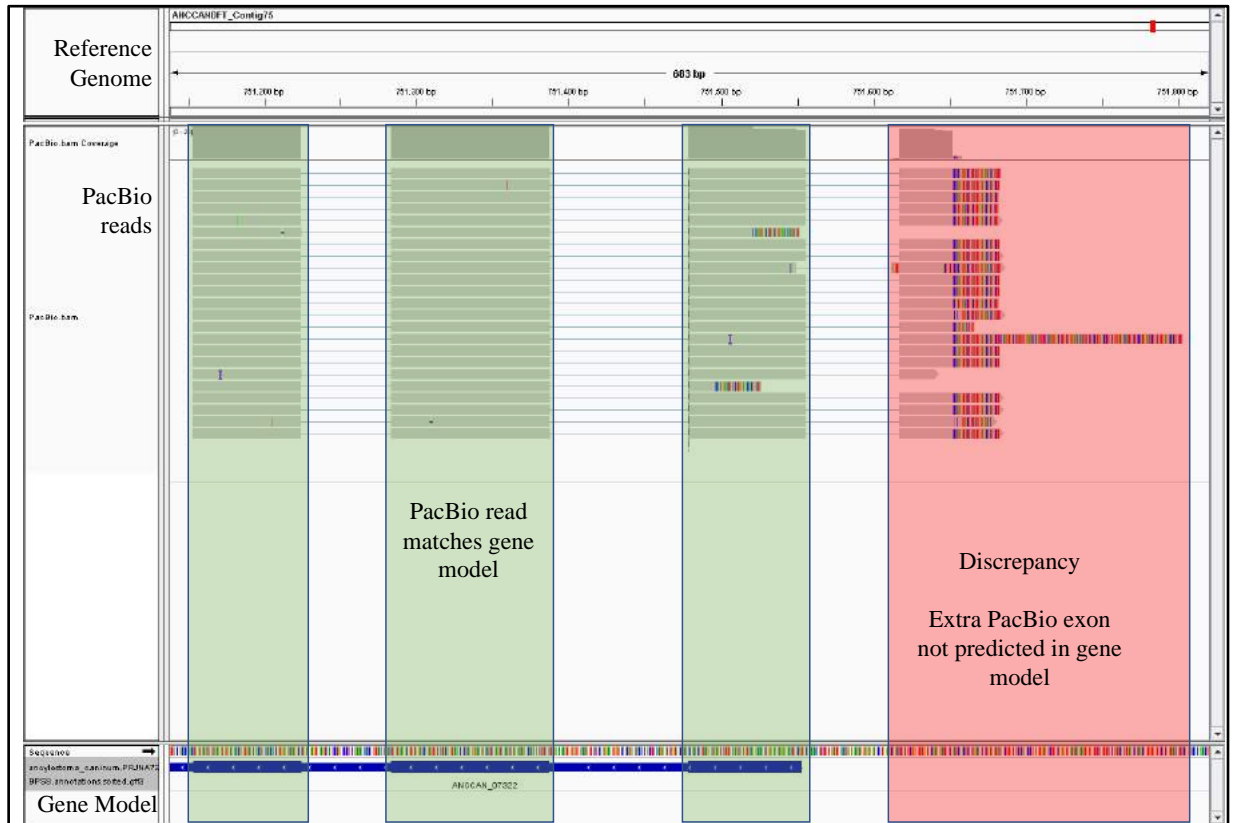
Figure 2-7 IGV image displaying the alignment of the reference A. caninum genome, PacBio reads and the gene model. Each horizontal row represents a single PacBio read aligned to the reference genome. This figure highlights an example of a discrepancy of an extra PacBio exon not predicted in the gene model.
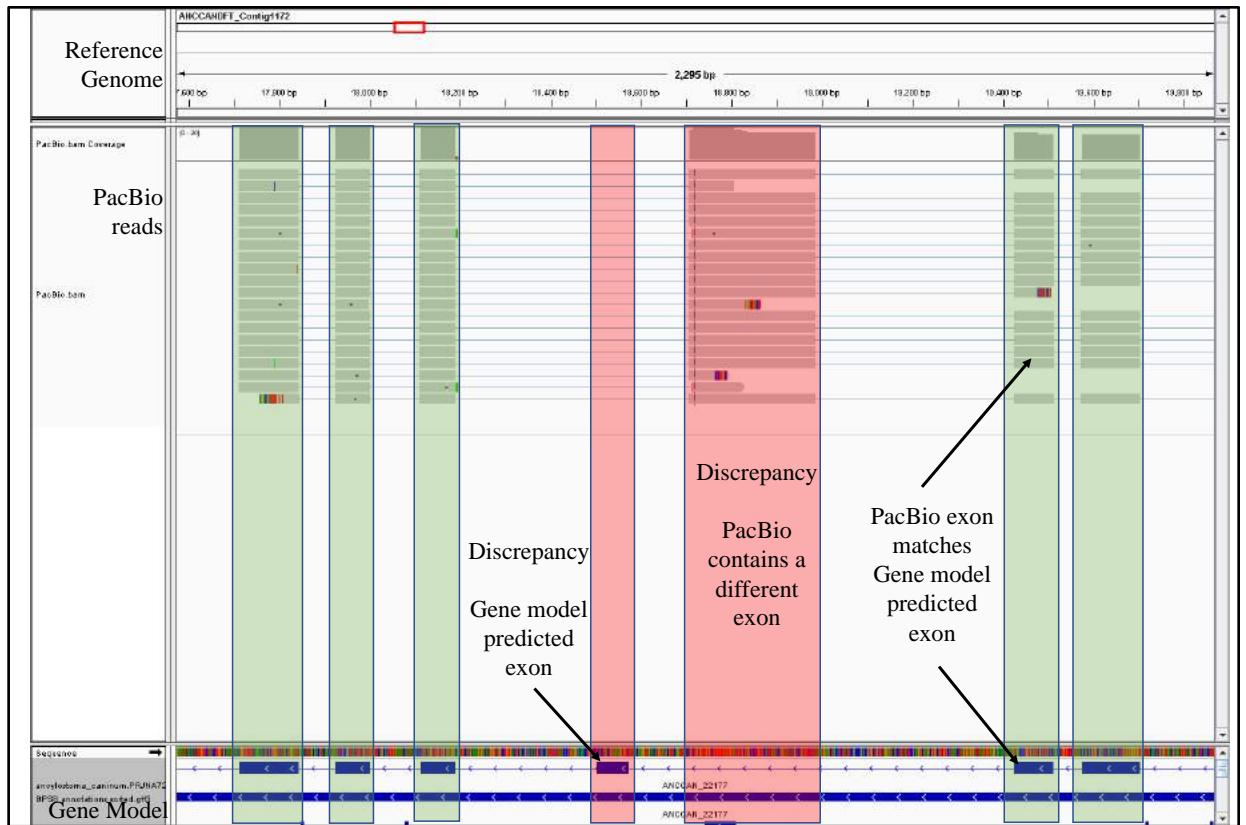
Figure 2-8 IGV image displaying the alignment of the reference A. caninum genome, PacBio reads and the gene model. This figure highlights an example of a discrepancy between the predicted gene model exon and the PacBio read that contained a different exon.
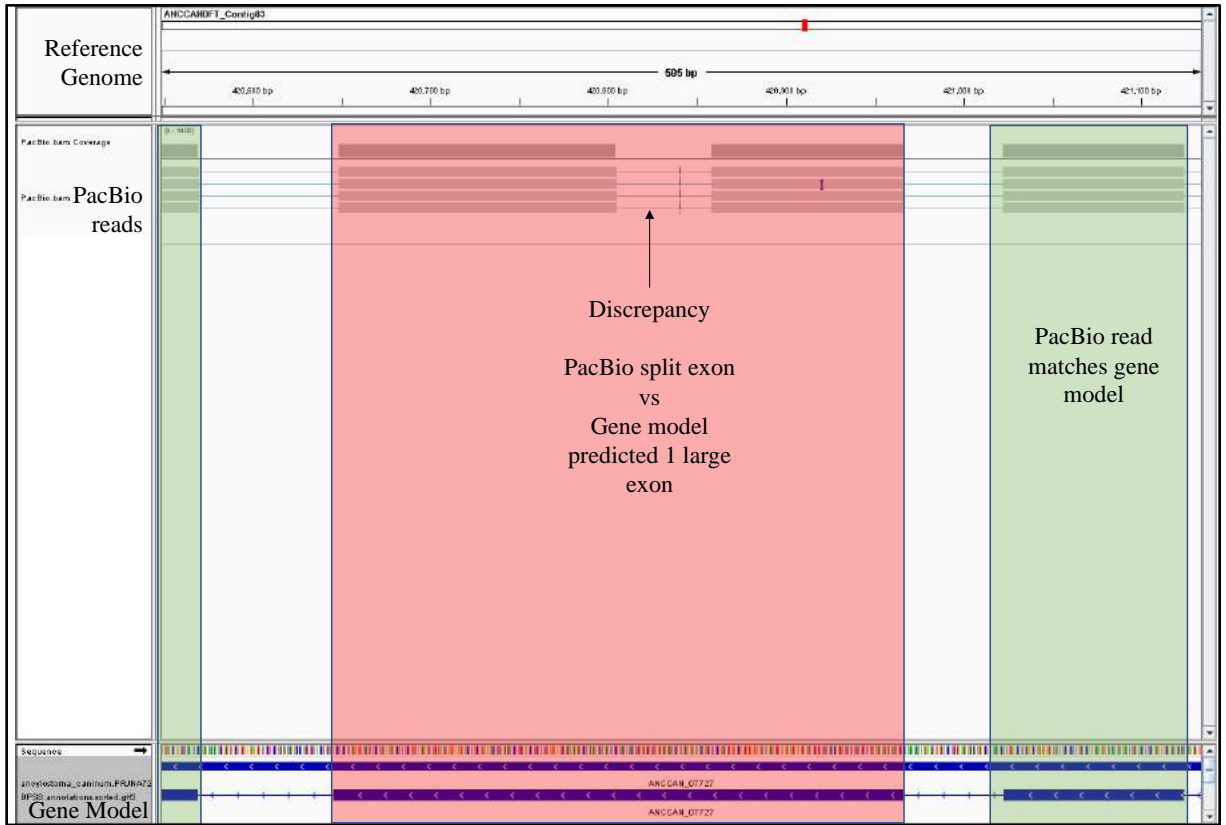
Figure 2-9 IGV image displaying the alignment of the reference A. caninum genome, PacBio reads and the gene model. This figure highlights an example of a discrepancy between the single large exon predicted by the gene model versus the PacBio read that splits a predicted single exon into two exons.
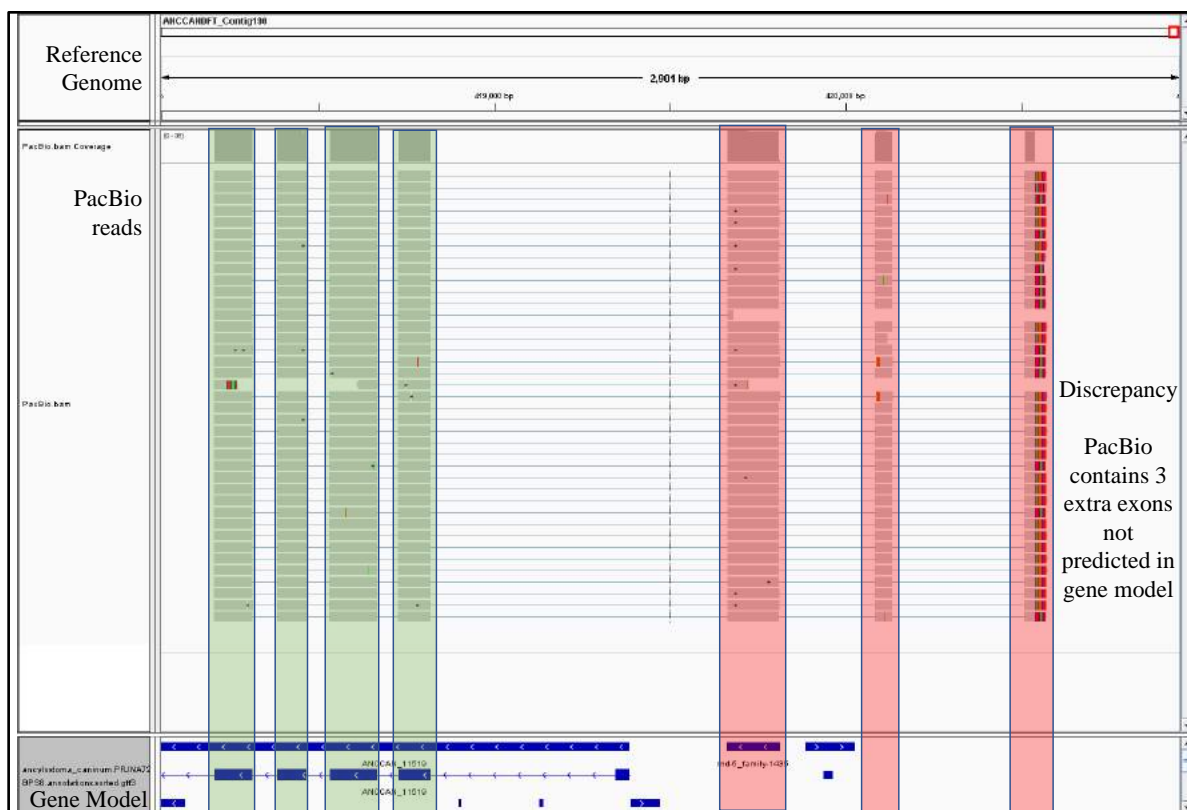
Figure 2-10 IGV image displaying the alignment of the reference A. caninum genome, PacBio reads and the gene model. This figure highlights an example of a discrepancy where the PacBio read contained three extra exons that were not predicted in the gene model.

After verification of the location of the start codon, SignalP online software was employed to identify whether the start codon was followed by a SP. If the start codon was not followed by an SP, then all six frames were examined to deduce if there was a change in the ORF to locate an SP. The location of the stop codon was determined and untranslated regions (UTRs) were also excluded. The final full-length protein-coding sequences were taken forward to step 9, and any identified SP and stop codons were removed from the corresponding nucleotide sequences to generate ORFs for cloning into the plasmid vector for cell-free protein expression.

A list of *Ac*ES protein-coding genes was compiled from the two input datasets - Mulvenna *et al.,* (2009)[211] and Datu *et al.,* (2008)[265] - based on predicted gene ontologies (Appendix 1). The GenBank™ accession numbers, top NCBI BLASTx hits (2016), identity coverage of homologues, and Pfam conserved domain accession numbers are provided in the appendix for further reference.

2.3.2 Cell-Free Lysate Protein Production in the LTE System

Protein CT Biotechnologies synthesised and ligated the requested protein-coding ORF sequences into the pLTE vector but 6 % were not synthesisable (7 of 114). The pLTE DNA was propagated and cell-free lysate protein expression was optimised at JCU. A further 6 % of the pLTE plasmids did not generate expressed protein after optimisation of lysate reaction conditions (6 of 107). eGFP-fused lysate protein expression was monitored in relative fluorescence units (RFU) over time on a POLARstar® Omega Plate Reader Spectrophotometer (Figure 2-11).
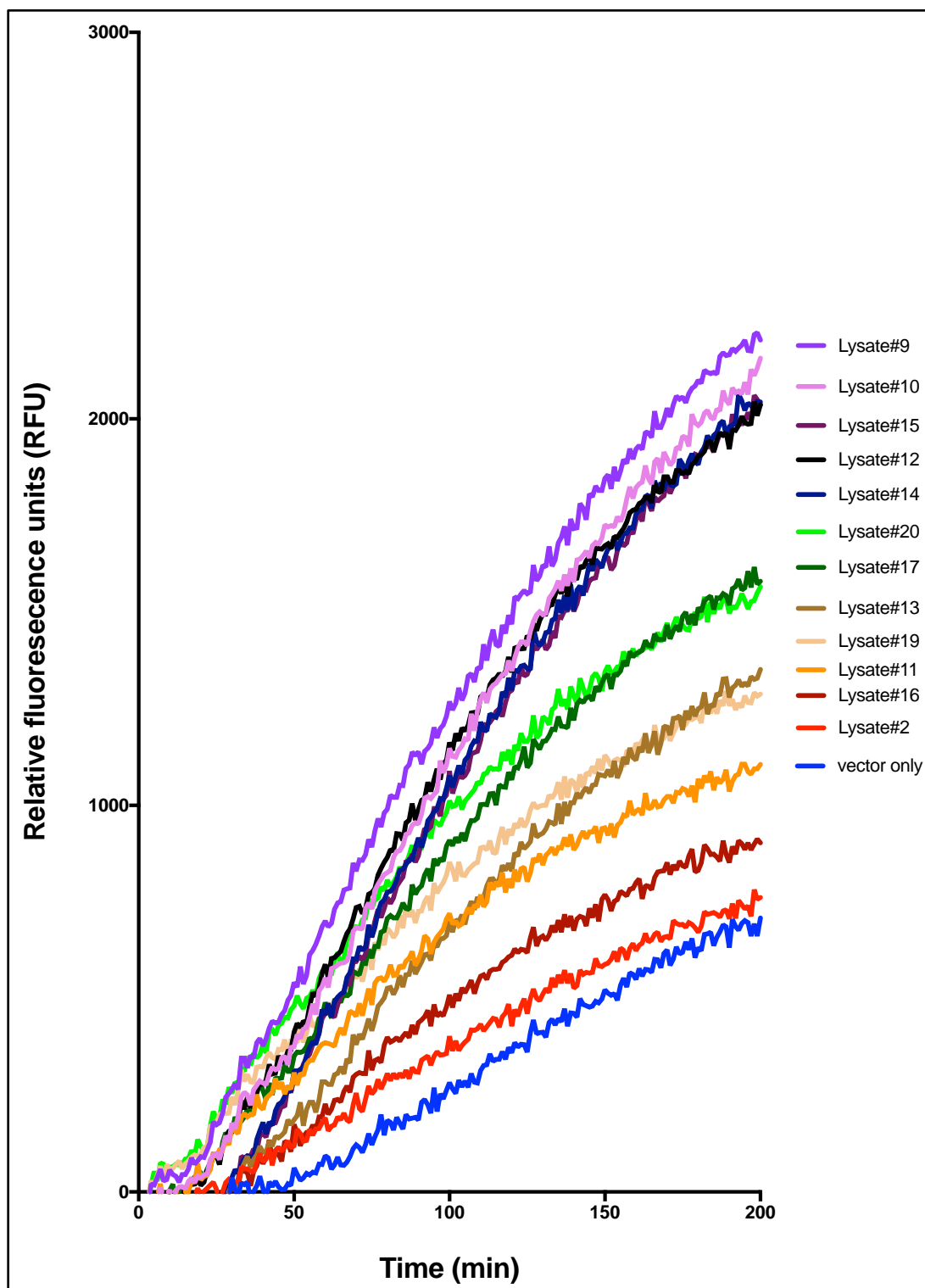
Figure 2-11 Detection of eGFP-expression from a selection of the 101 LTE fusion proteins. Expression was measured in relative fluorescence units (RFU) over time of the reaction in minutes a wavelength range of 485 nm excitation and 520 nm emission.

Protein expression was further validated by SDS-PAGE electrophoresis of the non-denatured cell-free lysate. Fluoresceinated proteins were visualised using the 485 nm excitation to 520 nm emission filter on a BIO-RAD™ VersaDoc Imaging System (Figure 2-12).
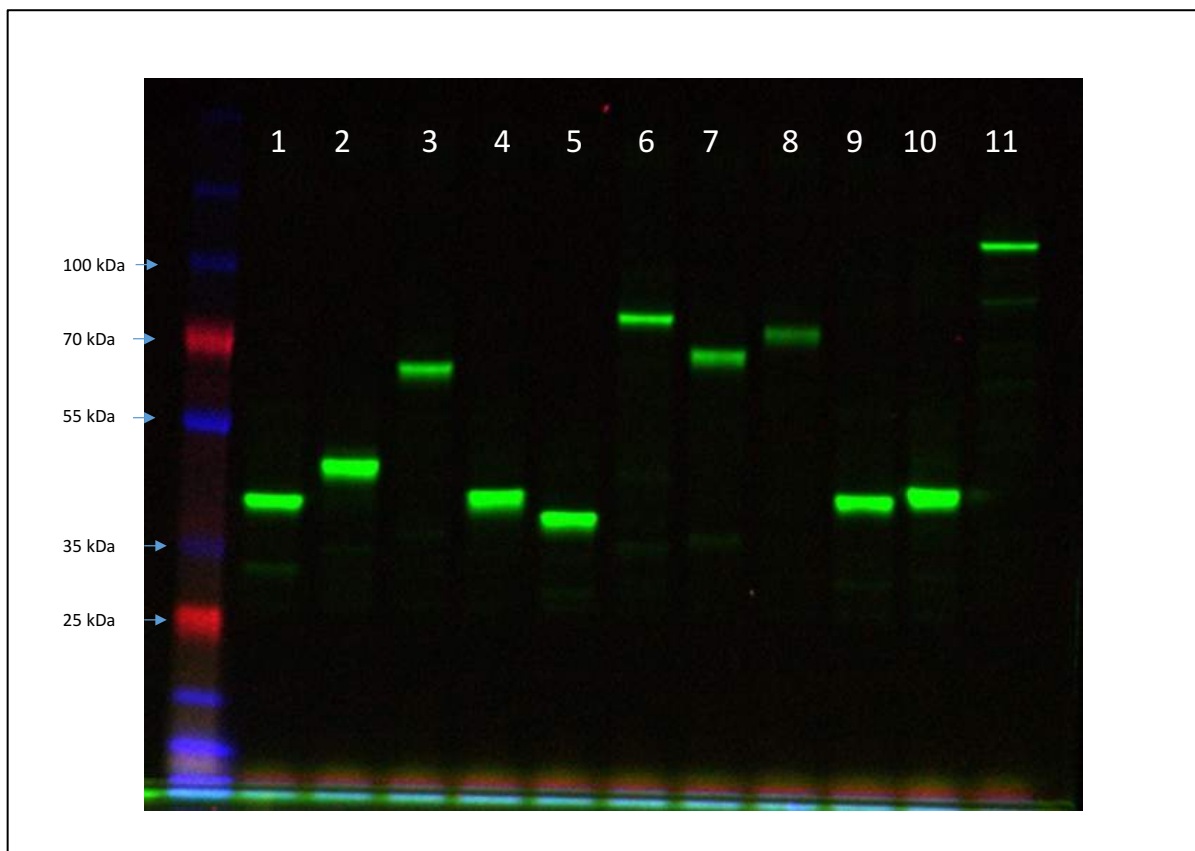
Figure 2-12 Fluorescence image displaying select eGFP-labelled lysate proteins expressed in the LTE cell-free expression system. SDS-PAGE gel visualised at 485 nm excitation and 520 nm emission to reveal eGFP fluorescence. Lysate numbers are shown at the top of each lane.

2.4 Discussion

The *A. caninum* secreted proteins were selected from the *Ac*ES proteome or from the SSH library of mRNAs that were upregulated upon transition from free-living to parasitic L3 stages of the hookworm. Evasion of the host immune response is essential for hookworms as the larvae migrate through the skin and sub-dermal tissues to the lungs, and when the adult worms are resident in the small intestine. As such, hookworms secrete many proteins with distinct mechanisms of action to target niche-specific immune responses. The 114 identified and verified *Ac*ES protein-coding sequences for this study were shown by NCBI (2016) BLASTx to have a diverse set of gene ontologies that categorised them into different protein groups with a diverse range of activities[265],[211]. In the context of strategically selecting *Ac*ES proteins with potential immuno-modulatory properties, the proteins selected either possessed a signal peptide or were members of a protein family that had previously described roles in interacting with mammalian tissues, with an emphasis on suppression of inflammation in any setting. Protein families of interest for this study included SCP/TAPS, metalloprotease inhibitors, lysozyme-like, retinol-binding, transthyretin-like, lectins, proteases (metallo-, cysteine, aspartyl, serine) and novel proteins with unknown functions.

The most abundantly represented Pfam group in the *Ac*ES secretome was the SCP/TAPS superfamily (26 of 114: 23 %; Pfam accession number PF00188, InterPro IPR014044). SCP/TAPS belong to a superfamily of cysteine-rich secretory proteins (CRISPs) that include vespid venom allergens, plant pathogenesis-related proteins and glycoproteins identified in mammalian epididymis and testis[282]. The extensive distribution of the CRISP family throughout diverse eukaryotic organisms implies that they function in

80

distinct and contrasting biological processes. SCP/TAPS possess a domain that is characterised by six relatively conserved sections littered with blocks of less conserved sequence. SCP/TAPS compose 28 % of all the proteins identified in the *Ac*ES proteome and have distinct homology to a sub-group referred to as *Ancylostoma*-secreted proteins (ASPs)[283]. In helminths, at least some ASPs have been described to possess angiogenic characteristics[284]. ASPs were initially identified as one of the dominant protein families secreted by the infective larval stage *A. caninum*, notably *Ac*-ASP-1 and *Ac*-ASP-2[285],[286]. Mulvenna and colleagues[211] then showed that ASPs accounted for 28 % of the adult hookworm ESP proteome, and Datu and colleagues[265] showed that 56 % of the 30 most highly upregulated mRNAs upon serum-stimulation encoded for ASPs[265]. Zhan went on to characterise seven of the msot abundant *Ac*ES ASPs in terms of their anatomic sites of expression using immunofluorescence and showed that most were localized to the gut and oesophageal glands[287]. SCP/TAPS were also shown to be a major feature in the genomes of two other soil-transmitted helminths, the human hookworm *Necator americanus* (137 SCP/TAPS protein-coding genes identified) and four different *Strongyloides* species (205 identified)[209],[288]. A four-fold expansion of these proteins was observed *N. americanus* in comparison to other nematodes which suggested that this protein family has separately expanded at least two times into both nematode clades IV and V[209]. More than half (69 of 137) of the SCP/TAPS identified in *N. americanus* were overexpressed in the adult life cycle stage suggesting that nematode SCP/TAPS proteins may be essential for successful infection to overcome host immune responses[209].

Indeed, the therapeutic potential of SCP/TAPS was recognised in the 1990s when Moyle and colleagues showed that Neutrophil Inhibitory Factor (NIF), a SCP/TAPS protein from *Ac*ES that binds to CD11b on leukocytes[220], had therapeutic potential in the

treatment of stroke[289],[290]. Finally, there are at least seventeen different SCP/TAPS-related proteins in the free-living nematode, *Caenorhabditis elegans*[287]. This family plays multi-functional roles in *C. elegans* where they are involved in antimicrobial activity[291], physiological development[292] and longevity of infection[293]. Despite frequent suggestions that SCP/TAPS proteins from helmiths have immunoregulatory properties, there are very few examples of this in the literature. Indeed there is conjecture around whether SCP/TAPS have an evolutionarily conserved function i.e. immunoregulation, or instead that the SCP domain has a versatile capacity to have distinct functions built onto it[294].

Another protein family of interest in the context of the this study is the lysozyme-like proteins, which accounted for 3 % of the final list (3 of 114). Lysozymes in humans are generated by the innate immune system and possess antimicrobial activity[295]. Lysozymes, also known as N-actetylmuramide glycanhydrolyase or muramidases, hydrolyse the 1,4-beta-linkages in peptidoglycans within the cell walls of gram positive bacteria[296]. Hydrolysis occurs between two or more carbohydrates, specifically N-acetylmuramic acid and N-acetyl-D-glucosamine residues in chitins[296]. Copious amounts of lysozyme are found in mucous, human milk, plasma, tears and saliva, as well as in cytoplasmic granules of macrophages and neutrophils[297]. A reduction in lysozyme levels in newborns has been associated with bronchopulmonary dysplasia[298]. Dysregulation of lysozyme expression has also been linked with IBD pathophysiology[299].

Transthyretin (TTR)-like proteins are another family of considerable interest because they are nematode-specific proteins that have weak homology to TTR proteins that bind and transport thyroid hormones (Pfam accession number PF01060, InterPro IPR001534)[300]. TTR-like proteins have been identified in ES products from *Ascaris*

suum[301], in the extracellular vesicles released from the ovine parasitic nematodes, *Teladorsagia circumcinta*[302] and *H. polygyrus*[303], and in abundance in the ESP of the murine gastrointestinal nematode *Nippostrongylus brasiliensis*[304]. TTRs of the filarial nematode *B. malayi* can be broken down into subunits that bind to host retinoids which may promote or suppress the regulatory arm of the immune system via FOXP3+ Treg cells[305],[306]. Considering this rationale, approximately 4 % (4 of 114) of the *A. caninum* proteins selected for expression herein were TTR-like proteins.

Fatty acid and retinol binding proteins (FAR) are a protein family group that constitute a unique family of nematode-specific proteins. They are α-helix-rich lipid-binding transporter and storage proteins identified exclusively in nematodes and are not present in other phyla[307]. Lipid synthesis is a crucial process in all organisms, including helminths. Helminths have an obligatory relationship with their host and rely on stored nutrients from the ingested food of their hosts. It has been hypothesised that this is due to their inability to synthesize fatty acids *de novo* and reliance therefore on capturing them from the host[308]. Nematodes secrete FARs into human, animal and plant host tissue in relatively high abundance, and these proteins are structurally distinct from host proteins that are known to bind lipids[156]. Helminth-derived lipid binding proteins deliver bioactive lipids and sequester lipidic intermediates, therefore they have the potential to regulate the host innate and acquired immune systems by interfering with secreted lipids and carrier proteins, and thus have been discussed as novel therapeutic targets[309].

Tissue inhibitors of metalloproteases (TIMPs) possess a netrin-like domain and function as endogenous protein regulators of matrix metalloprotease enzymes (Pfam accession number PF00965, InterPro IPR001134). They are involved in tissue restructuring and

cell communication to adhesion molecules and cytokines[310]. TIMP-like proteins from parasitic helminths have been suggested to be involved in immune evasion and the establishment of infection[311]. The crystal structure of a TIMP-like protein with a netrin domain (InterPro IPR001134) from *Ancylostoma ceylanicum* was solved, prompting the authors to speculate that the protein functioned as a cytokine decoy receptor[312]. A developmentally regulated TIMP that is abundant in *Ac*ES of adult *A. caninum* (*Ac*-TIMP-1) has been shown to be anti-inflammatory and protected against TNBS colitis[194].

Finally, proteins that had no homology or recognisable sequence similarity to known putative conserved domains were referred to as 'novel' for the purpose of this thesis. The bioactivity of novel proteins cannot be predicted by current bioinformatic software modelling systems. Therefore, parasite-specific novel proteins were hypothesised to potentially interact with host tissues during infection because there are no mammalian homologues. In the context of this thesis, 45 % of the *Ac*ES protein library (51 of 114) were considered to be novel.

A number of the ORFs selected for expression that corresponded to peptides or predicted ORFs identified by Mulvenna *et al.,* (2009)[211] and Datu *et al.,* (2008)[265], respectively, were based on truncated ESTs where the correct 5' initiator methionine had been incorrectly attributed. As such, some of the predicted proteins were thought to lack a signal peptide and deemed to be "non-secreted", at least via classical secretory pathways. To address this issue in collaboration with the Mitreva Lab, the full-length ORFs that corresponded to the partial sequences described by Mulvenna *et al.,* (2009)[211] and Datu *et al.,* (2008)[265] were identified.

2.5 Conclusion

In conclusion, 114 *Ac*ES protein-coding genes were selected and the integrity of the sequences was verified by the bioinformatics pipeline presented. Furthermore, the Mulvenna *et al.,* (2009)[211] and Datu *et al.,* (2008)[265] datasets were updated with evidence-based PacBio transcript reads to produce an up-to-date (2018) list of protein-coding *Ac*ES ORFs. These ORFs were then synthesized in an appropriate vector for the cell-free LTE system. In total, 86 % of the protein-coding ORFs identified were successfully expressed as fluorescently-labelled hookworm proteins, resulting in 104 *Ac*ES lysate proteins.

Chapter 3

In vivo Anti-Inflammatory Screening

of the Hookworm Cell-Free Secretome

3.1 Introduction

Understanding of IBD pathogenesis and clinical characteristics of the disease has been greatly improved by the use of experimental murine models. Mouse models enable induction of disease by a polarised T_H1 / T_H17 response mimicking CD or a T_H2 response mimicking UC[313],[314]. The TNBS-induced mouse model of colitis is an example of T cell-dependent, acute, abrasive and self-limiting colitis[102],[100]. The clinical presentation of disease is similar to an acute flare up of UC; however, the cytokine profile is more akin to that seen in CD as it is characterised by a predominantly T_H1 / T_H17 profile. The clinical course of TNBS-induced colitis includes manifestations such as bloody diarrhoea, inconsistent or occult stools, a dramatic loss in body weight, piloerection and decreased movement of the mice. The gastrointestinal lesions invoked by TNBS treatment mimics human CD because inflammation spreads in a transverse fashion and results in the development of transmural colitis[315]. Hallmarks such as distortion of crypts, formation of abscesses and mucosal oedema are also seen in this model[316]. This is a widely used model for the initial assessment of the therapeutic value of compounds and proteins because it requires relatively small amounts of the therapeutic product, has a quick turnaround, and is inexpensive[102].

Most of the recombinant proteins tested for efficacy in murine models are made in cell-based expression systems such as bacteria, yeast, insect, mammalian, or transgenic plants. Cell-based protein expression techniques are laborious and time consuming but often produce bioactive and post-translationally modified proteins[238]. To circumvent the time-constraints of these cell-based expression systems, an alternative cell-free expression system was employed for the purpose of this thesis in order to rapidly express

recombinant proteins. The *L. tarentolae* cell-free protein expression system uses a crude extract known as lysate which is produced from lysis of cultured *L. tarentolae*, a single celled eukaryotic parasite[261]. A simultaneous transcription and translation reaction occurs when template DNA is added to the supplemented lysate[243]. An important benefit of this organism is that it can be manipulated to exclusively translate only the specific gene of interest encoded by exogenous DNA[254]. The protein expression vector also contains an enhanced green fluorescent protein (eGFP) tag. The fluorescent tag allowed for the rate of protein expression to be tracked and visualised. This cell-free LTE system has great potential for production of many proteins at once and was determined to be a suitable system for expression of the hookworm recombinant secretome[261].

This chapter outlines the experimental protocols and procedures used throughout this section of the thesis in line with the research aims. In addition, this chapter presents the results and discusses the experimental strategy, statistical and bioinformatics workflows for the project. The aims of the studies described in this chapter are:

1 Establish whether non-recombinant cell-free lysate has an impact on TNBS colitis in mice.

2 Screen recombinant hookworm cell-free secretome using the mouse TNBS colitis model.

Figure 3-1 Research aims of chapter 3.

The basic schematic below was followed for the experimental workflow of chapter 3.
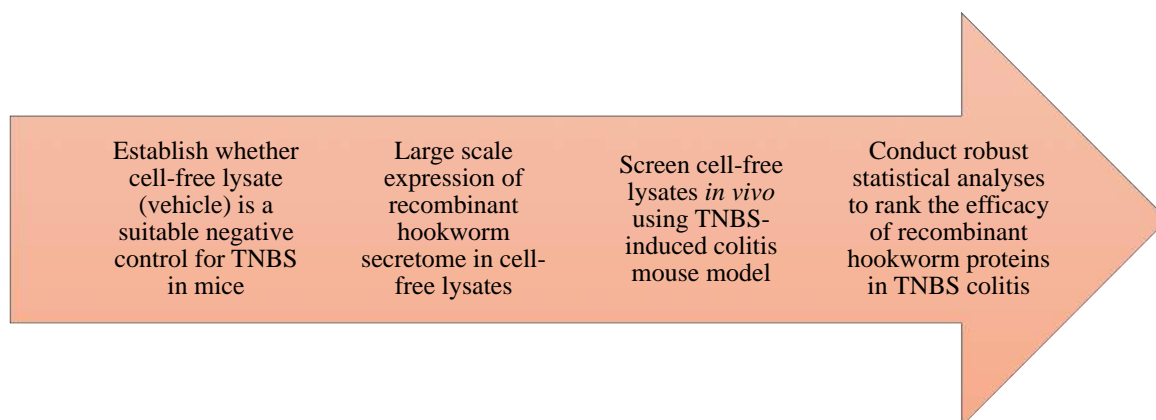
Figure 3-2 Schematic representation of the experimental workflow of chapter 3.

Herein, the *in vivo* screen of the recombinant hookworm secretome (identified and generated in chapter 2) in a mouse model of IBD has been presented. The use of an *in vivo* screen as opposed to a targeted *in vitro* screen was selected in an attempt to cast a wide net and make no assumptions about protective mechanisms of action. The high-throughput nature of cell-free protein expression makes the approach amendable to a range of *in vitro* and *ex vivo* applications, and is the first time that un-purified cell-free recombinant protein products have been screened for efficacy directly in an animal model of disease, highlighting the novelty of the approach.

3.2 Materials and Methods

3.2.1   Lysate Preparation

For each hookworm protein lysate that was tested in the *in vivo* screen, a 600 μL lysate reaction was performed as per the protocol stipulated in section 2.2.4. As quality control, a 10 μL sample of the lysate supernatant was electrophoresed on a non-reducing SDS-PAGE gel and the eGFP-fused protein was visualised as per the protocol stipulated in section 2.2.4.

3.2.2   Animal Procedures

All animal experiments were conducted under the parameters stipulated in the JCU Animal Ethics Committee approved project #A2180. Male BALB/c mice aged between 5 and 6 weeks old were purchased from the Animal Resource Centre (ARC) in Perth, Western Australia. BALB/c mice were chosen for use in this study because they are susceptible strain to TNBS-dependent colonic inflammation whereas the most widely used mouse inbred strain, C57BL/6 mice, are reasonably resistant[317]. Mice were weight-matched to within 1 g of each other prior to shipping to Cairns. Mice were housed in accordance with JCU animal rights and regulations under specific pathogen-free conditions (Cairns Campus). All procedures were performed after appropriate training was undertaken on the relevant handling procedures, and procedural records were kept by the manager of the facility. Mice were assessed for health status and body weight upon arrival to the facility. Based on their weight, mice were equally distributed into groups (n = 5 mice per group) and housed in plastic cages with unlimited access to food and water. Mice were rested for seven days prior to the commencement of an experiment.

In each experiment, each group of five mice received an injection of cell-free lysate containing a distinct hookworm recombinat protein. Each experiment had a naïve group that were administered with 100 μL DPBS (Gibco™ 14190144) via the i.p. route, a negative control group that received cell-free lysate containing empty pLTE vector expressing GFP alone, and 5 to 10 groups each of which receoved a different hookworm recombinant lysate (Table 3-1). The i.p. administration of lysate was chosen based on the rationale presented by Ferreira *et al.,*[194],[196] who showed that i.p. administration of *A. caninum* recombinant protein suppressed TNBS-induced inflammation and tissue damage. One hundred (100) μL of lysate was administered to each animal within an experimental group via IP injection 20 hours prior to the intra-rectal (i.r.) administration of TNBS.

Group	Treatment	n
1	Naïve (DPBS only)	5
2	TNBS + non-recombinant negative control (empty pLTE vector)	5
3+	TNBS + Experimental groups (Lysate with hookworm recombinant protein)	5

Table 3-1 Experimental groups for TNBS colitis experiments in mice. n = number of mice per group.

3.2.3 Preparation of Anaesthetic

Anaesthetic was prepared aseptically to a concentration of 6.25 % ketamine (as hydrochloride) (Ketamil; Provet) (50 mg/kg) and 6.25 % xylazine (2-2,6 Xylidine-5,6 dihydro-4H-1,3-thiazine hydrochloride) (Xylazil; Provet) (5 mg/kg) in sterile phosphate

buffered saline (DPBS) (Gibco™ 14190144) solution and i.p. administered to mice at a dose of 200 μL per mouse. Anaesthetic drugs were prepared on an *ad hoc* basis and stored at 4 °C until use under DS4-DS8 approval from the Queensland Government. A copy of the approval is held by JCU Australian Institute of Tropical Health and Medicine. Anaesthetic drugs were held in a secure location and all usage was recorded in drug usage logs.

3.2.4 Administration of TNBS to Mice

In a laminar flow cabinet, mice were administered a 200 μL i.p. injection of anaesthetic solution with a 29-gauge needle in the lower right quadrant of the peritoneum. During this procedure, animals were lightly restrained with the use of a scruff pad. After sedation, when each mouse was unresponsive to stimuli, their baseline weight was recorded. For administration of the TNBS solution, mice were inverted, lubricant (Durex K-Y Jelly) was placed on the rectum and a SRPLO I.V. soft catheter (Radiopaque/ETFE, Gauge 20G x11/4", I.D. 0.80x 32 mm) was inserted 4 mm into the colon. A volume of 100 μL of 1.5 mg 5 % (w/v) 2,4,6-Trinitrobenzenesulfonic acid solution (TNBS) (Sigma-Aldrich P2297) in sterile filtered 50 % ethanol in Type 1 ultrapure H_2O was slowly administered into the colon and mice were held upside down for 1 minute to prevent anal leakage[191]. Mice were returned to the appropriate cage and monitored for 30 minutes or until they regained consciousness.

3.2.5 Measuring and Monitoring

Each animal was monitored daily for the three days post-TNBS administration for changes in health and physical welfare (Figure 3-3).
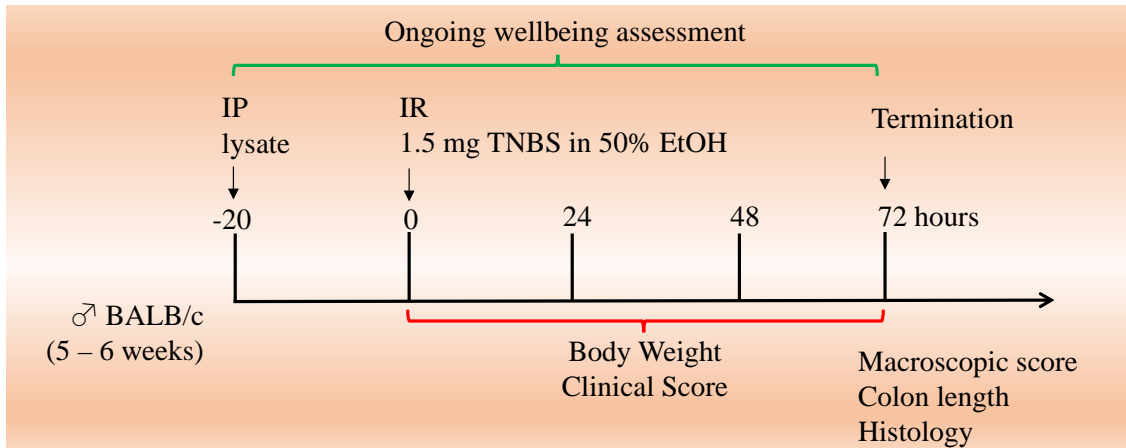
Figure 3-3 Schematic diagram of the experimental workflow used in TNBS-induced murine colitis.

The clinical score of each mouse was recorded daily which included body weight changes, decreased motor activity, piloerection, stool consistency and rectal bleeding (Table 3-2).

% Weight loss	Piloerection	Faeces	Mobility
0: Gain	0: None	0: Normal	0: Normal
1: Same	1: Mild	1: Mild diarrhoea	1: Mobile
2: Loss	2: Severe	2: Severe diarrhoea	2: Lethargic

Table 3-2 Clinical assessment parameters for scoring the daily physical welfare of each animal during the TNBS-Induced colitis procedure[318].

Animals exposed to TNBS treatment in the absence of therapeutic intervention were expected to cease weight loss by experimental day three. Any mouse suffering from undue distress or that lost more than one-third of its initial body weight over a 24-hour period was sacrificed based on ethical obligations in the approved protocol. In the event of this occurrence or any unexpected deaths, an "Adverse Event Form" was lodged with the JCU Animal Ethics Committee. It is widely accepted that there is no reliable positive control drug for use in TNBS colitis, and all of the standard immunosuppressive agents and biologics perform relatively poorly and inconsistently in this acute model of disease (A. Loukas, pers comm). As such, a positive control treatment was not included in these studies, and instead relied on groups of healthy mice that did not receive TNBS and negative control mice that received empty vector lysate and were administered TNBS.

3.2.6 Sacrifice and Tissue Collection

On the third day of the experiment, mice were euthanized by carbon dioxide asphyxiation and necropsied. After necropsy, the remnants of the mouse were autoclaved and disposed of via JCU approved channels. The colon was removed, measured and photographed. The macroscopic pathology score was assessed by longitudinally sectioning the colon, washing the intra-rectal contents out with sterile DPBS (Gibco™ 14190144) and the tissue integrity was observed under light microscopy (Olympus SX61, 0.67-45x). Macroscopic pathology score was used to assessed the severity of bowel wall thickening, adhesion to internal organs and tissues, ulceration, and mucosal oedema (Table 3-3).

	Adhesion	**Ulceration**	**Bowel wall thickening**	**Mucosal oedema**
0	Easily removed	None	Normal thin colon	No oedema
1	Minimal resistance	Minimal (1 ulcer)	Slight thickening	Slight
2	Adhesions	Mild (multiple)	Noticeable thickening	Clearly noticeable
3	Severe adhesion	Severe (necrosis)	Severe thickening	Severe

Table 3-3 Macroscopic pathology scoring assessment requirements for post-mortem colon analysis in TNBS-induced colitis[318].

3.2.7 Colon Sectioning

A 0.5 cm section of tissue proximal to the rectum was discarded (Figure 3-4). The next most proximal 0.5 cm section of tissue was flushed with DPBS (Gibco™ 14190144) and fixed in 4 % formaldehyde (Sigma-Aldrich HTF01128) for a maximum of 24 hours, after which the tissue was transferred to 70 % ethanol and stored at room temperature.

Figure 3-4 Schematic diagram of the colon sectioning protocol used in TNBS colitis.

3.2.8 Histology Procedure

Formalin-fixed tissue samples were processed at the JCU Advanced Analytical Centre (AAC) overnight in a Leica HistoCore PEARL automatic tissue processor then embedded into paraffin wax blocks with a Leica Arcadia Embedding Centre. Sections (5 µm) were cut using a Leica RM2125 rotary microtome, floated into a 40 °C water bath and carefully mounted onto slides. After air drying the slides were de-waxed in a series of 100 % xylene and 100 to 70 % ethanol solutions ending in a water bath. Slides were then kept hydrated and immediately stained with haematoxylin and eosin (H&E) using a Leica automatic Linear Slide Stainer. After cover-slipping the slides were viewed and imaged using a Leica Aperio CS2 Digital Pathology Scanner at 20x or 40x magnification for histopathological analyses.

3.2.9 Histopathological Blind Scoring Procedure

Scoring of pathology was performed from H&E stained slides by an individual blinded to the experimental group against the scoring criteria (Table 3-4). Tissue sections were scored on a scale of 0 to 5 for each of the following parameters; (1) epithelial pathology (crypt elongation, hyperplasia, erosion), (2) mural inflammation, and (3) oedema for an overall maximum total histology score of 15.

Parameters	Histopathology Score		
	Epithelial Pathology	Mural Inflammation	Oedema
Score	0 to 5	0 to 5	0 to 5

Table 3-4 Histopathology Scoring of H&E Stained Slides of Individual Mice from Experimental Groups.

3.2.10 Statistical Analysis of Different Outcomes to Determine Overall Significance of a Hookworm Protein Lysate's Performance Within an Experiment

Statistical comparisons between each hookworm recombinant protein lysate and the non-recombinant empty vector lysate control were performed in each experiment using R version 3.5.1[319]. The percentage weight change on day three and colon length were assessed using a two-sample t-test. Macroscopic and clinical scoring were assessed using a Mann-Whitney U test as this is most appropriate for ordinal data. P values were adjusted for multiple comparisons using Benjamini and Hochberg False Discovery Rate (FDR)[320]. The geometric mean of significance of these four outcomes was used to rank the protective capacity of the protein lysates (Figure 3-5).
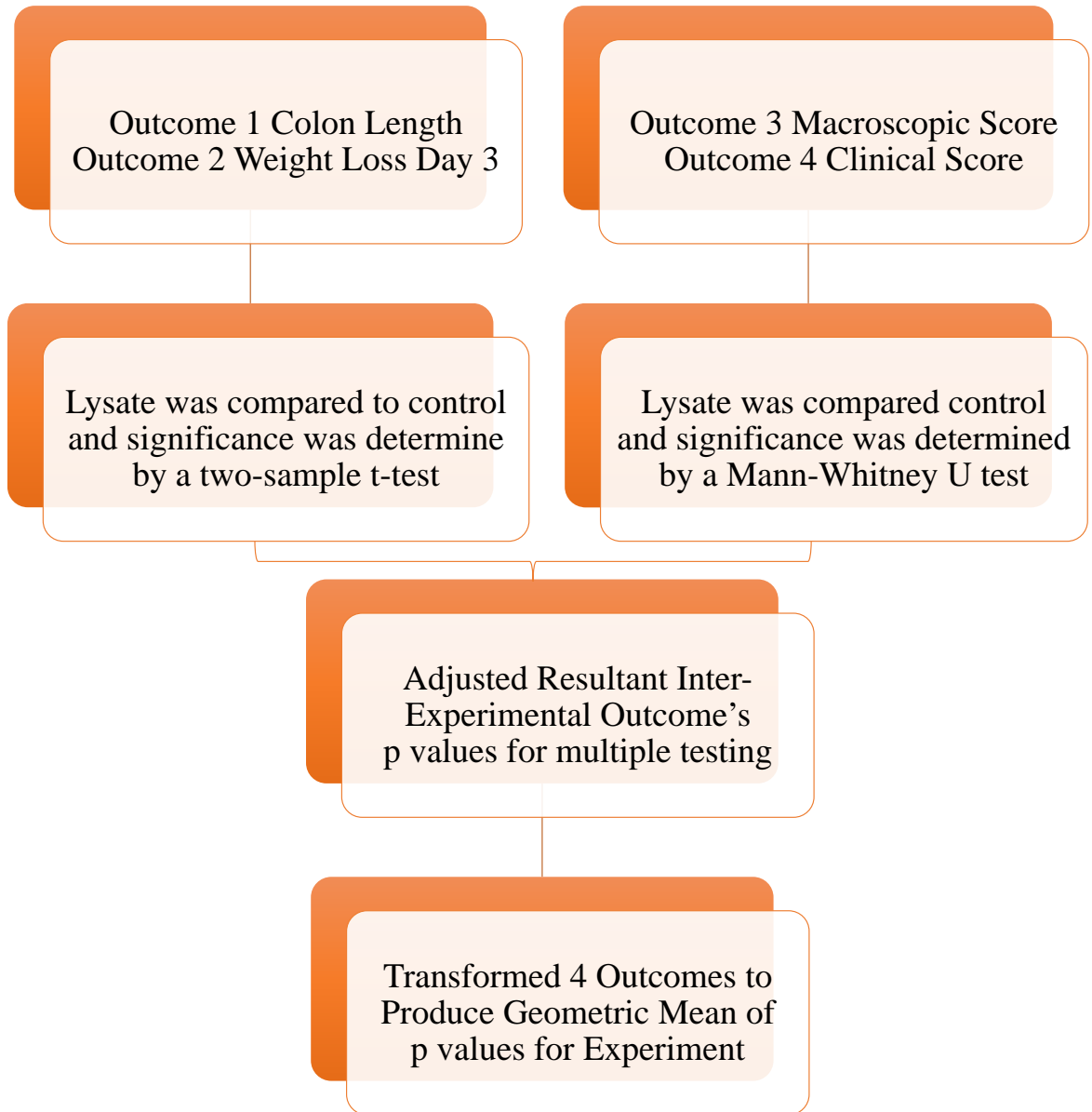
Figure 3-5 Flow chart showing statistical analysis of individual outcomes for determining overall significance of a hookworm recombinant protein lysate's performance within an experiment.

3.2.11 Statistical Analysis to Incorporate Different Outcomes to Determine Overall Significance of a Hookworm Recombinant Protein's Performance

In order to combine the four clinical outcomes into one value, the Z-score of each outcome for each animal was determined. The mean, standard deviation and sample size of the data set was determined and used to calculate the Z-score for each outcome of each animal. The Z-score transformation was applied to groups by subtracting the mean from each outcome, and the result was divided by the standard deviation. The signs of outcomes 3 and 4 were reversed because macroscopic scores (outcome 3) and clinical scores (outcome 4) are lower in healthy mice and elevated in diseased mice, whereas healthy mice have higher weights (outcome 1) and longer colons (outcome 2). A combined score was created by summing together the four Z-scores for each outcome. The significance of the combined Z-score of each protein lysate was determined using a Mann-Whitney one-tailed student's t-test of the combined Z-score of each animal within an experimental group compared to the negative control combined Z-scores and the data was adjusted to compensate for multiple testing[320].

Figure 3-6 Flow chart of calculation of combined Z-score p value for determining overall significance of a hookworm recombinant protein lysate's performance within the TNBS-colitis screen.

3.3 Results

3.3.1   Administration of Non-Recombinant Cell-Free Lysate to Mice Has No Effect on TNBS-Induced Colitis

There was no apparent effect of i.p. administration of non-recombinant lysate, either positive or negative, on the measured parameters of TNBS-induced colitis in mice (Figure 3-7). Thus, this result strengthened the rationale for using the TNBS-induced colitis model to test cell-free lysates containing hookworm recombinant proteins *in vivo*. The screen was conducted to assess the prophylactic effect of lysates on inducible colitis without the need to purify hookworm recombinant proteins.
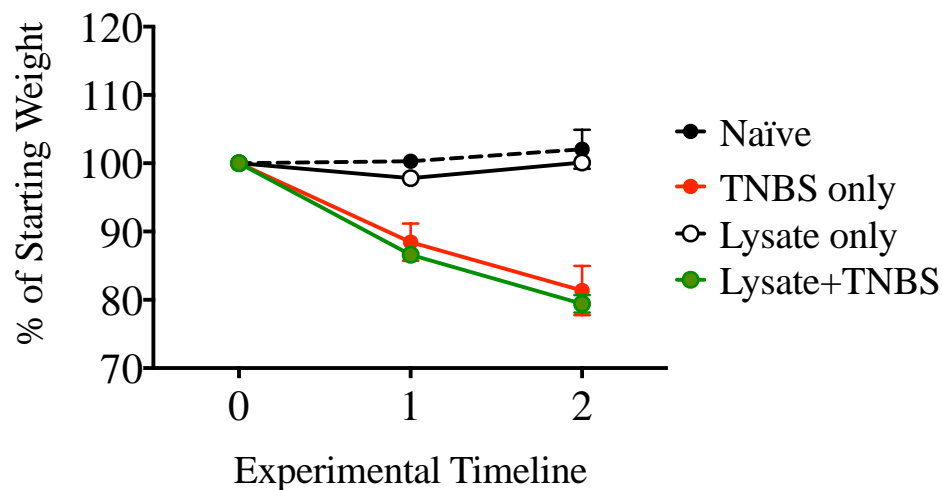
Figure 3-7 Non-recombinant cell-free lysate proof-of-concept trial. Mice were either treated with DPBS (Naïve), TNBS only, non-recombinant cell-free lysate (Lysate only) or both non-recombinant cell-free lysate and TNBS (Lysate+TNBS). Non-recombinant cell-free lysate-treated mice maintained the same weight as untreated mice, and treatment with non-recombinant cell-free lysate did not confer any protective benefit against TNBS-induced weight loss. Data points represent mean ± SEM and sample size (n = 4 mice / group).

3.3.2 Select Hookworm Recombinant Protein Lysates Protect Against TNBS-Induced Body Weight Loss

After the induction of colitis by TNBS, the mice developed various manifestations of acute colitis such as inconsistent stool formation, bloody diarrhoea and a dramatic loss of body weight. The negative control group (mice treated with non-recombinant cell-free lysate and then TNBS) quickly lost weight by day one post-TNBS administration and continued to do so until the termination of the experiment (Figure 3-8). Mice treated with cell-free lysates containing hookworm proteins prior to administration of TNBS displayed varying degrees of protection against weight loss. Mice treated with lysates 9 and 13 emained healthy and lost signficiantly less body weight by day 3 than negative control mice.
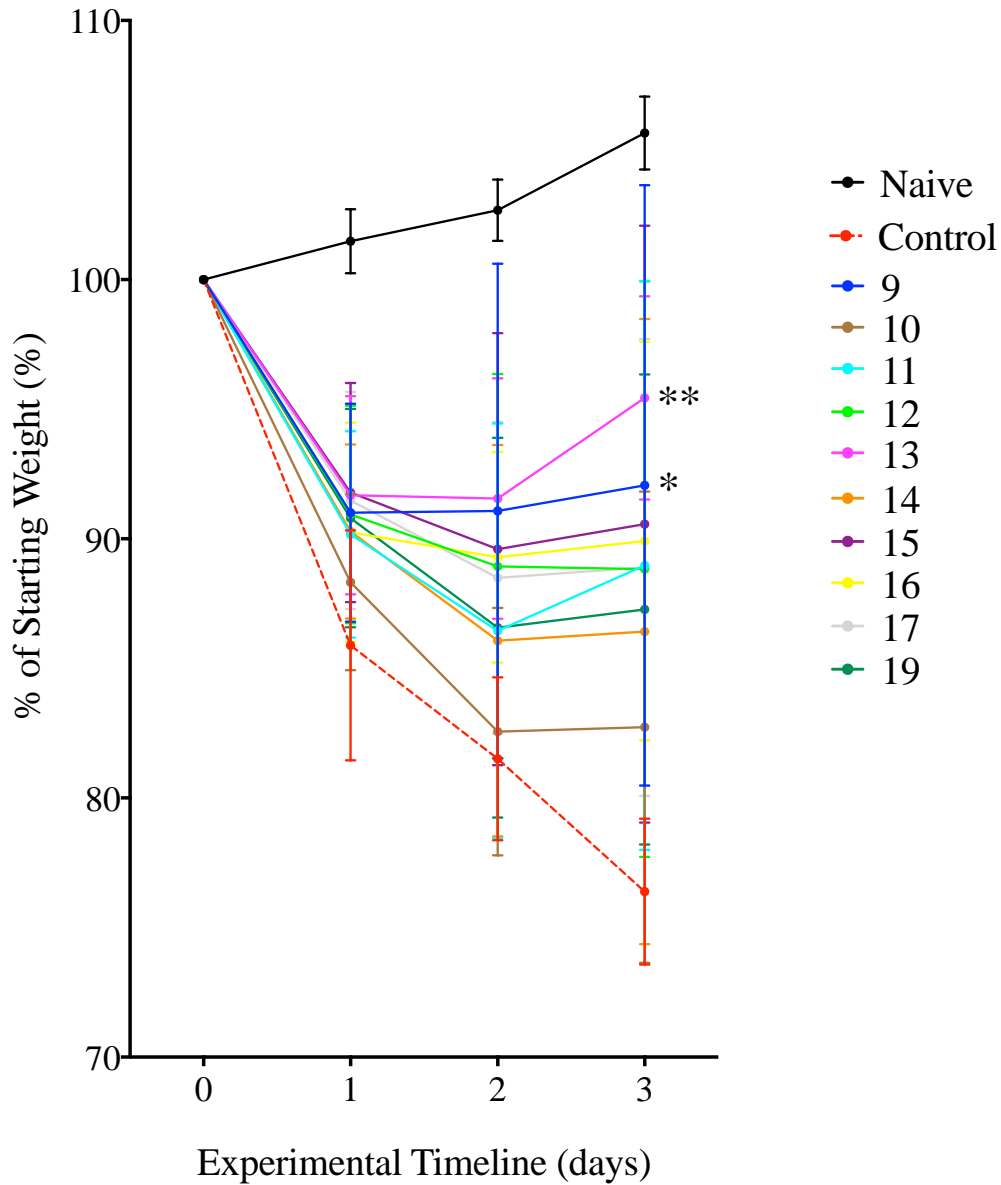
Figure 3-8 Example experiment showing daily weight change of mice receiving select hookworm protein-containing lysates prior to administration of TNBS. Naïve mice received DPBS only, control mice received non-recombinant cell-free lysate followed by TNBS and the remaining experimental groups received hookworm recombinant protein lysate followed by TNBS. Data points represent mean $\pm$ SEM and sample size (n = 5 mice / group). The significance was determined by using a two-sample t-test to compare weights from day three against the weights from the control group, and was adjusted for multiple testing denoted by $* p \leq 0.05$, and $** p \leq 0.01$.

Upon necropsy, the colons were removed from mice for measurement and further analysis. Photographs were taken for record keeping purposes (Figure 3-9). In the figure below, a representative colon removed from a mouse in the naïve group (A) appears to be healthy, while the colon removed from a mouse in the negative control group (non-recombinant protein cell-free lysate) (B) was severely inflamed and shortened. The colon removed from a mouse in the group that received hookworm recombinant protein 13-containing lysate prior to TNBS (C) was protected from TNBS-induced shortening of the colon.
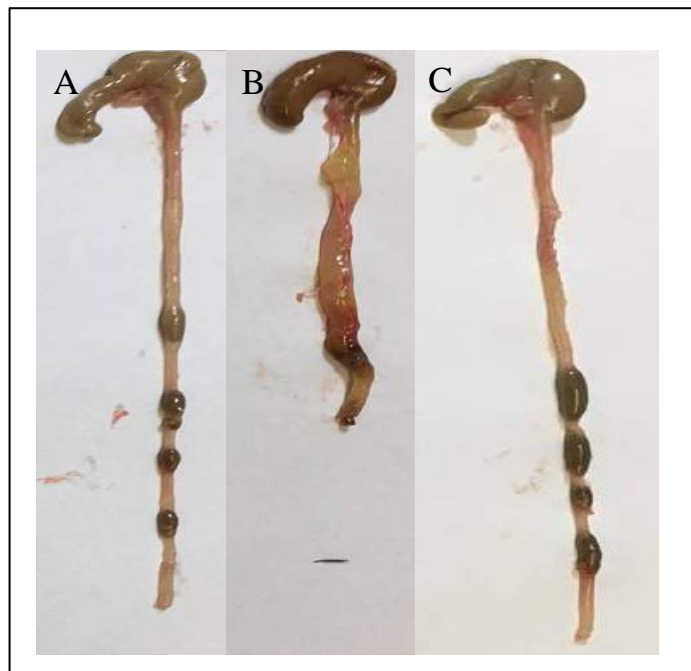
Figure 3-9 Example photographs showing colon lengths of mice receiving different hookworm protein-containing lysates prior to administration of TNBS. These images display the visual differences between the naïve (A), the non-recombinant protein cell-free lysate negative control (B) and the hookworm recombinant protein 13–containing lysate group (C).

3.3.3 Defined Hookworm Cell-Free Lysates Protect Against TNBS-Induced Macroscopic Pathology of the Colon

The macroscopic score assessed adhesion of the gut to the abdominal lining, presence of ulcers, bowel wall thickening and mucosal oedema. In an example experiment, the colons of the negative control group scored highly due to extensive colitic inflammation, whilst some groups receiving hookworm recombinant protein lysates (notably lysates 9, 11, 13, 16, and 19) maintained the integrity of the colon and their scores were significantly lower (Figure 3-10). Mice treated with lysate 9 were protected against TNBS-induced weight loss as well as macroscopic pathology.
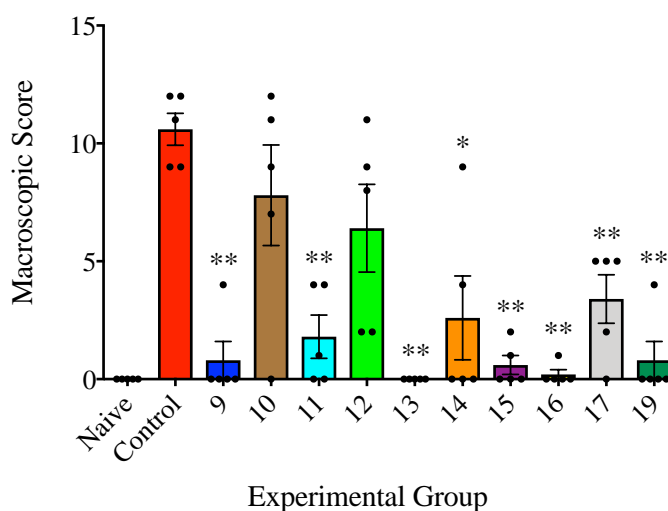
Figure 3-10 Example experiment showing macroscopic pathology scores of mice receiving select hookworm protein-containing lysates prior to administration of TNBS. Naïve mice received DPBS only, control mice received non-recombinant cell-free lysate followed by TNBS, and the remaining experimental groups received hookworm recombinant protein-containing lysate followed by TNBS. All individual data points are represented, mean ± SEM and sample size (n = 5 mice / group). The significance was determined by using a Mann-Whitney U test to compare each test group with the negative control group and adjusted for multiple testing. * p ≤0.05, ** p ≤0.01.

3.3.4 Defined Hookworm Cell-Free Lysates Protect Against TNBS-Induced Colon Shortening

Colon length is a good indicator of the extent of TNBS-induced colitis because in this model inflammation disseminates in a transverse manner, evenuating in transmural colitis with colon shortening[315]. Consistent with enhanced protection against TNBS-induced weight loss, some hookworm recombinant protein lysates test groups treated had longer (and less inflamed) colons than mice treated with TNBS and cell-free lysate control (Figure 3-11). Mice treated with lysates 10 and 13 had significantly longer colons than mice in the empty vector lysate control group.
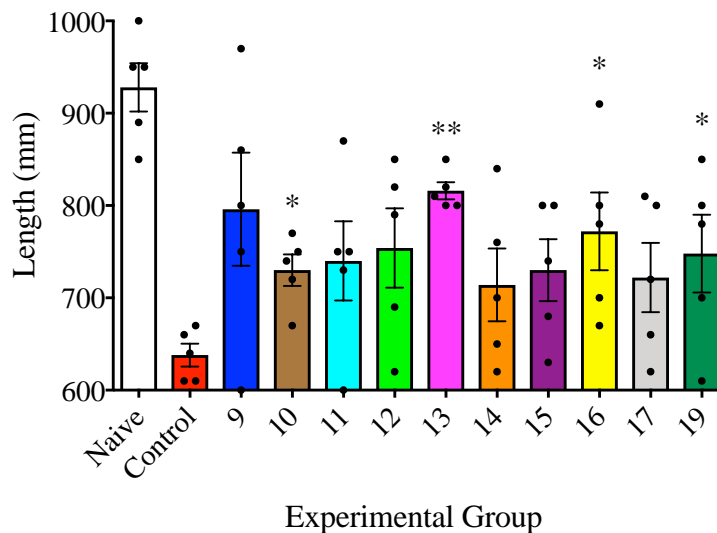
*Figure 3-11 Example experiment showing colon length of mice receiving select hookworm protein-containing lysates prior to administration of TNBS. Naïve mice received DPBS only, control mice received non-recombinant cell-free lysate followed by TNBS, and the remaining experimental groups received hookworm recombinant protein containing lysate followed by TNBS. All individual data points are represented, mean ± SEM and sample size (n = 5 mice / group). The significance was determined by using a two-sample t-test against the control group and was adjusted for multiple testing. * p ≤ 0.05, ** p ≤0.01, *** p ≤0.001.*

3.3.5 Defined Hookworm Cell-Free Lysates Protect Against TNBS-Induced Clinical Signs of Disease

The clinical score incorporated the non-specific physiological signs that pointed to an overall deterioration in the health and wellbeing of the animal, and included physical appearance (piloerection), facael consisteny, body weight change and behaviour (decreased movement and mobility) throughout the entirety of the experiment. A low clinical score is demonstrative of the protective properties of a hookworm recombinant protein lysate against TNBS-induced colitis. The negative control group had a significantly increased clinical score compared to the naïve group (Figure 3-12). Meanwhile mice that received cell-free lysates 9 and 13 had a clinical score comparable to the naïve group which was in congruence with the weight loss findings.
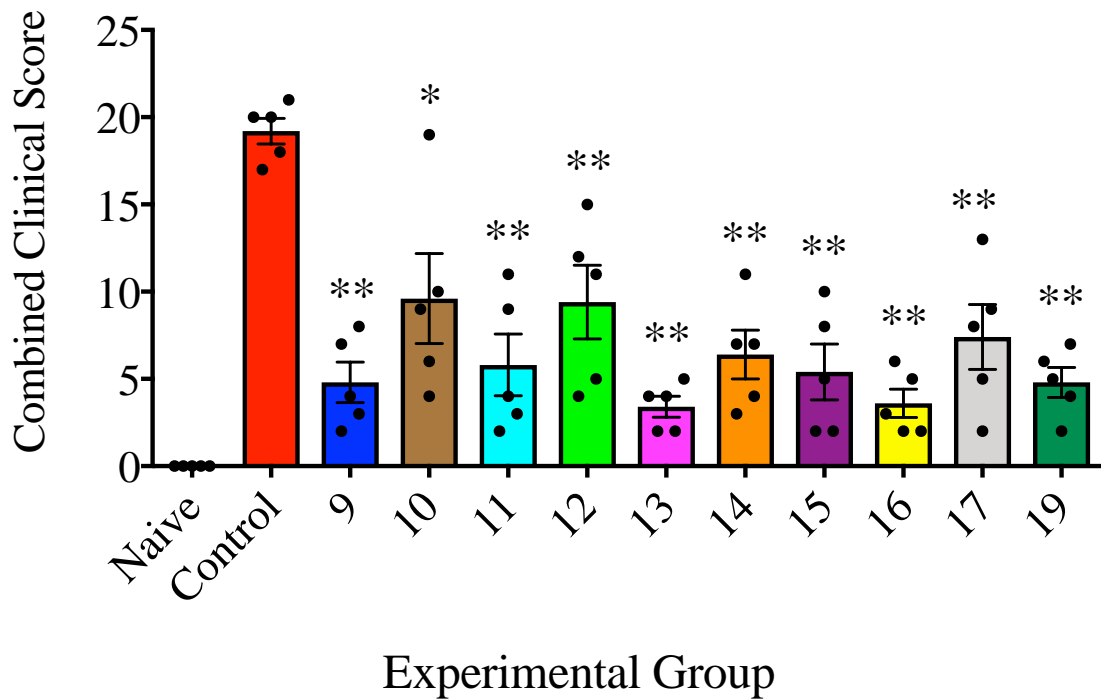
Figure 3-12 Combined clinical score of mice within each experimental group during the experiment. Throughout the three day experiment the extent of TNBS-colitis on the physical appearance of the animals was monitored. Naïve mice received DPBS only, control mice received non-recombinant cell-free lysate followed by TNBS, and the remaining experimental groups received hookworm recombinant protein containing lysate followed by TNBS. All individual data points are represented, mean ± SEM and sample size (n = 5 mice / group). The significance was determined by statistical comparisons assessed using Mann-Whitney U test against the control group and was adjusted for multiple testing. * p ≤ 0.05, ** p ≤ 0.01, *** p ≤ 0.001.

3.3.6 Comparison of Geometric Means from Intra-Experimental Statistical Analysis of Each Colitic Parameter of a TNBS Experiment

The inter-experimental statistical analysis highlighted the most significant protein-containing lysates within each experiment. The geometric mean was calculated for the p values for all four outcomes as per the flow chart (Figure 3-5). The geometric mean was chosen because it is less likely to be influenced by outliers and therefore would not skew the ranking of overall efficacy of a given protein. The significance of the geometric mean of the hookworm recombinant protein lysate versus control was determined.

In order to compare the overall performance of lysates between experiments, their average overall significance was ranked, revealing the top thirty most efficacious hookworm recombinant protein lysates from the TNBS screen (Table 3-5).

Lysate ID	Colon Length	Macroscopic Score	Weight Change	Clinical Score	Geometric Mean
13	0.0003	0.0239	0.0009	0.0239	0.0034
2	0.0143	0.0239	0.0239	0.0239	0.0210
16	0.0529	0.0239	0.0266	0.0239	0.0299
80	0.0302	0.0302	0.0617	0.0302	0.0361
9	0.0768	0.0239	0.0591	0.0239	0.0401
70	0.0318	0.0302	0.0926	0.0302	0.0405
15	0.0719	0.0239	0.0719	0.0239	0.0414
17	0.1007	0.0239	0.0529	0.0239	0.0417
19	0.0765	0.0239	0.0725	0.0239	0.0421
11	0.0877	0.0239	0.0768	0.0239	0.0442
85	0.0877	0.0302	0.0485	0.0302	0.0444
12	0.0725	0.0835	0.0798	0.0239	0.0583
73	0.1440	0.0302	0.0955	0.0302	0.0595
83	0.3520	0.0302	0.0402	0.0302	0.0599
14	0.1430	0.0335	0.1498	0.0239	0.0643
72	0.3252	0.0302	0.0661	0.0302	0.0665
67	0.2620	0.0302	0.0947	0.0302	0.0689
82	0.0148	0.0975	0.2076	0.0975	0.0735
74	0.9375	0.0302	0.0449	0.0302	0.0787
23	0.1329	0.0683	0.0726	0.0683	0.0819
68	0.0926	0.0302	0.3110	0.0520	0.0820
79	0.9763	0.0302	0.0661	0.0302	0.0876
20	0.2802	0.0690	0.1698	0.0239	0.0940
40	0.0148	0.1346	0.4351	0.0975	0.0958
21	0.1498	0.0728	0.1249	0.0683	0.0982
10	0.0239	0.3337	0.2078	0.0591	0.0994
77	1.0000	0.0661	0.0520	0.0302	0.1009

22	0.3514	0.0683	0.0903	0.0683	0.1103
25	0.1257	0.0683	0.2521	0.0710	0.1113
32	0.0975	0.1596	0.1640	0.1035	0.1275

Table 3-5 Best performing cell-free lysates from the geometric means calculated from intra-experimental statistical analysis of each colitic parameter of the TNBS colitis experiment. Dark green represents a significance value of <0.001, mid-green represents <0.01 and light green represents <0.05 of protection within a clinical outcome through to orange symbolising no significant protection. Throughout the screen n = 5 mice / group. Macroscopic and clinical scoring were assessed using a Mann-Whitney U test and all values were adjusted for multiple comparisons using FDR. The full version of this table is in appendix 3.1.

3.3.7 Heatmap Demonstrates Overall Prophylactic Performance Score of the Combined Experimental Parameters & Highlights Significantly Efficacious Proteins

After the average inter-experimental p values were ranked to demonstrate the best performing cell-free lysates, a heatmap was constructed in order to show the performance of each lysate within an outcome as well as their overall performance in the screen as a whole (Table 3-5). The highly protective hookworm recombinant protein lysates showed anti-inflammatory efficacy over multiple outcomes. Statistical comparisons between each test protein lysate (n = 5 mice / group) and the non-recombinant negative control lysate were performed and were adjusted for multiple testing.

Geometric Mean

Significance

***

**

*

ns

ein lysate in TNBS

ved by TNBS, and
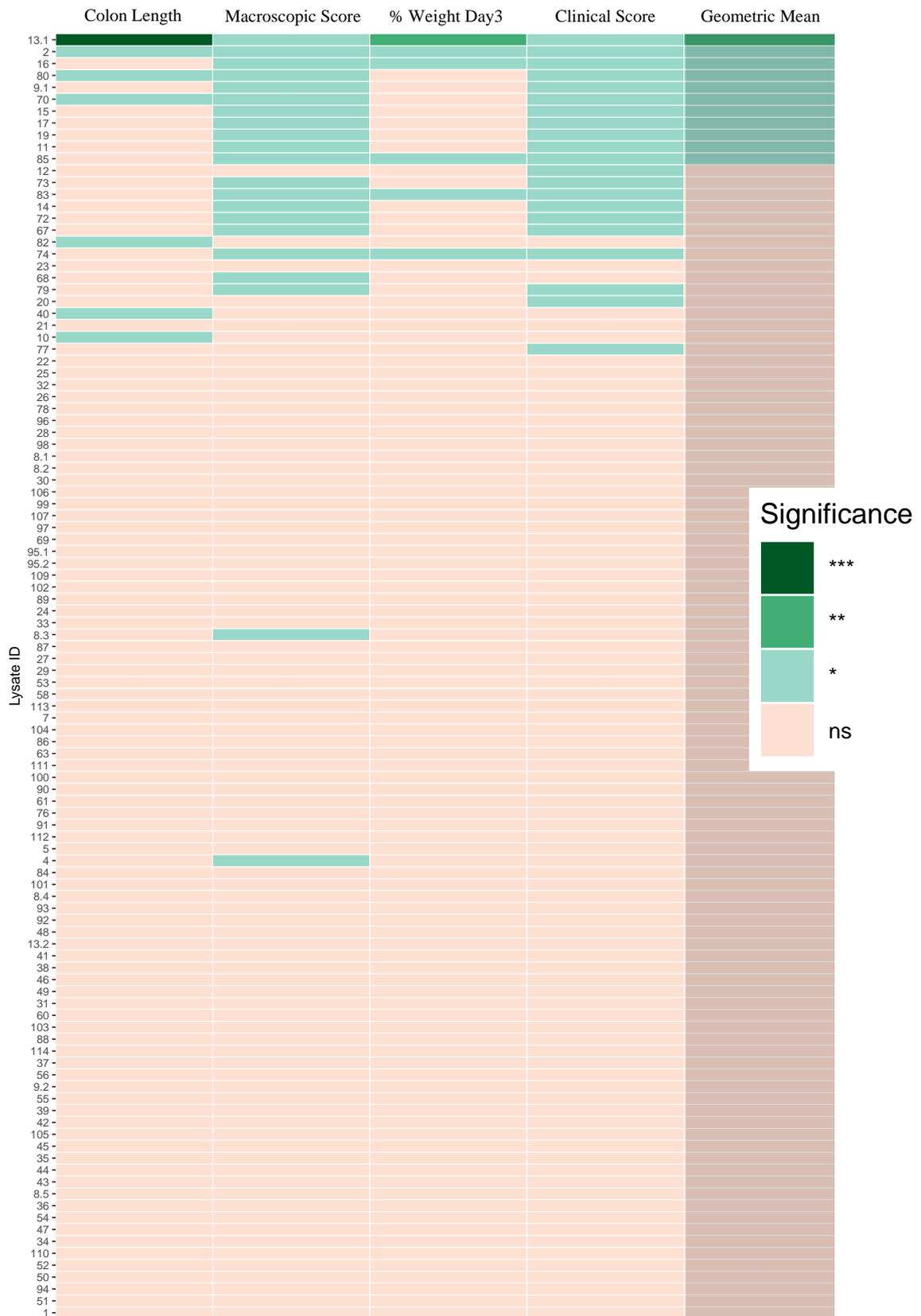
the experimental groups received hookworm recombinant protein containing lysate followed by TNBS. All individual data points were incorporated into statistical analyses and sample size was n = 5 mice / group. Statistical significance was determined by t-test (colon length and % of starting weight on day 3) and Mann Whitney U test (macroscopic score and clinical score), and values were adjusted for multiple comparisons using FDR. The four resultant p values were used to calculate the geometric mean to rank overall prophylactic performance. Analysis was performed in R version 3.5.1. Significantly protective lysates are shown in green, and non-protective lysates are shown in orange, denoted in legend by ns = non-significant. * p ≤ 0.05, ** p ≤ 0.01, *** p ≤ 0.001.

3.3.8 Calculation of Z-Scores Correlating the Four Measured Experimental Parameters of Colitis

Not only was the intra-experimental effect calculated but the raw data of the four outcomes was used to calculate a standard score, also known as a combined Z-score. The Z-score transformation combined the four major outcomes of TNBS colitis (percent of starting weight on day 3 (weight change), macroscopic pathology, clinical score and colon length) per mouse within a hookworm protein-containing lysate group. The Z-score transformed the raw data into units of standard deviation and showed whether the value of the raw score was below or above the population mean[321].

When the population mean scores of both the test (hookworm protein-containing lysate) and negative control (empty vector lysate) groups were the same value then the Z-score was 0. A positive Z-score is when the test group mean is higher than the negative control group mean, and a negative Z-score is when the test group score is less than the negative control population mean. The four assessed parameters were added together to produce

the combined Z-score value, which was compared to the negative control group of each experiment using a two-tailed student's t-test with two sample unequal variance (heteroscedastic). The determined p value then allowed the hookworm protein-containing lysate group to be compared against others across the entire screen.

Twenty (20) hookworm recombinant protein lysates had adjusted p values <0.05 and were ranked in order to highlight the efficiacy of candidate proteins as prophylactic hits (Table 3.3.2). A greater number of proteins were deemed significant based on their combined Z-score as opposed to the geometric mean of each individual protein's intra-experimental p value.

Lysate ID	Z-score p value*	Adjusted p value	Gene Name	Pfam	Life stage
13	0.0000	0.0001	ANCCAN_22177	SCP/TAPS	Adult
16	0.0004	0.0079	ANCCAN_12564	SCP/TAPS	Adult
23	0.0003	0.0079	ANCCAN_12569	SCP/TAPS	Adult
80	0.0004	0.0079	ANCCAN_07727	Annexin superfamily	Adult
85	0.0002	0.0079	ANCCAN_00478 *Ac*-ASP-2	SCP/TAPS	L3
2	0.0004	0.0080	ANCCAN_07322	Lysozyme-like	Adult
22	0.0007	0.0093	ANCCAN_26187	SCP/TAPS	Adult
70	0.0006	0.0093	ANCCAN_08034	TTR-52 superfamily	Adult
19	0.0019	0.0204	ANCCAN_07062	SCP/TAPS	Adult
73	0.0022	0.0204	ANCCAN_13497 *Ac*-TIMP-1	TIMP	Adult
79	0.0022	0.0204	ANCCAN_10127 *Ac*-FAR-2	Gp-FAR-1	Adult

83	0.0025	0.0204	ANCCAN_01926	No putative conserved domains	Adult
15	0.0030	0.0228	ANCCAN_19762	SCP/TAPS	Adult
72	0.0034	0.0244	ANCCAN_17044	TTR-52 superfamily	Adult
9	0.0041	0.0275	ANCCAN_06741	SCP/TAPS	Adult
74	0.0046	0.0295	None available	TIMP	Adult
11	0.0064	0.0366	ANCCAN_04194 *Ac*-NIF	SCP/TAPS	Adult
21	0.0064	0.0366	ANCCAN_11001	SCP/TAPS	Adult
17	0.0082	0.0445	ANCCAN_11010	SCP/TAPS	Adult
28	0.0087	0.0445	ANCCAN_11519	No putative conserved domains	Adult

Table 3-6 Ranking of adjusted p values from a t-test between combined Z-scores of control versus experimental groups. All results were adjusted for multiple tests in R version 3.5.1 (R Core Team, 2013). Lysate ID indicates the arbitrary identification number assigned to the hookworm recombinant protein lysate. Z-score p value and its

corresponding adjusted p value were used to rank hookworm recombinant proteins across the TNBS colitis screen. Gene names were identified using WormBase ParaSite Database (https://www.wormbase.org/). Protein family (Pfam) groups were determined by NCBI BLASTn using default parameters (nr/nt) (https://blast.ncbi.nlm.nih.gov/Blast.cgi?PAGE_TYPE=BlastSearch). Life cycle stage was taken from[211],[265].

3.3.9 Inter-Experimental Statistical Analysis Versus Intra-Experimental Z-Score Analysis Allowed for Dual Validation of Both Statistical Methodologies

The two methods of statistical analysis that allowed the protective proteins to be ranked were compared by plotting the adjusted p values determined by statistical method 1 against the adjusted p values determined by statistical method 2 (Table 3-6).

Statistical Method 1	Statistical Method 2
Average Significance	**Z-score Significance**
Outcome 1 Outcome 3 Outcome 2 Outcome 4	Calculated; mean, Std. Dev. of all outcomes
Lysate vs control & significance determined by two-sample t-test	Lysate vs control & significance determined by Mann Whitney U test	The Z-score transformation: (mean - outcome) / Std Dev.
	Reverse signs of Z –score for outcomes 3 & 4
	Combined 4 Z-scores
Adjusted resultant p values for multiple testing	T-test of Lysate vs control & significance determined by a two-sample t-test
Calculated geometric mean (LOG) of four p values of experiment	Adjusted resultant p values for multiple testing

Plot the Average Significance vs the Z-score Significance

to determine the correlation (R^2)

between the two statistical methods

Figure 3-14 Flow chart demonstrating the two different statistical methods simultaneously followed to validate the significance of prophylactic proteins.

The comparison of the intra-experimental statistical analysis and the Z-score analysis was plotted on a square root axis because it transformed the data and allowed for data values where p value < 0.05 could be visualised for interpretation. The correlation between the significant hits identified by both statistical methods was $R^2 = 0.78$ and highlighted the strength of the statistical criteria in the ranking metholodology of the prophylactic hits.
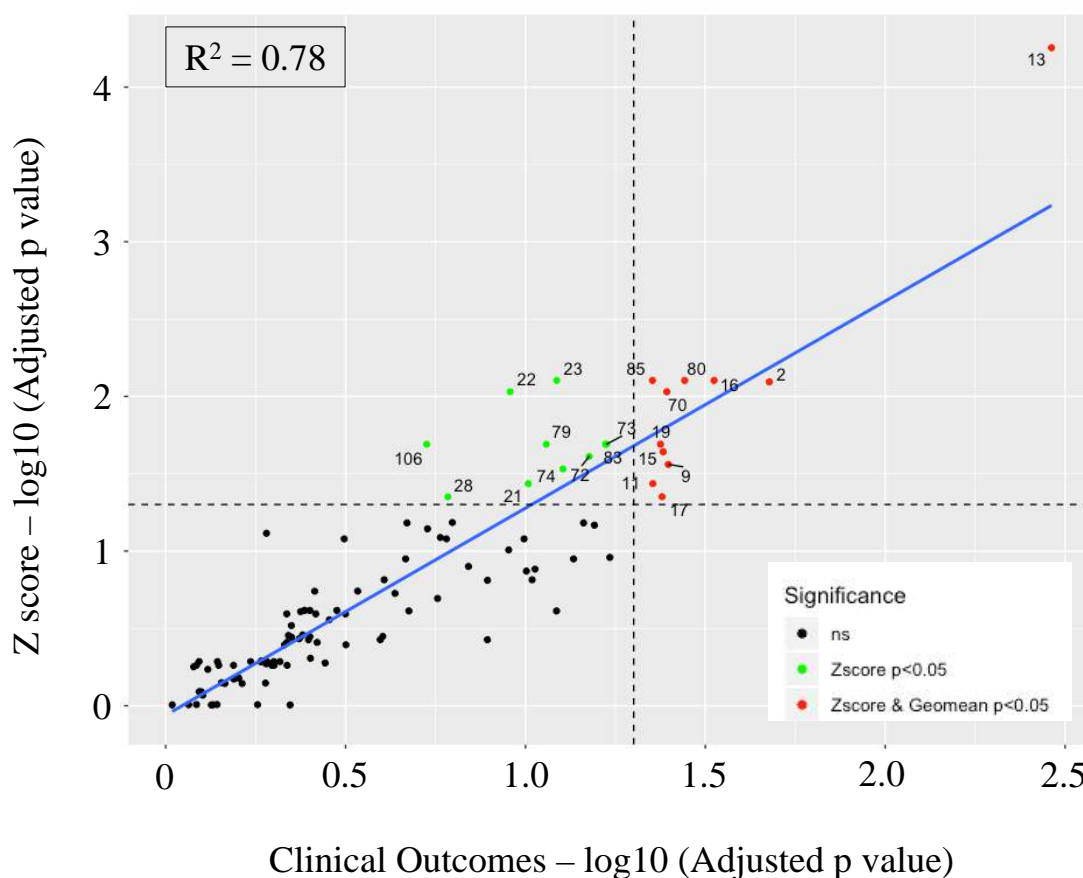
Figure 3-15 The average significance (p value) versus the combined Z-score of each candidate protein compared to the negative control group (non-recombinant cell-free lysate) of the TNBS colitis screen of the hookworm cell-free recombinant secretome. Lysate ID numbers indicate the arbitrary identification number assigned to the hookworm recombinant protein lysates. • ns = non significant, • Z-score p <0.05, • Z-score and Geomean p <0.05. Analysis was performed in R version 3.5.1.

Several candidate proteins were identified as highly protective by both the Z-score analysis and intra-experimental comparisons, notably lystaes 13, 80, 85, 23, 2, and 16. The top twenty hookworm proteins ranked by Z-score were tested for a second time (round 2) to ensure reproducibility of protein expresson and protection against TNBS colitis (Table 3-7).

Round 1 Rank	Lysate ID	Gene Name	Pfam	Life stage	Round 2 Rank
1 *	13	ANCCAN_22177	SCP/TAPS	Adult	1 *
2 *	85	ANCCAN_00478 *Ac*-ASP-2	SCP/TAPS	L3	na
3 *	23	ANCCAN_12569	SCP/TAPS	Adult	13 *
4 *	80	ANCCAN_00727	Annexin superfamily	Adult	9 ns
5 *	16	ANCCAN__12564	SCP/TAPS	Adult	11 ns
6 *	2	ANCCAN_07322	Lysozyme-like	Adult	12 ns
7 *	70	ANCCAN_08034	TTR-52 superfamily	Adult	na
8 *	22	ANCCAN_26187	SCP/TAPS	Adult	14 ns
9 *	19	ANCCAN_07062	SCP/TAPS	Adult	3 *
10 *	79	ANCCAN_10127 *Ac*-FAR-2	FAR	Adult	na
11 *	73	ANCCAN_13497 *Ac*-TIMP-1	TIMP	Adult	na

12 *	83	ANCCAN_01926	No putative conserved domains	Adult	7 *
13 *	15	ANCCAN_19762	SCP/TAPS	Adult	5 *
14 *	72	ANCCAN_17044	TTR-52 superfamily	Adult	na
15 *	9	ANCCAN_06741	SCP/TAPS	Adult	2 *
16 *	74	*Ac*-Novel-TIMP	TIMP	Adult	15*
17 *	11	ANCCAN_04194 *Ac*-NIF	SCP/TAPS	Adult	na
18 *	21	ANCCAN_12561	SCP/TAPS	Adult	4 *
19 *	17	ANCCAN_11005	SCP/TAPS	Adult	10 ns
20 *	28	ANCCAN_11519	SCP/TAPS	Adult	6 *

Table 3-7 Comparison of the performance of the top twenty ranked hookworm protein lysates from the first TNBS colitis experiment and ranking after replicate round 2 testing in mice. Proteins in this table are ranked based on their round-1 adjusted Z-score p values. Lysate ID indicates the arbitrary identification number assigned to the hookworm recombinant protein lysate. Gene names were identified using WormBase ParaSite Database (https://www.wormbase.org/). Protein family (Pfam) groups were determined

by   NCBI   BLASTn   using   default   parameters   (nr/nt)
(https://blast.ncbi.nlm.nih.gov/Blast.cgi?PAGE_TYPE=BlastSearch). Life cycle stage
*was taken from [211], and [265]. Significance * denoted adjusted Z-score p values <0.05, ns*
= non-significant and na = non-applicable (significance in round 2 testing could not be
determined due to unforeseen circumstances in the JCU Cairns Animal Facility).

3.3.10 Histological Assessment of Top Twenty Cell-Free Lysates in TNBS Colitis

The colon tissue from mice that received the top twenty cell-free lysates was processed for hispathology to establish whether the histopathological score was in congruence with the other colitis parameters tested. Transmural lesions are a characterisitic hallmark of TNBS-induced colitis and are characterised by infiltration of leukocytes into the mucosa and submucosa[322]. Tissue damage peaks at day 3 post-TNBS administration when neutrophils infiltrate the submucosal layers and this is associated with ulcerations, bowel wall thickening and loss of goblet cells throughout the colon.

In agreement with the overall prophylatic ranking, the top ranked lysate 13 showed the lowest levels of histopathology. The other lysate proteins with low histopathology scores were lysate 15 (ranked 13th) and lysate 11 (ranked 17th). A representative mouse from the no treatment group (naïve), the negative control group (non-recombinant lysate) and lysate group 13 have been presented (Figure 3-16). Mice in the naïve group that did not receive TNBS displayed normal gut architecture, whereas the negative control group that received non-recombinant lysate and TNBS displayed signs of severe colitis, shown by the major disruption of general gut architecture, loss of epithelial integrity, sub-mucosal oedema, loss of goblet cells and marked evidence of leukocytes and polymorphonuclear inflammatory cell infiltrates in the LP. Finally, the gut architecture of a representative

mouse treated with hookworm recombinant protein lysate 28 displayed substantially less

damage than that of the colitic control mouse, with normal gut architecture and mucosal

integrity, the presence of goblet cells, and well-formed crypts.

A) Naïve (Untreated Control)

Normal goblet cells →

B) Recombinant Protein-Free Lysate + TNBS Treatment

Loss of goblet cells →

Cellular infiltration →

Thickening of muscular layer →

Damaged mucosa & loss of epithelial integrity

C) Hookworm Protein Lysate 28 + TNBS Treatment

Presence of goblet cells →

Reduced cellular infiltration →

Maintained mucosal layer and epithelial integrity

Figure 3-16 Representative histology micrographs stained with H&E (x20) of distal colons. A) Naïve, No Treatment; B) TNBS + Negative Control Empty Vector Lysate; C) TNBS + Hookworm Recombinant Protein Lysate 28 and scale bar = 50 µm.

124

3.3.11 Blinded Histopathological Score Confirmed Ranking of TNBS-Screen Results

H&E stained slides were scored for pathology by an individual blinded to the experimental group. Tissue sections were scored on a scale of 0 to 5 for each of the following parameters; (1) epithelial pathology (crypt elongation, hyperplasia, erosion), (2) mural inflammation and (3) oedema for an overall maximal total histology score of 15 (Table 3-4). In this example experiment, mice treated with lysates 11, 13, and 15 were protected from colitis denoted by their significantly reduced histopathology scores.
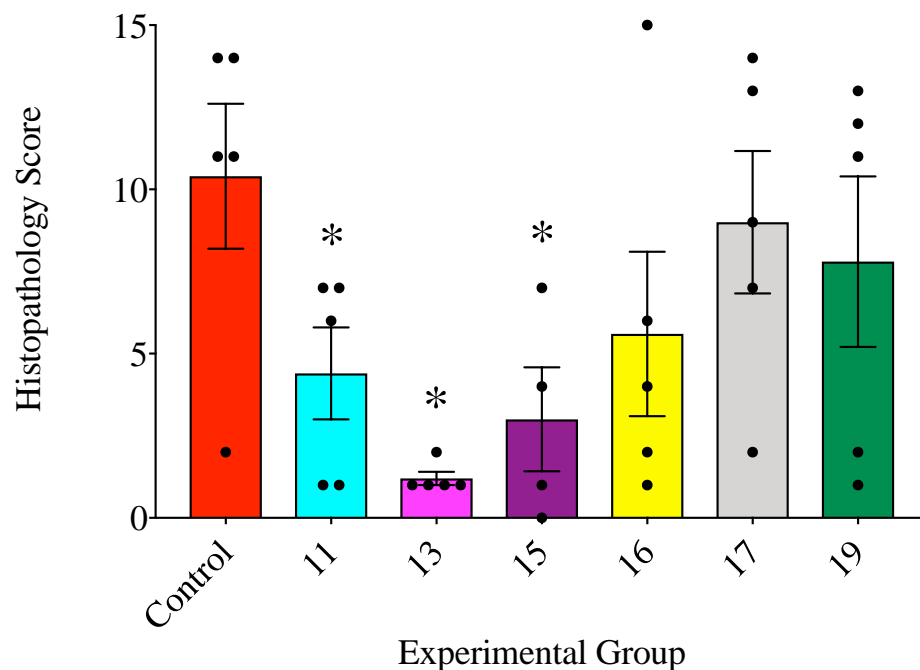
Figure 3-17 Aggregate blinded histopathology scores of H&E slides from lysate containing protein groups against experimental control. Control mice received non-recombinant cell-free lysate followed by TNBS, and the remaining experimental groups received hookworm protein containing lysate followed by TNBS. All individual data points are represented, mean ± SEM and sample size (n = 5 mice / group). Significance was determined by statistical comparisons assessed using Mann-Whitney U test against the control group and was adjusted for multiple testing. * p ≤ 0.05.

3.3.12 Histopathological Score Normalised to the Negative Control Group Highlights Trends of Reduced Histopathology of Defined Recombinant Protein Lysates

In order to compare multiple histopathological scores across separate experiments, the histopathological score of each hookworm recombinant lysate was normalised to its experimental control (Figure 3-18). There was obvious marked variablity within some hookworm recombinant lysate groups however it was clear that lysates 13, 15, 23, 28, and 80 displayed a trend towards diminished histopathology which correlated with their Z-scores and intra-experimental geometric mean p values.
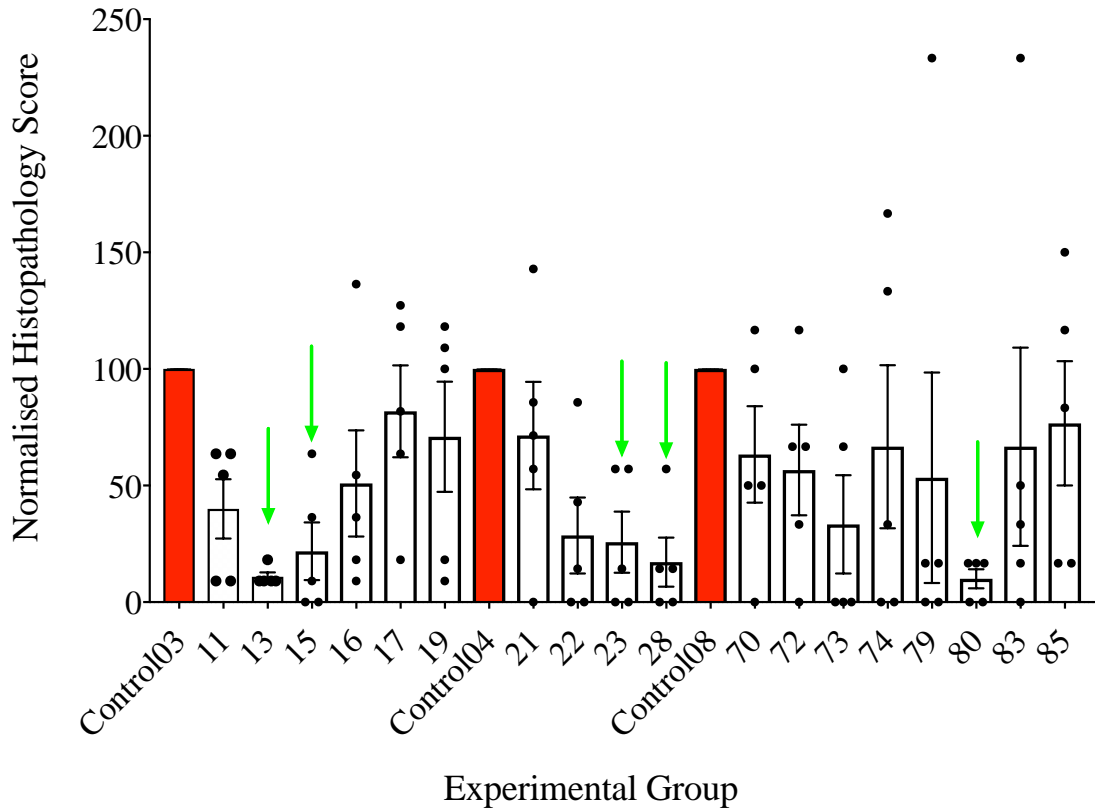
Figure 3-18 Histopathology scores normalised to the negative experimental control group in each experiment of TNBS colitis screen. Green arrows denote promising candidates by blinded histological analysis. Control 03, control 04, control 08 denotes groups of mice that received non-recombinant cell-free lysate followed by TNBS in three separate experiments. The remaining experimental groups received hookworm recombinant protein containing lysates followed by TNBS and histopathology scores were normalised to the control in each experiment. All individual data points of normalised hookworm recombinant lysate scores are represented, mean ± SEM and sample size (n = 5 mice / group).

3.4 Discussion

In this chapter, as many as twenty different hookworm recombinant protein-containing cell-free lysates protected against the onset of inducible TNBS-colitis. The empty vector cell-free lysate expressing GFP without a hookworm protein fusion partner (used as the negative control) did not have any protective properties in this model, suggesting that it was the hookworm recombinant proteins that conferred protection. The degree to which each lysate performed was ranked by significance of efficacy based on four key parameters that reflect disease status in TNBS-induced colitis in mice; weight change, colon length, macroscopic score, and clinical score. Histopathological scoring was performed on colons from the groups of mice treated with lysates that were deemed significant hits by Z-score in order to confirm which lysates conferred protection in TNBS colitis.

The TNBS model of colitis used in this thesis was modified from the protocol as described by Cobos *et al.,* (2018)[191]. Clinically, the animals presented with an acute colitic flare consisting of rapid body weight loss, diminished natural curiosity and reduced attentiveness to grooming. These changes were recorded in a clinical score until day three. Negative control mice typically begin to recuperate after day three so it is at this point that the mice were euthanised and *post-mortem* measurements and tissues were acquired. The quality and integrity of the architecture of the colon was assessed for markers of pathology upon necropsy.

There were several advantages to using the TNBS model as a screening tool in this study, including the short timeframe of the model and the small quantity of test material

128

required for one single treatment per animal. This resulted in conservation of lysate samples which made the screen economically feasible and the ability to gauge whether a lysate conferred protection in a timely manner possible. This *in vivo* screen permitted over 100 hookworm recombinant proteins to be screened in a relatively short time frame by a single investigator.

The intra-experimental statistical method did not identify any new therapeutic hits that the Z-score method had not already detected, but it added an extra level of stringency and rigour to the analysis. Therefore, it can be deduced that the Z-score method didn't miss any hits but produced more signficiant hits as it is less prone to FDR exclusions because fewer rounds of multiple testing are performed.

The three top ranked anti-colitic proteins identified by the TNBS colitis lysate screen were members of the SCP/TAPS protein family (Pfam accession number PF00188, InterPro IPR014044). Indeed, twelve of the top twenty protein hits were SCP/TAPS. There is a degree of uncertainty regarding whether SCP/TAPS have an evolutionarily conserved function, i.e. immunoregulation, or whether the SCP domain has a versatile capacity to perform distinct functions[294]. The most protective protein identified in the TNBS screen was ANCCAN_22177 that had been previously identified in adult *A. caninum* ESP by Mulvenna *et al.,* (2009)[211] but has not been further explored to our knowledge. Based on Z-score, the second-most protective protein from the screen was *Ac*-ASP-2 (ANCCAN_00478). *Ac*-ASP-2 generated significant protection against TNBS colitis in TNBS-1 but not in TNBS-2. *Ac*-ASP-2 is a dominant protein secreted by the infective larval stage of *A. caninum* upon transition from free-living to parasitic larvae, but further work must be undertaken to elucidate its immunoregulatory properties[270]. An

interesting aside is that a homologue of *Ac*-ASP-2 from the human hookworm *N. americanus*, *Na*-ASP-2, was shown to bind to CD49A on B cells and suppressed expression of genes involved in B cell signalling[323], suggesting a possible role in supressing inflammatory responses mediated by B cells. The conserved homology between these two molecules could be used as a rationale to further investigate the mechanism of action of this anti-inflammatory response.

Lysate 11 was identified as the seventeenth ranked protein in TNBS-1 but did not induce significant protection in the confirmation study TNBS-2. This protein is a member of the cysteine-rich secretory protein (CRISP) superfamily which contain many SCP/TAPS-like proteins. Lysate 11 is known as neutrophil inhibitory factor (*Ac*-NIF or ANCCAN_04194) and has been previously reported to be a glycoprotein ligand of the integrin CD11b / CD18 that inhibited neutrophil function[324]. Ligation of *Ac*-NIF to CD11b prevented neutrophil accumulation and reduced adhesion of neutrophils to human endothelial cell monolayers. The discrepancy between the two TNBS colitis trials might be due to the administration of different quantities of recombinant proteins to mice between trials, an unavoidable issue with the high-throughput nature of the approach used herein where unpurified cell lysates are prepared immediately before administration to mice. Moreover, cysteine-rich proteins such as SCP/TAPS are likely relatively unstable when expressed in a cell-free system where a reducing environment and the secretory organelles required for optimal folding and processing are absent.

The eleventh- and sixteenth-most significant hits were the TIMP-like proteins *Ac*-TIMP-1 (also known as *Ac*-AIP-1) and a previously unreported netrin domain-containing protein. *Ac*-AIP-1 has previously been expressed in yeast and was shown to be anti-

inflammatory in TNBS colitis[194]. Identification of this protein from the cell-free lysate screen validates the *in vivo* screening approach adopted herein for discovery of anti-inflammatory proteins using unpurified lysates. Furthermore evidence of the use of AIPs as anti-inflammatory therapeutics draws on data from a homologue of *Ac*-AIP-1, named *Ac*-AIP-2 which has been shown to induce FOXP3+Tregs in a mouse model of lung inflammation that re-established homeostasis[207]. The twelfth most significant hit possessed no known putative conserved domains and is a nematode-specific protein (ANCCAN_01926). The remaining hits belonged to multiple different Pfam protein families included a lysozyme-like protein, two TTR-like proteins, and a retinol-binding protein.

In the literature there has been considerable attention granted to lyzozymes in IBD. Expression of mammalian antimicrobial lysozyme C is upregulated in patients with UC and in organoids cultured from patients with UC compared to non-IBD controls[325]. Faecal lysozyme is used as a biomarker in the assessment of disease severity in IBD[326]. In UC, lysozyme is over-expressed by Paneth cells and gastric epithelial cells and is potentially produced by DCs and macrophages in the inflamed mucosa[325]. Furthermore, there is a correlation between lysozyme over-expression and abnormal or metaplastic changes in Paneth-like cells that potentially lead to stem cell alterations in the epithelium that may contribute to permanent pathological changes to patients with UC[326]. Lysozyme C is barely detectable in epithelial cells of non-IBD controls and interestingly it is down regulated in patients with UC in remission[325]. Therefore, the results of a trial where hen egg lysozyme was shown to protect against inflammation in a porcine model of DSS colitis and its ability to down-regulate gene expression of pro-inflammatory cytokines and up-regulate expression of TGF-β and IL-4 resulting in the restoration of immune

homeostasis are quite remarkable and counter-intuitive[327]. The reduction of innate cell pro-inflammatory cytokines, in conjunction with an up-regulation of anti-inflammatory cytokines indicates a restoration in gut homeostasis that may be potentially due to increased activation of Treg cells. Lysozymes are antibacterial proteins that break down peptidoglycans on Gram-positive bacteria, so perhaps the hookworm lysozyme (ANCCAN_07322) impacted on the microbiota to promote a regulatory phenotype to resolve TNBS-induced colitis? This hypothesis clearly now warrants further investigation.

The seventh- and fourteenth-most significant hits were TTR-like proteins. Much attention has been afforded to nematode TTR-like proteins in the literature due to their ability to be broken down into subunits that bind to host reserves of vitamin A, retinol[305],[306]. TTRs are carrier proteins that bind to lipocalin retinol-binding proteins (RBP). RBP have the ability to bind to retinol and the RBP-TTR complex is hypothesised to interact with specific target cells that require retinol which is then converted to retinoic acid[329]. Retinoic acid has been shown to synergise with TGF-β to induce FOXP3+ Tregs, so secretion by a hookworm of a TTR-like protein into host tissue might promote the uptake of vitamin A to enhance turnover of retinoic acid and promote the induction of Tregs[330]. Parasite TTR-like proteins could potentially form complexes with RBPs that bind to and sequester retinoic acid, making it unavailable so that more is produced by the host, or alternatively parasite-derived TTR-like proteins could be delivering retinol to specific target cells and inducing a regulatory phenotype, mediating peripheral tolerance and suppressing other inflammatory cells. A mechanism by which a therapeutic protein can induce Tregs from naïve T cells would be an appealing therapeutic avenue.

The tenth-most significant anti-colitic protein was a parasite-specific fatty acid- and retinol- binding (FAR) protein, *Ac*-FAR-2. These α-helix rich lipid-binding transporter proteins interfere with the delivery of bioactive lipids or can sequester lipidic intermediates, and interference with these processes can regulate the host immune response[309]. A FAR protein from the hookworm *A. ceylanicum* (*Ace*FAR-1) has been characterised and was shown to bind to low micromolar range fatty acids *in vitro*, further validating the likelihood that these proteins are implicated in obtaining host-derived fatty acids for the parasite.

In summary, twenty hookworm recombinant protein lysates were deemed prophylactically protective in a screen of the *A. caninum* cell-free recombinant secretome using the mouse model of TNBS colitis across multiple pathological parameters.

3.5 Conclusion

In summary, these results are notable for several reasons. First and foremost, a pipeline has been defined for identification of novel anti-inflammatories in a mouse model of TNBS-induced colitis, and this was achieved in a relatively short time period. 104 proteins were expressed and screened in just six months. This finding has ramifications for the drug discovery industry because it has the potential to accelerate the discovery of protein-based therapeutics using an *in vivo* clinical / pathological outcome rather than screening using an *in vitro* method that requires pre-selection of a defined mechanism of action. Furthermore, new intellectual property with commercial potential has been discovered; drugs with potential therapeutic efficacy in IBD. Encouraged by these results, in the next chapter the top twenty candidates were taken forward through the drug development pipeline and produced in an eukaryotic cell-based protein expression system, *P. pastoris*, and the purified proteins tested for anti-colitic efficacy in both acute (TNBS) and chronic (T cell transfer) murine models of colitis.

Chapter 4

Expression of Lead Proteins in Yeast and Validation in TNBS and T Cell Transfer Models of Colitis

4.1 Introduction

Of the top prophylatic hits identified in chapter 3, a select group of proteins were chosen for cell-based protein expression and purification in a eukaryotic system. In order to cast a wide net, and considering the time constraints of this project, an attempt was made to strike a balance between (i) including proteins from different families (based on Pfam categories) and (ii) ensuring that the most highly represented family of proteins – SCP/TAPS – were well represented in terms of distinct molecular groups within that larger family.

The different families of proteins chosen for cell-based expression were a fatty acid/retinol binding protein, a TIMP-like protein and at least one member of the SCP/TAPS family. Eleven of the top twenty hits belonged to the SCP/TAPS family, so one of the aims of this chapter was to use a phylogenetic rationale to justify selection of representative proteins for cell-based expression. Most of the SCP/TAPS proteins identified were members of ASP sub-group. Hookworms secrete ASPs with both single and double PRP domains[212] (Figure 4-1); single domain proteins contain a signal peptide, a PRP domain and a cysteine-rich hinge region, whereas double domain proteins contain a signal peptide, two PRP domains and two cysteine-rich hinge regions. Apart from their domain organisation, there has been further work on the classification of *A. caninum* ASPs based on the presence of two conserved histidine residues (at His-69 and His-129 based on the numberings of *Ac*-ASP-7) which has been proposed to be the metal binding site of the protein[331]. These conserved histidines have allowed ASPs to be grouped into three phylogenetic clades[283]. Group 1 proteins possess His-69 and His-129, group 2 proteins lack both His-69 and a conserved amino acid sequence preceding N-terminal

136

PRP motif, while group 3 lack both His-69 and His-129. Little is known about their function, however crystal structures[331],[332] and subsequent 3D modelling suggests that they possess an equatorial groove containing the conserved histidine residues that may bind to extended structures, such as peptides or glycans[333].
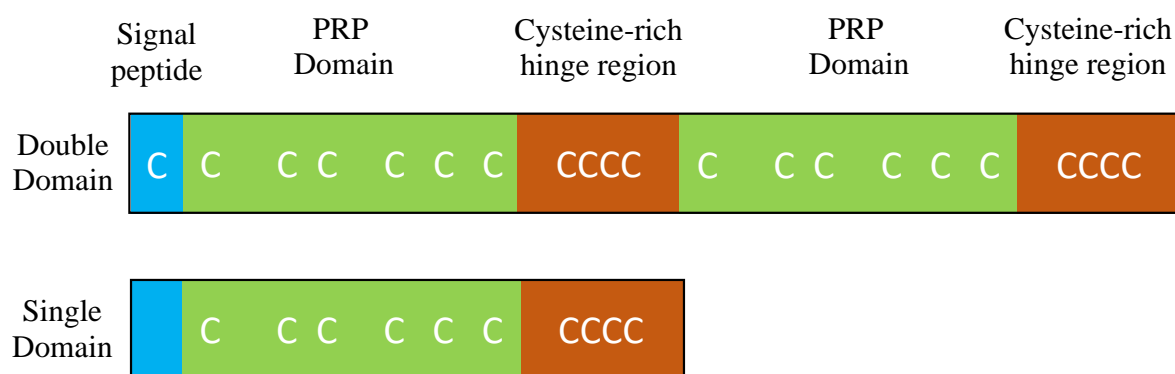
Figure 4-1 Double versus single PRP domains of SCPs. Adapted from[211].

Another protein family identified in the TNBS cell-free lysate screen was the fatty acid / retinol binding protein (FAR) family. This lipid-binding protein family is exclusively expressed in nematodes and has been hypothesised to interfere with cell to cell signalling processes[307]. Two TIMP-like proteins were identified in the TNBS cell-free lysate screen. *Ac*-TIMP-1 was chosen for cell-based expression because it has been previously shown to be anti-inflammatory in TNBS colitis[194]. To further assess its drug-like properties, *Ac*-TIMP-1 was selected to reproduce earlier findings in the TNBS model and to conduct further investigation including assessment in the T cell transfer model of chronic colitis and *in vitro* human cell cytokine analyses.

Once the cell-based expression candidates were chosen, the second aim of this chapter was to express and purify them in the *P. pastoris* yeast expression system and determine

whether they retained the anti-inflammatory efficacy displayed by their cell-free lysate counterparts in TNBS colitis, as well as the more human IBD relevant T cell transfer colitis model. The TNBS-induced model and the T cell transfer model are widely recognised experimental models of colitis that have aided in delineation of the immunological mechanisms of disease pathogenesis. However, the T cell transfer model is the most similar to human disease in terms of colonic gene expression changes[99]. In mice with TNBS colitis and CD45Rb (high) T cell transfer colitis, 21 and 582 genes were up-regulated more than two-fold, respectively, in the gastrointestinal mucosa compared to wild type mice[99]. The expression profiles were compared to a database of genes that are known to be up-regulated in human IBD (Figure 4-1-3), and the T cell transfer model was shown to most closely resemble human disease in terms of the numbers and identities of genes that underwent differential expression. I therefore selected this model to validate and further prioritise lead hookworm recombinant proteins for treating colitis.

This chapter outlines the experimental protocols and procedures used throughout the course of this section of this thesis in line with the research aims. In addition, this chapter presents the results and discusses the experimental strategy and statistical analyses for the project. Research aims are;
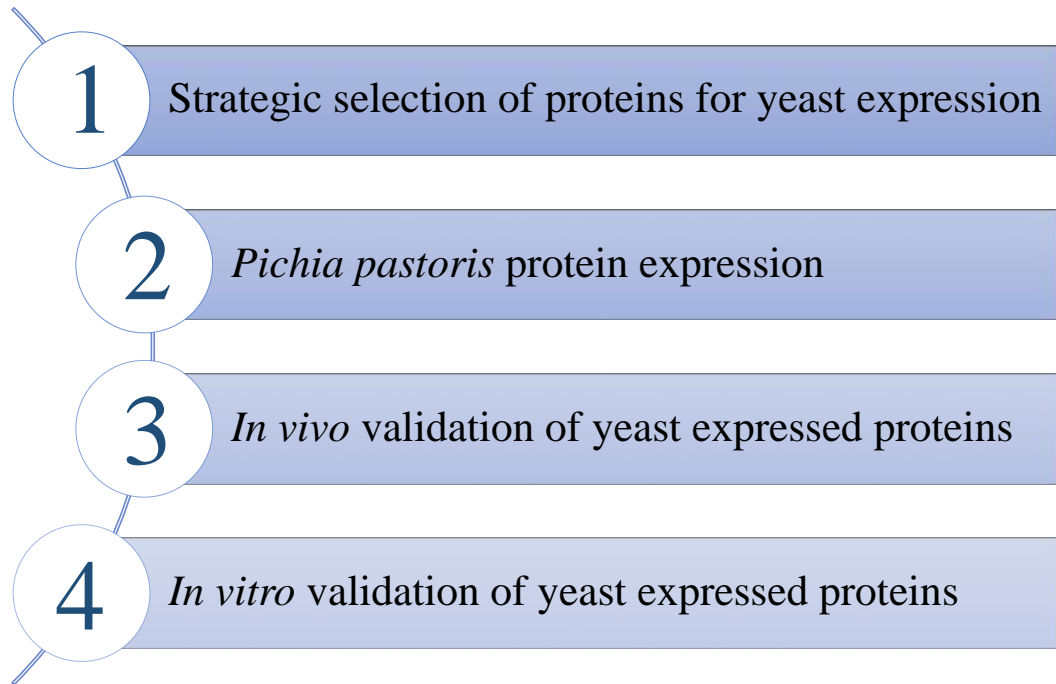
Figure 4-2 Research aims of chapter 4.

In this chapter, the work up of three proteins identified as potential therapeutic leads from the cell-free lysate protein screen in TNBS-induced colitis has been presented. Once the cell-based recombinant ES proteins were tested for efficacy in the two *in vivo* models of colitis, the next stage in therapeutic development was to ascertain their bioactivity on cytokine secretion by human PBMCs. The workflow followed in this chapter is detailed below.
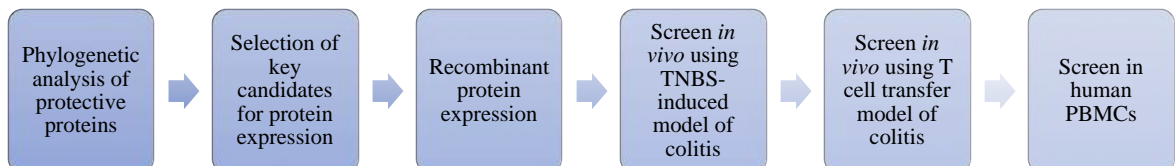
Figure 4-3 Chapter workflow in line with research aims.

This proposed workflow was designed to generate important pre-clinical data to allow early assessment of hookworm protein candidates and rank them for progression into formal pre-clinical development, and ultimately towards human clinical trials. The results from Chapter 3 (cell-free lysate TNBS screen) were corroborated herein using proteins produced in an expression system that is commonly used by biopharmaceutical companies to make therapeutic proteins.

4.2 Materials and Methods

4.2.1 Hookworm Recombinant ES Protein Expression in *Pichia pastoris* Expression System

The nucleotide sequences of the selected hookworm proteins for eukaryotic expression were verified, cloned into the relevant vector, and electroporated into yeast for protein production and purification as per the workflow (Figure 4-4).
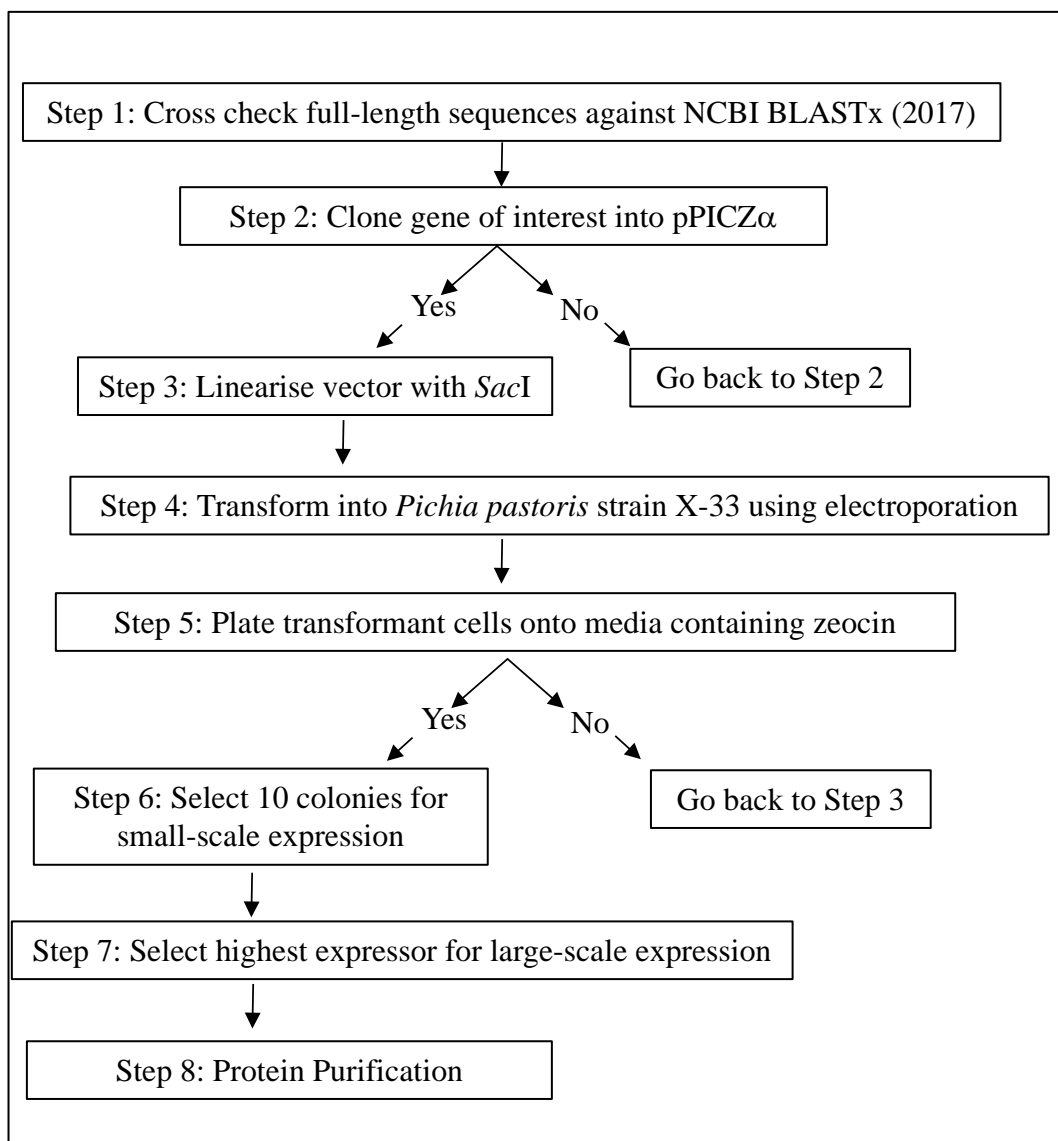
Figure 4-4 Overview of protein expression protocol in the P. pastoris yeast expression system.

4.2.2 Sequence Analysis

All of the top eleven SCP/TAPS proteins identified in TNBS cell free lysate screen were considered based on their phylogenetic diversity. The FASTA sequences from the SCP/TAPS leads, as well as members of all three ASP groups (sourced from the literature), were converted into Newick file format. The Newick files were used by the online software tool iTOL (Interactive Tree of Life), and aligned for a phylogenetic analysis.

4.2.3 Protein Structure Modelling

Protein structures of selected candidates were modelled using I-TASSER protein structure and function prediction software, which involved: reading template identification, iterative structure assembly simulation, model selection and refinement, and structure-based function annotation[334]. The highest ranked reading templates for the models of *Ac*-NIF, *Ac*-FAR-2 and *Ac*-TIMP-1 were based on the structures of *Na*-ASP-1 (PDB code 3NT8), *Na*-FAR-1 (PDB code 4UET) and human TIMP-3 (PDB code 3CKI), respectively. The models with the highest C-scores were chosen for display, and corresponded to values of -0.81 for *Ac*-NIF, 0.48 for *Ac*-FAR-1 and -0.73 for *Ac*-TIMP-1. The C-score represents the confidence in the model; values are typically in the range -5 to 2, and higher values correspond to models with higher confidence.

4.2.4 Cloning and DNA Propagation of Sequences

Plasmids (pPICZαA – Sigma-Aldrich V19520) containing ORFs that were codon optimised for yeast expression were synthesised by GENEWIZ®, U.S.A. Lyophilised DNA was re-suspended in Type 1 ultrapure H_2O at 10 ng/μL. *E. coli* DH5α strain was heat shocked to transform the recombinant plasmids into cells. One (1) μL of plasmid

DNA (10 ng/μL) was transformed into 50 μL of chemically competent (CaCl$_2$) *E. coli* DH5α cells and incubated on ice for 20 minutes. The reaction was incubated at 42 °C for 45 seconds and was immediately incubated on ice for two minutes. Five hundred (500) μL of low salt LB broth was aseptically added to the reaction and incubated at 37 °C for one hour with shaking at 150 RPM. The transformation reaction was centrifuged at 11,000 *g* for two minutes, supernatant was discarded and the pellet re-suspended in 200 μL of low salt LB broth. The mixture was then plated on low salt LB agar plates containing 100 μg/mL zeocin. Plates were incubated at 37 °C in the dark overnight. Transformant colonies were picked to inoculate 5 mL LB low salt medium containing 50 μg/mL and incubated at 37 °C with shaking at 150 RPM overnight. Recombinant plasmids were purified from overnight cultures using an ISOLATE II Plasmid Mini Kit (BIOLINE) as per the manufacturer's instructions.

4.2.5 Restriction Endonuclease Digestion

Isolated DNA plasmids were subjected to restriction endonuclease digestion (Table 4-1) and reactions were incubated overnight at 37 °C in a water bath.

Component	50 μL Reaction
Plasmid DNA	5 μg
*EcoR*I (New England Biolabs R01456S)	1 μL
*Xba*I (New England Biolabs R0101)	1 μL
Cutsmart buffer (10x) (New England Biolabs)	50 μL

Table 4-1 Components required for the restriction endonuclease digestion of pPIC-ZαA plasmid DNA.

The reaction was subjected to 1 % agarose gel electrophoresis for 30 minutes and stained with ethidium bromide. The digested band of DNA was excised and purified from the agarose gel using an ISOLATE II PCR and Gel Kit (BIOLINE) as per the manufacturer's instructions.

4.2.6   Ligation of Recombinant Sequences into pPICZαA Vector

Purified DNA inserts were ligated into pPICZαA at the restriction sites *EcoR*I and *Xba*I in the alcohol oxidase (AOX1) promoter region as per (Figure 4-5) below.
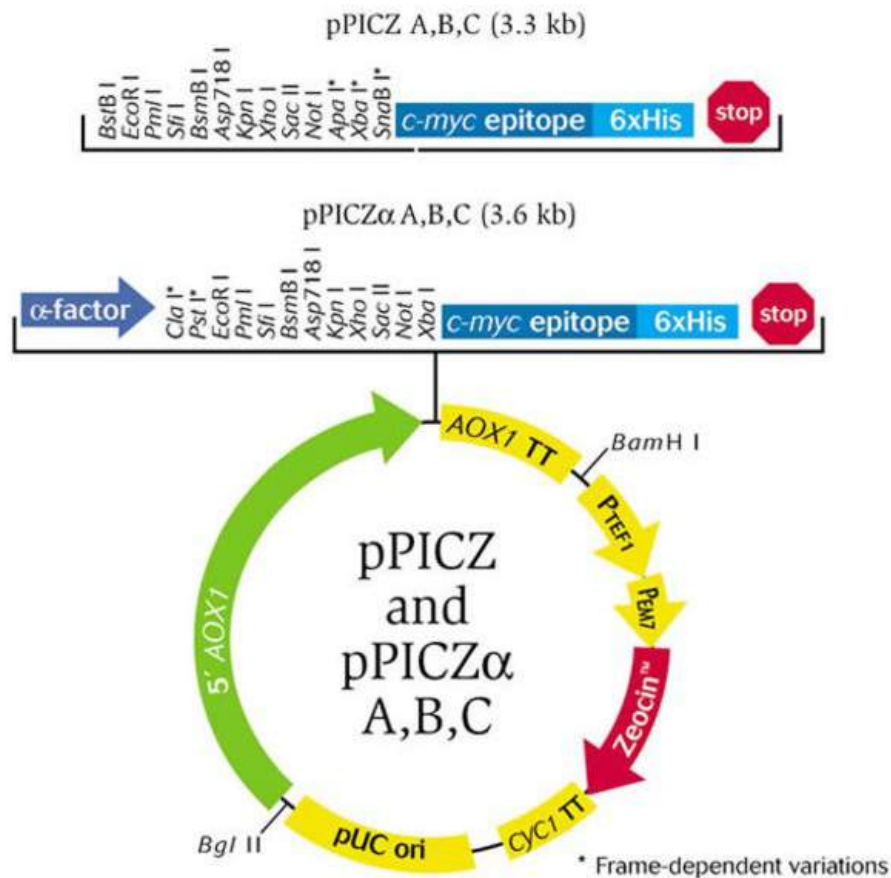
Figure 4-5 pPICZαA zeocin plasmid map containing cDNA of genes of interest. Taken from EasySelect™Pichia expression kit protocol (Invitrogen™K1740-01).

144

The online tool NEBioCalculator (v1.7.1) was used to calculate the DNA insert to vector ligation ratio. Ligation reactions were made up to 20 µL in Type 1 ultrapure H_2O (Table 4-2) and incubated at 24 °C for 3 hours.

Component	20 µL reaction
T4 DNA Ligase Buffer (10x) (NEBiolab B0202S)	2 µL
T4 DNA Ligase (NEBiolab M0202)	1 µL
Gene of interest DNA	5 µg
pPICZαA (Sigma-Aldrich V19520)	1 µL (100 ng)

Table 4-2 Components required for the ligation of DNA in pPICZαA plasmid.

Ten (10) µL of ligation reaction was added to *E. coli* DH5α cells and the transformation protocol was conducted as per section 4.2.4. Ligation mixture was plated onto a low salt LB agar medium plate containing zeocin at 50 µg/mL and incubated at 37 °C in the dark overnight. Transformant colonies were picked to inoculate 50 mL low salt LB broth containing zeocin at 50 µg/mL and incubated at 37 °C at 150 RPM overnight. Plasmids were purified using an ISOLATE Plasmid Mini Kit (BIOLINE) as per manufacturer's instructions. The protocol was amended to increase the quantity of isolated DNA 10-fold to produce approximately 10 µg plasmid DNA. Linearisation of plasmid DNA was performed by restriction endonuclease digestion using *Sac*I-HF as per section 4.2.4 including the following amendments: combined, 2 µL *Sac*I-HF restriction enzyme (NEBiolab R3156) with 6 µL of 10 X CutSmart Buffer and 10 µg plasmid DNA for a total reaction volume of 60 µL in Type 1 ultrapure H_2O. The linearised plasmid was

145

precipitated using an ISOLATE PCR and Gel Kit (BIOLINE) as per the manufacturer's instructions.

4.2.7   Electroporation of Recombinant Expression Plasmid into *P. pastoris*

The protocol for the preparation of *P. pastoris*-expressed recombinant proteins was followed as per instructions below. Yeast were grown using aseptic techniques at a growth temperature of 28- 30 °C and $OD_{600} = \sim 5 \times 10^7$ cells/mL. A glycerol stock of the reconstituted prototrophic X-33 strain of *P. pastoris* with a wild-type genotype and phenotype (sourced from Life Technologies) was streaked onto yeast extract peptone dextrose (YPD) agar plate and incubated at 30 °C overnight. A single colony was used to inoculate a 50 mL tube containing 5 mL YPD broth incubated at 30 °C at 150 RPM overnight. Fresh YPD medium (245 mL) was inoculated with 25 µL of overnight culture in a 2 L aerated baffled shake flask and incubated at 30 °C at 150 RPM overnight to an $OD_{600} = 1.3 - 1.5$. The culture was then centrifuged at 2,000 *g* at 4 °C for 20 minutes. The supernatant was discarded and the pellet was re-suspended in 250 mL of ice cold sterile H_2O. Repeated centrifugation and H_2O wash steps were conducted. The supernatant was discarded and the cell pellet was resuspended with 20 mL of ice cold 1 M sorbitol. The cells were centrifuged at 2,000 *g* at 4 °C for 20 minutes. The supernatant was discarded and the cell pellet was re-suspended in 2 mL of ice cold 1 M sorbitol which produced a final volume of 4.5 mL.

For electroporation, 10 µL of linearised plasmid was added to an ice cold electroporation cuvette (0.2 cm path length; BIO-RAD™ 1652086) followed by the addition of 80 µL of competent *P. pastoris* cells. The cuvette was incubated on ice for 5 minutes and subjected

to electroporation using a BIO-RAD™ Gene Pulsar Xcell system (*P. pastoris* setting).

Cells were immediately re-suspended in 1 mL ice cold 1 M sorbitol and the mixture was

transferred to a 15 mL tube and incubated at 30 °C without shaking for 3 hours. Two

hundred (200) μL of cells were plated on YPD agar with 500 μg/mL zeocin. Plates were

incubated at 30 °C for 5 days in the dark. Transformant colonies from the YPD agar 500

μg/mL zeocin plates were patched onto YPD agar with 2 mg/mL zeocin and incubated

at 30 °C for 5 days in the dark.

4.2.8 Yeast Colony Polymerase Chain Reaction (PCR)

Five to ten of the zeocin-resistant *Pichia* transformants were selected and the presence

of insert integrated into the *Pichia* genome was confirmed using PCR. The yeast

transformant colonies were re-suspended in 20 μL H_2O, and 10 μL was transferred to 20

μL of 20 mM NaOH and incubated at 95 °C for 30 minutes then centrifuged at 2,000 *g*

for 5 minutes. Five (5) μL of DNA supernatant was used in a 25 μL PCR reaction.

The PCR reaction contained 1 μL forward primer (FP) (5' AOXI *Pichia* 5'-

gactgcttcaattgacaagc-3'), 1 μL reverse primer (RP) (3' AOXI *Pichia*

5'GCAAATGGCATTCTGACATCC-3'), 0.5 μL MyTaq polymerase (Bioline BIO-

21105), 5 μL Mytaq Red Reaction Buffer (Bioline BIO-3712), and 12.5 μL dH_2O.

Untransformed *Pichia* displayed a single band at 2.2 kb on an agarose gel whereas the

transformed inserts displayed two bands; one at 2.2 kb and one at the size of the gene of

interest (GOI).

PCR positive *Pichia* transformant colonies were picked with a sterile pipette tip and inoculated into 5 mL BMGY broth medium (Buffer recipe in Appendix 3) and incubated at 30 °C overnight. Cultures were centrifuged at 2,000 *g* for 5 minutes and the supernatant was discarded. The pellet was re-suspended in 5 mL of BMMY broth and incubated at 30 °C overnight. Twenty-five (25) µL of 100 % methanol was added at 24 and 48 hour time points. Aliquots of 50 µL were taken at 0, 24, 48 and 72 hours and centrifuged at 2,000 *g* for 5 minutes. Supernatant was retained and stored at -20 °C for analysis by SDS-PAGE and western blotting.

4.2.9 SDS-PAGE Electrophoresis

Protein analysis by SDS-PAGE used 12-well gel cassettes composed of 4 % stacking and 12 % separation gels except where otherwise stated. Thirty (30) µL of protein sample was mixed with 10 µL 4x SDS-PAGE loading dye and the mixture was incubated at 95 °C for 10 minutes on a heat block. Thirty (30) µL of loading sample was applied to each well of the gel cassette and an additional lane was included that contained 7 µL of 10-180 kDa PageRuler™ Prestained Protein Ladder (ThermoFisher Scientific™ 26616). A c-myc-tagged recombinant protein was included on the gel as a positive control protein for quality control purposes. Cassettes were submerged in 1x SDS-PAGE Tris-glycine running buffer in an assembled negative electrode chamber. Electrophoresis was conducted at 125 V for 90 minutes.

4.2.10 Coomassie Brilliant Blue Protein Staining

Following electrophoresis, the polyacrylamide gel was removed from the cassette and incubated in 0.3 % Coomassie Brilliant Blue stain on a platform rocker for two hours.

Following staining, the gel was removed and incubated in a de-staining solution (40 % methanol, 10 % glacial acetic acid and Type 1 ultrapure H_2O) overnight.

4.2.11 Electrophoretic Transfer of Proteins from Polyacrylamide Gels to Nitrocellulose Sheets

After SDS-PAGE, polyacrylamide gels were removed from their cassettes and placed in a cartridge that contained a sandwich of four layers of chromatography paper with the gel adjacent to the nitrocellulose membrane in the centre. The cartridge was submerged into an XCell SureLock™ transfer chamber containing western blot transfer buffer (25 mM Tris, 192 mM Glycine, pH 8.3, 0.25 % SDS, 20 % methanol) that was assembled as per the manufacturer's protocol and subjected to a constant voltage of 100 mA for 60 minutes.

4.2.12 Western Blotting

After the proteins were transferred from the polyacrylamide gel onto the nitrocellulose membrane, the membrane was incubated in blocking buffer (5 % BSA in PBS / 0.05 % Tween-20 (1 X PBS-T)) at 4 °C overnight. The membrane was washed in 1x PBS-T for 10 minutes three times and incubated in 1:5,000 monoclonal anti-c-myc mouse mAb (Sigma-Aldrich M4439) in 1x PBS at 4 °C overnight. The primary antibody was removed and the membrane was washed twice in PBS-T and once with PBS for 10 minutes each. Blots were incubated with an anti-c-myc antibody (ThermoFisher Scientific™ R951-25) at 4 °C for 1 hour. The secondary antibody was removed and the membrane washed as described above. The membrane was developed by the addition of ECL™ Prime Western Blotting Detection Reagents (GE Healthcare Life Sciences RPN2232) as per the

manufacturer's instructions. A BIO-RAD™ VersaDoc Imaging System was used to visualise the membrane by UV trans-illumination.

4.2.13 Immobilised Metal Ion Affinity Chromatography to Purify Recombinant Proteins

An ÄKTA Start FPLC Chromatography System (GE Healthcare Life Sciences) was used to purify the recombinant protein from the yeast culture supernatant by Immobilised Metal Ion Affinity Chromatography (IMAC). A 5 mL HisTrap™ excel nickel column (GE Healthcare Life Sciences 17371206) was used with a linear 0-250 mM imidazole elution gradient at a flow rate of 5 mL/min. The purified 5 mL fractions were collected in 15 mL tubes and concentrated through an Amicon® Ultra-15, PLHK Ultracel-PL 3 or 10 kDa Membrane Centrifugal Filter unit (Sigma-Aldrich Z740210) by centrifugation at 3,000 g to produce a final volume of 5 mL. *Ac*-FAR-2 and *Ac*-TIMP-1 were buffer exchanged and concentrated using a 3 kDa molecular weight cut-off (MWCO) centrifugal filter and *Ac*-NIF was purified using a 10 kDa MWCO filter. Concentrated proteins were buffer exchanged by the addition of 15 mL sterile 1 X PBS to the protein and centrifuged at 3,000 g for 15 minutes and repeated five times to yield a final volume of 5 mL.

4.2.14 Quality Control of Purified Proteins

Validation of the expected molecular weight of the proteins in the eluate fractions was verified against the ÄKTA Start chromatogram and bands detected by SDS-PAGE and western blotting. Quantitation of protein was assessed using Pierce™ Bicinchoninic acid (BCA) Protein Assay Kit (ThermoFisher Scientific™ 23225) as per the manufacturer's protocol. LPS analysis was preformed using a QCL-1000™ Endpoint Chromogenic

Limulus Amoebocyte Lysate (LAL) Assay (Lonza 50-648U) for endotoxin detection as per the manufacturer's protocol. The above assays were visualised on a POLARstar Omega microplate reader (BMG Labtech) and conducted in BD Falcon® Clear 96-well flat bottomed Microtest Plates. Removal of endotoxin from proteins where required (in order for them to be suitable for cell culture and *in vivo* use) was performed using EndoTrap® HD Endotoxin Removal System (Hyglos 200053) as per the manufacturer's protocol.

4.2.15 Trypsinising Yeast Expressed Hookworm Recombinant Protein for Use as Negative Control

The following protocol was used for denaturation, trypsinisation and alkalinisation of *Ac*-FAR-2 for use as a negative control protein. *Ac*-FAR-2 was diluted into PBS at 1 mg/mL [207]. Protein was transferred to a 1.5 mL eppendorf tube to be trypsinised and alkalised. The sample was frozen at -80 °C and then freeze-dried at 300 *g* and 0 hPa using a ScanVac CoolSafe Freeze Dryer. Freeze-dried protein was re-suspended in 10 μL of 50 mM ammonium bicarbonate followed by addition of 1,4-dithiothreitol (DTT) to 2 mM final concentration (2 μL of 50 mM ammonium bicarbonate and 3 μL of 10 mM DTT). The sample was incubated at 60 °C for 20 minutes followed by addition of 2 μL of 55 mM iodoacetamide and 3 μL of 50 mM ammonium bicarbonate. The sample was incubated in darkness at 30 °C for 30 minutes followed by addition of DTT to 10 mM final concentration (2.5 μL of 50 mM ammonium bicarbonate and 2.5 μL of 100 mM DTT). The sample was incubated at 30 °C for 30 minutes then 800 μL of trypsin (25 μg/mL) was added. The sample was incubated overnight at 37 °C then 100 μL of 3 % formic acid was added. The sample was incubated at 37 °C for 30 minutes and then

diluted in 1 mL of sterile PBS and boiled for 4 hours at 100 °C. The efficiency of the

digestion of trypsinised/denatured (Td) protein was verified by SDS-PAGE and the

Td*Ac*-FAR-2 sample will now be referred to as denatured control.

4.2.16 TNBS-Induced Colitis Study with Yeast Expressed Recombinant Proteins

All protocols used for TNBS-induced colitis with yeast expressed proteins were as per

chapter 3 with the exception of the IP injection of yeast proteins at a concentration of 1

mg/kg body weight (mpk), equivalent to ~20 µg to a 20 g mouse.

Group	Treatment
1	Naïve
2	*Ac*-TIMP-1
3	*Ac*-FAR-2
4	*Ac*-NIF
5	Denatured Control

Table 4-3 Experimental groups for TNBS-Induced colitis experiment with yeast expressed hookworm recombinant proteins.

4.2.17 T Cell Transfer Colitis

All animal experiments were conducted under the parameters stipulated in the JCU

Animal Ethics Committee approved project #A2379. Male WT C57BL/6 mice aged

between 5 to 6 weeks and male RAG1$^{-/-}$ strain mice aged between 4 to 6 weeks were

purchased from the ARC in Perth, Western Australia. Mice were housed in accordance

with JCU animal rights and regulations under specific pathogen-free conditions (Cairns

Campus). Weights of all mice were recorded on arrival of mice and based on their weight, mice were equally distributed into groups (n = 6 mice per experimental group) based on power and sample size calculations and housed in plastic cages with unlimited access to food and water.

In this model, naïve T cells (CD4+, CD25-) from WT mice are transferred into recipient RAG1$^{-/-}$ mice, that are deficient in T and B cells. After 18 to 20 days the signs of gastrointestinal inflammation and colitis are observed and mice with active disease experience diarrhoea, weight loss and deterioration of general physical appearance. The recipient RAG1$^{-/-}$ mice were ear tagged and weighed twice weekly until weight loss was observed. The body weight and clinical score were recorded biweekly until day 18 after which weights were recorded every third day (Figure 4-6).
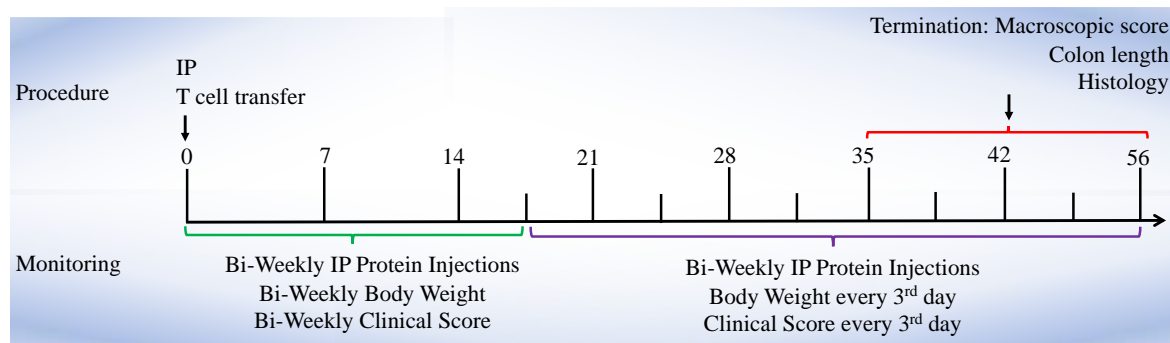
Figure 4-6 Schematic diagram of the T cell transfer colitis experiment.

The spleen, mesenteric lymph nodes (MLN), inguinal lymph nodes (iLN), and the brachial lymph nodes (bLN) were removed from C57BL/6 donor mice into 2 % fetal calf serum (FCS) RPMI-1640 Medium (Sigma-Aldrich R8755) using 15 mL falcon tubes. Cells were isolated from the harvested organs by pouring the contents into a gentleMACS™ C tube (Miltenyi Biotec 130-093-237) for tissue dissociation and

153

homogenised for 55 seconds. The tubes were centrifuged at 300 g for 1 minute at 4 °C. Contents were strained through a 70 μm Corning® cell strainer (Sigma-Aldrich CLS431750) and centrifuged at 450 g for 5 minutes at 4 °C. The supernatant was aspirated and pelleted cells were re-suspended in red blood cell (RBC) lysis buffer (Roche 11814389001) for 5 minutes. Lysed cells were washed with RPMI-1640 Medium and centrifuged for 5 minutes at 450 g at 4 °C. Pooled lymph node cell preparations were not treated with RBC lysis buffer but instead received 5 mL RPMI-1640 medium and were centrifuged at 450 g for 5 minutes at 4 °C. The supernatant was aspirated and pelleted cells were re-suspended in 2 mL RPMI-1640 Medium. Lymph node and spleen cell suspensions were combined, counted and their viability assessed using 0.04 % Trypan Blue Solution (ThermoFisher Scientific™ 15250061). Cells (~300 million) were centrifuged at 450 g for 10 minutes at 4 °C.

Isolation of CD4+ cells from other lymphocytes was performed using a EasySep Mouse™ CD4+ T cell Negative Selection Kit (STEMCELL Technologies: 191812A). Rat serum (200 μL, 1:200 dilution) was added to block Fc groups. CD4+ T cell Isolation Cocktail (200 μL) was added, mixed well and incubated for 10 minutes at room temperature. RapidSpheres provided in the kit were vortexed rapidly for 30 seconds and 300 μL (75 μL / 1 mL suspension) was added, mixed well and incubated for 2.5 minutes at room temperature. EasySep™ Magnet (STEMCELL Technologies 18000) purification allowed for isolation of the relevant cell type. The sample was centrifuged at 450 g for 5 minutes, supernatant was aspirated and the pellet re-suspended in a minimal volume of FACS buffer for flow cytometry.

4.2.18 Isolated Specific CD4+ Subset for *in vivo* Administration

All steps containing flow cytometry antibodies were conducted with minimal light and the plate was covered with aluminium foil for any incubation periods to avoid exposing antibodies to the light. The staining panel antibody cocktail was CD4: APC 1/300, CD25: PE 1/300. The cell pellet was re-suspended in the antibody cocktail and incubated on ice in the dark for approximately 30 minutes. Ten (10) mL of FACS buffer was added, centrifuged at 450 g for 5 minutes and the supernatant was discarded. The pellet was re-suspended in 5 mL of FACS buffer and strained into a filtered cap FACS tube and incubated on ice in the dark.

The population of CD4+CD25- cells was sorted (*Fig. 4.2.4*) and collected into 2 mL of 50 % FCS and RPMI-1640 medium. The sorted cells were centrifuged at 450 g for 5 minutes at 4 ºC to remove FCS and were re-suspended with sterile PBS (Sigma-Aldrich P3813) for the approximate volume for 4 million cells / mL in a 100 μL injection to RAG1$^{-/-}$ mice. A 26-gauge needle was used for i.p. injections to administer cells and 27-gauge needle was used for i.p. injections of hookworm recombinant proteins.

For T cell transfer experiments, an expression-matched negative control protein (recombinant human albumin - rHA) was used. This protein was thought to be a rigorous control due to its presumed inert effect on inducible colitis in mice and because it was expressed and purified in an identical fashion as the test hookworm recombinant proteins[335]. All recombinant proteins were administered bi-weekly (20 μg/mouse). One (1) mg of the α-mouse IL-12p40 mAb Clone C17.8 (BioXcell BE0051) was administered to each mouse once a week as a positive control for the treatment of T cell transfer colitis.

Cell transfer	Group	Number
No cells + PBS	Naïve	4
CD4+CD25- cells + αIL-12	Positive control 1	4
CD4+CD25- cells + rHA	Negative control	8
CD4+CD25- cells + *Ac*-TIMP-1	Experimental group 1	7
CD4+CD25- cells + *Ac*-NIF	Experimental group 2	5

Table 4-4 Experimental groups for T cell transfer colitis experiment with yeast expressed hookworm recombinant proteins.

4.2.19 Sacrifice and Tissue Collection

On the final day of the experiment, mice were euthanized by carbon dioxide asphyxiation and necropsied. The colon was removed and measured, photographic evidence was taken and the colon was necropsied (Figure 4-7).
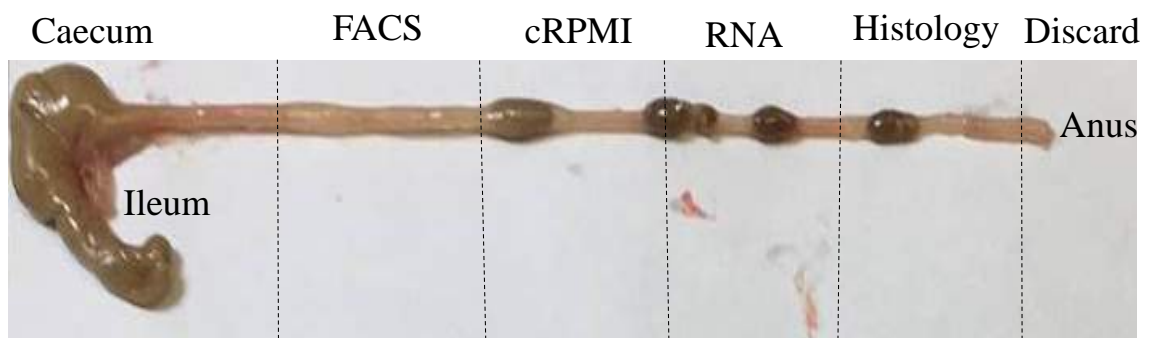
Figure 4-7 Diagram depicting colon sectioning protocol in T cell transfer colitis.

Colon tissue approximately 0.5 cm proximal to the anus was discarded and 0.5 cm sections were removed for histology and RNA extraction (RNAlater, Sigma-Aldrich

R0901), a 1 cm section was transferred to RPMI-1640 medium and the remaining 1-5 cm was stored in RPMI-1640 medium for FACS analysis.

The macroscopic pathology score was assessed by longitudinally sectioning the colon, washing the intra-rectal contents out with sterile PBS and assessing the tissue integrity under light microscopy (Olympus SX61, 0.67-45x). The parameters of the macroscopic pathology score that were assessed included the severity of bowel wall thickening, adhesion to internal organs and tissues, ulceration, and mucosal oedema (Table 3-3). The MLN were collected in 2 % FCS RPMI-1640 Medium.

4.2.20 Histology Procedure

Histological assessment was carried out as per the procedure outlined in sections 3.2.8 and 3.2.9 with the additional parameter of goblet cells. The goblet cell index was scored on a scale of 0-5 where a score of 3 represented a naïve healthy mouse colon, scores of 0-2 represented a loss of goblet cells and scores of 4-5 represented goblet cell hyperplasia. Significance was determined by statistical comparisons assessed using Mann-Whitney U test against the control group and was adjusted for multiple testing.

4.2.21 Isolation of Human Peripheral Blood Mononuclear Cells

To assess the impact of recombinant hookworm proteins on cytokine production by human immune cells, human blood was acquired from healthy volunteers by venepuncture. At the time of blood draw each donor gave written informed consent. The JCU Human Ethics Committee (Cairns, Australia) gave ethical approval for this research (H7010). PBMCs were isolated from peripheral blood using density gradient Ficoll-Paque media as per the manufacturer's instructions (isolation of mononuclear cells, GE

157

Healthcare, Bio-Sciences AB, Uppsala, Sweden). Vapour phase nitrogen was used to cryopreserve PBMCs until required. The culture media (R10) used for all PBMC assays contains the following; RPMI-1640 Medium, [-] L-Glutamine (Gibco 21870-076), 10 % FCS, and penicillin-streptomycin (100x) (Gibco 15140122). The selected cryogenic tube was removed from liquid nitrogen storage and sufficient cells were thawed for 100,000 PBMCs in 100 µL media/well. After the PBMCs were thawed, the freezing media was removed and the cells were resuspended in RPMI-1640 medium supplemented with 10 % FCS (R10) (ThermoFisher Scientific™) and DNase I Solution (10 µg/mL) (Stemcell 07900). Cells were incubated for 1 hour at 37 °C. Ten (10) µL of cells were diluted with 10 µL of Trypan blue stain 0.4 % (Gibco 15250-061) and counted on a haemocytometer. The cells were centrifuged at 450 *g* for 5 minutes at 24 °C.

For induction of T cell cytokines, a cell stimulation cocktail of 50 ng/mL of phorbol 12-myristate 13-acetate (PMA) (Sigma-Aldrich 79346) and 1 µg/mL of Ionomycin (Sigma-Aldrich 56092) was used to activate PBMCs. The immunoregulatory effects of hookworm recombinant proteins were assessed under three conditions: (i) unstimulated PBMCs; (ii) PMA-Ionomycin activated cells; (iii) LPS activated cells. For each condition, cells were resuspended in sufficient R10 media to allow for seeding of 100,000 cells in 30 µL per well of a round bottom 96-well culture plate (Corning® CLS3789). Unstimulated PBMCs were treated in triplicate with recombinant proteins (see below) or remained untreated.

For stimulation of myeloid cell-associated cytokines, 10 ng/mL LPS from *E. coli* o55:b5 for cell-culture γ-irradiated (Sigma-Aldrich L6529) was used to activate PBMCs. LPS-

stimulated PBMCs were treated with hookworm recombinant proteins or remained untreated.

Tissue culture plates were incubated at 37 °C and supplemented with 6.5 % CO_2 for 24 hours. Plates were centrifuged for 5 minutes at 450 g at 4 °C. Fifty (50) μL of culture supernatants were collected for cytokine analysis and stored at -80 °C. Ten (10) μL of supernatant was used for cytometric bead array (CBA) analysis.

Treatment Groups for CBA Analysis of human PBMCs

Untreated - R10 media only

PMA + Ionomycin

LPS

Cyclosporin A (CsA) (Sigma-Aldrich 30024)

Protein dosage was based on previous dose response work from our laboratory[194]:

Ac-TIMP-1 sample (100 μg/mL)

Ac-FAR-2 sample (100 μg/mL)

Ac-NIF sample (100 μg/mL)

Treatment Groups for CBA Analysis of human PBMCs with *Ac*-FAR-2

Untreated - R10 media only

PMA + Ionomycin

LPS

CsA

Dexamethasone (Dex) (Sigma-Aldrich D1756)

rHA (control)

159

Ac-FAR-2 sample (100 µg/mL)

4.2.22 BD™ Cytometric Bead Array

The BD™ Cytometric Bead Array (BD™ Biosciences 558265) was used to quantify the amount of IL-1β, IL-2, IL-6, IL-8, IL-10, IFN-γ, TNF and monocyte chemoattractant protein-1 (MCP-1) in a cell culture supernatant according to the manufacturer's protocol.

Cytokine	Catalogue No.
IL-1β	558279
IL-2	558270
IL-6	558276
IL-8	558277
IL-10	558274
IL-12/23p40	560154
IL-17A	560383
IFN-γ	558269
MCP-1	558287
TGF-β	560429
TNF	558273

Table 4-5 Cytokines detected in the human CBA kit with corresponding BD Biosciences catalogue numbers.

Master mix capture beads (MCB) were vortexed and resuspended thoroughly as per the manufacturer's instructions. Ten (10) µL of MCB was added to the appropriate wells of

160

a V-bottom 96 well plate. Ten (10) µL of standards and diluted samples were added to the appropriate wells and the plate was covered with foil, mixed for 5 minutes on a shaker and left to incubate for 1 hour at room temperature. The Master Mix PE Detection Beads (MDB) were prepared as below. Ten (10) µL of MDB were added to all wells of the V-bottom 96 well plate. The plate was covered with foil and mixed on a shaker for 5 minutes at room temperature then incubated at room temperature for 2 hours. One hundred (100) µL of wash buffer was added to each well and the plate was centrifuged at 800 g for 5 minutes. The supernatant was discarded and the pellet was resuspended in 80 µL of wash buffer for HTS analysis on a five laser BD LSRFortessa™X-20 (BD, Franklin Lakes, NJ, USA) using software version Diva 8.0.1. The concentration of cytokines in pg/mL was calculated using a comparison of the sample mean fluorescence intensity (MFI) to the cytokine standard curves using Analysis Software BD FCAP Array v3 version 3.0.19.2091. All the graphs and statistical analysis were performed using GraphPad Prism version 7.02 (GraphPad Software Inc, La Jolla, CA, USA).

4.3 Results

The results of this chapter document the cell-based expression of a select group of lead proteins identified in Chapter 3 (Table 3-5). After cell-based protein expression, the anti-inflammatory properties of these lead proteins were further validated using a mouse model of chronic colitis and *in vitro* bioactivity assays with human PBMCs.

Rank	Gene Name	Pfam	Life stage
1	ANCCAN_22177	SCP/TAPS	Adult
2	ANCCAN_00478	SCP/TAPS (*Ac*-ASP-2)	L3
3	ANCCAN_12569	SCP/TAPS	Adult
4	ANCCAN_07727	Annexin superfamily	Adult
5	ANCCAN_12564	SCP/TAPS	Adult
6	ANCCAN_07322	Lysozyme-like	Adult
7	ANCCAN_08034	TTR-52 superfamily	Adult
8	ANCCAN_26187	SCP/TAPS	Adult
9	ANCCAN_07062	SCP/TAPS	Adult
10	ANCCAN_10127	Gp-FAR-1 (*Ac*-FAR-2)	Adult
11	ANCCAN_13497	TIMP (*Ac*-TIMP-1)	Adult
12	ANCCAN_01926	No putative conserved domains	Adult
13	ANCCAN_19762	SCP/TAPS	Adult
14	ANCCAN_17044	TTR-52 superfamily	Adult
15	ANCCAN_06741	SCP/TAPS	Adult
16	*Ac*_Novel_TIMP	TIMP	Adult
17	ANCCAN_04194	SCP/TAPS (*Ac*-NIF)	
18	ANCCAN_12561	SCP/TAPS	Adult
19	ANCCAN_11005	SCP/TAPS	Adult
20	ANCCAN_11519	No putative conserved domains	Adult

Table 4-6 The top 20 hookworm cell-free lysate secretome proteins based on TNBS colitis. Lysates are ranked by significance of the Z-Score.

4.3.1 Phylogenetic Analysis Highlighted a Diverse Range of SCP/TAPS for Recombinant Protein Expression

The FASTA sequences in the form of Newick files from *A. caninum* SCP/TAPS proteins identified in the TNBS screen were aligned against published SCP/TAPS from the three phylogenetically diverse ASP groups[331],[336]. A phylogenetic tree was constructed to determine which group each of the new anti-inflammatory proteins belonged (Figure 4-8). The majority of *A. caninum* SCP/TAPS candidate proteins clustered into ASP group 3.
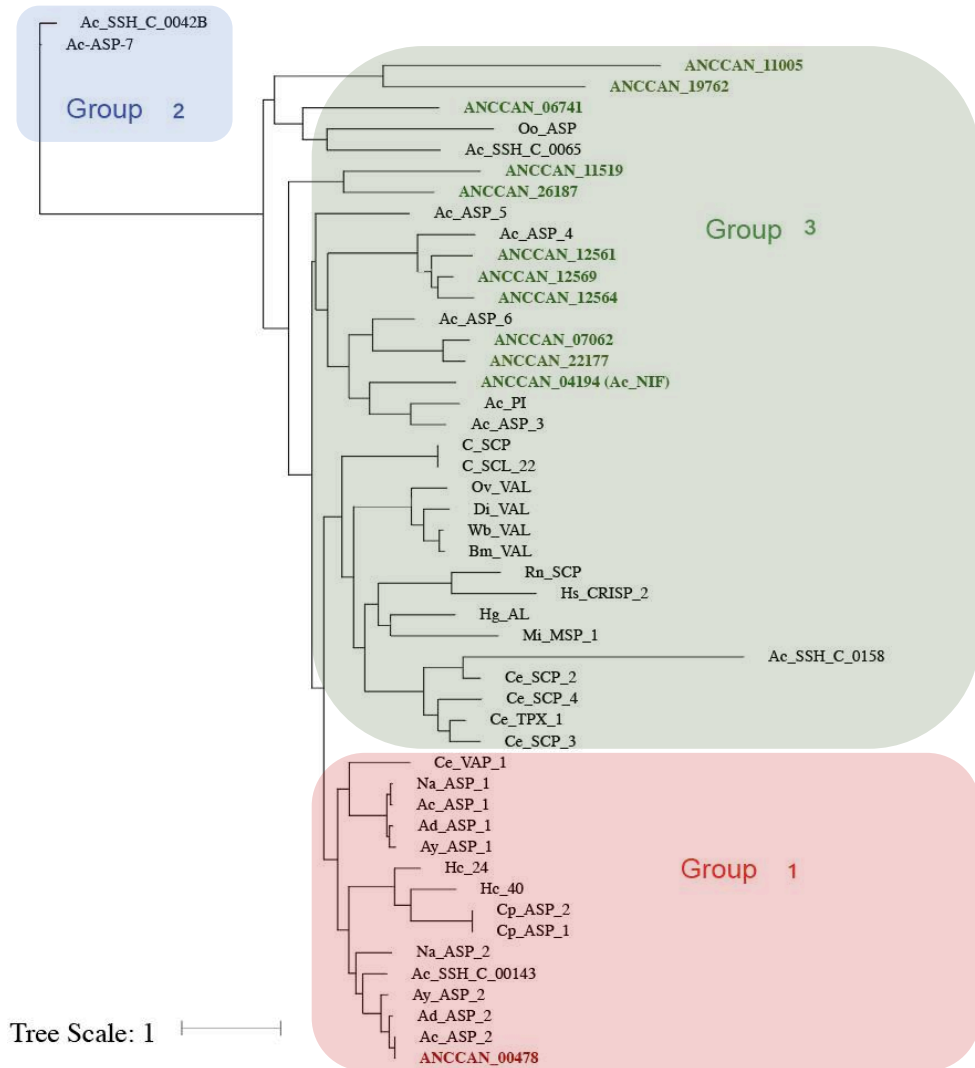
Figure 4-8 Phylogenetic tree of SCP/TAPS identified in the cell-free lysate TNBS screen. Proteins were compared with known members of the SCP/TAPS family from the published literature. The bolded coloured font indicates proteins identified from the A. caninum secretome cell-free lysate TNBS-screen. The accession numbers for all sequences not already provided are in the Appendix (Table 6-1).

4.3.2 Selection of Nine Hookworm Recombinant Proteins for Cell-Based Expression

Nine *Ac*ES proteins were selected for expression in *P. pastoris* based on their Pfam diversity (Figure 4-8*)*.

Lysate ID	Putative Function	Gene Model	SP?	bp	aa	MWt (Da)	MWt + tag (Da)
79	Gp_FAR	ANCCAN_10127 *Ac*-FAR-2	AFS-APN	495	165	18802.76	22202.32
73	TIMP	ANCCAN_13497 *Ac*-TIMP-1	AHA-CKC	360	120	13975	17374
11	SCP/TAPS	ANCCAN_04194 *Ac*-NIF	AHS-NEH	771	257	28926.77	32326.32
85	SCP/TAPS	ANCCAN_00478 *Ac*-ASP-2	VHG-NSM	603	201	22227.18	25626.74
13	SCP/TAPS	ANCCAN_22177	SFA-QAP	1338	446	48212	51612.34
15	SCP/TAPS	ANCCAN_19762	SQG-QSL	657	219	25064	28464.37
23	SCP/TAPS	ANCCAN_12569	n/a	654	218	24075	27474.73
22	SCP/TAPS	ANCCAN_26187	VEA-TTR	1299	433	45953	49352
9	SCP/TAPS	ANCCAN_06741	STA-IEF	564	188	18673.2	22072.76

Table 4-7 Selected proteins for expression in P. pastoris yeast expression system.

Putative function was predicted using NCBI BLASTx and Gene Model ANCANN number

was identified using WormBase ParaSite TBLASTN. Presence of a predicted signal peptide (SP) was established using SignalP 4.1. Molecular weight (MWt) of predicted amino acid sequences with and without vector-derived tags was predicted using ExPASy: SIB Bioinformatics Resource Portal Compute pI/Mw tool. bp = base pairs; aa = amino acids.

4.3.3 Recombinant Protein Expression in *P. pastoris* System Validated by SDS-PAGE & Western Blotting

Three of the nine proteins were successfully expressed in yeast. Large scale volumes of *Ac*-FAR-2 (ANCCAN_10127), *Ac*-TIMP-1 (ANCCAN_13497) and *Ac*-NIF (ANCCAN_04194) were successfully expressed in the P. pastoris system and sufficient supernatant media was purified by IMAC using the ÄKTA Start FPLC Chromatography System. The recombinant proteins were eluted into fractions that correlated with the absorbance peaks identified by the chromatography traces (Figure 4-9, Figure 4-11, Figure 4-13). The flow-through of unbound media was also collected after each protein purification. The eluate fractions were subjected to SDS-PAGE and staining with Coomassie brilliant blue and western blotting (Figure 4-10, Figure 4-12, Figure 4-14).

4.3.4   Purification of *Ac*-FAR-2 (ANCCAN_10127)

One (1) L of culture media containing *Ac*-FAR-2 (ANCCAN_10127) was purified by IMAC. The FPLC trace (Figure 4-9) shows an absorbance peak between fractions B11 and C10 and correspond to the presence of bands of the expected size (~22 kDa including purification tag) by SDS-PAGE (Figure 4-10).
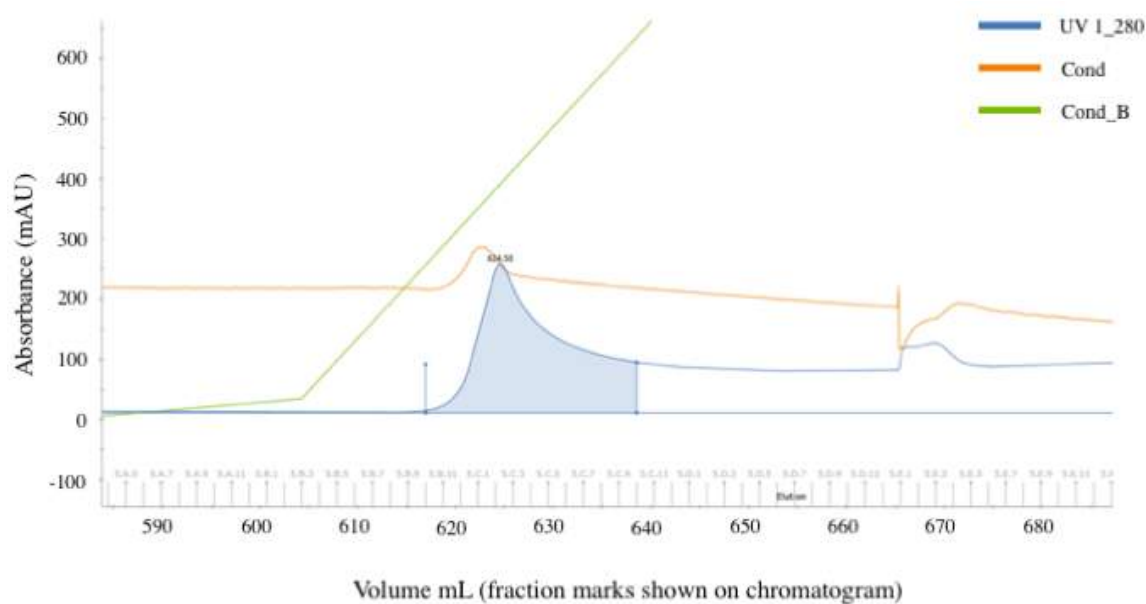
Figure 4-9 ÄKTA Start FPLC chromatogram of Ac-FAR-2 purification by immobilised metal ion affinity chromatography showing absorbance (mAU) over volume (mL) of sample. The blue line indicates ultra-violet absorption at 280 nm, the orange line indicates the salt concentration and the green line indicates the imidazole concentration.
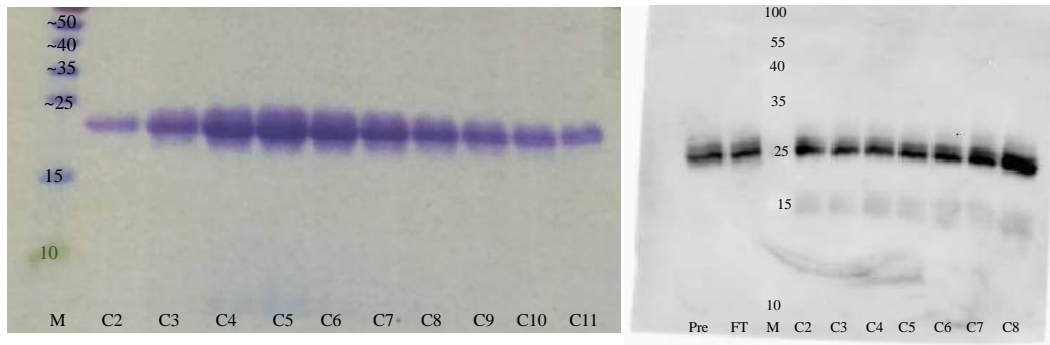
Figure 4-10 SDS-PAGE (A) and Western Blot (B) Showing FLPC Eluate Fractions of Ac-FAR-2. M = molecular weight standards;C2 – C11 = IMAC eluate fractions; Pre = culture media starting material pre-purification; FT = unbound column flow-through post-purification. Samples were subjected to electrophoresis on a 10 % SDS-PAGE gel and stained with Coomassie Brilliant Blue. Western blot was probed with mouse monoclonal anti-c-myc-HRP antibody.

4.3.5 Purification of *Ac*-TIMP-1 (ANCCAN_13497)

The ÄKTA trace (Figure 4-11) shows an absorbance peak between fractions B11 and C9. These fractions correspond to fractions identified by SDS-PAGE that contain a purified protein of the correct molecular weight of ~17 kDa including the purification tag (Figure 4-12).
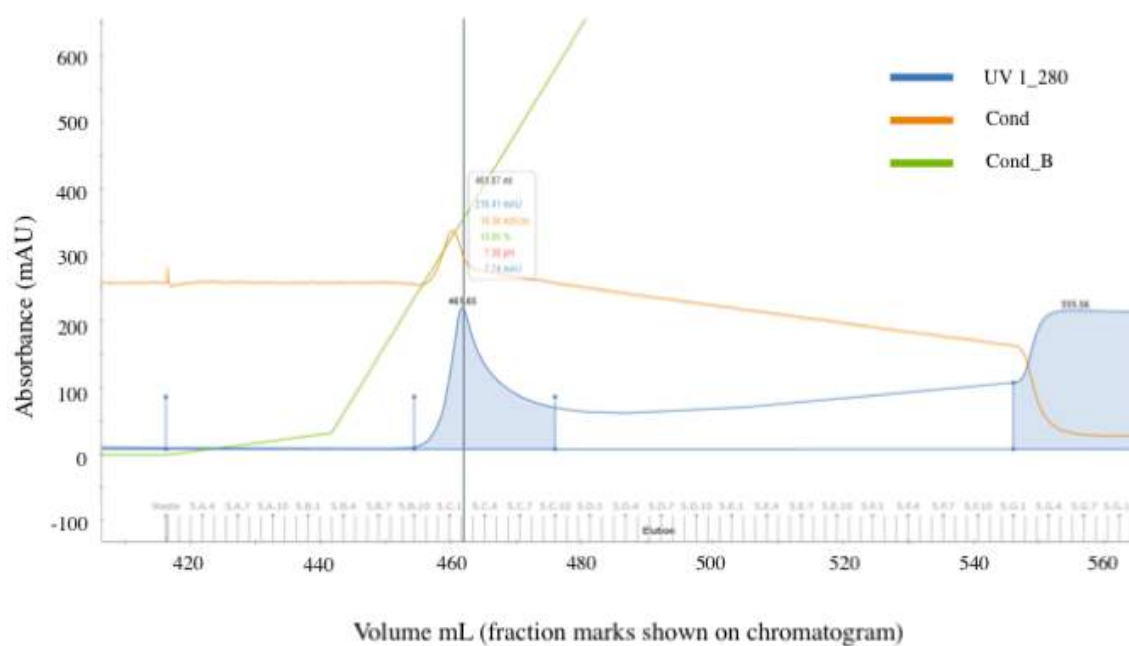
Figure 4-11 ÄKTA Start FPLC chromatogram of Ac-TIMP-1 purification by immobilised metal ion affinity chromatography showing absorbance (mAU) over volume (mL) of sample. The blue line indicates ultra-violet absorption at 280 nm, the orange line indicates the salt concentration and the green line indicates the imidazole concentration.
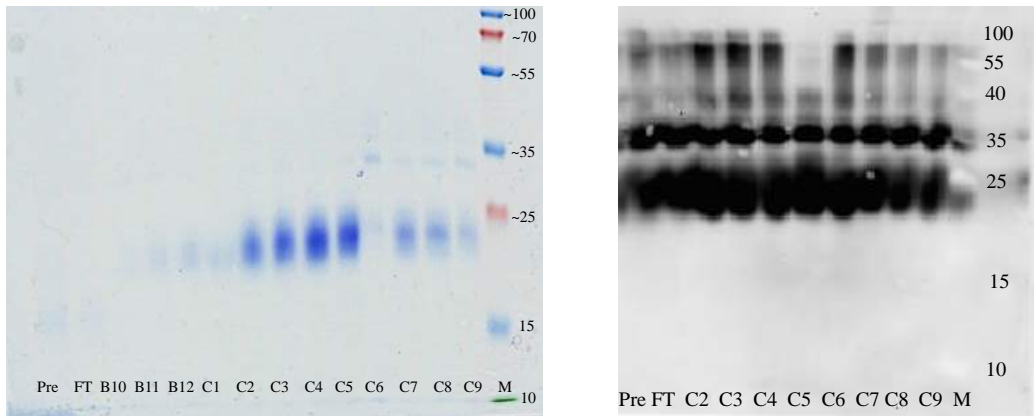
Figure 4-12 SDS-PAGE (A) and Western Blot (B) Showing FLPC Eluate Fractions of Ac-TIMP-1. M = molecular weight standards;B10 – C9 = IMAC eluate fractions; Pre = culture media starting material pre-purification; FT = unbound column flow-through post-purification. Samples were subjected to electrophoresis on a 12 % SDS-PAGE gel and stained with Coomassie Brilliant Blue. Western blot was probed with mouse monoclonal anti-c-myc-HRP antibody.

4.3.6   Purification of *Ac*-NIF (ANCCAN_04194)

The ÄKTA trace (Figure 4-13) shows an absorbance peak between fractions A11 and B8. These fractions correspond to fractions identified by SDS-PAGE that contain a purified protein of the correct molecular weight of ~32 kDa including the purification tag (Figure 4-14).
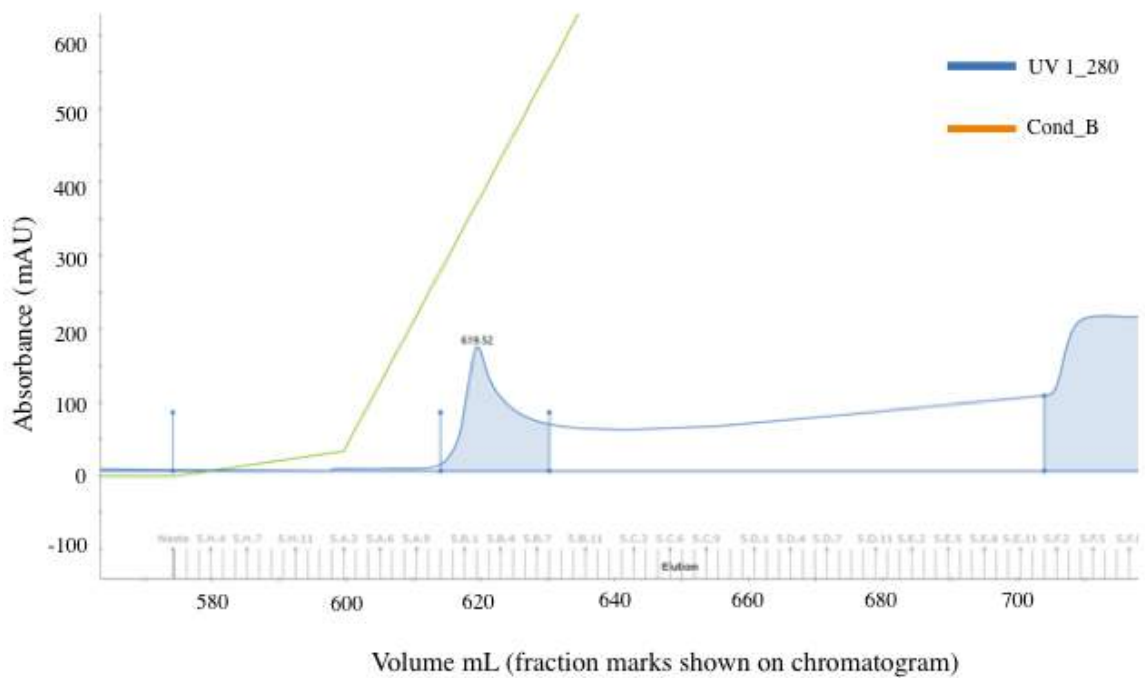
Figure 4-13 ÄKTA Start FPLC chromatogram of the Ac-NIF protein purification by immobilised metal ion affinity chromatography showing absorbance (mAU) over volume (mL) of sample. The blue line indicates ultra-violet absorption at 280 nm, and the orange line indicates the salt concentration.
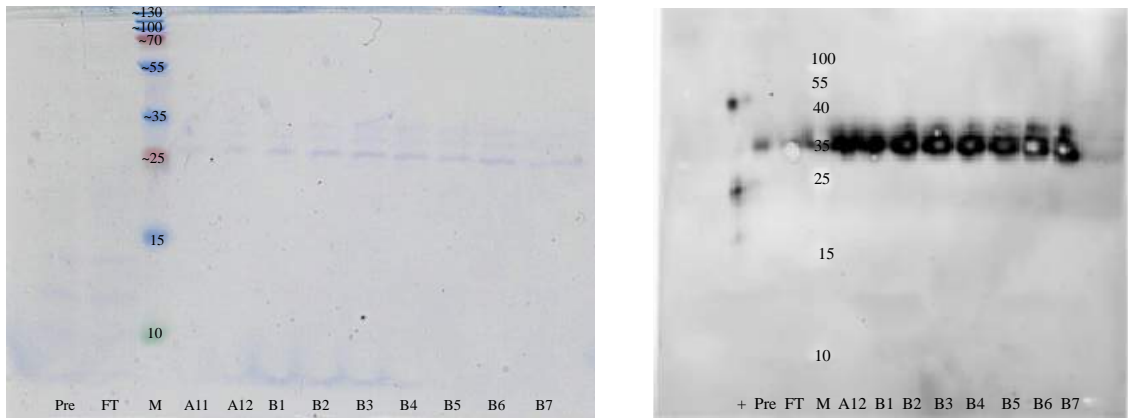
Figure 4-14 SDS-PAGE (A) and Western Blot (B) Showing FLPC Eluate Fractions of Ac-NIF. M = molecular weight standards;A11 – B7 = IMAC eluate fractions; Pre = culture media starting material pre-purification; FT = unbound column flow-through post-purification. Samples were subjected to electrophoresis on a 12 % SDS-PAGE and stained with Coomassie Brilliant Blue. Western blot was probed with mouse monoclonal anti-c-myc-HRP antibody. The Ac-NIF protein shows signs of extensive glycosylation evident by the presence of additional higher molecular weight bands.

The relevant features, yields after purification and endotoxin concentrations of each of the purified proteins expressed in *P. pastoris* is presented in Table 4-8.

Protein	Predicted MWt	Actual MWt#	Potential N-glycosylation sites	Yield (mg/L)	LPS (EU/mg)
Ac-FAR-2	~22 kDa	~24 kDa	0	1.7	0.336
Ac-TIMP-1	~17 kDa	~20 kDa	1	1.5	ND*
Ac-NIF	~29 kDa	~33 kDa	7	1	ND*

*Table 4-8 Features of purified hookworm recombinant proteins. The predicted and actual molecular weight (MWt), number of putative N-linked glycosylation sites, yield and endotoxin levels are shown. Endotoxin was measured using the LAL assay and values are expressed as EU/mg of purified proteins. The LPS level was higher for Ac-FAR-2 because the purified protein was relatively dark in colour and gave a baseline reading at 405 nm which is likely to have adversely affected the LPS reading. Nonetheless, the OD_{405} was below the maximum concertation recommended for cell culture of 0.5 EU/mg. *ND – endotoxin level below the limit of detection of the assay employed. #MWt measured under reducing and denaturing conditions by SDS-PAGE.*

4.3.7   Predicted 3D Structures of Lead Hookworm Proteins

Molecular models of the tertiary structures of the three proteins expressed in *P. pastoris* highlight the structural diversity between the secreted proteins (Figure 4-15). Varying degrees of alpha helicity were predicted, with *Ac*-FAR-2 consisting of mostly alpha helices joined by short strands based on the crystal structure *Na*-FAR-1 (PDB code 4UET). *Ac*-NIF and *Ac*-TIMP-1 contain several beta sheets at the core of their structures compared with *Ac*-FAR-2[337].

A) *Ac*-FAR-2   **B) *Ac*-NIF**   **C) *Ac*-TIMP-1**
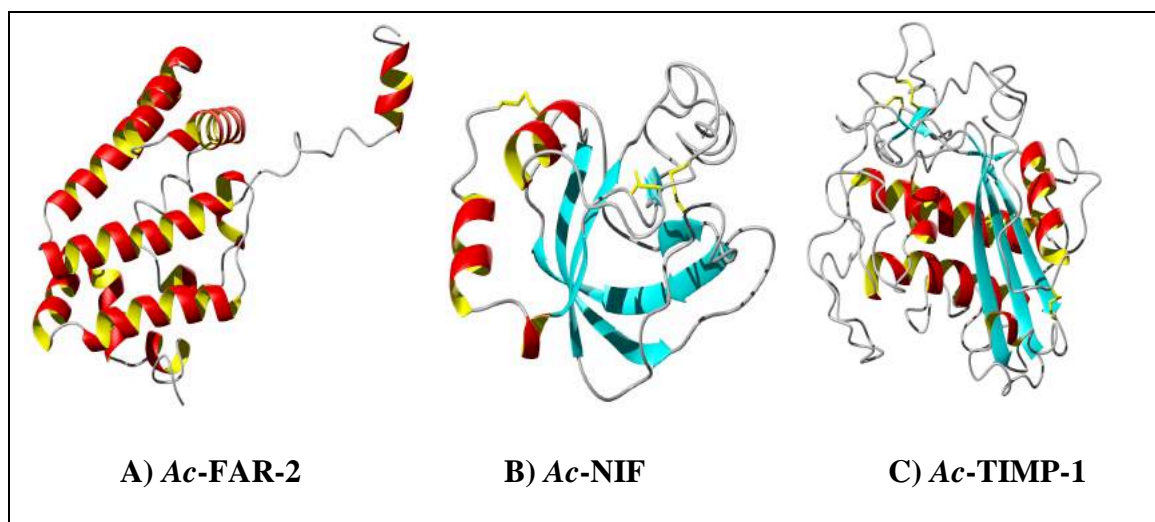
Figure 4-15 Predicted structural models of Ac-FAR-2 (A), Ac-NIF (B) and Ac-TIMP-1 (C) were modelled on the crystal structures of Na-FAR-1 (PDB code 4UET), Na-ASP-1 (PDB code 3NT8), and human TIMP-3 (PDB code 3CKI), respectively. The models with the highest C-scores were chosen for display, and corresponded to values of 0.48 for Ac-FAR-1, -0.81 for Ac-NIF, and -0.73 for Ac-TIMP-1. The C-score represents the confidence in the model; values are typically in the range -5 to 2, and higher values correspond to models with higher confidence. The models were created using I-TASSER protein structure and function prediction software and the macromolecular display figures were made using MOLMOL[334],[337].

4.3.8 Assessment of Prophylactic Efficacy of Purfied Yeast-Derived Recombinant *Ac*-FAR-2, *Ac*-TIMP-1, and *Ac*-NIF in TNBS Colitis

The hookworm proteins that were successfully expressed in *P. pastoris* were used to validate the prophylactic efficacy observed with their cell-free counterparts in chapter 3. Proteins were administered i.p. once at a dose of 1 mpk 6 hours prior to intra-rectal administration of TNBS. Recombinant yeast-expressed *Ac*-FAR-2 and *Ac*-TIMP-1 proteins protected against weight loss in TNBS colitis. As per the experimental rationale put forward in chapter 3 the percentage weight change of each mouse was monitored over the course of the three-day experiment.

4.3.9 Defined Yeast Expressed Hookworm Proteins Protect Against TNBS-Induced Weight Loss

Recombinant yeast expressed *Ac*-FAR-2 and *Ac*-TIMP-1 proteins protected against weight loss in the TNBS colitis experiment. As per the experimental rationale put forward in chapter 3 the percentage weight change of each mouse was monitored over the course of the three-day experiment. Figure 4-16 demonstrates that mice that received yeast expressed *Ac*-FAR-2 and *Ac*-TIMP-1 were protected from TNBS-induced body weight loss in comparison to the trypanised and denatured protein negative control.
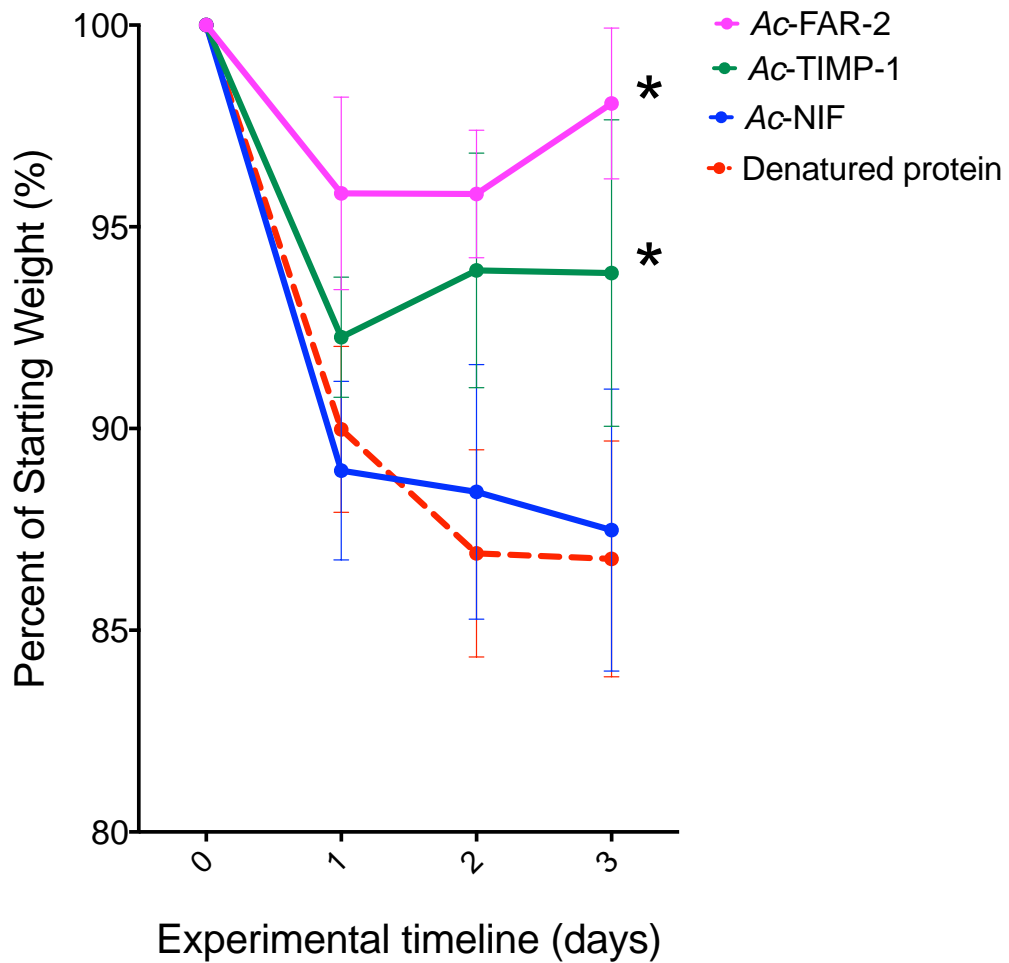
Figure 4-16 Daily weight change of groups of mice treated with recombinant proteins prior to the administration of TNBS. Data points represent mean ± SEM, sample size (n = 6 mice / group). The significance was determined by using a two-sample t-test to compare weights from day three of each test group against the weight of the control group (denatured Ac-FAR-2), and was adjusted for multiple testing. *p ≤ 0.05.

4.3.10 Yeast-Derived Recombinant Proteins Protect Against TNBS-Induced Macroscopic Inflammation of the Colon

The level of superficial (macroscopic) inflammation was assessed upon opening the peritoneal cavity at necropsy, and generating a macroscopic score that is composed of adhesions, ulceration, bowel wall thickening and mucosal oedema. The colons of mice treated with denatured *Ac*-FAR-2 and *Ac*-NIF received high macroscopic pathology scores due to extensive inflammation, whilst the group treated with *Ac*-FAR-2 had a signficantly reduced macroscopic score and maintained colon integrity. There was a trend towards reduced macroscopic score for *Ac*-TIMP-1 but it did not reach significance (p value = 0.119) (Figure 4-17).
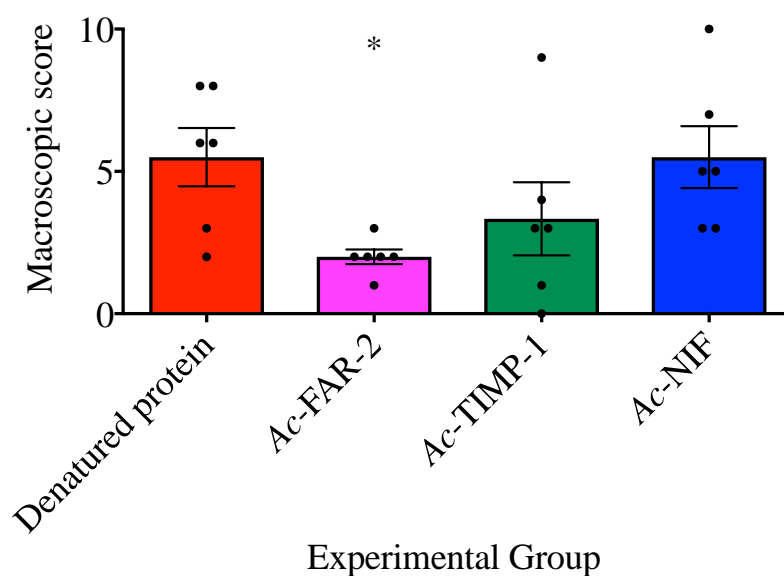
*Figure 4-17 Macroscopic pathology score of mice treated with yeast-expressed Ac-FAR-2, Ac-TIMP-1 and Ac-NIF prior to administration of TNBS. Control mice received denatured Ac-FAR-2 followed by TNBS. All individual data points are represented, as well as the mean ±SEM, sample size n = 6 mice / group. The significance was determined by statistical comparisons using a Mann-Whitney U test to compare each test group with the negative control group and adjusted for multiple testing denoted by * p ≤0.05.*

4.3.11 Yeast-Expressed *Ac*-FAR-2 and *Ac*-TIMP-1 Protect Against TNBS-Induced Colon Shortening

The extent of colitis was monitored by the measurement of colon length. Mice treated with yeast-expressed *Ac*-FAR-2 and *Ac*-TIMP-1 had significantly longer colons than control mice treated with denatured *Ac*-FAR-2 (Figure 4-18).
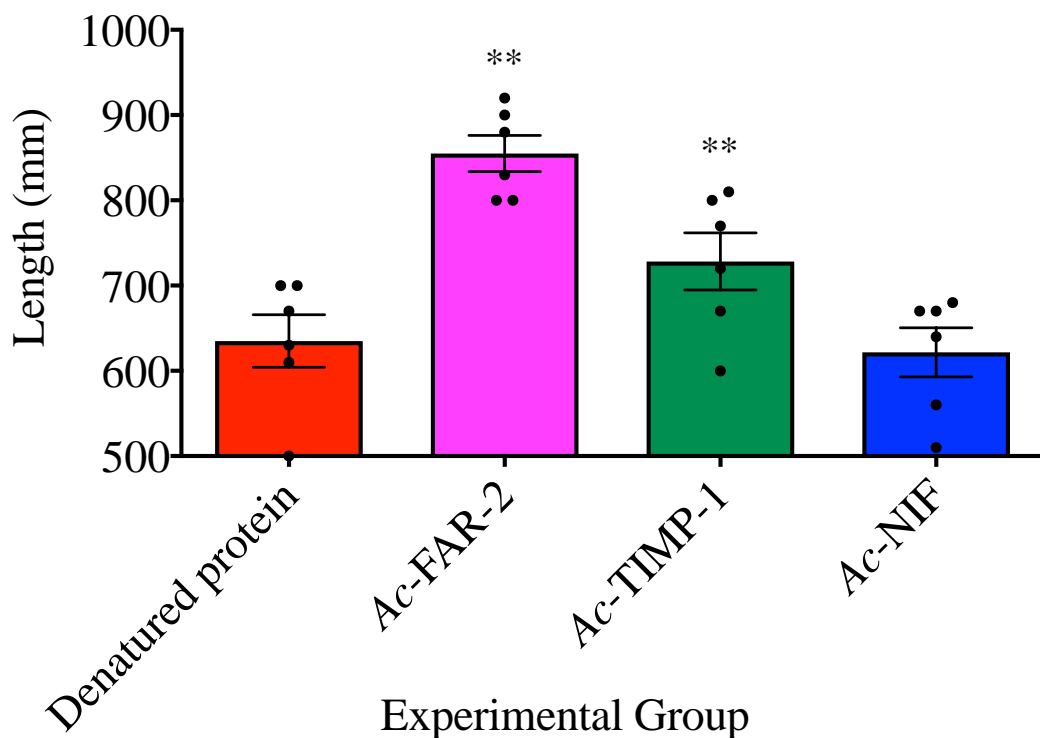
*Figure 4-18 Mice treated with yeast-derived recombinant Ac-FAR-2 and Ac-TIMP-1 had signficantly longer colons than control mice after administration of TNBS. All individual data points are represented, mean ± SEM, sample size n = 6 mice / group. The significance was determined by statistical comparisons using a two-sample t-test against the control group and was adjusted for multiple testing. ** p ≤0.01.*

4.3.12 Photomicrographs of Representative *Post-Mortum* Colons

At the termination of the experiment, the colon was removed from each animal, photographs were taken and a macroscopic score assessing the extent of inflammation and the impact of the physical structure of the colon was conducted (Figure 4-19).

| A | B | C | D |
| Denatured protein | *Ac*-FAR-2 | *Ac*-TIMP-1 | *Ac*-NIF |
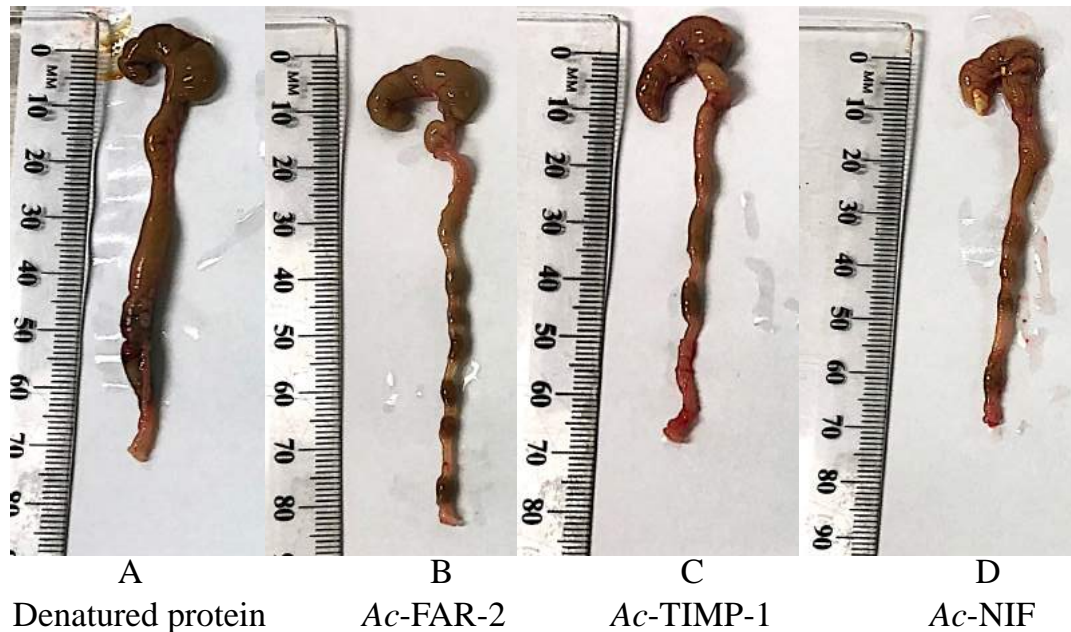
Figure 4-19 Photographs of Representative Colons at Necropsy of Mice Treated with Yeast-Expressed Hookworm Proteins Prior to Administration of TNBS. Photographs display one representative image from each experimental group to highlight the superficial differences between the control group treated with denatured Ac-FAR-2 and the test groups treated with Ac-FAR-2, Ac-TIMP-1 and Ac-NIF. Note the thickened and stunted colon of the control group. These photographs display one representative image from each experimental group to convey the visual differences between the denatured protein, Ac-FAR-2, Ac-TIMP-1 and Ac-NIF experimental groups.

4.3.13 Yeast-Expressed *Ac*-FAR-2 Protects Against TNBS-Induced Clinical Signs of Colitis

The experimental group that was administered recombinant *Ac*-FAR-2 had significantly lower mean clinical score than the control group treated with denatured *Ac*-FAR-2 (Figure 4-20). *Ac*-TIMP-1 also showed a trend towards protection (p value = 0.0563) but this group did not reach significance because of one outlier.
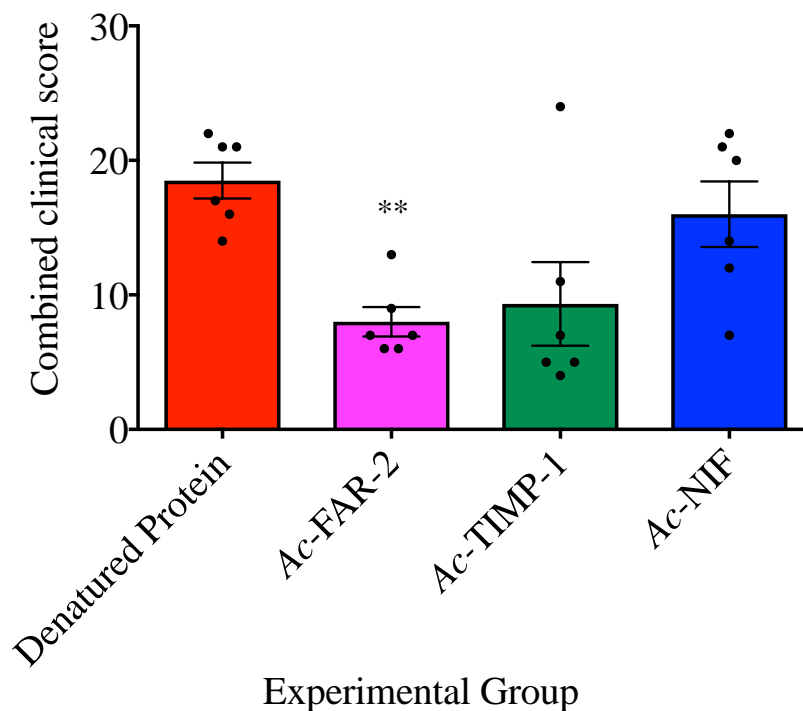
*Figure 4-20 Mice treated with yeast-derived recombinant Ac-FAR-2 had significantly reduced clinical scores compared to the control group. Throughout the three day experiment the extent of TNBS-colitis on the physical appearance of the animals was monitored. Control mice received denatured Ac-FAR-2 followed by TNBS. All individual data points are represented, mean ± SEM, sample size n = 6 mice / group. The significance was determined by statistical comparisons using Mann-Whitney U test to compare test groups with the control group and adjusted for multiple testing. ** p ≤0.01.*

4.3.14 Yeast-Expressed and Purified *Ac*-FAR-2 and *Ac*-TIMP-1 Protect Against Histopathology in TNBS-Induced Colitis

Histological sections were obtained from colonic tissue of mice that were treated with recombinant yeast-expressed hookworm proteins prior to administration of TNBS. The negative control group (received denatured *Ac*-FAR-2 protein) displayed signs of severe colitis, shown by the major disruption to the general gut architecture, loss of epithelial integrity, sub-mucosal oedema and loss of goblet cells. Furthermore, there was evidence of infiltration of inflammatory cells in the lamina propria and thickening of the underlying muscularis (Figure 4-21). Evidence of protection from transmural lesions, a characteristic hallmark of TNBS-induced colitis, was present in mice that received *Ac*-FAR-2 and *Ac*-TIMP-1, and to a lesser extent *Ac*-NIF. Mice administered *Ac*-FAR-2 and *Ac*-TIMP-1 displayed significantly less disruption to overall gut architecture and had less evidence of inflammatory cell infiltration and greater numbers of goblet cells than control animals.

A) Naïve

B) Denatured Protein
+ TNBS

C) *Ac*-NIF
+ TNBS

D) *Ac*-FAR-2
+ TNBS

E) *Ac*-TIMP-1
+ TNBS
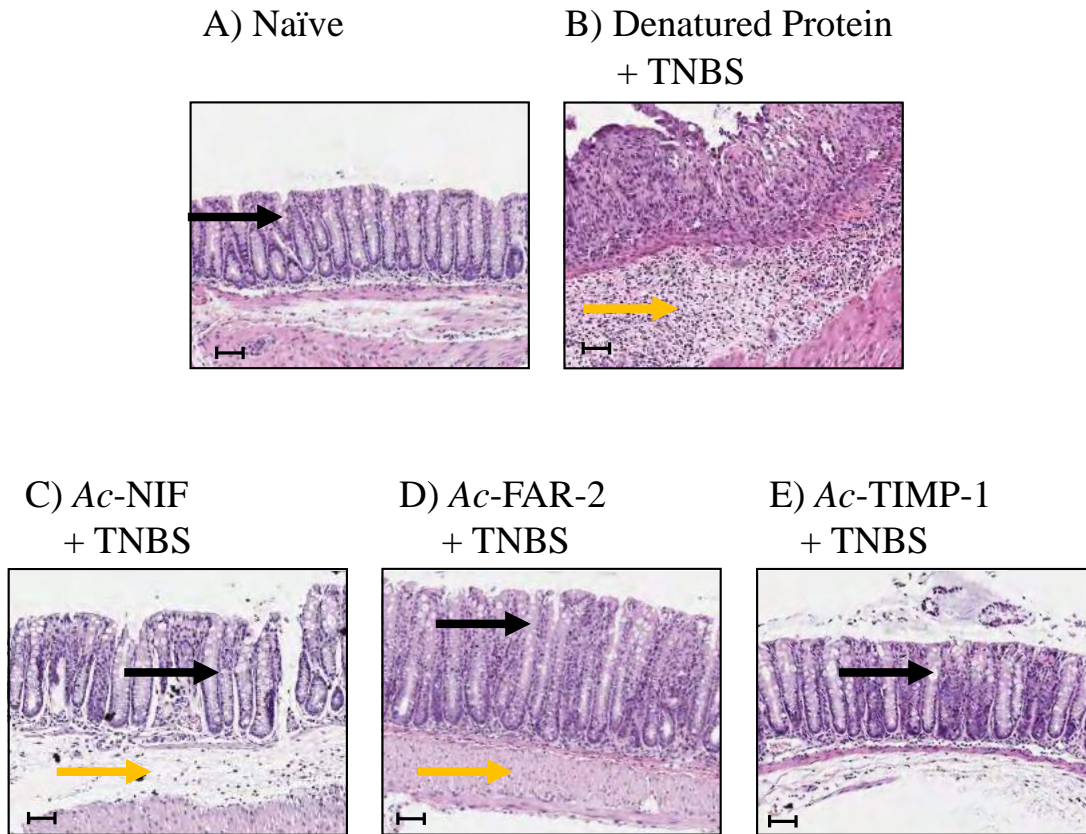
Figure 4-21 Representative micrographs showing colon histopathology of mice treated with recombinant purified hookworm proteins expressed in yeast. Naïve image (A) displays normal goblet cells (denoted by the black arrow), and normal gut architecture of crypts and villi. Control mice that received denatured Ac-FAR-2 (B) display loss of goblet cell in the mucosa, cellular infiltration of the mucosa and thickening of the lamina propria (denoted by the yellow arrow). Treatment with Ac-NIF (C), Ac-FAR-2 (D), Ac-TIMP-1 (E) maintained the mucosal architecture and epithelial integrity, the presence of goblet cells (denoted by the black arrow) and limited the extent of inflammation. Scale bar = 50 μm.

4.3.15 Yeast-Expressed and Purified *Ac*-FAR-2 and *Ac*-TIMP-1 Signficantly Protect Against Blinded Histopathology Scores in TNBS-Induced Colitis

H&E stained slides were scored for pathology by an individual blinded to the experimental group. Tissue sections were scored on a scale of 0 to 5 for each of the following parameters; (1) epithelial pathology (crypt elongation, hyperplasia, erosion), (2) mural inflammation and (3) oedema for an overall maximal total histology score of 15 (Table 3-4). *Ac*-FAR-2 and *Ac*-TIMP-1 were significantly protected from colitis in terms of a significantly reduced histopathology score.
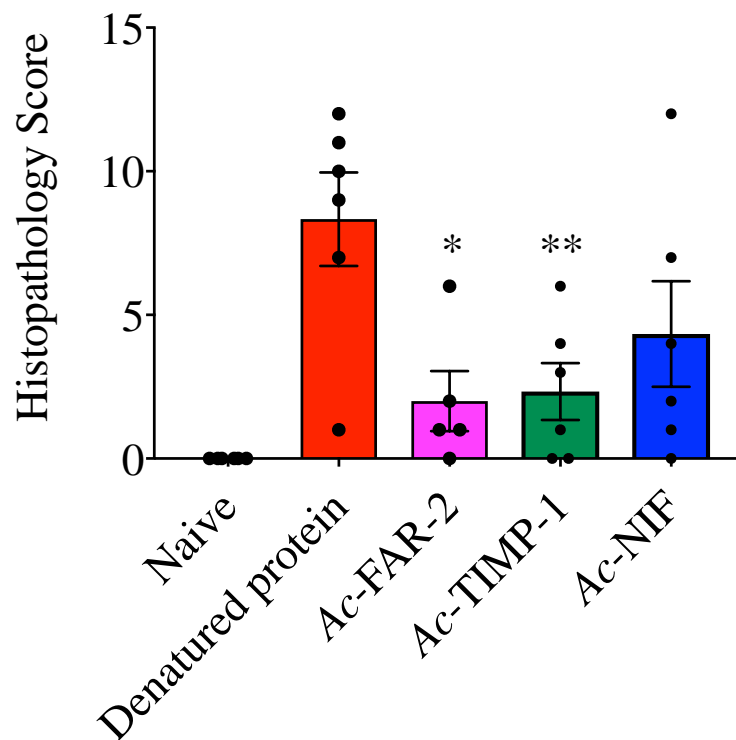
*Figure 4-22 Blinded histopathology scores for yeast expressed proteins in TNBS-induced colitis. Control mice received denatured protein followed by TNBS, and the remaining experimental groups received hookworm proteins followed by TNBS. All individual data points are represented, mean ± SEM, sample size n = 6 mice / group. Significance was determined by statistical comparisons assessed using Mann-Whitney U test against the control group and was adjusted for multiple testing. * p ≤0.05; **p ≤0.01.*

4.3.16 Yeast Expressed Hookworm *Ac*-TIMP-1 Protein Protected Against Weight Loss in T Cell Transfer Colitis

The results presented in the proceeding section are from the CD4+ CD25- T cell transfer experiment, where mice were treated with either yeast-expressed recombinant hookworm proteins *Ac*-TIMP-1 and *Ac*-NIF or the rHA *Pichia* expression-matched negative control. Due to an unforeseen technical occurrence, yeast-expressed *Ac*-FAR-2 was not tested in this study because the mice in this group were accidently injected with twice the amount of T cells in the engraftment process. As a positive control, anti-IL-12p40 mAb at a dose of 1 mg/mouse was administered every 7 days.

RAG1$^{-/-}$ mice that received *Ac*-TIMP-1 i.p. at a dose of 1 mpk every third day from the time of T cell transfer showed significant protection against weight loss on days 20 (p value < 0.05) and 27 (p value < 0.01) in comparison to the negative control group that received rHA (Figure 4-23). Mice that received anti-IL-12p40 displayed highly significant protection (p value < 0.0001) against weight loss at all time points from day 20 onwards.
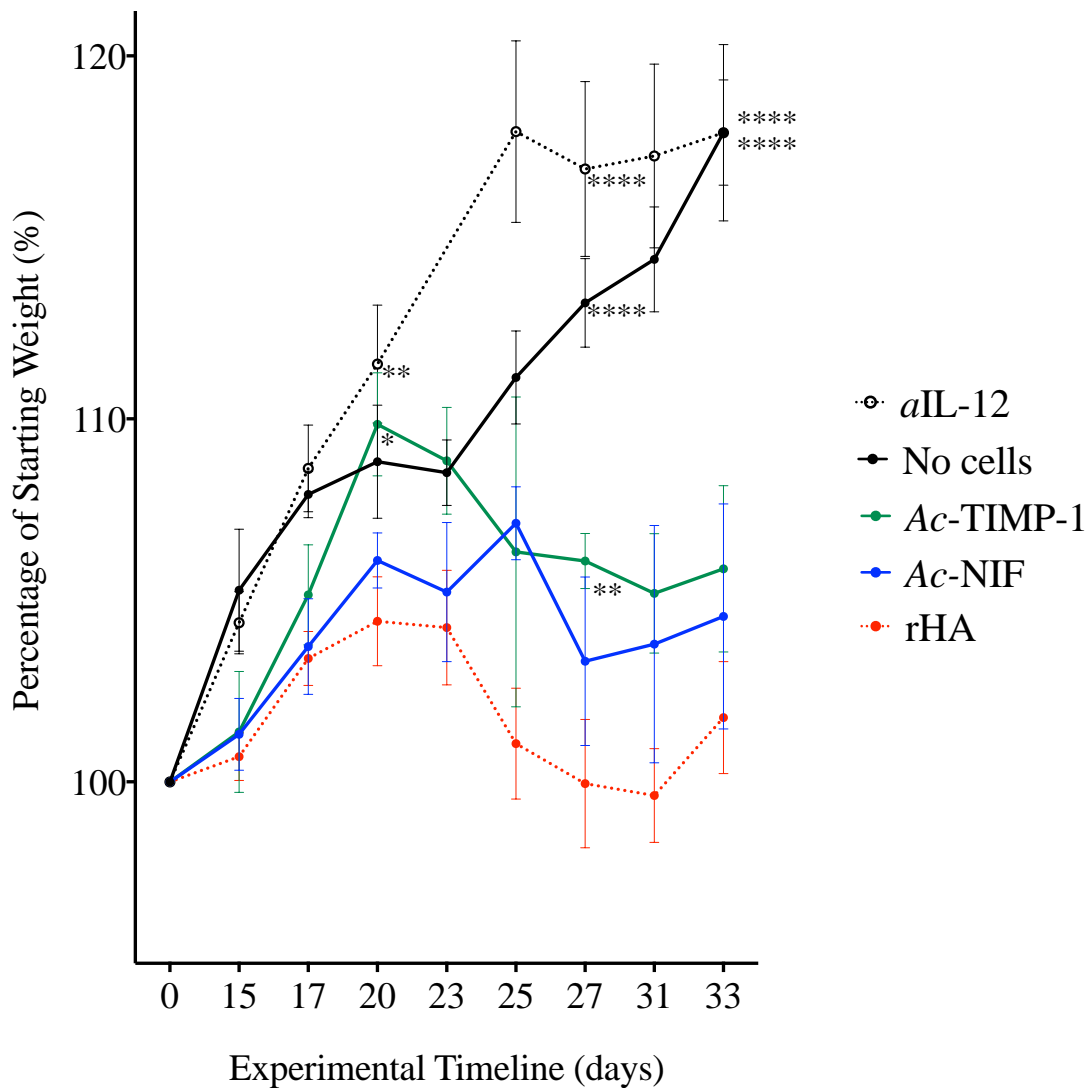
*Figure 4-23 Naïve RAG1$^{-/-}$ mice that received anti-IL-12p40 or recombinant Ac-TIMP-1 displayed significant protection against weight loss after T cell transfer. Naïve RAG1$^{-/-}$ mice received no cells (n = 4), the negative control mice received recombinant human albumin (rHA) every third day and transferred T cells (n = 8) at day 0. Positive control mice received αIL-12 antibody and transferred T cells (n = 4), and the remaining experimental groups received hookworm recombinant proteins (Ac-TIMP-1; n = 7, Ac-NIF; n = 5) and transferred T cells. Data points represent mean ±SEM. The significance was determined by using a two-sample t-test to compare weights from days 20, 27 and 33 against the weights from the negative control group, and was adjusted for multiple testing. * p ≤0.05, ** p ≤0.01, ****p ≤0.0001.*

4.3.17 Yeast-Expressed *Ac*-TIMP-1 and *Ac*-NIF Protect Against Clinical Signs of Disease in T Cell Transfer Colitis

As per the experimental rationale, outward clinical signs of disease in animals is an excellent indicator of the severity of colitis. Mice that received *Ac*-NIF and *Ac*-TIMP-1 were protected against clinical signs of disease on days 27 and 33 reflected as significantly reduced clinical scores (p value < 0.05) in comparison to the rHA negative control group (Figure 4-24). Anti-IL-12p40 treatment also resulted in reduced clinical scores at these same time points (p value < 0.05)[338].
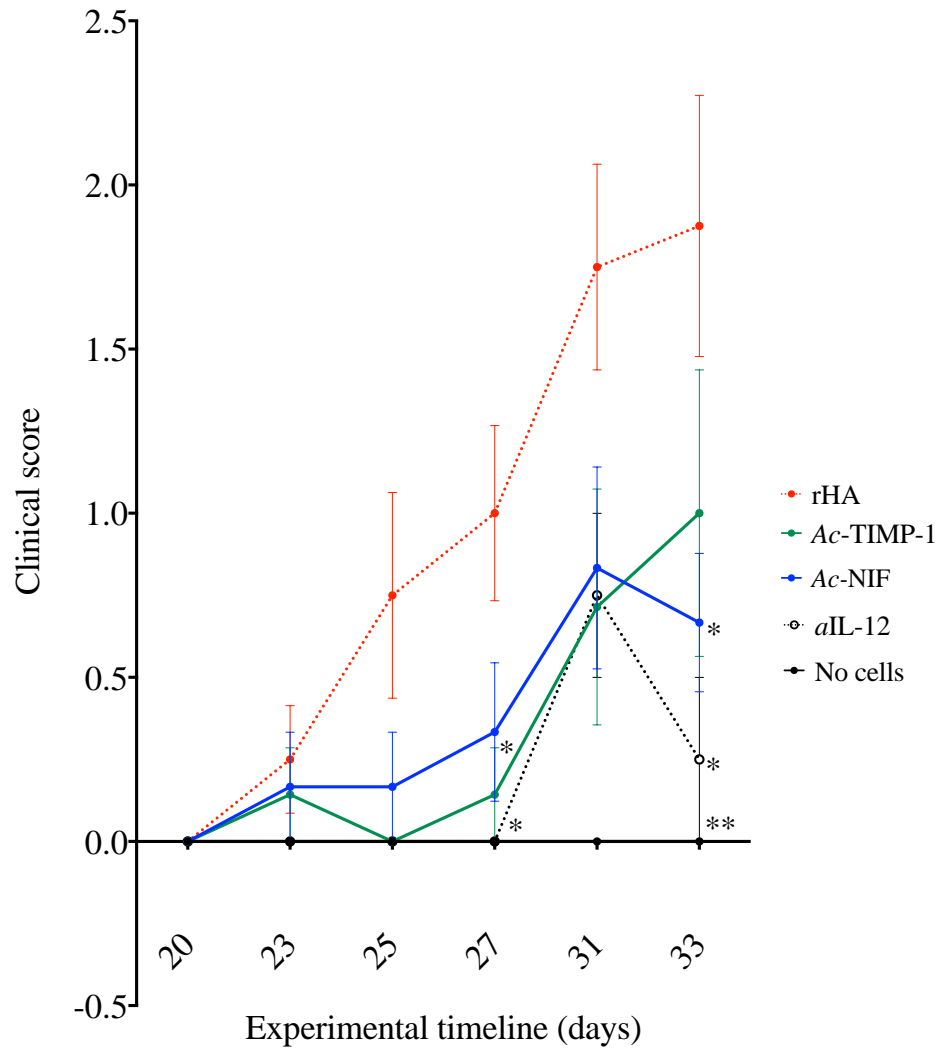
Figure 4-24 Mice that received recombinant Ac-TIMP-1 and Ac-NIF displayed reduced clinical scores compared to negative control mice that received rHA in the T cell transfer model of colitis. Three weeks after the administration of T cells the physical appearance of the animals began to deteriorate. Naïve RAG1⁻ᐟ⁻ mice received no cells (n = 4), negative control mice received rHA and transferred T cells (n =8), positive control mice received αIL-12 antibody and transferred T cells (n = 4), and the remaining experimental groups received hookworm recombinant protein (Ac-TIMP-1; n = 7, Ac-NIF; n = 5) and transferred T cells. All data points are represented, mean ± SEM. The significance was determined by a two sample two-tailed student's t test comapring test groups with the negative control (rHA) group on days 27 and 33.* p ≤0.05, ** p ≤0.01.

4.3.18 Yeast-Expressed *Ac*-TIMP-1 Protects Against Macroscopic Inflammation of the Colon in T Cell Transfer Colitis

The extent of macroscopic colonic inflammation was significantly less in mice that received *Ac*-TIMP-1 compared to the negative control rHA group (Figure 4-25).

Experimental Group
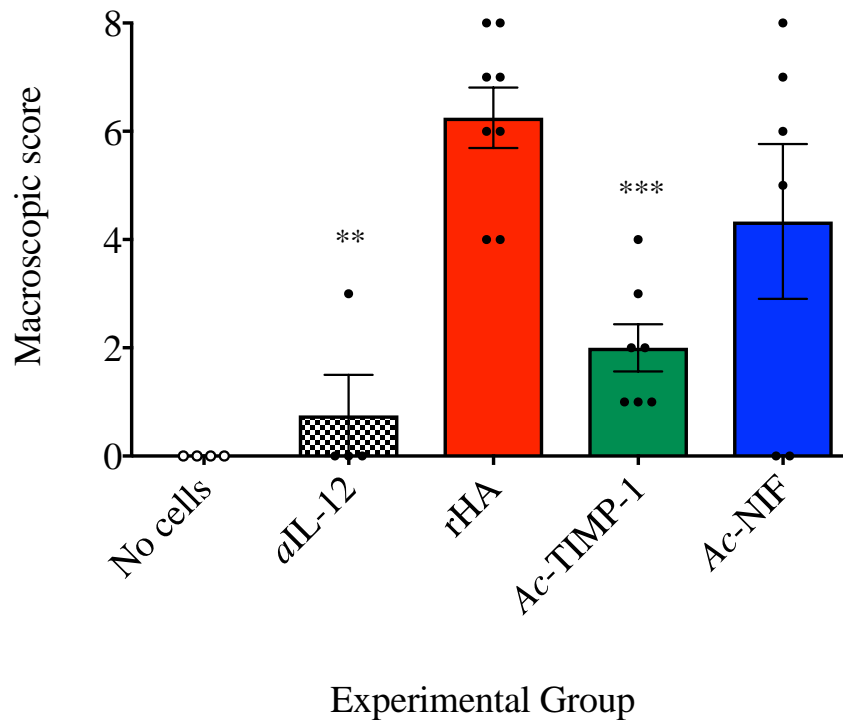
*Figure 4-25 RAG1$^{-/-}$ mice treated with recombinant Ac-TIMP-1 had a significantly reduced macroscopic pathology score compared to rHA-treated negative control mice in T cell transfer colitis. Naïve RAG1$^{-/-}$ mice received no cells (n = 4), in the negative control group mice received recombinant human albumin (rHA) and T cells (n = 8), in the positive control group mice received αIL-12 antibody and by T cells (n = 4), and the remaining experimental groups received hookworm recombinant protein and T cells (Ac-TIMP-1; n = 7, Ac-NIF; n = 5). All individual data points are represented, mean ± SEM. The significance was determined by statistical comparisons using a Mann-Whitney U test to compare each test group with the negative control group and adjusted for multiple testing denoted by ** p ≤ 0.01, *** p ≤ 0.001.*

4.3.19 Yeast-Expressed Hookworm Protein *Ac*-NIF Showed Protection Against Shortening of the Colon in T Cell Transfer Colitis

In T cell transfer colitis, the extent of inflammation can be directly correlated to the length of the colon, because increased inflammation causes shortening (and thickening) of the colon[318]. Administration of *Ac*-NIF protein significantly protected against inflammation demonstrated by the maintenance of colon length in comparison to the rHA negative control group, which was comparable to the positive control group αIL-12 (Figure 4-26).
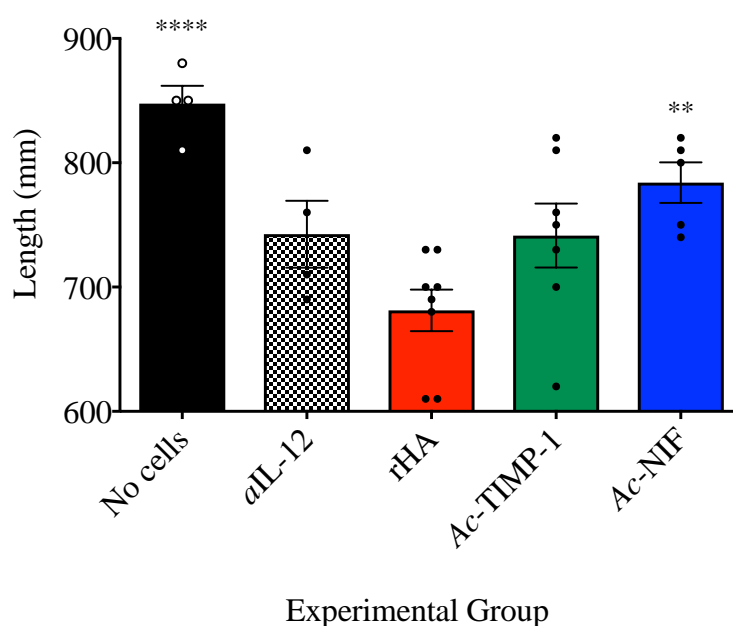
*Figure 4-26 RAG1^{-/-} mice treated with recombinant Ac-NIF had significantly reduced colon shortening compared to rHA-treated negative control mice in T cell transfer colitis. Naïve RAG1^{-/-} mice received no cells (n = 4), negative control mice received recombinant human albumin (rHA) and transferred T cells (n = 8), positive control mice received αIL-12 mAb and transferred T cells (n = 4), and the remaining experimental groups received hookworm recombinant protein and transferred T cells (Ac-TIMP-1; n = 7, Ac-NIF; n = 5). All individual data points are represented, mean ± SEM. The significance was determined by statistical comparisons using a two-sample t-test against the rHA control group and was adjusted for multiple testing. ** p ≤ 0.01, **** p ≤ 0.0001.*

4.3.20 Yeast-Expressed *Ac*-NIF Treatment Resulted in Signficantly Decreased Histopathological Scores in T Cell Transfer Colitis

Histological sections were prepared from colons of mice in all experimental groups of the T cell transfer experiment.
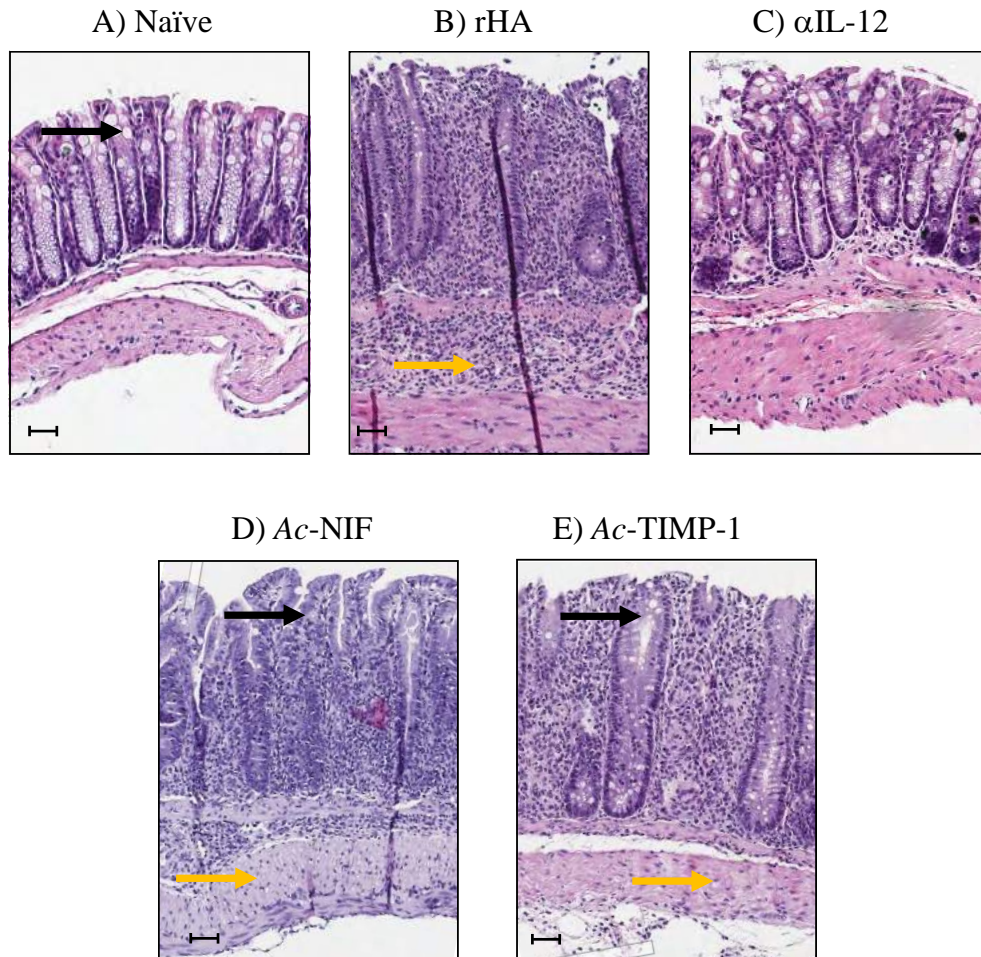
Figure 4-27 Representative histology micrographs stained with H&E of colon sections from T cell transfer experiment with yeast expressed hookworm proteins. Naïve mice (A) display normal goblet cells (denoted by the black arrow), and normal gut architecture of crypts and villi. Control mice that received rHA (B) display a loss of goblet cells in the mucosa, cellular infiltration of the mucosa and thickening of the lamina propria (denoted by the yellow arrow). Treatment with αIL-12 (C), Ac-NIF (D) and Ac-TIMP-1 (E) maintained the mucosal architecture and epithelial integrity, the presence of goblet cells

(denoted by the black arrow) and limited the extent of inflammation (denoted by the yellow arrow). Scale bar = 30 μm.

Longitudinal sections (3-4 μm) of colon were stained with H&E and were scored for pathology by an individual blinded to the experimental group. Goblet cell index was scored on a scale from 0 - 5, where a score of 3 represented typical goblet cell presence in naïve colons (no cell transfer). Score of 0 - 2 represents a loss of goblet cells (rHA negative control), and a score of 4 - 5 represents goblet cell hyperplasia. All five mice in the rHA experimental group showed a marked loss of goblet cells and two mice in both the *Ac*-NIF and *Ac*-TIMP-1 groups also showed evidence of a loss of goblet cells.
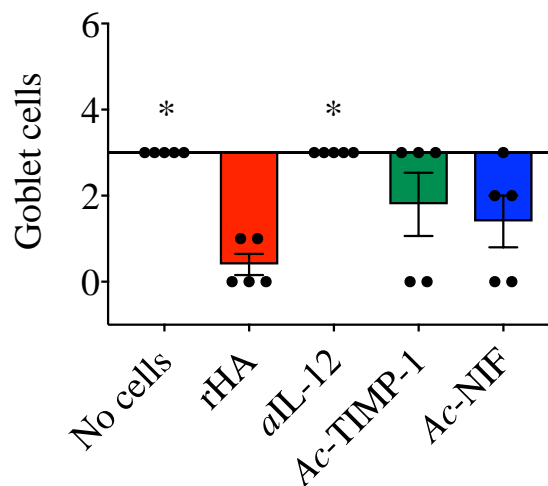
Figure 4-28 Blinded goblet cell score of histology sections from RAG1$^{-/-}$ mice in T cell transfer colitis. Control mice received denatured protein followed by T cell transfer, and the remaining experimental groups received hookworm protein followed by T cell transfer. All individual data points are represented, mean ± SEM, sample size (n = 6 mice / group). Significance was determined by statistical comparisons assessed using Mann-Whitney U test against the negatice control group (rHA) and was adjusted for multiple testing. * p ≤ 0.05.

As per the TNBS screen in chapter 3, tissue sections were scored on a scale of 0 - 5 for each of the following parameters; (1) epithelial pathology (crypt elongation, hyperplasia, erosion), (2) mural inflammation and (3) oedema for an overall maximum total histology score of 15 (Figure 4-29). *Ac*-NIF significantly protected against crypt elongation and hyperplasia (p value = 0.0317), while both *Ac*-TIMP-1 (p value = 0.0043) and *Ac*-NIF protected against oedema (p value = 0.0079). The overall histopathology of the positive control group (αIL-12) was a good indicator of gut architecture after effective therapeutic treatment in the T cell transfer experiment below. Mice treated with *Ac*-TIMP-1 showed a similar degree of histopathology to mice treated with *Ac*-NIF but their overall histology scores were not significantly different to that of the rHA group. These results were evident in all three parameters of the blinded histopathology score.
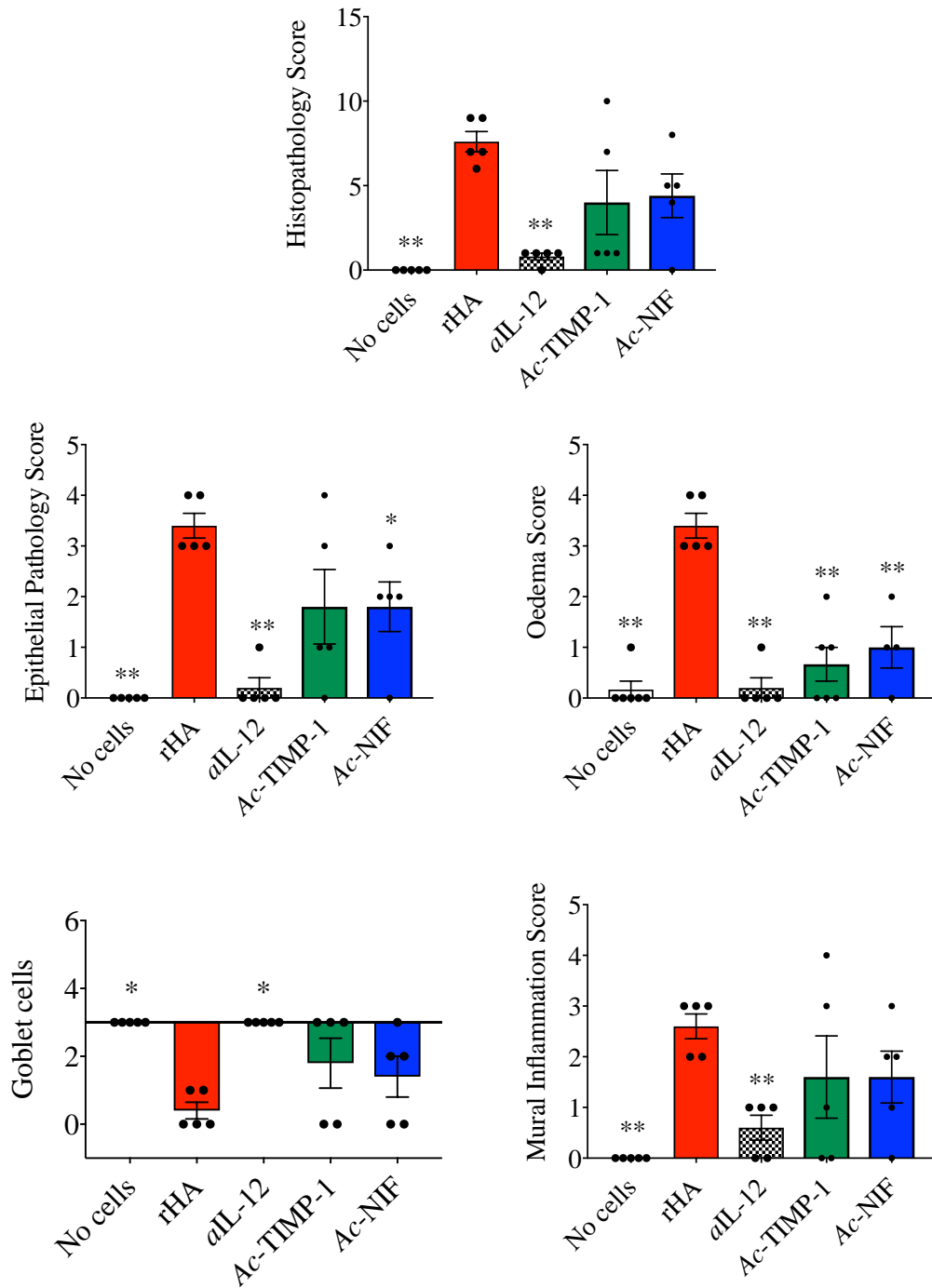
Figure 4-29 Blinded histopathology scoring of H&E stained sections of colon from T cell transfer induced-colitis. All individual data points are represented, mean ± SEM. Sample size n = 5 colon sections for analysis. The significance was determined by a unpaired two sample two-tailed parametric student's t test against the negative control (rHA) (* p ≤ 0.05, ** p ≤ 0.01.

4.3.21 Effect of Yeast-Expressed *Ac*-TIMP-1, *Ac*-NIF, and *Ac*-FAR-2 on Inflammatory Cytokine Production by Human Peripheral Blood Myeloid Cells

PBMCs were isolated from human blood by density centrifugation. Cells were either untreated or stimulated with PMA-Ionomycin (for T cell cytokines) or LPS (myeloid cell cytokines). Toll-like receptor (TLR)-4 on antigen presenting cells is engaged by LPS which activates NADPH oxidase and NF-κB and drives innate cell pro-inflammatory cytokine release. PMA activates protein kinase C, while ionomycin is a calcium ionophore, and stimulation with these compounds bypasses the T cell membrane receptor complex and leads to activation of several intracellular signalling pathways, resulting in T cell activation and production of cytokines.

To assess the impact of *Ac*-TIMP-1, *Ac*-FAR-2 and *Ac*-NIF on human immune cell cytokine production, PBMCs were treated with or without yeast-expressed hookworm proteins, and expression of IL-1β, IL-2, IL-6, IL-10, and TNF was analysed by CBA. PBMCs from a single donor were treated with recombinant proteins alone or were stimulated with LPS and recombinant proteins simultaneously. Addition of *Ac*-FAR-2 resulted in highly significant suppression of secretion of all cytokines analysed, including the anti-inflammatory cytokine IL-10. Addition of *Ac*-TIMP-1 however resulted in significant suppression of TNF (p value < 0.001), IL-8 (p value < 0.05) and IL-1β (p value < 0.01) production, but instead caused up-regulation of the anti-inflammatory cytokine IL-10 (p value < 0.05). *Ac*-NIF suppressed TNF production (p value < 0.01) and, like *Ac*-TIMP-1, induced up-regulation of IL-10 (p value < 0.01) (Figure 4-3-22).
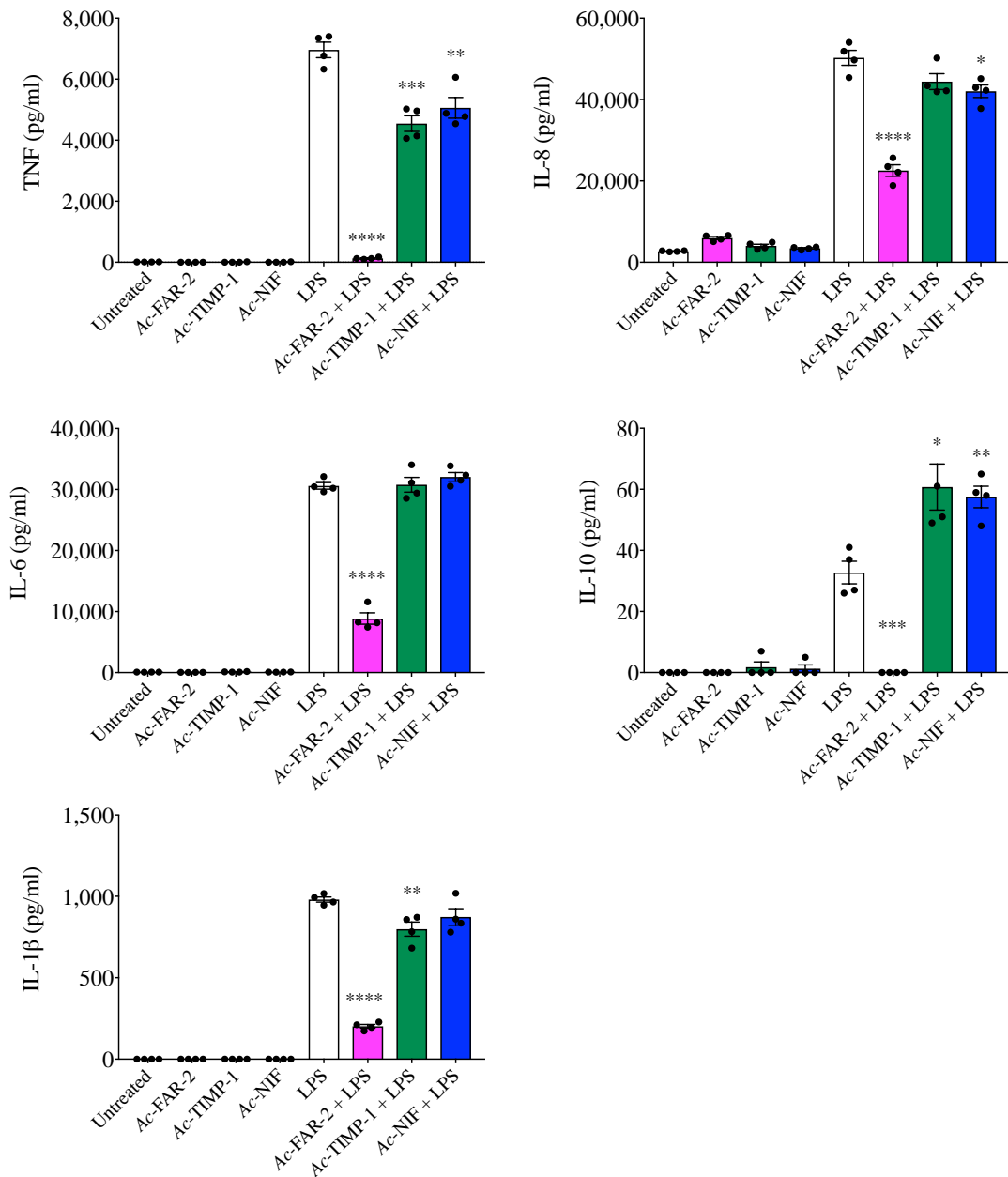
*Figure 4-30 Soluble analyte levels captured by CBA beads of supernatant from LPS-stimulated PBMCs co-cultured with yeast expressed recombinant proteins Ac-FAR-2, Ac-NIF and Ac-TIMP-1. All individual data points are represented, mean ±SEM, sample size (n = 4). The significance was determined by an unpaired, two sample, two-tailed parametric student's t test against the relevant positive control (Untreated cells or LPS-treated cells). Significant increases or decreases against LPS-treated cells * p ≤0.05, ** p ≤0.01, *** p ≤0.001, **** p ≤0.0001.*

4.3.22 Effect of Yeast-Expressed *Ac*-TIMP-1, *Ac*-NIF and *Ac*-FAR-2 on Inflammatory Cytokine Production by Human Peripheral Blood T Cells

The cells treated with protein only showed no increase in pro-inflammatory markers which corresponds to their undetectable LPS measurements. PBMCs were treated with proteins alone or were stimulated with PMA-Ionomycin and recombinant proteins. In like fashion to its effect on innate cells, addition of *Ac*-FAR-2 to PBMCs stimulated with PMA-Ionomycin resulted in significant suppression of IL-2, IL-8 and TNF. *Ac*-TIMP-1 on the other hand significantly up-regulated the production of IL-2, and IL-10 and had no effect on TNF and IL-8 production in comparison to PMA-Ionomycin-treated cells. *Ac*-NIF caused significant up-regulation of IL-10 production and subtle but significant down-regulation of TNF and IL-8 (Figure 4-31).
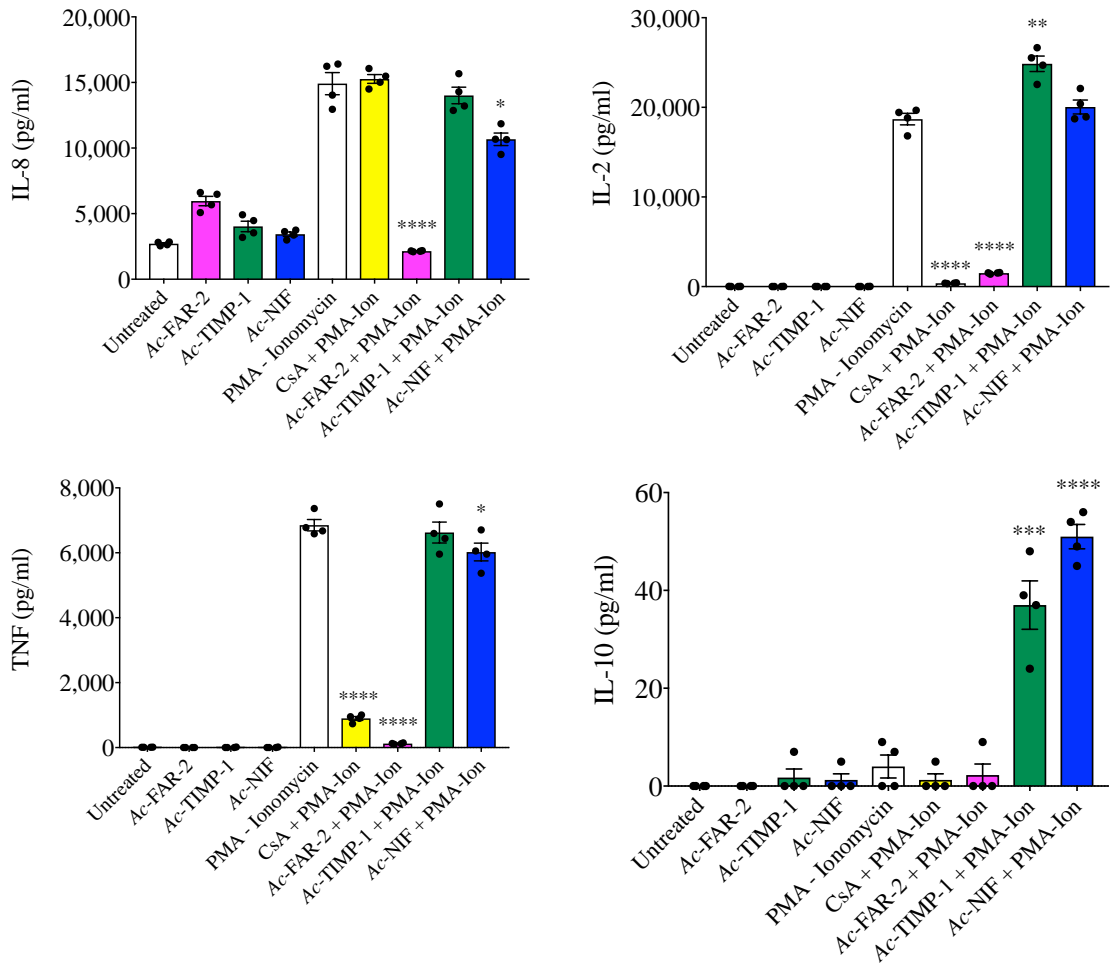
*Figure 4-31 Soluble analyte levels captured by CBA beads of supernatant from PMA-Ionomycin stimulated PBMCs co-cultured with yeast expressed proteins Ac-FAR-2, Ac-NIF and Ac-TIMP-1. All individual data points are represented, mean ± SEM, sample size n = 4. Significance was determined by an unpaired, two sample, two-tailed parametric student's t test against the relevant positive control (Untreated cells or PMA–Ionomycin-treated cells). Significant increases or decreases against PMA-Ionomycin treated cells * p ≤ 0.05, ** p ≤ 0.01, *** p ≤ 0.001, **** p ≤ 0.0001.*

4.3.23 *Ac*-FAR-2 Yeast Expressed Hookworm Protein Repeatedly Suppressed Inflammatory Cytokine TNF Production by PBMCs

The results of the PBMC assay highlighted the dramatic anti-inflammatory properties of *Ac*-FAR-2 on human immune cells. *Ac*-FAR-2 treatment of PBMCs resulted in suppression of the production of multiple inflammatory cytokines when CD3+ cells were stimulated by PMA-Ionomycin including IL-2, and IL-8 (Figure 4-31). When cells were stimulated with LPS, the production of IL-1β, IL-6, IL-8, and IL-10 cytokines was also suppressed by treatment with *Ac*-FAR-2 (Figure 4-30). After consideration of the marked suppression of cytokine production after treatment with *Ac*-FAR-2, the PBMC experiment was replicated with inclusion of additional control treatments of dexamethasone and a LPS negative control to ensure the reproducibility of the assay and data (Figure 4-32).
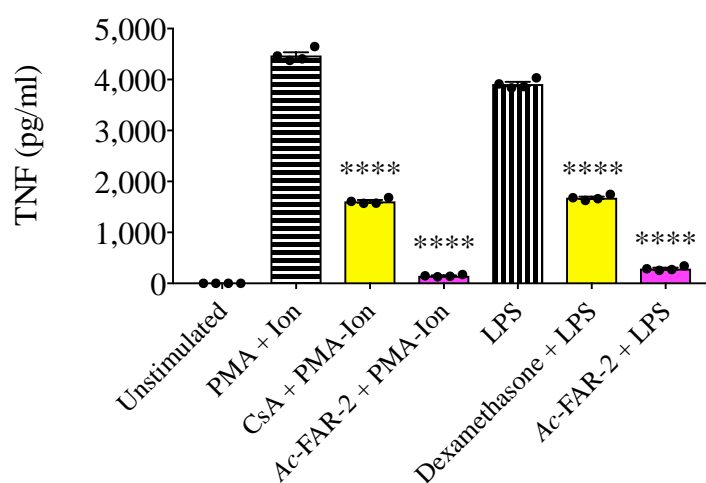
Figure 4-32 Soluble TNF analyte levels captured by CBA beads from human PBMCs co-cultured with yeast-expressed Ac-FAR-2 recombinant protein. TNF levels were significantly reduced in cells treated with PMA-Ionomycin or LPS in the presence of Ac-FAR-2. All individual data points are represented, mean ± SEM, sample size (n = 4). Significance was determined by an unpaired one-tailed parametric student's t test against the relevant positive control; PMA–Ionomycin or LPS. **** p ≤0.0001.

4.4 Discussion

The results from Chapter 3 (TNBS screen of the cell-free lysates) identified many new anti-inflammatory proteins. Some of those proteins were expected to be anti-inflammatory based on their GOs, but other novel proteins with no homologues of known function were also identified. In this chapter, several of the hookworm anti-inflammatory protein candidates identified in Chapter 3 were expressed in a cell-based system, and displayed differing levels of efficacy in two distinct models of murine colitis and in suppression of cytokine production by human PBMCs.

Candidates were selected from three GO groups - a fatty acid binding protein (*Ac*-FAR-2), a TIMP-like protein (*Ac*-TIMP-1) and a group 3 ASP (*Ac*-NIF). The expression of ten additional candidates from the list of lead secretome proteins was endeavoured, but insurmountable protein expression problems were encountered, and there was insufficient time available to express them during the tenure of this PhD thesis. Extensive optimisation and trouble-shooting of the yeast expression system revealed no apparent reasons for the lack of expression. Optimisation of the temperature, culture pH, harvesting time and nutrient supply were all explored and it was concluded that these proteins were not permissive to the yeast expression system[339].

The common advantages of using the methylotrophic *P. pastoris* system for recombinant protein expression include its ability to post-translationally process the protein, fold them effectively, and produce high yields. Moreover, *N*-glycosylation by *Pichia* is closer to higher eukaryotes than it is to bacteria or the yeast *S. cerevisiae*, however, it must be noted that it is still different to mammalian cells. Most importantly from the perspective

199

of this project, the yeast expression system is relatively endotoxin-free if care is taken to ensure pyrogen-free labware is used wherever possible, which is paramount in assessing the anti-inflammatory properties of a protein in both *in vivo* and *in vitro* applications. Firstly, minimal LPS is important for the safety of the mice in the study, and secondly, LPS contamination of recombinant proteins could mask any anti-inflammatory effects.

The proteins that were successfully secreted were subjected to one or more post-translational modifications. These include the addition of disulphide bonds to cysteine pairs, protein folding into its native state, as well as *N-* and *O-* glycosylation. Glycosylation is important because it affects the bioactivity of some proteins as it may protect against proteolysis and promote stability in the extracellular milieu [340]. As previously mentioned, *P. pastoris* does have the propensity to hyperglycosylate recombinant proteins because yeast produce high mannose glycan structures, which was evident in the expression of *Ac*-NIF which contained seven *N*-glycosylation sites. Hyperglycosylation can be circumvented by genetic engineering mutation strategies of troublesome glycosylation sites, and future studies with *Ac*-NIF should consider mutation of glycosylated Asn residues to allow for expression of a glycan-free protein. Of course a glycan-free *Ac*-NIF might not adopt correct fold and could be less stable with increased susceptibility to proteolysis.

The TNBS model of colitis used in this chapter was modified from the protocol described in Chapter 3. Clinically, the animals presented with the same manifestations as observed in the cell-free lysate screen, which included diminished natural curiosity, rapid body weight loss and reduced attentiveness to grooming. The quality and integrity of the architecture of the colon was assessed and sections were analysed by H&E staining to

determine the extent of histopathology. The technique by which the colon tissue is dissected and prepared for histology could be improved in future studies by implementing a swiss roll technique [341]. This would improve histology images and enhance the quality of intestinal epithelial morphology to display intact structural features after sectioning.

Yeast-expressed *Ac*-FAR-2 protected against all parameters measured in the TNBS experiment including weight loss, macroscopic score, cumulative clinical score and colon length. The TNBS experiment will need to be repeated in order to validate the reproducibility of this result. A potential mechanism of action by which *Ac*-FAR-2 protects against TNBS-induced colitis could be via decreased homing of lymphocytes to inflamed colonic tissue by binding to lipid signalling molecules. Furthermore, fatty acid lipid metabolism is crucial in the development, functionality and survival of lymphocytes because fatty acids are sources of cellular energy (triglycerides) and as precursors of membrane phospholipids and cholesterol[342]. Sequestering of fatty acids by *Ac*-FAR-2 could inhibit their incorporation into downstream pathways which could affect immunometabolism and interfere with lymphocyte differentiation or function altering the balance between a pro-inflammatory and an anti-inflammatory response. The mechanism of action of *Ac*-FAR-2 could be confirmed by probing a human proteome array with the protein to find its receptor ligand[323], but this is based on an assumption that it binds to proteins and not lipids.

Chronic models of intestinal inflammation are frequently used to delineate the mechanisms of action of therapeutic proteins. Moreover, these chronic models of disease often resemble the human condition better than acute models do[343]. For this reason, the

recombinant hookworm proteins were chosen to be tested in the T cell transfer model of chronic colitis. In this model, *Ac*-TIMP-1 protected recipient Rag1-knockout mice from T cell transfer induced body weight loss. *Ac*-NIF did not induce significant protection but followed the same trend as *Ac*-TIMP-1. *Ac*-TIMP-1 induced significant protection against macroscopic deterioration of the colon and *Ac*-NIF induced significant protection against colon shortening. As per the TNBS colitis experiment, the T cell transfer results require repeating to validate the reproducibility of this model.

Adoptive transfer of T cells into Rag1-knockout mice induced a mixed T_H1 / T_H17 response with the production of IFN-γ causing inflammation in the small bowel and colon which is similar to CD[344]. The T cell transfer experiment should be repeated to ensure reproducibility but also it could be repeated using a different strain of recipient mice. The analysis of the adoptive transfer of T cells into severe combined immunodeficiency (SCID) mice instead of Rag1-knock out mice is well documented in the literature[109]. The spontaneous mutation of a protein kinase (*Prkdc*) gene in SCID mice creates a premature stop codon which stops the genetic recombination of components of antibodies and T cell receptors[345]. This results in a lack of mature T and B cells. SCID were some of the first available immune deficient mice, and thus have been widely used in research and there is a plethora of publications and historical data on this strain. The SCID mouse model has some "leakiness", which refers to the development of some T or B cells over time, while the Rag-knock out mice are more stable in terms of their lymphocyte deficiency[346]. The knockout of the Rag protein prevents appropriate recombination events that blocks the maturation pathways of T and B cells[347]. Recombination in Rag-knockout mice cannot be initiated like it can in SCID mice, providing the experimental rationale to adopt this chronic model of colitis in my study.

Lead proteins from the hookworm secretome should go on to be tested in other murine models of colitis because no single model faithfully recapitulates the histopathological and clinical characteristics of human IBD. Whether the model focuses on chronic homing of T cells to the gut, or enteric bacteria causing inflammation, or merely being a result of the genetic background of the mice, researchers can use this information to elucidate mechanisms of action of therapeutic proteins. One such model is the Winnie mouse model of spontaneous chronic colitis because its symptoms are highly representative of human IBD[348]. The mice used in this model have a missense mutation in the *muc2* gene which results in dysfunctional control of motor functions in the colon.

In the intestinal mucosa of IBD patients, there is an overproduction of TNF, which in turn induces mucosal barrier cell apoptosis. Apoptosis of the cells diminishes the barrier function of epithelial cells and increases the permeability of the epithelial membrane [349]. During the active phase of IBD flare ups, pathogens within the enteric cavity capitalise on the permeability of the mucosal barrier and translocate into the LP and activate immune cells which in turn produces inflammatory cytokines. TNF, IL-1β, and IL-2 drive inflammation and epithelial cell apoptosis in colitis, providing the experimental rationale for assessing the production of these cytokines by human PBMCs[336],[350]. PBMCs that were treated with *Ac*-FAR-2 showed a dramatic suppression of all cytokines analysed by CBA to a high level of significance (p value < 0.0001). *Ac*-FAR-2 showed major suppression of both T cell and myeloid cell inflammatory cytokines. Unlike *Ac*-TIMP-1 and *Ac*-NIF which promoted secretion of the anti-inflammatory cytokine IL-10, *Ac*-FAR-2 ablated IL-10 production.

A cytokine produced by myeloid cells as a result of the ligation of specific PAMPs to TLRs is IL-6. LPS stimulation of peripheral blood myeloid cells resulted in IL-6 production and this was potently suppressed by recombinant *Ac*-FAR-2. A cytokine that is also known as neutrophil chemotactic factor that promotes homing of neutrophils to sites of inflammation and increases histamine release is IL-8. This is secreted from myeloid cells via ligation of TLRs by LPS, and its secretion was also suppressed by treatment with *Ac*-FAR-2.

The ability of *Ac*-FAR-2 to suppress T cell cytokine expression was demonstrated by stimulating PBMCs with PMA-Ionomycin. *Ac*-FAR-2 was as potent at suppressing IL-2 as the immunosuppressive agent CsA. Indeed, the extent of the suppressive effect of *Ac*-FAR-2 on PBMC cytokine production was so potent that it could have been cytotoxic, and reduced cytokine secretion may have reflected metabolically inactive cells that were dying. While the cells appeared to be healthy by simple visual inspection microscopically, cell toxicity assays to determine the viability of PBMCs after protein treatment should be considered for future work. Moreover, relatively high concentrations of recombinant proteins (100 µg/ml) were used, and a dose-response curve is warranted to identify the optimal therapeutic dose while minimising potential toxicity.

The yeast expressed *Ac*-TIMP-1 protein did not appear to suppress T cell responses which could be a result of suppression of co-stimulatory markers on APCs which has been previously shown by AIPs[194],[207]. LPS-stimulated PBMC that were co-cultured with *Ac*-TIMP-1 secreted significantly less TNF (p value <0.0001), and there was a trend towards down-regulation of the production of IL-1β whilst there was an increase in the production the anti-inflammatory IL-10 (p value = 0.0158) (Figure 4-30). In the presence

204

of LPS, *Ac*-TIMP-1 treatment resulted in significantly reduced levels of TNF and IL-1β. IL-1β is a cytokine produced by activated macrophages and is a pivotal mediator of the pro-inflammatory response by regulating several processes including apoptosis, cell proliferation and differentiation[351].

In PMA-Ionomycin-stimulated cells, *Ac*-TIMP-1 treatment significantly up-regulated the production of IL-2 and IL-10 and there is evidence in the literature, that low dose IL-2 therapy expands Tregs[352]. IL-2 is a cytokine produced by T cells that promotes their differentiation into effector T cells and memory T cells upon initial antigen stimulation. When PBMCs were stimulated with PMA-Ionomycin in the presence of *Ac*-TIMP-1, T cells produced significantly more IL-2 than control cells treated with vehicle. Furthermore, recent studies have found that IL-2 mediates the expansion and the ability of naïve human Tregs to home to the gut in early life[353],[352]. IL-10 is a pleiotropic cytokine with multiple effects in immunoregulation of myeloid and T cells. IL-10 can down-regulate T$_H$1 cytokine expression and can block NF-κB activity. IL-10 can activate T$_H$1 cells to differentiate into Type 1 regulatory (T$_R$1) cells. T$_R$1 cells can regulate tolerance towards antigens from any origin and in the presence of IL-10 can down-regulate inflammation and boost regulatory DCs. IL-10 was upregulated by *Ac*-TIMP-1 in both myeloid and T cell stimulated cultures, and this finding supports *in vivo* mouse data showing an increase in systemic IL-10 levels in *Ac*-TIMP-1-treated animals[194].

4.5 Conclusion

In this chapter, select lead hookworm recombinant proteins identified in the cell-free lysate TNBS-screen were shown to retain their anti-inflammatory properties when produced in yeast. Two distinct *in vivo* murine models were utilised to show the therapeutic effects of these proteins in acute and chronic modes of colitis. Furthermore, the proteins showed varying levels of anti-inflammatory properties on human immune cells, important findings if these proteins are to be considered as potential therapeutics for treating patients with inflammatory diseases. To further assess the drug-like properties of these proteins, additional studies are required to delineate mechanism of action, dose-response kinetics and formulation properties for optimal delivery and efficacy. Additional experiments might also include testing the bioactivity of these proteins on human gut biopsy tissue from IBD patients to determine potency at the site of drug action.

Chapter 5

General Discussion

There is a necessity to develop treatments for IBD that are efficacious, safe, easily produced and well-tolerated by patients because current treatments, notably the biologics, are very costly and come with a host of side effects. The two common forms of IBD have an unknown aetiology. Consequently, many of the therapeutic treatments that are currently available, such as glucocorticoids or anti-TNF antibodies, only provide symptomatic relief, and mop up circulating inflammatory molecules as opposed to targeting early events that trigger inflammatory pathways and actually providing a cure.

The incidence of inflammatory disorders, including IBD, that result from a dysregulated immune system has escalated in the past few decades, particularly in economically developed countries[354]. This geographical association is thought to be directly related to the increased levels of sanitation, improved living conditions and access to antibiotics[355]. Clinical, experimental and epidemiological data indicate that the eradication of many pathogens, such as helminths is at least partially responsible for the increased susceptibility to IBD and other inflammatory diseases[182]. Therefore, research efforts have focused on determining whether helminth infections underpin the urban-rural difference in risk factors for developing inflammatory disorders[356]. Helminths, have evolved mechanisms that suppress and subvert the immune system away from a phenotype that is detrimental to themselves. Moreover, human clinical trials using live hookworm treatment have harnessed the immunoregulatory power of helminths to alter the immune system. To date there have been ten clinical trials that have assessed the safety and / or efficacy of low-dose helminth infection in patients with IBD or other gastrointestinal inflammatory disorders. All of the above trials have shown the infections to be safe, well tolerated, and indeed some trials resulted in clinically beneficial outcomes[357,358,172]. Nevertheless, there are four main drawbacks to live helminth infection: (i) difficulty in

the standardisation of Current Good Manufacturing Practice (cGMP) of live worms on a sufficiently large scale; (ii) potential pathology and clinical unpredictability caused by infection (i.e. alterations in gastro-motility can result in gastrointestinal discomfort); (iii) public perception and the psychological impact on the patient harbouring a parasitic infection, and (iv) regulatory problems (medical regulators have no idea how to approach this because it is such a foreign concept for a drug)[359],[207],[194],[360]. In response to these caveats, much work has been done to elucidate whether the worm could be removed from the equation altogether, by utilising helminths secretomes as therapeutic tools and understanding the protective mechanisms by which worms and their secreted molecules attenuate inflammation.

Our research group in collaboration with the Mitreva lab used a proteogenomic approach to comprehensively analyse the secretomes of several different hookworms, and the proteomic data was used to re-annotate the genomes[361],[362]. Hundreds of new protein candidates that have the potential to be therapeutic leads in the treatment of inflammatory diseases have been identified[363],[364],[187],[196]. Carrying on from the promising work done in this field, some researchers have gone on to express individual recombinant proteins and have shown them to be therapeutic in a multitude of different inflammatory disorders in mice and in some instances provided *ex vivo* supporting data with human cells and tissues[365],[366],[217].

In the context of parasite-derived ES proteins, this thesis aimed to investigate the pharmaceutical potential of 105 hookworm secreted proteins in an experimental mouse model of colitis. This represents the first attempt, to the best of my knowledge, to express and screen such a large number of proteins in a cell-free protein expression system for

anti-inflammatory efficacy *in vivo*. From the results presented in this thesis, a "strike rate" of roughly one-in-five proteins resulted in significant protection against the various parameters of colitis, where 20 out of 105 cell-free lysates tested were deemed to be significantly anti-inflammatory after rigorous statistical filtering. Several proteins were expressed in a cell-based expression system, and these lead proteins retained their anti-inflammatory capacity in at least one mouse model of colitis and significantly attenuated inflammatory cytokine secretion by human PBMCs in culture (Figure 5-1).
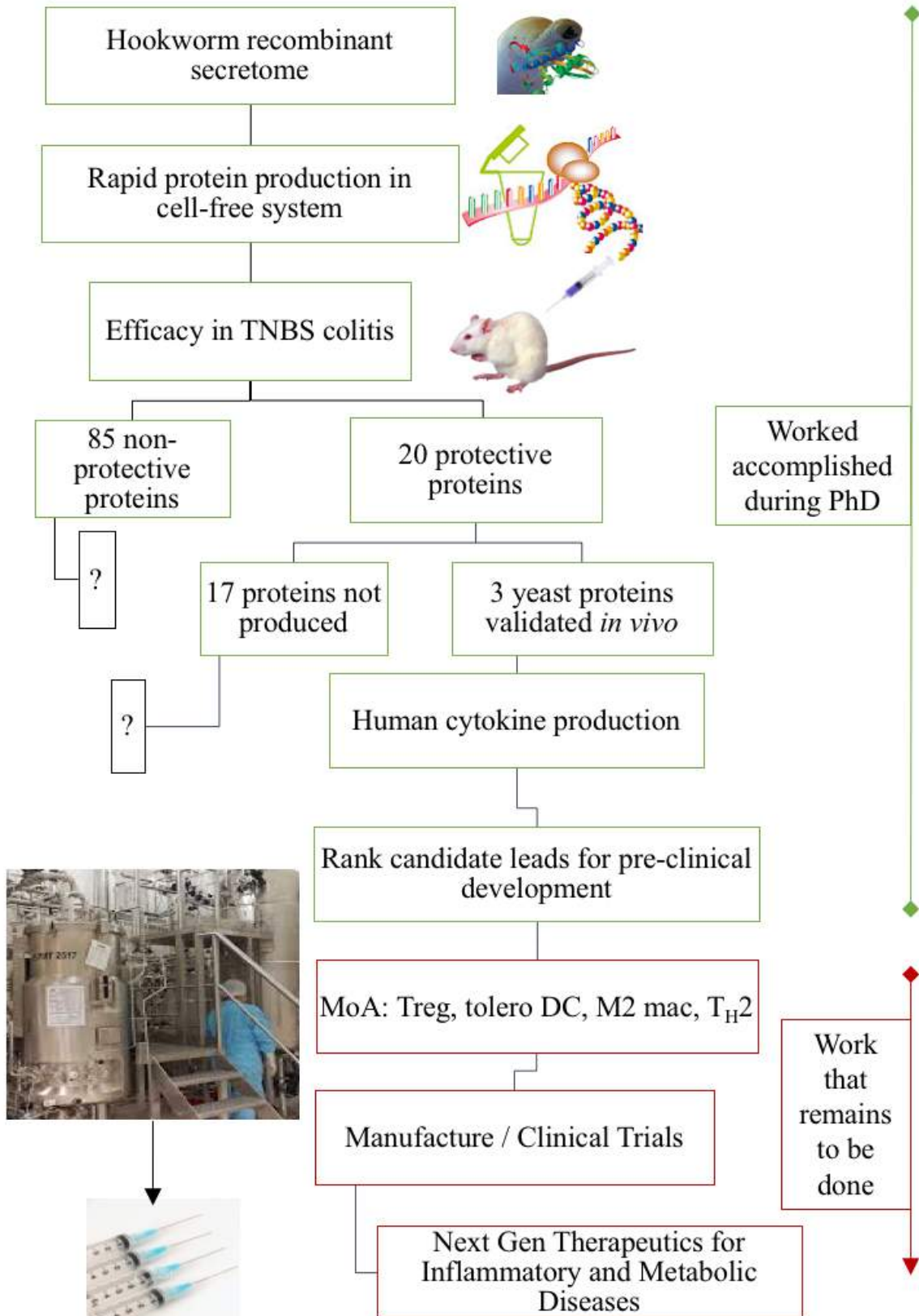
Figure 5-1 Screening the hookworm recombinant secretome for next-generation biologics.

This rapid cell-free protein expression system can produce hookworm-derived ES proteins, many of which retained their biological activity and confer protection against colitis *in vivo*. Altogether, this research has led to the production of a ranked list of hookworm recombinant ES proteins in the form of cell-free lysates, and validation of a small number of lead hits expressed in a cell-based system with both *in vivo* and *in vitro* read-outs. The impact of these findings is substantial because many hundreds of helminth secreted proteins have been described in recent years with the advances in proteomics and genomics, and the approach described herein could facilitate rapid testing for a multitude of different downstream applications and phenotypes. Moreover, the technique lends itself not only to discovery of biologics for treating inflammatory diseases, but also for identifying vaccine and diagnostic biomarker candidates.

In this thesis, the focus was placed upon the most abundant proteins of *Ac*ES, and since the commencement of this PhD tenure, a subsequent re-analysis of *Ac*ES using more sensitive mass spectrometry techniques[361] found that there were twice as many ES proteins as originally proposed by Mulvenna *et al.,* (2009)[211]. Given that many immunologically relevant proteins display bioactivity at very low concentrations (such as cytokines), there is now a need to generate cell-free versions of the remaining *Ac*ES proteins and test them for anti-inflammatory properties.

In order to rigorously validate the screening approach, it has been clearly demonstrated that the body weight of mice was unaffected by the administration of cell-free lysate, both with and without the intrarectal administration of TNBS. As described in Chapter 3, any anti-inflammatory properties observed in the TNBS colitis model with cell-free lysates was therefore attributed to the recombinant hookworm protein expressed by the

212

lysate. Furthermore, it was essential that the proteins were protective over multiple clinical parameters in each experiment and thus used two robust statistical methods to generate an average significance score within an experiment and an average significance score over the entire population screened in the TNBS colitis model was employed. Both methodologies produced the same top twenty lead proteins, which provided confidence in the model and allowed me to proceed with downstream analyses of the lead candidates.

While the methodologies employed in this thesis have yielded a wealth of information and new drug leads, at least some of the proteins that did not protect against TNBS colitis when tested in cell-free lysate form may have been false negatives. This is a drawback of the high-throughput nature of the cell-free protein expression system whereby some proteins are misfolded due to the lack of secretory organelles such as endoplasmic reticulum and golgi apparatus in this system. This would have resulted in some recombinant proteins not possessing the proper conformation and subsequent impaired bioactivity. If time and funding allowed, the hookworm secretome could instead be produced in a cell-based system such as yeast, insect or mammalian cells, and individual proteins purified and assessed for function. Another alternative that could be considered, draws on literature that shows that hookworms and other helminths have recently been shown to secrete EVs, providing other possible alternative therapies by which to screen the secretome for bioactivity. Although more time consuming, this would allow for proper folding, disulphide bond pairing and active secretion across the cell membrane, and could reveal even more therapeutic hits in *in vitro* and *in vivo* models of IBD.

Another limitation of this high-throughput screening of lysate proteins was the direct progression of lysates straight into *in vivo* screening in a mouse model of colitis. Instead

of testing 105 cell-free lysates in an animal model, *in vitro* or *ex vivo* screening protocols could have been employed to identify proteins with defined bioactivities. This approach, however, assumes a pre-conceived idea of the mechanism of action of interest. To address this issue, and given the impact of helminth ES products on APCs[367] the cell-free lysates could be tested for immunomodulatory effects on mixed populations of human immune cells (e.g. human PBMCs) or specific immune cell lines (e.g. THP-1 monocyte-derived DCs or macrophages) that could be immunomodulatory targets for helminth-derived products. These *in vitro* approaches would circumvent the use of animals as a first line screening technique and align future research with the 3Rs concept of replacement, reduction and refinement[368,369]. This methodology would also identify protein interactions with human cells that may have been missed by screening in mice. However, these selective approaches of screening for bioactivity in targeted cell lines may result in an inability to identify complex immunomodulatory pathways that operate only *in vivo*, which is why parallel assessments in a more biologically-relevant *in vivo* setting may still be required. Hence, this was the justification for deciding to go directly *in vivo* with cell-free lysates, to define protection against the onset of colitis at a whole organism level. There are many ways to prevent the onset of inducible colitis, and having a primary endpoint of protection against clinical disease and associated histopathology meant that a broad diversity of proteins with distinct mechanisms of action would be discovered. That indeed was the case, as six different GO categories were identified in the top 20 lead proteins.

A limitation of this thesis is that only three of the anti-inflammatory lead proteins identified in the cell-free lysate screen were progressed to yeast expression and efficacy validation. To validate the anti-inflammatory activity of the proteins that were not

successfully expressed in the cell-based expression system, expression conditions and parameters need to be adjusted, and / or a different expression host cell lines such as mammalian or insect cells need to be explored[370]. *E. coli* is a user-friendly expression host but presents numerous limitations for the expression of hookworm secreted proteins, including the absence of a eukaryotic secretion pathway, difficulty in correctly pairing cysteine residues into disulphide bonds, and the potential for LPS contamination of purified proteins.

Another important factor that needs to be addressed is the risk of hookworm-derived therapies potentially suppressing inflammation and therefore increasing the risk of cancer. Some platyhelminths (*Schistosoma species*) and liver flukes (*Opisthorchis viverrini* and *Clornorchis sinensis*) are involved in the initiation of human cancers, but this is mainly due to chronic inflammation that results from decades long infections[371]. In addition to this association, the long-term use of immunomodulators such as anti-TNF therapy has long been associated with the increased risks of malignancies[372]. This is a concern that would need to be addressed in later stages of drug development. Attention should be paid to any drug that promotes regulatory immune responses and suppresses inflammatory pathways; increased Treg cell function and numbers concurrentlydecreases the ability of T cells to fight tumour cells, sometimes resulting in malignancy[373]. Moreover, worm infection or treatment with anti-inflammatory worm molecules can suppress the T_H1 arm of the immune system and affect an individual's ability to respond to vaccination and infectious diseases such as TB, malaria or influenza.

Based on the successful application herein of cell-free protein expression technology to the discovery of novel biologics sourced from canine hookworms, the secretomes of

other helminths could now be mined for new therapeutics. Specifically, the secretome of the human hookworm, *N. americanus*, has recently been published[362], and this secretome likely contains novel biologics for treating human disease given the coevolution of this host-parasite partnership and subsequent arms race to generate immunity (by the human host) and modulate immunity (by the parasite). *A. caninum* is a parasite of dogs that does not typically mature in humans to establish chronic infection, most likely due to its coevolution with dogs and not humans[362]. In the quest to discover novel human IBD therapeutics, there is strong experimental rationale to explore the *Necator* secretome. At the time of the commencement of this PhD project, the *A. caninum* secretome was available but the *N. americanus* secretome was not. This is primarily due to the difficulty in obtaining sufficient quantities of adult *N. americanus* ESP material for proteomic studies. Moreover, the only reliable animal model for maintaining the *Necator* life cycle involves hamsters, a species which is not permitted for any type of use in Australia. Nonetheless, now that the *Necator* secretome is available, there is growing interest in mining the proteome of this exquisitely adapted human parasite for novel anti-inflammatories (www.paragenbio.com).

The cell-free technology used herein has important implications for all parasitic helminths (including roundworms and flatworms) that have been shown to have therapeutic potential. For example, the secretome of *T. suis* has been published[374] and this whipworm was shown to be well tolerated and efficacious in early phase clinical trials of multiple sclerosis and IBD[375]. Despite the success of early phase trials with iatrogenic whipworm infection, information on the proteins responsible for suppressing inflammatory cytokine production by myeloid cells is only just now being revealed using brute force chromatographic fractionation techniques[374]. Cell-free expression of the

protein components of extracellular vesicles from helminths such as *F. hepatica*[376], and *N. brasiliensis*[377], both of which are known to prevent colitis in murine models, would facilitate rapid discovery of the bioactive proteins. Moreover, a cell-free protein expression approach has also been used to discover potential vaccine and diagnostic antigens from helminths. For example, an *E. coli*-based *in vitro* transcription-translation system was used to produce a subset of the recombinant *S. mansoni* surface proteome for subsequent printing on protein microarrays. The microarrays were probed to show the antibody response signatures of resistant individuals to *S. mansoni* infection for vaccine development[378].

The *A. caninum* proteins identified as a result of this PhD show promise in the treatment of colitis, however they could also be beneficial in the treatment of many other inflammatory disorders. Parasite-derived proteins and their drug-like analogues have been shown to alter inflammatory immune responses and used for the treatment of numerous allergies and autoimmune diseases in mouse models, including systemic lupus erythematosus (SLE)[379], asthma[380], type 1 diabetes[381], multiple sclerosis[365] and rheumatoid arthritis (RA)[357]. Treatment of RA focuses on symptomatic relief rather than curative targeted treatment and results in the global suppression of the immune system. Research endeavours have looked to block or modulate pro-inflammatory macrophages from producing TNF[382]. This has been achieved with a glycoprotein from a filarial nematode, ES-62, for articular inflammation[360]. A galectin that was isolated from the adult stage of the gastrointestinal nematode parasite *Toxascaris leonine* was shown to attenuate colitis but surprisingly inhibited remission of experimental autoimmune encephalomyelitis by up-regulating autoantibody production[383]. This demonstrates that these novel parasite-derived molecules cannot be a pan-anti-inflammatory therapy but

instead exhibit specific mechanisms of action that will be useful in the treatment of specific diseases.

Peptides derived from parasitic helminths are also being explored as therapeutic products alongside proteins. The FhHDM-1 peptide secreted by *F. hepatica* has shown therapeutic efficacy in a mouse model of MS, where efficacy is mediated by IL-5 and the induction of Treg cells in experimental autoimmune encephalomyelitis[384]. Furthermore this same peptide also inhibited mixed granulocytic inflammation and airway hyper-reactivity in experimental asthma[380]. FhHDM-1 to preferentially bind to macrophages instead of lymphocytes and neutrophils when it was administered into the peritoneum of mice and upregulated anti-inflammatory pathways in IL-17-mediated allergic inflammation and prevents inflammasome activation[385]. It has also been shown to target the macrophage lysosome which has been hypothesised as a novel therapeutic option for autoimmune disease[382]. Furthermore, this peptide has also been shown to ameliorate autoimmune disease in a preclinical mouse model of type 1 diabetes[365].

One of the main findings in this thesis was that the proteins identified as anti-inflammatory cell-free lysates in TNBS colitis retained their anti-inflammatory properties when expressed as purified proteins in yeast. Each of three lead yeast-expressed hookworm proteins showed differing levels of anti-colitis efficacy, and some proteins outperformed others depending on the colitic parameters assessed. Moreover, the impact of co-culturing each of the three proteins with human PBMCs showed distinct effects on LPS- and PMA-induced cytokine secretion. This indicates that each protein is likely inducing distinct anti-inflammatory effects via different mechanisms of action. Importantly from a translational perspective, the effect of each protein on PBMC

cytokine production can now be exploited for the development of reproducible potency assays. For example, suppression of human TNF using the CBA technique (chapter 4; section 4.2.21) can be now be adapted to an ELISA format to assess hookworm recombinant protein activity on human PBMCs. Furthermore, from an industry perspective, adapting this methodology to replace PBMCs with a renewable reagent such as an immortal cell line (e.g. THP-1 human monocyte line) would be desirable[368]. Moreover, a human monocyte cell line such as THP-1, assuming it responds to *ex vivo* exposure to a hookworm recombinant protein of interest, could be differentiated into dendritic cells and/or macrophages *in vitro* to further delineate mechanism of action.

Currently the biologically active agents used against IBD are glucocorticoid steroids or biologics. Hookworm derived biologics have offer a potentially safe and well-tolerated option due to their evolutionary tailoring to exist within the human gut. Most of the current mAb therapies on the market are designed to simply mop up excess cytokine within the body, such as TNF. Hookworm-derived proteins on the other hand likely display differentiated and unique mechanisms of action from existing biologics by acting upstream of current targets and switching off initiators of inflammatory responses and skewing towards a regulatory phenotype and tolerance, thus preventing the induction of colitis and other chronic inflammatory conditions.

An avenue that warrants exploration is the mechanisms of action of the hookworm protein leads identified herein. *Ac*-FAR-2 exhibited anti-inflammatory effects *in vivo* and *ex vivo* by suppressing PBMC cytokine production, suggesting that it is likely to skew the immune response towards a suppressor phenotype, but studies to address this in-depth have yet to be carried out. The retinol-binding capabilities of FAR proteins might account

219

for the activity seen in my studies as the protein could interfere with the delivery of bioactive lipids or their intermediates. Previous studies have shown that *Ac*-NIF binds to CD11b / CD18 and it has been hypothesised to inhibit vascular lesions in diabetic retinopathy by antagonising CD11b that mediates damage on endothelial cells by activated leukocytes[386], but the mechanisms by which *Ac*-NIF protcted against colitis remain to be explored. Treatment of mice with *Ac*-TIMP-1 has been shown to upregulate CXCL11 expression in lung tissue, a notable chemokine involved in wound healing[387]. Chemokines are also imperative in shaping the balance between subsets of T cells. In a mouse model of EAE, CXCL11 polarised T_H0 cells into a regulatory phenotype with increased IL-10 levels[388]. Herein, it has been shown that *Ac*-TIMP-1 treatment resulted in a significant increase in IL-10 produced by PMA-stimulated human peripheral blood T cells, further corroborating mouse mechanistic findings.

Another approach to explore mechanisms of action of hookworm secreted proteins is via the use of human proteome microarrays to determine which, if any receptors these proteins would target on the cell surface. This approach was used to identify a role for recombinant *Na*-ASP-2 from *N. americanus* in suppressing B cell receptor signalling [323]. Furthermore, immuno-precipitation of recombinant proteins with host target cell extracts, known as "receptor fishing", can be utilised to pull-down recombinant proteins and their binding partners from lysed target cell populations. Given the g.i. location of adult hookworms, gut biopsy material from IBD patients could also be used to assess the impact of co-culture with hookworm recombinant proteins. Biopsy cells could then be co-stained with defined markers to identify cell populations that interact with the protein. Furthermore, in terms of mechanism of action, next-generation RNA sequencing is frequently used to show the effect of a drug on the transcriptome of target cells[389]. By

identifying gene pathways that are affected by a treatment, specific experiments can be tailored to determine whether that treatment blocks or activities a particular pathway. Moreover, validation of gene sequencing findings often utilise targeted mouse knockout experiments of key driver pathways, or more recently the use of CRISPR-Cas9 to knock-out define genes in cell lines or animals[390],[391],[392].

Another key aspect of any drug development pathway for a hookworm protein therapeutic is dosing route and frequency[393]. Optimal dosing conditions need to be identified to maximise the efficacy while minimizing any side effects. The dosing route used in this thesis was the i.p. route of administration. This is a frequently used dosing route for initial efficacy studies in mice but is rarely used in humans. Moreover, most biologics for treating IBD rely on either intra-venous or sub-cutaneous (s.c.) administration, and any competitive new product for treating IBD would need to be delivered ideally s.c. or preferably as an oral therapy[394]. Oral administration is favoured due to improved patient compliance, and there is less likelihood of a patient developing antibodies to the foreign protein. Moreover, oral delivery targets drugs specifically to the site of action for IBD and therefore minimises systemic exposure and the risk of drug accumulating in other organs.

Finally, structural analysis of the lead hookworm therapeutic proteins is essential if informative structure-activity relationship (SAR) studies are to be undertaken. SAR can help tailor the development of a pre-clinical candidate and identify a minimally active fragment. For example, the granulin growth factor secreted by parasitic liver flukes is a cysteine-rich protein with potent wound-healing properties but the recombinant protein is difficult to express in an industrially scalable form[395],[396]. SAR analyses allowed for the synthesis of a bioactive peptide fragment of liver fluke granulin that retained the

wound healing properties[397] but was easy to synthesise and likely less immunogenic due to its reduced molecular weight. Further to the structural modelling of the three lead therapeutic hookworm proteins in this thesis, experimental determination of the three-dimensional structures using isotopically labelled protein with NMR (nuclear magnetic resonance) spectroscopy or X-ray crystallography would facilitate SAR studies for these proteins[191].

The community of researchers mining helminth secretomes for the development of novel immunotherapeutics is still small, but there is an increasing number of high impact publications in this area[367]. Moreover, pharmaceutical companies are paying attention and biotechnology companies are being formed to specifically discover and develop helminth proteins to treat inflammatory diseases. Indeed, the work presented in this thesis has been used as part of a package of data to attract investment into a new spin-out biotech company formed at JCU, Paragen Bio (www.paragenbio.com). Paragen Bio investors include Australian venture capital groups as well AbbVie, the US pharmaceutical company that produces the world's most profitable drug for treating IBD, the anti-TNF mAb Humira. Through the auspices of Paragen Bio and efforts of other groups around the world, the potential of helminth secreted proteins to form a scaffold for next-generation anti-inflammatories will finally be realised.

The work presented in this thesis describes an entirely novel screening platform that has identified new lead proteins that might one day be translated into a commercial product that will benefit the millions of people around the world suffering from a chronic inflammatory disorder.

Appendices

6.1 Appendix Table 1

1	EU523698.1 ACB13195.1	tissue inhibitor of metalloprotease-2 [*Ancylostoma caninum*]	100%: 100%	NTR_like superfamily	cd03585
2	gi 157997648 EX544266.1	Protein F28E10.1, isoform c [*Haemonchus contortus*]	85%:72%	No putative conserved domains	
3	gi 85672997 DW718354 DW718354.1	hypothetical protein ANCCEY_09468 [*Ancylostoma ceylanicum*]	91%: 82%	GH25_muramidase superfamily	cd00599 cl10448
4	gi 157988383 EX535002.1	hypothetical protein Y032_0157g3200 [*Ancylostoma ceylanicum*]	91%: 89%	GH25_muramidase superfamily	cd06416 cl10448
5	gi 158007955 EX554573.1	hypothetical protein Y032_0255g319 [*Ancylostoma ceylanicum*]	99%: 86%	vWFA superfamily+ CLECT superfamily	cd01477 cd03589 cl00057+cl02 432
6	gi 157990551 gb EX537170.1 EX537170.1	hypothetical protein Y032_0255g315 [*Ancylostoma ceylanicum*]	99%: 89%	vWFA superfamily	cd01477 cl00057
7	gi 158012665 gb EX559283.1 EX559283.1	hypothetical protein Y032_0064g3539 [*Ancylostoma ceylanicum*]	93%: 99%	GLECT superfamily	cd00070 cl00071
8	gi 156185039 gb EW743831.1 EW74831.1	galactoside-binding lectin [*Ancylostoma ceylanicum*]	87%: 96%	GLECT superfamily	cd00070 cl00071 Pfam00337
9	gi 21808086 gb BQ666404.1	hypothetical protein Y032_0256g347 [*Ancylostoma ceylanicum*]	96%: 49%	SCP superfamily	

10	gi 29124850 gb AY217004.1	secreted protein 3 precursor [*Ancylostoma caninum*]	87%: 100%	SCP_euk	cd00168 cl00133
11	NIF - 3415520 L27427.1	neutrophil inhibitory factor [*Ancylostoma caninum*]	95%: 100%	SCP superfamily	cd00168 cl00133 Pfam 00188
12	gi 158009220 gb EX555838.1	SCP_like protein [*Ancylostomma duodenale*]	98%: 73%	SCP superfamily	cd00168 cl00133 Pfam 00189
13	gi 158009159 EX555777.1	SCP_like protein [*Ancylostomma duodenale*]	89%: 71%	SCP superfamily	cd00168 cl00133 Pfam 00190
14	gi 15028472 AF399709.1	platelet inhibitor, partial [*Ancylostoma caninum*]	86%: 100%	SCP superfamily	cd00168 cl00133 Pfam 00191
15	gi 158007422 gb EX554040.1	hypothetical protein ANCDUO_14992, partial [*Ancylostoma duodenale*]	99%: 84%	SCP superfamily	
16	gi 158005927 gb EX552545.1	SCP-like protein, partial [*Ancylostoma duodenale*]	79%: 89%	SCP superfamily	cd00168 cl00133 Pfam 00191
17	gi 157996739 gb EX543357.1	SCP-like protein [*Ancylostoma duodenale*]	98%: 47%	SCP superfamily	
18	gi 158009159 gb EX555777.1	SCP-like protein, partial [*Ancylostoma duodenale*]	89%: 71%	SCP superfamily	cd00168 cl00133 Pfam 00191
19	gi 158009298 gb EX555916.1	SCP-like protein [*Ancylostoma duodenale*]	96%: 58%	SCP superfamily	
20	gi 156183831 gb EW742623.1	hypothetical protein Y032_0004g2028 [*Ancylostoma ceylanicum*]	95%: 77%	SCP superfamily	cd00168 cl00133 Pfam 00191
21	gi 59189474 gb CZ200328.1	hypothetical protein Y032_0005g2414 [*Ancylostoma ceylanicum*]	40%: 89%	SCP superfamily	
22	gi 59254161 gb CZ227136.1	hypothetical protein Y032_0151g2844 [*Ancylostoma ceylanicum*]	46%: 57%	SCP superfamily	
23	gi 157991240 gb EX537859.1	hypothetical protein Y032_0005g2414 [*Ancylostoma ceylanicum*]	86%: 83%	SCP superfamily	cd00168 cl00133 Pfam 00191

24	gi 157997544 gb EX544162.1	hypothetical protein Y032_0477g2171 [*Ancylostoma ceylanicum*]	82%: 80%	SCP superfamily	cd00168 cl00133 Pfam 00191
25	gi 55391839| gb CW709169.1	hypothetical protein ANCDUO_20021, partial [*Ancylostoma duodenale*]	45%: 58%	SCP superfamily	
26	gi 158002778 gb EX549396.1	hypothetical protein Y032_0030g2174 [*Ancylostoma ceylanicum*]	99%: 59%	SCP superfamily	
27	gi 158009220 gb EX555838.1	SCP-like protein [*Ancylostoma duodenale*]	98%: 73%	SCP superfamily	cd00169 cl00134 Pfam 00192
28	gi 158008599 gb EX555217.1	hypothetical protein ANCCEY_09859 [*Ancylostoma ceylanicum*]	60%: 59%	SCP superfamily	
29	gi 156183730 gb EW742522.1	hypothetical protein Y032_0010g1025 [*Ancylostoma ceylanicum*]	82%: 69%	SCP superfamily	cd00169 cl00134 Pfam 00192
30	gi 158019488 gb EX566106.1	hypothetical protein Y032_0045g1167 [*Ancylostoma ceylanicum*]	78%: 75%	SCP superfamily	
31	gi 158007580 gb EX554198.1	hypothetical protein Y032_0045g1167 [*Ancylostoma ceylanicum*]	78%: 67%	SCP superfamily	
32	gi 14318583 gb AF273084.3	zinc metallopeptidase 1 [*Ancylostoma caninum*]	93%: 100%	GluZincin superfamily	cd08662 cl14813 Pfam01431
33	gi 156183344 gb EW742136.1	hypothetical protein Y032_0295g1651 [*Ancylostoma ceylanicum*]	99%: 76%	Asp superfamily	cl26008 Pfam00026
34	gi 157988693 gb EX535312.1	astacin [*Ancylostoma duodenale*]	99%: 94%	Astacin superfamily	cd04280 cl27699 Pfam01400
35	gi 110007378 gb DQ665302.1	metalloprotease-2 [*Ancylostoma caninum*]	82%: 100%	ZnMc superfamily	cd04280 cl00064 Pfam01400
36	gi 984959 gb U18912.1	cathepsin B proteinase, partial [*Ancylostoma caninum*]	92%: 100%	Peptidase_C1 superfamily	cd02620 cl23744 Pfam00112

37	gi 158012119 gb EX558737.1	hypothetical protein Y032_0028g1832 [*Ancylostoma ceylanicum*]	90%: 78%	Peptidase_C1 superfamily	cd02620 cl23744 Pfam00112
38	gi 158012027 gb EX558645.1	hypothetical protein Y032_0154g3018 [*Ancylostoma ceylanicum*]	96%: 78%	Peptidase_C1 superfamily	cd02620 cl23744 Pfam00112
39	gi 158019664 gb EX566282.1	astacin [*Ancylostoma duodenale*]	95%: 80%	ZnMc superfamily	cd04280 cl00064
40	gi 158010776 gb EX557394.1	hypothetical protein Y032_0073g740 [*Ancylostoma ceylanicum*]	99%: 66%	Tetraspanin family	
41	gi 21808958 gb BQ667276.1	hypothetical protein Y032_0627g815 [*Ancylostoma ceylanicum*]	69%: 84%	SCP superfamily	
42	gi 21808590 gb BQ666908.1	hypothetical protein Y032_0999g3344, partial [*Ancylostoma ceylanicum*]	68%: 69%	KU superfamily	cd00109 cl00101 Pfam00014
43	gi 21808088 gb BQ666406.1	hypothetical protein Y032_0443g1548 [*Ancylostoma ceylanicum*]	95%: 87%	SCP superfamily	cd00168 cl00133 Pfam 00191
44	gi 1181142 emb Z69345.1	cysteine proteinase [*Haemonchus contortus*]	95%: 100%	Peptidase_C1 superfamily	cd02620 cl23744 Pfam00112
45	gi 21808232 gb BQ666550.1	putative GPI-anchored protein pfl2 [*Mizuhopecten yessoensis*]	89%: 51%	V-ATPase_G_2 superfamily	cl25545
46	gi 15766285 gb BI744483.1	eukaryotic aspartyl protease [*Ancylostoma duodenale*]	99%: 97%	Pepsin_retropepsin_like superfamily	cd05477 cl26008 Pfam00026
47	gi 21809002 gb BQ667320.1	hypothetical protein Y032_0145g2468 [*Ancylostoma ceylanicum*]	88%: 86%	No putative conserved domains	
48	gi 21808324 gb BQ666642.1	hypothetical protein Y032_0222g2619 [*Ancylostoma ceylanicum*]	91%: 87%	SCP superfamily	
49	gi 21808108 gb BQ666426.1	ASP-7 [*Ancylostoma caninum*]	89%: 82%	SCP superfamily	

50	gi 85672966 DW718323.1	hypothetical protein Y032_1361g3846, partial [*Ancylostoma ceylanicum*]	74%: 41%	No putative conserved domains	
51	gi 85672867 DW718224.1	hypothetical protein Y032_1361g3846, partial [*Ancylostoma ceylanicum*]	71%: 42%	No putative conserved domains	
52	gi 55382664 CW700088.1	hypothetical protein Y032_0387g468 [Ancylostoma ceylanicum]	20%: 59%	No putative conserved domains	
53	gi 59628717 gb CZ243276.1 CZ243276.1	No significant similarity found			
54	gi 158006265 gb EX552883.1	hypothetical protein Y032_0001g60 [*Ancylostoma ceylanicum*]	79%: 35%	No putative conserved domains	
55	gi 156184318 gb EW743110.1	malate dehydrogenase, NAD-dependent [*Ancylostoma ceylanicum*]	99%: 97%	NADB_Rossmann superfamily	cd01336 cl28073 Pfam02866
56	gi 156182715 gb EW741507.1	hypothetical protein Y032_0009g830 [*Ancylostoma ceylanicum*]	76%: 46%	SCP superfamily	
57	gi 21808737 gb BQ667055.1	putative histidine operon leader peptide, partial [*Ancylostoma duodenale*]	100%: 98%	NPA superfamily	cl24891 Pfam16469
58	gi 158012765 gb EX559383.1	putative histidine operon leader peptide, partial [*Ancylostoma duodenale*]	99%: 92%	NPA superfamily	cl24891 Pfam16469
59	gi 158003804 gb EX550422.1	putative histidine operon leader peptide, partial [*Ancylostoma duodenale*]	98%: 96%	NPA superfamily	cl24891 Pfam16469
60	gi 158006869 gb EX553487.1	nematode fatty acid retinoid binding protein [*Ancylostoma ceylanicum*]	73% 89%	Gp-FAR-1	cl05414 Pfam05823
61	gi 158008118 gb EX554736.1	hypothetical protein Y032_0002g1070	79%: 91%	SCP superfamily	

		[*Ancylostoma ceylanicum*]			
62	gi 156184318 gb EW743110.1	malate dehydrogenase, NAD-dependent [*Ancylostoma ceylanicum*]	99%: 97%	NADB_Rossmann superfamily	cd01336 cl28073 Pfam02866
63	gi 59630114 gb CZ244673.1	No significant similarity found			
64	gi 59631715 gb CZ246274.1	No significant similarity found			
65	gi 156184887 gb EW743679.1	hypothetical protein ANCCEY_01248 [*Ancylostoma ceylanicum*]	96%: 90%	No putative conserved domains	
66	gi 157997476 gb EX544094.1	hypothetical protein Y032_0073g740 [*Ancylostoma ceylanicum*]	97%: 59%	No putative conserved domains	
67	gi 21808303 gb BQ666621.1	hypothetical protein Y032_0596g435 [*Ancylostoma ceylanicum*]	96%: 80%	No putative conserved domains	
68	gi 158011812 EX558430.1	Transthyretin-like family protein [*Necator americanus*]	57%: 100%	TTR-52 superfamily	
69	gi 85672960 gb DW718317.1	Transthyretin-like family protein [*Ancylostoma duodenale*]	47%: 99%	TTR-52 superfamily	cl03084 Pfam01060
70	gi 16924887 gb BM077851.1	Transthyretin-like family protein [*Ancylostoma duodenale*]	79%: 98%	TTR-52 superfamily	cl03084 Pfam01060
71	gi 158011916 gb EX558534.1	Transthyretin-like family protein [*Ancylostoma duodenale*]	98%: 80%	TTR-52 superfamily	cl03084 Pfam01060
72	gi 157989171 gb EX535790.1	Transthyretin-like family protein [*Ancylostoma ceylanicum*]	86%: 56%	TTR-52 superfamily	cl03084 Pfam01060
73	gi 22347361 AF397162.1	putative tissue metalloprotease inhibitor Aca14 [*Ancylostoma caninum*]	75%: 100%	NTR_like superfamily	cd03577 cl02512 Pfam01759
74	gi 158017850 EX564468.1	hypothetical protein ANCCEY_04214 [*Ancylostoma ceylanicum*]	44%: 33%	No putative conserved domains	
75	gi 170295877 ACB13195.1	tissue inhibitor of metalloprotease-2	100%: 100%	NTR_like superfamily	cd03577 cl02512 Pfam00965

		[*Ancylostoma caninum*]			
76	gi 158014078 gb EX560696.1	hypothetical protein ANCDUO_09587 [*Ancylostoma duodenale*]	92%: 94%	No putative conserved domains	
77	gi 158017414 gb EX564032.1	hyaluronoglucosaminidase [*Ancylostoma ceylanicum*]	99%: 80%	Glyco_hydro_56	cl03288 Pfam01630
78	gi 47717440 gb AY605283.1	glutathione S-transferase [*Ancylostoma caninum*]	83%: 100%	GST_C_family superfamily	cd03192 cl02776 Pfam14497
79	gi 22532420 gb AF533365.1	fatty acid- and retinol-binding protein 2 [*Ancylostoma caninum*]	88%: 100%	Gp-FAR-1	cl05414 Pfam05823
80	gi 12727575 gb BG232400.1	Annexin, partial [Oesophagostomum dentatum]	93%: 97%	Annexin superfamily	cl02574 Pfam00191
81	gi 16924702 gb BM077666.1	14-3-3 protein [*Ancylostoma ceylanicum*]	98%: 89%	14-3-3 superfamily	cd11310 cl02098 Pfam00244
82	gi 156185538 gb EW744330.1	putative dihydrolipoyl dehydrogenase [*Ancylostoma duodenale*]	100%: 98%	Pyr_redox_superfamily	cl26177 Pfam07992
83	gi 157988805 gb EX535424.1	hypothetical protein Y032_0073g740 [*Ancylostoma ceylanicum*]	96%: 71%	No putative conserved domains	
84	gi 23268454 gb AY136548.1	secreted-protein 1 precursor [*Ancylostoma ceylanicum*]	96%: 100%	SCP superfamily	cd00169 cl00134 Pfam 00192
85	gi 3608492 gb AF089728.1	secreted protein ASP-2 precursor [*Ancylostoma caninum*]	79%: 100%	SCP superfamily	cd00169 cl00134 Pfam 00192
86	gi 71483117 gb AAR03712.2	secreted protein 3 precursor [*Ancylostoma ceylanicum*]	100%: 100%	SCP superfamily	cd00169 cl00134 Pfam 00192
87	gi 29124852 gb AY217005.1	secreted protein 4 precursor [*Ancylostoma caninum*]	90%: 100%	SCP superfamily	cd00169 cl00134 Pfam 00192
88	gi 29124854 gb AY217006.1	secreted protein 5 precursor [*Ancylostoma caninum*]	91%: 100%	SCP superfamily	cd00169 cl00134 Pfam 00192
89	gi 29124856 gb AY217007.1	secreted protein 6 precursor	92%: 100%	SCP superfamily	cd00169 cl00134 Pfam 00192

		[*Ancylostoma caninum*]			
90	gi 21808236 gb BQ666554.1	ASP-7 [*Ancylostoma caninum*]	98%: 99%	SCP superfamily	
91	gi 158012264 gb EX558882.1	hypothetical protein Y032_0085g1832 [*Ancylostoma ceylanicum*]	99%: 79%	SCP superfamily	cd00169 cl00134 Pfam 00192
92	augustus-NECAMEDFT_ Contig39-abinit-gene-5.8-mRNA-1	hypothetical protein NECAME_03290 [*Necator americanus*]	42%: 100%	No putative conserved domains	
93	maker-NECAMEDFT_ Contig676-augustus-gene-0.66-mRNA-1	hypothetical protein NECAME_14139 [*Necator americanus*]	98%: 100%	No putative conserved domains	
94	maker-NECAMEDFT_ Contig16-pred_gff_fgenes h-gene-5.5-mRNA-1	hypothetical protein NECAME_01785 [*Necator americanus*]	99%: 100%	No putative conserved domains	
95	maker-NECAMEDFT_ Contig181-pred_gff_snap-gene-0.7-mRNA-1	hypothetical protein NECAME_07865 [*Necator americanus*]	98%: 100%	No putative conserved domains	
96	maker-NECAMEDFT_ Contig560-pred_gff_snap-gene-0.23-mRNA-1	hypothetical protein NECAME_13112 [*Necator americanus*]	99%: 100%	No putative conserved domains	
97	maker-NECAMEDFT_ Contig575-augustus-gene-0.145-mRNA-1	hypothetical protein NECAME_13264 [*Necator americanus*]	99%: 100%	No putative conserved domains	
98	maker-NECAMEDFT_ Contig60-augustus-gene-3.63-mRNA-1	hypothetical protein NECAME_04282 [*Necator americanus*]	98%: 100%	No putative conserved domains	
99	maker-NECAMEDFT_ Contig664-pred_gff_fgenes h-gene-0.8-mRNA-1	hypothetical protein NECAME_14037 [*Necator americanus*]	99%: 100%	No putative conserved domains	
100	maker-NECAMEDFT_ Contig670-augustus-gene-0.79-mRNA-1	hypothetical protein NECAME_14084 [*Necator americanus*]	98%: 100%	No putative conserved domains	

101	maker-NECAMEDFT_Contig8-augustus-gene-0.45-mRNA-1	hypothetical protein NECAME_00948 [*Necator americanus*]	71%: 100%	No putative conserved domains	
102	maker-NECAMEDFT_Contig82201-augustus-gene-0.1-mRNA-1	hypothetical protein NECAME_07255 [*Necator americanus*]	74%: 80%	No putative conserved domains	
103	maker-NECAMEDFT_Contig82698-pred_gff_fgenesh-gene-0.1-mRNA-1	hypothetical protein NECAME_07255 [*Necator americanus*]	56%: 75%	No putative conserved domains	
104	augustus-NECAMEDFT_Contig1405-abinit-gene-0.0-mRNA-1	hypothetical protein NECAME_17161 [*Necator americanus*]	52%: 100%	No putative conserved domains	
105	maker-NECAMEDFT_Contig1154-pred_gff_fgenesh-gene-0.1-mRNA-1	hypothetical protein NECAME_16625 [*Necator americanus*]	82%: 100%	No putative conserved domains	
106	maker-NECAMEDFT_Contig18-augustus-gene-5.130-mRNA-1	hypothetical protein NECAME_01945 [*Necator americanus*]	99%: 100%	No putative conserved domains	
107	maker-NECAMEDFT_Contig999-pred_gff_snap-gene-0.25-mRNA-1	hypothetical protein NECAME_15991 [*Necator americanus*]	99%: 100%	No putative conserved domains	
108	Na-ASP-2	secreted protein ASP-2 [*Necator americanus*]	83%: 100%	SCP superfamily	cd00169 cl00134 Pfam 00192
109	augustus-NECAMEDFT_Contig10-abinit-gene-10.5-mRNA-1	none		No significant similarity found	
110	maker-NECAMEDFT_Contig119-augustus-gene-0.59-mRNA-1	hypothetical protein NECAME_06315 [*Necator americanus*]		No significant similarity found	
111	maker-NECAMEDFT_Contig581-pred_gff_fgenesh-gene-0.8-mRNA-1	hypothetical protein NECAME_13304 [*Necator americanus*]	99%: 100%	No putative conserved domains	
112	maker-NECAMEDFT_	hypothetical protein	98%: 100%	No putative conserved domains	

	Contig62330-pred_gff_snap-gene-0.2-mRNA-1	NECAME_18587, partial [*Necator americanus*]			
113	maker-NECAMEDFT_Contig63567-augustus-gene-0.4-mRNA-1	hypothetical protein NECAME_18730 [*Necator americanus*]	100%: 100%	No putative conserved domains	
114	maker-NECAMEDFT_Contig67356-pred_gff_snap-gene-0.0-mRNA-1	hypothetical protein NECAME_19195 [*Necator americanus*]	98%: 100%	No putative conserved domains	

Table 6-1 Appendix Table 1 Expressed Sequence Tags (ESTs) chosen from the Mulvenna

et al., (2009)[211] and Datu et al., (2008)[265].

6.2 Appendix Table 2

pLTE DNA expression results in *L. tarentolae* cell-free protein expression system.

No.	ES Protein Group	GenBank™	Positive Protein Expression
1	AIP-2		y
2	Lysozyme-like 1	EX544266.1	y
3	Lysozyme-like 2	DW718354.1	Unsynthesised
4	Lysozyme-like 3	EX535002.1	y
5	Lectins 1	EX554573.1	y
6	Lectins 3	EX537170.1	Unsynthesised
7	Lectins 4	EX559283.1	y
8	Lectins 5	EW74831.1	y
9	Secreted 1	BQ666404.1	y
10	Secreted 3	AY217004.1	y
11	Secreted 4	L27427.1	y
12	Secreted 5	EX555838.1	y
13	Secreted 6	EX555777.1	y
14	Secreted 7	AF399709.1	y
15	Secreted 8	EX554040.1	y
16	Secreted 9	EX552545.1	y
17	Secreted 10	EX543357.1	y
18	Secreted 12	EX555777.1	Unsynthesised
19	Secreted 13	EX555916.1	y
20	Secreted 14	EW742623.1	y
21	Secreted 15	CZ200328.1	y
22	Secreted 16	CZ227136.1	y
23	Secreted 17	EX537859.1	y
24	Secreted 18	EX544162.1	y
25	Secreted 19	CW709169.1	y
26	Secreted 20	EX549396.1	y
27	Secreted 21	EX555838.1	y
28	Secreted 22	EX555217.1	y
29	Secreted 23	EW742522.1	y
30	Secreted 24	EX566106.1	y
31	Secreted 25	EX554198.1	y
32	Protease 1	AF273084.3	y
33	Protease 2	EW742136.1	y
34	Protease 3	EX535312.1	y
35	Protease 4	DQ665302.1	y
36	Protease 5	U18912.1	y

37	Protease 6	EX558737.1	y
38	Protease 7	EX558645.1	y
39	Protease 8	EX566282.1	y
40	Strutural 1	EX557394.1	y
41	L3 Upreg 1	BQ667276.1	y
42	L3 Upreg 4	BQ666908.1	y
43	L3 Upreg 5	BQ666406.1	y
44	L3 Upreg 13	Z69345.1	y
45	L3 Upreg 17	BQ666550.1	y
46	L3 Upreg 18	BI744483.1	y
47	L3 Upreg 19	BQ667320.1	y
48	L3 Upreg 20	BQ666642.1	y
49	L3 Upreg 29	BQ666426.1	y
50	Unknown Func 1	DW718323.1	y
51	Unknown Func 2	DW718224.1	y
52	Unknown Func 3	CW700088.1	y
53	Unknown Func 5	CZ243276.1	y
54	Unknown Func 6	EX552883.1	y
55	Unknown Func 7	EW743110.1	y
56	Unknown Func 8	EW741507.1	y
57	Unknown Func 10	BQ667055.1	y
58	Unknown Func 11	EX559383.1	y
59	Unknown Func 12	EX550422.1	Unsynthesised
60	Unknown Func 13	EX553487.1	y
61	Unknown Func 14	EX554736.1	y
62	Unknown Func 15	EW743110.1	Unsynthesised
63	Unknown Func 16	CZ244673.1	y
64	Unknown Func 17	CZ246274.1	y
65	Unknown Func 19	EW743679.1	y
66	Unknown Func 20	EX544094.1	Unsynthesised
67	Unknown Func 21	BQ666621.1	y
68	Transthyretin-like 1	EX558430.1	y
69	Transthyretin-like 2	DW718317.1	y
70	Transthyretin-like 3	BM077851.1	y
71	Transthyretin-like 4	EX558534.1	Unsynthesised
72	Transthyretin-like 5	EX535790.1	y
73	AIP-1 / Met Inhib 1	AF397162.1	y
74	Met Inhib 2	EX564468.1	y
75	Met Inhib 3	ACB13195.1	Non expressor
76	Miscellaneous 1	EX560696.1	y
77	Miscellaneous 2	EX564032.1	y

234

78	Miscellaneous 3	AY605283.1	y
79	Miscellaneous 5	AF533365.1	y
80	Miscellaneous 6	BG232400.1	y
81	Miscellaneous 7	BM077666.1	y
82	Miscellaneous 8	EW744330.1	y
83	Miscellaneous 9	EX535424.1	y
84	ASP-1 / L3 Upreg 10	AY136548.1	y
85	ASP-2 / L3 Upreg 8	AF089728.1	y
86	ASP-3 / L3 Upreg 12	AAR03712.2	y
87	ASP-4 Secreted 11	AY217005.1	y
88	ASP-5	AY217006.1	y
89	ASP-6 / Secreted 26	AY217007.1	y
90	ASP-7 / L3 Upreg 6	BQ666554.1	y
91	ASP-8	EX558882.1	y
92	NECAME_03290	augustus-NECAMEDFT_Contig39-abinit-gene-5.8-mRNA-1	y
93	NECAME_14139	maker-NECAMEDFT_Contig676-augustus-gene-0.66-mRNA-1	y
94	NECAME_01785	maker-NECAMEDFT_Contig16-pred_gff_fgenesh-gene-5.5-mRNA-1	y
95	NECAME_07865	maker-NECAMEDFT_Contig181-pred_gff_snap-gene-0.7-mRNA-1	y
96	NECAME_13112	maker-NECAMEDFT_Contig560-pred_gff_snap-gene-0.23-mRNA-1	y
97	NECAME_13264	maker-NECAMEDFT_Contig575-augustus-gene-0.145-mRNA-1	y
98	NECAME_04282	maker-NECAMEDFT_Contig60-augustus-gene-3.63-mRNA-1	y
99	NECAME_14037	maker-NECAMEDFT_Contig664-pred_gff_fgenesh-gene-0.8-mRNA-1	y
100	NECAME_14084	maker-NECAMEDFT_Contig670-augustus-gene-0.79-mRNA-1	y
101	NECAME_00948	maker-NECAMEDFT_Contig8-augustus-gene-0.45-mRNA-1	y
102	NECAME_07255.1	maker-NECAMEDFT_Contig82201-augustus-gene-0.1-mRNA-1	y
103	NECAME_07255.2	maker-NECAMEDFT_Contig82698-pred_gff_fgenesh-gene-0.1-mRNA-1	y
104	NECAME_17161	augustus-NECAMEDFT_Contig1405-abinit-gene-0.0-mRNA-1	y
105	NECAME_16625	maker-NECAMEDFT_Contig1154-pred_gff_fgenesh-gene-0.1-mRNA-1	y
106	NECAME_01945	maker-NECAMEDFT_Contig18-augustus-gene-5.130-mRNA-1	y
107	NECAME_15991	maker-NECAMEDFT_Contig999-pred_gff_snap-gene-0.25-mRNA-1	y
108	Na-ASP-2	Na-ASP2	Non expressor
109	NECAME_Contig10	augustus-NECAMEDFT_Contig10-abinit-gene-10.5-mRNA-1	y
110	NECAME_06315	maker-NECAMEDFT_Contig119-augustus-gene-0.59-mRNA-1	y
111	NECAME_13304	maker-NECAMEDFT_Contig581-pred_gff_fgenesh-gene-0.8-mRNA-1	y
112	NECAME_18587	maker-NECAMEDFT_Contig62330-pred_gff_snap-gene-0.2-mRNA-1	y
113	NECAME_18730	maker-NECAMEDFT_Contig63567-augustus-gene-0.4-mRNA-1	y
114	NECAME_19195	maker-NECAMEDFT_Contig67356-pred_gff_snap-gene-0.0-mRNA-1	y

Table 6-2 pLTE DNA expression results in L. tarentolae cell-free protein expression

system.

References

1. Danese S, Fiocchi C. Ulcerative colitis. *N Engl J Med.* Nov 3 2011;365(18):1713-1725. doi: 10.1056/NEJMra1102942.
2. Su H-J, Chiu Y-T, Chiu C-T, et al. Inflammatory bowel disease and its treatment in 2018: Global and Taiwanese status updates. *J Formos Med Assoc.* 2018/07/24/ 2018. doi: https://doi.org/10.1016/j.jfma.2018.07.005.
3. Binder V. Epidemiology of IBD during the twentieth century: an integrated view. *Best Pract Res Clin Gastroenterol.* Jun 2004;18(3):463-479. doi: 10.1016/j.bpg.2003.12.002.
4. Baumgart DC, Sandborn WJ. Inflammatory bowel disease: clinical aspects and established and evolving therapies. *Lancet.* May 12 2007;369(9573):1641-1657. doi: 10.1016/s0140-6736(07)60751-x.
5. Korolkova OY, Myers JN, Pellom ST, Wang L, M'Koma AE. Characterization of Serum Cytokine Profile in Predominantly Colonic Inflammatory Bowel Disease to Delineate Ulcerative and Crohn's Colitides. *Clin Med Insights Gastroenterol.* 2015;8:29-44. doi: 10.4137/CGast.S20612.
6. Wilson J, Hair C, Knight R, et al. High incidence of inflammatory bowel disease in Australia: a prospective population-based Australian incidence study. *Inflamm Bowel Dis.* Sep 2010;16(9):1550-1556. doi: 10.1002/ibd.21209.
7. Jostins L, Ripke S, Weersma RK, et al. Host-microbe interactions have shaped the genetic architecture of inflammatory bowel disease. *Nature.* Nov 1 2012;491(7422):119-124. doi: 10.1038/nature11582.
8. Kaplan GG. The global burden of IBD: from 2015 to 2025. *Nat Rev Gastroenterol Hepatol.* Dec 2015;12(12):720-727. doi: 10.1038/nrgastro.2015.150.
9. Molodecky NA, Soon IS, Rabi DM, et al. Increasing incidence and prevalence of the inflammatory bowel diseases with time, based on systematic review. *Gastroenterology.* Jan 2012;142(1):46-54.e42; quiz e30. doi: 10.1053/j.gastro.2011.10.001.
10. Baumgart DC, Bernstein CN, Abbas Z, et al. IBD Around the world: comparing the epidemiology, diagnosis, and treatment: proceedings of the World Digestive Health Day 2010--Inflammatory Bowel Disease Task Force meeting. *Inflamm Bowel Dis.* Feb 2011;17(2):639-644. doi: 10.1002/ibd.21409.
11. Mulder DJ, Noble AJ, Justinich CJ, Duffin JM. A tale of two diseases: the history of inflammatory bowel disease. *J Crohns Colitis.* May 2014;8(5):341-348. doi: 10.1016/j.crohns.2013.09.009.
12. Wolff WI. Colonoscopy: history and development. *Am J Gastroenterol.* Sep 1989;84(9):1017-1025.
13. Button LA, Roberts SE, Goldacre MJ, Akbari A, Rodgers SE, Williams JG. Hospitalized prevalence and 5-year mortality for IBD: record linkage study. *World J Gastroenterol.* Jan 28 2010;16(4):431-438.
14. Loftus EV, Jr., Silverstein MD, Sandborn WJ, Tremaine WJ, Harmsen WS, Zinsmeister AR. Ulcerative colitis in Olmsted County, Minnesota, 1940-1993: incidence, prevalence, and survival. *Gut.* Mar 2000;46(3):336-343.
15. Neurath MF. Cytokines in inflammatory bowel disease. *Nat Rev Immunol.* May 2014;14(5):329-342. doi: 10.1038/nri3661.

References

16. Probert CS, Jayanthi V, Pinder D, Wicks AC, Mayberry JF. Epidemiological study of ulcerative proctocolitis in Indian migrants and the indigenous population of Leicestershire. *Gut.* May 1992;33(5):687-693.

17. Pinsk V, Lemberg DA, Grewal K, Barker CC, Schreiber RA, Jacobson K. Inflammatory bowel disease in the South Asian pediatric population of British Columbia. *Am J Gastroenterol.* May 2007;102(5):1077-1083. doi: 10.1111/j.1572-0241.2007.01124.x.

18. Yazdanbakhsh M, Kremsner PG, van Ree R. Allergy, parasites, and the hygiene hypothesis. *Science.* Apr 19 2002;296(5567):490-494. doi: 10.1126/science.296.5567.490.

19. Cho JH, Brant SR. Recent insights into the genetics of inflammatory bowel disease. *Gastroenterology.* May 2011;140(6):1704-1712. doi: 10.1053/j.gastro.2011.02.046.

20. Ikeya K, Hanai H, Sugimoto K, et al. The Ulcerative Colitis Endoscopic Index of Severity More Accurately Reflects Clinical Outcomes and Long-term Prognosis than the Mayo Endoscopic Score. *J Crohns Colitis.* Mar 2016;10(3):286-295. doi: 10.1093/ecco-jcc/jjv210.

21. Fiocchi C. Inflammatory bowel disease: etiology and pathogenesis. *Gastroenterology.* Jul 1998;115(1):182-205.

22. Lennard-Jones JE, Shivananda S. Clinical uniformity of inflammatory bowel disease a presentation and during the first year of disease in the north and south of Europe. EC-IBD Study Group. *Eur J Gastroenterol Hepatol.* Apr 1997;9(4):353-359.

23. Ochsenkuhn T, D'Haens G. Current misunderstandings in the management of ulcerative colitis. *Gut.* Sep 2011;60(9):1294-1299. doi: 10.1136/gut.2010.218180.

24. Solberg IC, Lygren I, Jahnsen J, et al. Clinical course during the first 10 years of ulcerative colitis: results from a population-based inception cohort (IBSEN Study). *Scand J Gastroenterol.* 2009;44(4):431-440. doi: 10.1080/00365520802600961.

25. Charpentier C, Salleron J, Savoye G, et al. Natural history of elderly-onset inflammatory bowel disease: a population-based cohort study. *Gut.* Mar 2014;63(3):423-432. doi: 10.1136/gutjnl-2012-303864.

26. Arai M, Naganuma M, Sugimoto S, et al. The Ulcerative Colitis Endoscopic Index of Severity is Useful to Predict Medium- to Long-Term Prognosis in Ulcerative Colitis Patients with Clinical Remission. *J Crohns Colitis.* Nov 2016;10(11):1303-1309. doi: 10.1093/ecco-jcc/jjw104.

27. Van Assche G, Vermeire S, Noman M, et al. Infliximab administered with shortened infusion times in a specialized IBD infusion unit: a prospective cohort study. *J Crohns Colitis.* Sep 2010;4(3):329-333. doi: 10.1016/j.crohns.2009.12.012.

28. Cunningham KE, Turner JR. Myosin light chain kinase: pulling the strings of epithelial tight junction function. *Ann N Y Acad Sci.* Jul 2012;1258:34-42. doi: 10.1111/j.1749-6632.2012.06526.x.

29. Mankertz J, Schulzke JD. Altered permeability in inflammatory bowel disease: pathophysiology and clinical implications. *Curr Opin Gastroenterol.* Jul 2007;23(4):379-383. doi: 10.1097/MOG.0b013e32816aa392.

30. Villanacci V, Antonelli E, Geboes K, Casella G, Bassotti G. Histological healing in inflammatory bowel disease: a still unfulfilled promise. *World J Gastroenterol.* Feb 21 2013;19(7):968-978. doi: 10.3748/wjg.v19.i7.968.

237

References

31. Geremia A, Jewell DP. The IL-23/IL-17 pathway in inflammatory bowel disease. *Expert Rev Gastroenterol Hepatol.* Apr 2012;6(2):223-237. doi: 10.1586/egh.11.107.

32. Anderson CA, Boucher G, Lees CW, et al. Meta-analysis identifies 29 additional ulcerative colitis risk loci, increasing the number of confirmed associations to 47. *Nat Genet.* Mar 2011;43(3):246-252. doi: 10.1038/ng.764.

33. Franke A, McGovern DP, Barrett JC, et al. Genome-wide meta-analysis increases to 71 the number of confirmed Crohn's disease susceptibility loci. *Nat Genet.* Dec 2010;42(12):1118-1125. doi: 10.1038/ng.717.

34. Biancone L, Michetti P, Travis S, et al. European evidence-based Consensus on the management of ulcerative colitis: Special situations. *J Crohns Colitis.* Mar 2008;2(1):63-92. doi: 10.1016/j.crohns.2007.12.001.

35. Cui G, Yuan A. A Systematic Review of Epidemiology and Risk Factors Associated With Chinese Inflammatory Bowel Disease. *Front Med (Lausanne).* 2018;5:183. doi: 10.3389/fmed.2018.00183.

36. Glocker EO, Kotlarz D, Klein C, Shah N, Grimbacher B. IL-10 and IL-10 receptor defects in humans. *Ann N Y Acad Sci.* Dec 2011;1246:102-107. doi: 10.1111/j.1749-6632.2011.06339.x.

37. Hisamatsu T, Kanai T, Mikami Y, Yoneno K, Matsuoka K, Hibi T. Immune aspects of the pathogenesis of inflammatory bowel disease. *Pharmacol Ther.* Mar 2013;137(3):283-297. doi: 10.1016/j.pharmthera.2012.10.008.

38. Sales-Campos H, Basso PJ, Alves VB, et al. Classical and recent advances in the treatment of inflammatory bowel diseases. *Braz J Med Biol Res.* Feb 2015;48(2):96-107. doi: 10.1590/1414-431x20143774.

39. Hampe J, Franke A, Rosenstiel P, et al. A genome-wide association scan of nonsynonymous SNPs identifies a susceptibility variant for Crohn disease in ATG16L1. *Nat Genet.* Feb 2007;39(2):207-211. doi: 10.1038/ng1954.

40. Halfvarson J. Genetics in twins with Crohn's disease: less pronounced than previously believed? *Inflamm Bowel Dis.* Jan 2011;17(1):6-12. doi: 10.1002/ibd.21295.

41. Ponder A, Long MD. A clinical review of recent findings in the epidemiology of inflammatory bowel disease. *Clin Epidemiol.* 2013;5:237-247. doi: 10.2147/clep.S33961.

42. Iwasaki A, Medzhitov R. Control of adaptive immunity by the innate immune system. *Nat Immunol.* Apr 2015;16(4):343-353. doi: 10.1038/ni.3123.

43. Heller F, Florian P, Bojarski C, et al. Interleukin-13 is the key effector Th2 cytokine in ulcerative colitis that affects epithelial tight junctions, apoptosis, and cell restitution. *Gastroenterology.* Aug 2005;129(2):550-564. doi: 10.1016/j.gastro.2005.05.002.

44. Perez-Lopez A, Behnsen J, Nuccio SP, Raffatellu M. Mucosal immunity to pathogenic intestinal bacteria. *Nat Rev Immunol.* Mar 2016;16(3):135-148. doi: 10.1038/nri.2015.17.

45. Jager S, Stange EF, Wehkamp J. Inflammatory bowel disease: an impaired barrier disease. *Langenbecks Arch Surg.* Jan 2013;398(1):1-12. doi: 10.1007/s00423-012-1030-9.

46. Antoni L, Nuding S, Wehkamp J, Stange EF. Intestinal barrier in inflammatory bowel disease. *World J Gastroenterol.* Feb 7 2014;20(5):1165-1179. doi: 10.3748/wjg.v20.i5.1165.

47. Cao X. Self-regulation and cross-regulation of pattern-recognition receptor signalling in health and disease. *Nat Rev Immunol.* Jan 2016;16(1):35-50. doi: 10.1038/nri.2015.8.

48. Gautier EL, Shay T, Miller J, et al. Gene-expression profiles and transcriptional regulatory pathways that underlie the identity and diversity of mouse tissue macrophages. *Nat Immunol.* Nov 2012;13(11):1118-1128. doi: 10.1038/ni.2419.

49. Janeway CA, Jr. The priming of helper T cells. *Semin Immunol.* Sep 1989;1(1):13-20.

50. Buchmann K. Evolution of Innate Immunity: Clues from Invertebrates via Fish to Mammals. *Front Immunol.* 2014;5:459. doi: 10.3389/fimmu.2014.00459.

51. Parkes M, Barrett JC, Prescott NJ, et al. Sequence variants in the autophagy gene IRGM and multiple other replicating loci contribute to Crohn's disease susceptibility. *Nat Genet.* Jul 2007;39(7):830-832. doi: 10.1038/ng2061.

52. Hugot JP, Chamaillard M, Zouali H, et al. Association of NOD2 leucine-rich repeat variants with susceptibility to Crohn's disease. *Nature.* May 31 2001;411(6837):599-603. doi: 10.1038/35079107.

53. Wu W, He C, Liu C, et al. miR-10a inhibits dendritic cell activation and Th1/Th17 cell immune responses in IBD. *Gut.* Nov 2015;64(11):1755-1764. doi: 10.1136/gutjnl-2014-307980.

54. Park JH, Kwon JG, Kim SJ, et al. Alterations of colonic contractility in an interleukin-10 knockout mouse model of inflammatory bowel disease. *J Neurogastroenterol Motil.* Jan 1 2015;21(1):51-61. doi: 10.5056/jnm14008.

55. Gkouskou KK, Deligianni C, Tsatsanis C, Eliopoulos AG. The gut microbiota in mouse models of inflammatory bowel disease. *Front Cell Infect Microbiol.* 2014;4:28. doi: 10.3389/fcimb.2014.00028.

56. Wang SL, Shao BZ, Zhao SB, et al. Impact of Paneth Cell Autophagy on Inflammatory Bowel Disease. *Front Immunol.* 2018;9:693. doi: 10.3389/fimmu.2018.00693.

57. Fuchs A, Vermi W, Lee JS, et al. Intraepithelial type 1 innate lymphoid cells are a unique subset of IL-12- and IL-15-responsive IFN-gamma-producing cells. *Immunity.* Apr 18 2013;38(4):769-781. doi: 10.1016/j.immuni.2013.02.010.

58. Bernink JH, Peters CP, Munneke M, et al. Human type 1 innate lymphoid cells accumulate in inflamed mucosal tissues. *Nat Immunol.* Mar 2013;14(3):221-229. doi: 10.1038/ni.2534.

59. Buonocore S, Ahern PP, Uhlig HH, et al. Innate lymphoid cells drive interleukin-23-dependent innate intestinal pathology. *Nature.* Apr 29 2010;464(7293):1371-1375. doi: 10.1038/nature08949.

60. Yamada A, Arakaki R, Saito M, Tsunematsu T, Kudo Y, Ishimaru N. Role of regulatory T cell in the pathogenesis of inflammatory bowel disease. *World J Gastroenterol.* Feb 21 2016;22(7):2195-2205. doi: 10.3748/wjg.v22.i7.2195.

61. Wertheim B. Genomic basis of evolutionary change: evolving immunity. *Front Genet.* 2015;6:222. doi: 10.3389/fgene.2015.00222.

62. Hogquist KA, Baldwin TA, Jameson SC. Central tolerance: learning self-control in the thymus. *Nat Rev Immunol.* Oct 2005;5(10):772-782. doi: 10.1038/nri1707.

63. Ellestad KK, Thangavelu G, Haile Y, Lin J, Boon L, Anderson CC. Prior to Peripheral Tolerance, Newly Generated CD4 T Cells Maintain Dangerous Autoimmune Potential: Fas- and Perforin-Independent Autoimmunity Controlled by Programmed Death-1. *Front Immunol.* 2018;9:12. doi: 10.3389/fimmu.2018.00012.

64. Perry JSA, Russler-Germain EV, Zhou YW, et al. Transfer of Cell-Surface Antigens by Scavenger Receptor CD36 Promotes Thymic Regulatory T Cell Receptor Repertoire Development and Allo-tolerance. *Immunity*. Jun 19 2018;48(6):1271. doi: 10.1016/j.immuni.2018.05.011.

65. Mayer L, Shao L. Therapeutic potential of oral tolerance. *Nat Rev Immunol*. Jun 2004;4(6):407-419. doi: 10.1038/nri1370.

66. Abbas AK, Benoist C, Bluestone JA, et al. Regulatory T cells: recommendations to simplify the nomenclature. *Nat Immunol*. Apr 2013;14(4):307-308. doi: 10.1038/ni.2554.

67. Rook GA. Review series on helminths, immune modulation and the hygiene hypothesis: the broader implications of the hygiene hypothesis. *Immunology*. Jan 2009;126(1):3-11. doi: 10.1111/j.1365-2567.2008.03007.x.

68. Maul J, Loddenkemper C, Mundt P, et al. Peripheral and intestinal regulatory CD4+ CD25(high) T cells in inflammatory bowel disease. *Gastroenterology*. Jun 2005;128(7):1868-1878.

69. Read S, Greenwald R, Izcue A, et al. Blockade of CTLA-4 on CD4+CD25+ regulatory T cells abrogates their function in vivo. *J Immunol*. Oct 1 2006;177(7):4376-4383.

70. Marchiando AM, Shen L, Graham WV, et al. Caveolin-1-dependent occludin endocytosis is required for TNF-induced tight junction regulation in vivo. *J Cell Biol*. Apr 5 2010;189(1):111-126. doi: 10.1083/jcb.200902153.

71. Hoffman W, Lakkis FG, Chalasani G. B Cells, Antibodies, and More. *Clin J Am Soc Nephrol*. Jan 7 2016;11(1):137-154. doi: 10.2215/cjn.09430915.

72. Fillatreau S, Sweenie CH, McGeachy MJ, Gray D, Anderton SM. B cells regulate autoimmunity by provision of IL-10. *Nat Immunol*. Oct 2002;3(10):944-950. doi: 10.1038/ni833.

73. Steel AW, Mela CM, Lindsay JO, Gazzard BG, Goodier MR. Increased proportion of CD16(+) NK cells in the colonic lamina propria of inflammatory bowel disease patients, but not after azathioprine treatment. *Aliment Pharmacol Ther*. Jan 2011;33(1):115-126. doi: 10.1111/j.1365-2036.2010.04499.x.

74. Griseri T, Arnold IC, Pearson C, et al. Granulocyte Macrophage Colony-Stimulating Factor-Activated Eosinophils Promote Interleukin-23 Driven Chronic Colitis. *Immunity*. Jul 21 2015;43(1):187-199. doi: 10.1016/j.immuni.2015.07.008.

75. Griseri T, McKenzie BS, Schiering C, Powrie F. Dysregulated hematopoietic stem and progenitor cell activity promotes interleukin-23-driven chronic intestinal inflammation. *Immunity*. Dec 14 2012;37(6):1116-1129. doi: 10.1016/j.immuni.2012.08.025.

76. Lampinen M, Ronnblom A, Amin K, et al. Eosinophil granulocytes are activated during the remission phase of ulcerative colitis. *Gut*. Dec 2005;54(12):1714-1720. doi: 10.1136/gut.2005.066423.

77. Nemoto Y, Kanai T, Tohda S, et al. Negative feedback regulation of colitogenic CD4+ T cells by increased granulopoiesis. *Inflamm Bowel Dis*. Nov 2008;14(11):1491-1503. doi: 10.1002/ibd.20531.

78. Sadik CD, Kim ND, Luster AD. Neutrophils cascading their way to inflammation. *Trends Immunol*. Oct 2011;32(10):452-460. doi: 10.1016/j.it.2011.06.008.

79. Amulic B, Cazalet C, Hayes GL, Metzler KD, Zychlinsky A. Neutrophil function: from mechanisms to disease. *Annu Rev Immunol*. 2012;30:459-489. doi: 10.1146/annurev-immunol-020711-074942.

80. Kuhl AA, Kakirman H, Janotta M, et al. Aggravation of different types of experimental colitis by depletion or adhesion blockade of neutrophils. *Gastroenterology.* Dec 2007;133(6):1882-1892. doi: 10.1053/j.gastro.2007.08.073.

81. Peterson LW, Artis D. Intestinal epithelial cells: regulators of barrier function and immune homeostasis. *Nat Rev Immunol.* Mar 2014;14(3):141-153. doi: 10.1038/nri3608.

82. Kirchberger S, Royston DJ, Boulard O, et al. Innate lymphoid cells sustain colon cancer through production of interleukin-22 in a mouse model. *J Exp Med.* May 6 2013;210(5):917-931. doi: 10.1084/jem.20122308.

83. Geremia A, Arancibia-Carcamo CV, Fleming MP, et al. IL-23-responsive innate lymphoid cells are increased in inflammatory bowel disease. *J Exp Med.* Jun 6 2011;208(6):1127-1133. doi: 10.1084/jem.20101712.

84. Powell N, Lo JW, Biancheri P, et al. Interleukin 6 Increases Production of Cytokines by Colonic Innate Lymphoid Cells in Mice and Patients With Chronic Intestinal Inflammation. *Gastroenterology.* Aug 2015;149(2):456-467.e415. doi: 10.1053/j.gastro.2015.04.017.

85. Cella M, Fuchs A, Vermi W, et al. A human natural killer cell subset provides an innate source of IL-22 for mucosal immunity. *Nature.* Feb 5 2009;457(7230):722-725. doi: 10.1038/nature07537.

86. Colonna M. Interleukin-22-producing natural killer cells and lymphoid tissue inducer-like cells in mucosal immunity. *Immunity.* Jul 17 2009;31(1):15-23. doi: 10.1016/j.immuni.2009.06.008.

87. Kobori A, Yagi Y, Imaeda H, et al. Interleukin-33 expression is specifically enhanced in inflamed mucosa of ulcerative colitis. *J Gastroenterol.* Oct 2010;45(10):999-1007. doi: 10.1007/s00535-010-0245-1.

88. Pastorelli L, Garg RR, Hoang SB, et al. Epithelial-derived IL-33 and its receptor ST2 are dysregulated in ulcerative colitis and in experimental Th1/Th2 driven enteritis. *Proc Natl Acad Sci U S A.* Apr 27 2010;107(17):8017-8022. doi: 10.1073/pnas.0912678107.

89. Sipos F, Molnar B, Zagoni T, Berczi L, Tulassay Z. Growth in epithelial cell proliferation and apoptosis correlates specifically to the inflammation activity of inflammatory bowel diseases: ulcerative colitis shows specific p53- and EGFR expression alterations. *Dis Colon Rectum.* Apr 2005;48(4):775-786. doi: 10.1007/s10350-004-0831-5.

90. Yan F, Cao H, Cover TL, et al. Colon-specific delivery of a probiotic-derived soluble protein ameliorates intestinal inflammation in mice through an EGFR-dependent mechanism. *J Clin Invest.* Jun 2011;121(6):2242-2253. doi: 10.1172/jci44031.

91. Monticelli LA, Osborne LC, Noti M, Tran SV, Zaiss DM, Artis D. IL-33 promotes an innate immune pathway of intestinal tissue protection dependent on amphiregulin-EGFR interactions. *Proc Natl Acad Sci U S A.* Aug 25 2015;112(34):10762-10767. doi: 10.1073/pnas.1509070112.

92. Al-Haddad S, Riddell RH. The role of eosinophils in inflammatory bowel disease. *Gut.* Dec 2005;54(12):1674-1675. doi: 10.1136/gut.2005.072595.

93. Fulkerson PC, Rothenberg ME. Targeting eosinophils in allergy, inflammation and beyond. *Nat Rev Drug Discov.* Feb 2013;12(2):117-129. doi: 10.1038/nrd3838.

94. Ahrens R, Waddell A, Seidu L, et al. Intestinal macrophage/epithelial cell-derived CCL11/eotaxin-1 mediates eosinophil recruitment and function in pediatric ulcerative colitis. *J Immunol.* Nov 15 2008;181(10):7390-7399.

95. Forbes E, Murase T, Yang M, et al. Immunopathogenesis of experimental ulcerative colitis is mediated by eosinophil peroxidase. *J Immunol.* May 1 2004;172(9):5664-5675.

96. Elson CO, Sartor RB, Tennyson GS, Riddell RH. Experimental models of inflammatory bowel disease. *Gastroenterology.* Oct 1995;109(4):1344-1367.

97. Heller F, Fuss IJ, Nieuwenhuis EE, Blumberg RS, Strober W. Oxazolone colitis, a Th2 colitis model resembling ulcerative colitis, is mediated by IL-13-producing NK-T cells. *Immunity.* Nov 2002;17(5):629-638.

98. Strober W, Fuss IJ, Blumberg RS. The immunology of mucosal models of inflammation. *Annu Rev Immunol.* 2002;20:495-549. doi: 10.1146/annurev.immunol.20.100301.064816.

99. te Velde AA, de Kort F, Sterrenburg E, et al. Comparative analysis of colonic gene expression of three experimental colitis models mimicking inflammatory bowel disease. *Inflamm Bowel Dis.* Mar 2007;13(3):325-330. doi: 10.1002/ibd.20079.

100. te Velde AA, Verstege MI, Hommes DW. Critical appraisal of the current practice in murine TNBS-induced colitis. *Inflamm Bowel Dis.* Oct 2006;12(10):995-999. doi: 10.1097/01.mib.0000227817.54969.5e.

101. Jiminez JA, Uwiera TC, Douglas Inglis G, Uwiera RR. Animal models to study acute and chronic intestinal inflammation in mammals. *Gut Pathog.* 2015;7:29. doi: 10.1186/s13099-015-0076-y.

102. Antoniou E, Margonis GA, Angelou A, et al. The TNBS-induced colitis animal model: An overview. *Ann Med Surg (Lond).* Nov 2016;11:9-15. doi: 10.1016/j.amsu.2016.07.019.

103. Neurath MF, Fuss I, Kelsall BL, Stuber E, Strober W. Antibodies to interleukin 12 abrogate established experimental colitis in mice. *J Exp Med.* Nov 1 1995;182(5):1281-1290.

104. Chassaing B, Aitken JD, Malleshappa M, Vijay-Kumar M. Dextran sulfate sodium (DSS)-induced colitis in mice. *Curr Protoc Immunol.* Feb 4 2014;104:Unit 15.25. doi: 10.1002/0471142735.im1525s104.

105. Ren G, Sun A, Deng C, et al. The anti-inflammatory effect and potential mechanism of cardamonin in DSS-induced colitis. *Am J Physiol Gastrointest Liver Physiol.* Oct 1 2015;309(7):G517-527. doi: 10.1152/ajpgi.00133.2015.

106. Im JP, Ye BD, Kim JM, Jung HC, Song IS, Kim JS. Rectal administration of lipopolysaccharide and ovalbumin ameliorates acute murine colitis. *Dig Dis Sci.* Aug 2011;56(8):2292-2298. doi: 10.1007/s10620-011-1630-1.

107. Suresh R, Mosser DM. Pattern recognition receptors in innate immunity, host defense, and immunopathology. *Adv Physiol Educ.* Dec 2013;37(4):284-291. doi: 10.1152/advan.00058.2013.

108. Meers GK, Bohnenberger H, Reichardt HM, Luhder F, Reichardt SD. Impaired resolution of DSS-induced colitis in mice lacking the glucocorticoid receptor in myeloid cells. *PLoS One.* 2018;13(1):e0190846. doi: 10.1371/journal.pone.0190846.

109. Ostanin DV, Bao J, Koboziev I, et al. T cell transfer model of chronic colitis: concepts, considerations, and tricks of the trade. *Am J Physiol*

Gastrointest Liver Physiol. Feb 2009;296(2):G135-146. doi: 10.1152/ajpgi.90462.2008.

110.   Iyer SS, Cheng G. Role of interleukin 10 transcriptional regulation in inflammation and autoimmune disease. *Crit Rev Immunol.* 2012;32(1):23-63.

111.   Keubler LM, Buettner M, Hager C, Bleich A. A Multihit Model: Colitis Lessons from the Interleukin-10-deficient Mouse. *Inflamm Bowel Dis.* Aug 2015;21(8):1967-1975. doi: 10.1097/mib.0000000000000468.

112.   Belkaid Y, Hand TW. Role of the microbiota in immunity and inflammation. *Cell.* Mar 27 2014;157(1):121-141. doi: 10.1016/j.cell.2014.03.011.

113.   Calderon-Gomez E, Bassolas-Molina H, Mora-Buch R, et al. Commensal-Specific CD4(+) Cells From Patients With Crohn's Disease Have a T-Helper 17 Inflammatory Profile. *Gastroenterology.* Sep 2016;151(3):489-500.e483. doi: 10.1053/j.gastro.2016.05.050.

114.   Dou W, Zhang J, Li H, et al. Plant flavonol isorhamnetin attenuates chemically induced inflammatory bowel disease via a PXR-dependent pathway. *J Nutr Biochem.* Sep 2014;25(9):923-933. doi: 10.1016/j.jnutbio.2014.04.006.

115.   Waljee AK, Wiitala WL, Govani S, et al. Corticosteroid Use and Complications in a US Inflammatory Bowel Disease Cohort. *PLoS One.* 2016;11(6):e0158017. doi: 10.1371/journal.pone.0158017.

116.   Baert F, Moortgat L, Van Assche G, et al. Mucosal healing predicts sustained clinical remission in patients with early-stage Crohn's disease. *Gastroenterology.* Feb 2010;138(2):463-468; quiz e410-461. doi: 10.1053/j.gastro.2009.09.056.

117.   Lim WC, Wang Y, MacDonald JK, Hanauer S. Aminosalicylates for induction of remission or response in Crohn's disease. *Cochrane Database Syst Rev.* Jul 3 2016;7:Cd008870. doi: 10.1002/14651858.CD008870.pub2.

118.   Pineton de Chambrun G, Peyrin-Biroulet L, Lemann M, Colombel JF. Clinical implications of mucosal healing for the management of IBD. *Nat Rev Gastroenterol Hepatol.* Jan 2010;7(1):15-29. doi: 10.1038/nrgastro.2009.203.

119.   Goel RM, Blaker P, Mentzer A, Fong SC, Marinaki AM, Sanderson JD. Optimizing the use of thiopurines in inflammatory bowel disease. *Ther Adv Chronic Dis.* May 2015;6(3):138-146. doi: 10.1177/2040622315579063.

120.   Park SC, Jeen YT. Anti-integrin therapy for inflammatory bowel disease. *World J Gastroenterol.* May 7 2018;24(17):1868-1880. doi: 10.3748/wjg.v24.i17.1868.

121.   Rutgeerts P, Van Assche G, Sandborn WJ, et al. Adalimumab induces and maintains mucosal healing in patients with Crohn's disease: data from the EXTEND trial. *Gastroenterology.* May 2012;142(5):1102-1111.e1102. doi: 10.1053/j.gastro.2012.01.035.

122.   Gisbert JP, Marin AC, Chaparro M. The Risk of Relapse after Anti-TNF Discontinuation in Inflammatory Bowel Disease: Systematic Review and Meta-Analysis. *Am J Gastroenterol.* May 2016;111(5):632-647. doi: 10.1038/ajg.2016.54.

123.   Bodger K, Kikuchi T, Hughes D. Cost-effectiveness of biological therapy for Crohn's disease: Markov cohort analyses incorporating United Kingdom patient-level cost data. *Aliment Pharmacol Ther.* Aug 2009;30(3):265-274. doi: 10.1111/j.1365-2036.2009.04033.x.

References

124.   Guo Y, Lu N, Bai A. Clinical use and mechanisms of infliximab treatment on inflammatory bowel disease: a recent update. *Biomed Res Int.* 2013;2013:581631. doi: 10.1155/2013/581631.

125.   Teng MW, Bowman EP, McElwee JJ, et al. IL-12 and IL-23 cytokines: from discovery to targeted therapies for immune-mediated inflammatory diseases. *Nat Med.* Jul 2015;21(7):719-729. doi: 10.1038/nm.3895.

126.   Mannon PJ, Fuss IJ, Mayer L, et al. Anti-interleukin-12 antibody for active Crohn's disease. *N Engl J Med.* Nov 11 2004;351(20):2069-2079. doi: 10.1056/NEJMoa033402.

127.   Kruis W, Fric P, Pokrotnieks J, et al. Maintaining remission of ulcerative colitis with the probiotic Escherichia coli Nissle 1917 is as effective as with standard mesalazine. *Gut.* Nov 2004;53(11):1617-1623. doi: 10.1136/gut.2003.037747.

128.   von Lampe B, Barthel B, Coupland SE, Riecken EO, Rosewicz S. Differential expression of matrix metalloproteinases and their tissue inhibitors in colon mucosa of patients with inflammatory bowel disease. *Gut.* Jul 2000;47(1):63-73.

129.   Matsuno K, Adachi Y, Yamamoto H, et al. The expression of matrix metalloproteinase matrilysin indicates the degree of inflammation in ulcerative colitis. *J Gastroenterol.* 2003;38(4):348-354. doi: 10.1007/s005350300062.

130.   Arihiro S, Ohtani H, Hiwatashi N, Torii A, Sorsa T, Nagura H. Vascular smooth muscle cells and pericytes express MMP-1, MMP-9, TIMP-1 and type I procollagen in inflammatory bowel disease. *Histopathology.* Jul 2001;39(1):50-59.

131.   Crohn BB, Ginzburg L, Oppenheimer GD. Regional ileitis; a pathologic and clinical entity. *Am J Med.* Nov 1952;13(5):583-590.

132.   Danese S, Vuitton L, Peyrin-Biroulet L. Biologic agents for IBD: practical insights. *Nat Rev Gastroenterol Hepatol.* Sep 2015;12(9):537-545. doi: 10.1038/nrgastro.2015.135.

133.   Schnitzler F, Fidder H, Ferrante M, et al. Mucosal healing predicts long-term outcome of maintenance therapy with infliximab in Crohn's disease. *Inflamm Bowel Dis.* Sep 2009;15(9):1295-1301. doi: 10.1002/ibd.20927.

134.   Yu Q, Mao R, Lian L, et al. Surgical management of inflammatory bowel disease in China: a systematic review of two decades. *Intest Res.* Oct 2016;14(4):322-332. doi: 10.5217/ir.2016.14.4.322.

135.   Peyrin-Biroulet L, Panes J, Sandborn WJ, et al. Defining Disease Severity in Inflammatory Bowel Diseases: Current and Future Directions. *Clin Gastroenterol Hepatol.* Mar 2016;14(3):348-354.e317. doi: 10.1016/j.cgh.2015.06.001.

136.   Wiercinska-Drapalo A, Jaroszewicz J, Flisiak R, Prokopowicz D. Plasma matrix metalloproteinase-1 and tissue inhibitor of metalloproteinase-1 as biomarkers of ulcerative colitis activity. *World J Gastroenterol.* Dec 2003;9(12):2843-2845.

137.   Bach JF. The effect of infections on susceptibility to autoimmune and allergic diseases. *N Engl J Med.* Sep 19 2002;347(12):911-920. doi: 10.1056/NEJMra020100.

138.   Strachan DP. Hay fever, hygiene, and household size. *BMJ.* Nov 18 1989;299(6710):1259-1260.

139.   Bjorksten B. Diverse microbial exposure - consequences for vaccine development. *Vaccine.* Jun 19 2012;30(29):4336-4340. doi: 10.1016/j.vaccine.2011.10.074.

140.   McCoy KD, Koller Y. New developments providing mechanistic insight into the impact of the microbiota on allergic disease. *Clin Immunol.* Aug 2015;159(2):170-176. doi: 10.1016/j.clim.2015.05.007.

141.   Figueiredo CA, Alcantara-Neves NM, Veiga R, et al. Spontaneous cytokine production in children according to biological characteristics and environmental exposures. *Environ Health Perspect.* May 2009;117(5):845-849. doi: 10.1289/ehp.0800366.

142.   Wammes LJ, Mpairwe H, Elliott AM, Yazdanbakhsh M. Helminth therapy or elimination: epidemiological, immunological, and clinical considerations. *Lancet Infect Dis.* Nov 2014;14(11):1150-1162. doi: 10.1016/s1473-3099(14)70771-6.

143.   Fumagalli M, Pozzoli U, Cagliani R, et al. Parasites represent a major selective force for interleukin genes and shape the genetic predisposition to autoimmune conditions. *J Exp Med.* Jun 8 2009;206(6):1395-1408. doi: 10.1084/jem.20082779.

144.   Fumagalli M, Pozzoli U, Cagliani R, et al. The landscape of human genes involved in the immune response to parasitic worms. *BMC Evol Biol.* Aug 31 2010;10:264. doi: 10.1186/1471-2148-10-264.

145.   Li Q, Lee CH, Peters LA, et al. Variants in TRIM22 That Affect NOD2 Signaling Are Associated With Very-Early-Onset Inflammatory Bowel Disease. *Gastroenterology.* May 2016;150(5):1196-1207. doi: 10.1053/j.gastro.2016.01.031.

146.   Cooper PJ, Chico ME, Rodrigues LC, et al. Reduced risk of atopy among school-age children infected with geohelminth parasites in a rural area of the tropics. *J Allergy Clin Immunol.* May 2003;111(5):995-1000.

147.   Denson LA, Long MD, McGovern DP, et al. Challenges in IBD research: update on progress and prioritization of the CCFA's research agenda. *Inflamm Bowel Dis.* Mar-Apr 2013;19(4):677-682. doi: 10.1097/MIB.0b013e31828134b3.

148.   Sonnenberg GF, Artis D. Innate lymphoid cells in the initiation, regulation and resolution of inflammation. *Nat Med.* Jul 2015;21(7):698-708. doi: 10.1038/nm.3892.

149.   Tahapary DL, de Ruiter K, Martin I, et al. Helminth infections and type 2 diabetes: a cluster-randomized placebo controlled SUGARSPIN trial in Nangapanda, Flores, Indonesia. *BMC Infect Dis.* Mar 18 2015;15:133. doi: 10.1186/s12879-015-0873-4.

150.   Zhang J, Dou W, Zhang E, et al. Paeoniflorin abrogates DSS-induced colitis via a TLR4-dependent pathway. *Am J Physiol Gastrointest Liver Physiol.* Jan 1 2014;306(1):G27-36. doi: 10.1152/ajpgi.00465.2012.

151.   Atarashi K, Tanoue T, Shima T, et al. Induction of colonic regulatory T cells by indigenous Clostridium species. *Science.* Jan 21 2011;331(6015):337-341. doi: 10.1126/science.1198469.

152.   Frank DN, St Amand AL, Feldman RA, Boedeker EC, Harpaz N, Pace NR. Molecular-phylogenetic characterization of microbial community imbalances in human inflammatory bowel diseases. *Proc Natl Acad Sci U S A.* Aug 21 2007;104(34):13780-13785. doi: 10.1073/pnas.0706625104.

References

153.   Hotez PJ, Alvarado M, Basanez MG, et al. The global burden of disease study 2010: interpretation and implications for the neglected tropical diseases. *PLoS Negl Trop Dis.* Jul 2014;8(7):e2865. doi: 10.1371/journal.pntd.0002865.

154.   Frolkis A, Dieleman LA, Barkema HW, et al. Environment and the inflammatory bowel diseases. *Can J Gastroenterol.* Mar 2013;27(3):e18-24.

155.   Chen F, Liu Z, Wu W, et al. An essential role for TH2-type responses in limiting acute tissue damage during experimental helminth infection. *Nat Med.* Jan 15 2012;18(2):260-266. doi: 10.1038/nm.2628.

156.   Hewitson JP, Grainger JR, Maizels RM. Helminth immunoregulation: the role of parasite secreted proteins in modulating host immunity. *Mol Biochem Parasitol.* Sep 2009;167(1):1-11. doi: 10.1016/j.molbiopara.2009.04.008.

157.   Helmby H. Human helminth therapy to treat inflammatory disorders - where do we stand? *BMC Immunol.* Mar 26 2015;16:12. doi: 10.1186/s12865-015-0074-3.

158.   Rook GA, Brunet LR. Old friends for breakfast. *Clin Exp Allergy.* Jul 2005;35(7):841-842. doi: 10.1111/j.1365-2222.2005.02112.x.

159.   Rook GA, Adams V, Hunt J, Palmer R, Martinelli R, Brunet LR. Mycobacteria and other environmental organisms as immunomodulators for immunoregulatory disorders. *Springer Semin Immunopathol.* Feb 2004;25(3-4):237-255. doi: 10.1007/s00281-003-0148-9.

160.   Elliott DE, Urban JJ, Argo CK, Weinstock JV. Does the failure to acquire helminthic parasites predispose to Crohn's disease? *FASEB J.* Sep 2000;14(12):1848-1855.

161.   Maizels RM, McSorley HJ. Regulation of the host immune system by helminth parasites. *J Allergy Clin Immunol.* Sep 2016;138(3):666-675. doi: 10.1016/j.jaci.2016.07.007.

162.   Allen JE, Sutherland TE. Host protective roles of type 2 immunity: parasite killing and tissue repair, flip sides of the same coin. *Semin Immunol.* Aug 2014;26(4):329-340. doi: 10.1016/j.smim.2014.06.003.

163.   Ramanan D, Bowcutt R, Lee SC, et al. Helminth infection promotes colonization resistance via type 2 immunity. *Science.* Apr 29 2016;352(6285):608-612. doi: 10.1126/science.aaf3229.

164.   Harris NL, Loke P. Recent Advances in Type-2-Cell-Mediated Immunity: Insights from Helminth Infection. *Immunity.* Dec 19 2017;47(6):1024-1036. doi: 10.1016/j.immuni.2017.11.015.

165.   Cantacessi C, Giacomin P, Croese J, et al. Impact of experimental hookworm infection on the human gut microbiota. *J Infect Dis.* Nov 1 2014;210(9):1431-1434. doi: 10.1093/infdis/jiu256.

166.   Giacomin P, Zakrzewski M, Jenkins TP, et al. Changes in duodenal tissue-associated microbiota following hookworm infection and consecutive gluten challenges in humans with coeliac disease. *Sci Rep.* Nov 9 2016;6:36797. doi: 10.1038/srep36797.

167.   Zaiss MM, Rapin A, Lebon L, et al. The Intestinal Microbiota Contributes to the Ability of Helminths to Modulate Allergic Inflammation. *Immunity.* Nov 17 2015;43(5):998-1010. doi: 10.1016/j.immuni.2015.09.012.

168.   McFarlane AJ, McSorley HJ, Davidson DJ, et al. Enteric helminth-induced type I interferon signaling protects against pulmonary virus infection through interaction with the microbiota. *J Allergy Clin Immunol.* Oct 2017;140(4):1068-1078.e1066. doi: 10.1016/j.jaci.2017.01.016.

References

169.   Scholmerich J, Fellermann K, Seibold FW, et al. A Randomised, Double-blind, Placebo-controlled Trial of Trichuris suis ova in Active Crohn's Disease. *J Crohns Colitis.* Apr 1 2017;11(4):390-399. doi: 10.1093/ecco-jcc/jjw184.

170.   Fleming J, Hernandez G, Hartman L, et al. Safety and efficacy of helminth treatment in relapsing-remitting multiple sclerosis: Results of the HINT 2 clinical trial. *Mult Scler.* Oct 1 2017:1352458517736377. doi: 10.1177/1352458517736377.

171.   Bager P, Arnved J, Ronborg S, et al. Trichuris suis ova therapy for allergic rhinitis: a randomized, double-blind, placebo-controlled clinical trial. *J Allergy Clin Immunol.* Jan 2010;125(1):123-130.e121-123. doi: 10.1016/j.jaci.2009.08.006.

172.   Croese J, O'Neil J, Masson J, et al. A proof of concept study establishing Necator americanus in Crohn's patients and reservoir donors. *Gut.* Jan 2006;55(1):136-137. doi: 10.1136/gut.2005.079129.

173.   Giacomin P, Zakrzewski M, Croese J, et al. Experimental hookworm infection and escalating gluten challenges are associated with increased microbial richness in celiac subjects. *Sci Rep.* Sep 18 2015;5:13797. doi: 10.1038/srep13797.

174.   Shepherd C, Wangchuk P, Loukas A. Of dogs and hookworms: man's best friend and his parasites as a model for translational biomedical research. *Parasit Vectors.* Jan 25 2018;11(1):59. doi: 10.1186/s13071-018-2621-2.

175.   Feary JR, Venn AJ, Mortimer K, et al. Experimental hookworm infection: a randomized placebo-controlled trial in asthma. *Clin Exp Allergy.* Feb 2010;40(2):299-306. doi: 10.1111/j.1365-2222.2009.03433.x.

176.   Blount D, Hooi D, Feary J, et al. Immunologic profiles of persons recruited for a randomized, placebo-controlled clinical trial of hookworm infection. *Am J Trop Med Hyg.* Nov 2009;81(5):911-916. doi: 10.4269/ajtmh.2009.09-0237.

177.   Varyani F, Fleming JO, Maizels RM. Helminths in the gastrointestinal tract as modulators of immunity and pathology. *Am J Physiol Gastrointest Liver Physiol.* Jun 1 2017;312(6):G537-g549. doi: 10.1152/ajpgi.00024.2017.

178.   Yang J, Zhao J, Yang Y, et al. Schistosoma japonicum egg antigens stimulate CD4 CD25 T cells and modulate airway inflammation in a murine model of asthma. *Immunology.* Jan 2007;120(1):8-18. doi: 10.1111/j.1365-2567.2006.02472.x.

179.   Reardon C, Sanchez A, Hogaboam CM, McKay DM. Tapeworm infection reduces epithelial ion transport abnormalities in murine dextran sulfate sodium-induced colitis. *Infect Immun.* Jul 2001;69(7):4417-4423. doi: 10.1128/iai.69.7.4417-4423.2001.

180.   Navarro S, Ferreira I, Loukas A. The hookworm pharmacopoeia for inflammatory diseases. *Int J Parasitol.* Mar 2013;43(3-4):225-231. doi: 10.1016/j.ijpara.2012.11.005.

181.   Loukas A, Hotez PJ, Diemert D, et al. Hookworm infection. *Nat Rev Dis Primers.* Dec 8 2016;2:16088. doi: 10.1038/nrdp.2016.88.

182.   Weinstock JV, Elliott DE. Helminth infections decrease host susceptibility to immune-mediated diseases. *J Immunol.* Oct 1 2014;193(7):3239-3247. doi: 10.4049/jimmunol.1400927.

183.   Coakley G, Buck AH, Maizels RM. Host parasite communications-Messages from helminths for the immune system: Parasite communication and

cell-cell interactions. *Mol Biochem Parasitol.* Jul 2016;208(1):33-40. doi: 10.1016/j.molbiopara.2016.06.003.

184.   McSorley HJ, Maizels RM. Helminth infections and host immune regulation. *Clin Microbiol Rev.* Oct 2012;25(4):585-608. doi: 10.1128/cmr.05040-11.

185.   Grainger JR, Smith KA, Hewitson JP, et al. Helminth secretions induce de novo T cell Foxp3 expression and regulatory function through the TGF-beta pathway. *J Exp Med.* Oct 25 2010;207(11):2331-2341. doi: 10.1084/jem.20101074.

186.   Odeh AN, Simecka JW. Regulatory CD4+CD25+ T Cells Dampen Inflammatory Disease in Murine Mycoplasma Pneumonia and Promote IL-17 and IFN-gamma Responses. *PLoS One.* 2016;11(5):e0155648. doi: 10.1371/journal.pone.0155648.

187.   McSorley HJ, O'Gorman MT, Blair N, Sutherland TE, Filbey KJ, Maizels RM. Suppression of type 2 immunity and allergic airway inflammation by secreted products of the helminth Heligmosomoides polygyrus. *Eur J Immunol.* Oct 2012;42(10):2667-2682. doi: 10.1002/eji.201142161.

188.   Jang JC, Nair MG. Alternatively Activated Macrophages Revisited: New Insights into the Regulation of Immunity, Inflammation and Metabolic Function following Parasite Infection. *Curr Immunol Rev.* Aug 1 2013;9(3):147-156. doi: 10.2174/1573395509666131210232548.

189.   Nair MG, Cochrane DW, Allen JE. Macrophages in chronic type 2 inflammation have a novel phenotype characterized by the abundant expression of Ym1 and Fizz1 that can be partly replicated in vitro. *Immunol Lett.* Jan 22 2003;85(2):173-180.

190.   Murray PJ. Macrophage Polarization. *Annu Rev Physiol.* Feb 10 2017;79:541-566. doi: 10.1146/annurev-physiol-022516-034339.

191.   Cobos C, Bansal PS, Jones L, et al. Engineering of an Anti-Inflammatory Peptide Based on the Disulfide-Rich Linaclotide Scaffold. *Biomedicines.* Oct 6 2018;6(4). doi: 10.3390/biomedicines6040097.

192.   Shepherd C, Navarro S, Wangchuk P, Wilson D, Daly NL, Loukas A. Identifying the immunomodulatory components of helminths. *Parasite Immunol.* Jun 2015;37(6):293-303. doi: 10.1111/pim.12192.

193.   Ruyssers NE, De Winter BY, De Man JG, et al. Therapeutic potential of helminth soluble proteins in TNBS-induced colitis in mice. *Inflamm Bowel Dis.* Apr 2009;15(4):491-500. doi: 10.1002/ibd.20787.

194.   Ferreira IB, Pickering DA, Troy S, Croese J, Loukas A, Navarro S. Suppression of inflammation and tissue damage by a hookworm recombinant protein in experimental colitis. *Clin Transl Immunology.* Oct 2017;6(10):e157. doi: 10.1038/cti.2017.42.

195.   Zakeri A, Hansen EP, Andersen SD, Williams AR, Nejsum P. Immunomodulation by Helminths: Intracellular Pathways and Extracellular Vesicles. *Front Immunol.* 2018;9:2349. doi: 10.3389/fimmu.2018.02349.

196.   Ferreira I, Smyth D, Gaze S, et al. Hookworm excretory/secretory products induce interleukin-4 (IL-4)+ IL-10+ CD4+ T cell responses and suppress pathology in a mouse model of colitis. *Infect Immun.* Jun 2013;81(6):2104-2111. doi: 10.1128/iai.00563-12.

197.   Cancado GG, Fiuza JA, de Paiva NC, et al. Hookworm products ameliorate dextran sodium sulfate-induced colitis in BALB/c mice. *Inflamm Bowel Dis.* Nov 2011;17(11):2275-2286. doi: 10.1002/ibd.21629.

198.   Motomura Y, Wang H, Deng Y, El-Sharkawy RT, Verdu EF, Khan WI. Helminth antigen-based strategy to ameliorate inflammation in an experimental model of colitis. *Clin Exp Immunol.* Jan 2009;155(1):88-95. doi: 10.1111/j.1365-2249.2008.03805.x.

199.   Yang X, Yang Y, Wang Y, et al. Excretory/secretory products from Trichinella spiralis adult worms ameliorate DSS-induced colitis in mice. *PLoS One.* 2014;9(5):e96454. doi: 10.1371/journal.pone.0096454.

200.   Cho MK, Park MK, Kang SA, et al. TLR2-dependent amelioration of allergic airway inflammation by parasitic nematode type II MIF in mice. *Parasite Immunol.* Apr 2015;37(4):180-191. doi: 10.1111/pim.12172.

201.   Kron MA, Metwali A, Vodanovic-Jankovic S, Elliott D. Nematode asparaginyl-tRNA synthetase resolves intestinal inflammation in mice with T-cell transfer colitis. *Clin Vaccine Immunol.* Feb 2013;20(2):276-281. doi: 10.1128/cvi.00594-12.

202.   Khatri V, Amdare N, Tarnekar A, Goswami K, Reddy MV. Brugia malayi cystatin therapeutically ameliorates dextran sulfate sodium-induced colitis in mice. *J Dig Dis.* Oct 2015;16(10):585-594. doi: 10.1111/1751-2980.12290.

203.   Khatri V, Amdare N, Yadav RS, Tarnekar A, Goswami K, Reddy MV. Brugia malayi abundant larval transcript 2 protein treatment attenuates experimentally-induced colitis in mice. *Indian J Exp Biol.* Nov 2015;53(11):732-739.

204.   Kim JY, Cho MK, Choi SH, et al. Inhibition of dextran sulfate sodium (DSS)-induced intestinal inflammation via enhanced IL-10 and TGF-beta production by galectin-9 homologues isolated from intestinal parasites. *Mol Biochem Parasitol.* Nov 2010;174(1):53-61. doi: 10.1016/j.molbiopara.2010.06.014.

205.   Wang W, Wang S, Zhang H, et al. Galectin Hco-gal-m from Haemonchus contortus modulates goat monocytes and T cell function in different patterns. *Parasit Vectors.* Jul 23 2014;7:342. doi: 10.1186/1756-3305-7-342.

206.   Du L, Liu L, Yu Y, Shan H, Li L. Trichinella spiralis excretory-secretory products protect against polymicrobial sepsis by suppressing MyD88 via mannose receptor. *Biomed Res Int.* 2014;2014:898646. doi: 10.1155/2014/898646.

207.   Navarro S, Pickering DA, Ferreira IB, et al. Hookworm recombinant protein promotes regulatory T cell responses that suppress experimental asthma. *Sci Transl Med.* Oct 26 2016;8(362):362ra143. doi: 10.1126/scitranslmed.aaf8807.

208.   Pineda MA, Lumb F, Harnett MM, Harnett W. ES-62, a therapeutic anti-inflammatory agent evolved by the filarial nematode Acanthocheilonema viteae. *Mol Biochem Parasitol.* Mar-Apr 2014;194(1-2):1-8. doi: 10.1016/j.molbiopara.2014.03.003.

209.   Tang YT, Gao X, Rosa BA, et al. Genome of the human hookworm Necator americanus. *Nat Genet.* Mar 2014;46(3):261-269. doi: 10.1038/ng.2875.

210.   Schwarz EM, Hu Y, Antoshechkin I, Miller MM, Sternberg PW, Aroian RV. Erratum: the genome and transcriptome of the zoonotic hookworm Ancylostoma ceylanicum identify infection-specific gene families. *Nat Genet.* Jun 2015;47(6):689. doi: 10.1038/ng0615-689a.

References

211.　　Mulvenna J, Hamilton B, Nagaraj SH, Smyth D, Loukas A, Gorman JJ. Proteomics analysis of the excretory/secretory component of the blood-feeding stage of the hookworm, Ancylostoma caninum. *Mol Cell Proteomics.* Jan 2009;8(1):109-121. doi: 10.1074/mcp.M800206-MCP200.

212.　　Cantacessi C, Hofmann A, Pickering D, Navarro S, Mitreva M, Loukas A. TIMPs of parasitic helminths - a large-scale analysis of high-throughput sequence datasets. *Parasit Vectors.* May 30 2013;6:156. doi: 10.1186/1756-3305-6-156.

213.　　Cuellar C, Wu W, Mendez S. The hookworm tissue inhibitor of metalloproteases (Ac-TMP-1) modifies dendritic cell function and induces generation of CD4 and CD8 suppressor T cells. *PLoS Negl Trop Dis.* May 19 2009;3(5):e439. doi: 10.1371/journal.pntd.0000439.

214.　　Glocker E, Grimbacher B. Inflammatory bowel disease: is it a primary immunodeficiency? *Cell Mol Life Sci.* Jan 2012;69(1):41-48. doi: 10.1007/s00018-011-0837-9.

215.　　Caffrey CR, Goupil L, Rebello KM, Dalton JP, Smith D. Cysteine proteases as digestive enzymes in parasitic helminths. *PLoS Negl Trop Dis.* Aug 2018;12(8):e0005840. doi: 10.1371/journal.pntd.0005840.

216.　　Harnett MM, Melendez AJ, Harnett W. The therapeutic potential of the filarial nematode-derived immunodulator, ES-62 in inflammatory disease. *Clin Exp Immunol.* Mar 2010;159(3):256-267. doi: 10.1111/j.1365-2249.2009.04064.x.

217.　　Danilowicz-Luebert E, Steinfelder S, Kuhl AA, et al. A nematode immunomodulator suppresses grass pollen-specific allergic responses by controlling excessive Th2 inflammation. *Int J Parasitol.* Mar 2013;43(3-4):201-210. doi: 10.1016/j.ijpara.2012.10.014.

218.　　Ma Y, Liu J, Hou J, et al. Oral administration of recombinant Lactococcus lactis expressing HSP65 and tandemly repeated P277 reduces the incidence of type I diabetes in non-obese diabetic mice. *PLoS One.* 2014;9(8):e105701. doi: 10.1371/journal.pone.0105701.

219.　　Coronado S, Barrios L, Zakzuk J, et al. A recombinant cystatin from Ascaris lumbricoides attenuates inflammation of DSS-induced colitis. *Parasite Immunol.* Apr 2017;39(4). doi: 10.1111/pim.12425.

220.　　Moyle M, Foster DL, McGrath DE, et al. A hookworm glycoprotein that inhibits neutrophil function is a ligand of the integrin CD11b/CD18. *J Biol Chem.* Apr 1 1994;269(13):10008-10015.

221.　　Ferrer-Miralles N, Domingo-Espin J, Corchero JL, Vazquez E, Villaverde A. Microbial factories for recombinant pharmaceuticals. *Microb Cell Fact.* Mar 24 2009;8:17. doi: 10.1186/1475-2859-8-17.

222.　　Mattanovich D, Branduardi P, Dato L, Gasser B, Sauer M, Porro D. Recombinant protein production in yeasts. *Methods Mol Biol.* 2012;824:329-358. doi: 10.1007/978-1-61779-433-9_17.

223.　　Sorensen HP. Towards universal systems for recombinant gene expression. *Microb Cell Fact.* Apr 30 2010;9:27. doi: 10.1186/1475-2859-9-27.

224.　　Zhu J. Mammalian cell protein expression for biopharmaceutical production. *Biotechnol Adv.* Sep-Oct 2012;30(5):1158-1170. doi: 10.1016/j.biotechadv.2011.08.022.

225.　　Porro D, Gasser B, Fossati T, et al. Production of recombinant proteins and metabolites in yeasts: when are these systems better than bacterial

production systems? *Appl Microbiol Biotechnol.* Feb 2011;89(4):939-948. doi: 10.1007/s00253-010-3019-z.

226.   Goffeau A, Barrell BG, Bussey H, et al. Life with 6000 genes. *Science.* Oct 25 1996;274(5287):546, 563-547.

227.   De Schutter K, Lin YC, Tiels P, et al. Genome sequence of the recombinant protein production host Pichia pastoris. *Nat Biotechnol.* Jun 2009;27(6):561-566. doi: 10.1038/nbt.1544.

228.   Hamilton SR, Davidson RC, Sethuraman N, et al. Humanization of yeast to produce complex terminally sialylated glycoproteins. *Science.* Sep 8 2006;313(5792):1441-1443. doi: 10.1126/science.1130256.

229.   Kurtzman CP. Biotechnological strains of Komagataella (Pichia) pastoris are Komagataella phaffii as determined from multigene sequence analysis. *J Ind Microbiol Biotechnol.* Nov 2009;36(11):1435-1438. doi: 10.1007/s10295-009-0638-4.

230.   Hedfalk K. Further advances in the production of membrane proteins in Pichia pastoris. *Bioengineered.* Nov-Dec 2013;4(6):363-367. doi: 10.4161/bioe.23886.

231.   Rabert C, Weinacker D, Pessoa A, Jr., Farias JG. Recombinants proteins for industrial uses: utilization of Pichia pastoris expression system. *Braz J Microbiol.* 2013;44(2):351-356. doi: 10.1590/s1517-83822013005000041.

232.   Zahrl RJ, Pena DA, Mattanovich D, Gasser B. Systems biotechnology for protein production in Pichia pastoris. *FEMS Yeast Res.* Nov 1 2017;17(7). doi: 10.1093/femsyr/fox068.

233.   Vieira Gomes AM, Souza Carmo T, Silva Carvalho L, Mendonca Bahia F, Parachin NS. Comparison of Yeasts as Hosts for Recombinant Protein Production. *Microorganisms.* Apr 29 2018;6(2). doi: 10.3390/microorganisms6020038.

234.   Teh SH, Fong MY, Mohamed Z. Expression and analysis of the glycosylation properties of recombinant human erythropoietin expressed in Pichia pastoris. *Genet Mol Biol.* Jul 2011;34(3):464-470. doi: 10.1590/s1415-47572011005000022.

235.   Goud GN, Bottazzi ME, Zhan B, et al. Expression of the Necator americanus hookworm larval antigen Na-ASP-2 in Pichia pastoris and purification of the recombinant protein for use in human clinical trials. *Vaccine.* Sep 15 2005;23(39):4754-4764. doi: 10.1016/j.vaccine.2005.04.040.

236.   Curti E, Seid CA, Hudspeth E, et al. Optimization and revision of the production process of the Necator americanus glutathione S-transferase 1 (Na-GST-1), the lead hookworm vaccine recombinant protein candidate. *Hum Vaccin Immunother.* 2014;10(7):1914-1925. doi: 10.4161/hv.28872.

237.   Seid CA, Curti E, Jones RM, et al. Expression, purification, and characterization of the Necator americanus aspartic protease-1 (Na-APR-1 (M74)) antigen, a component of the bivalent human hookworm vaccine. *Hum Vaccin Immunother.* 2015;11(6):1474-1488. doi: 10.1080/21645515.2015.1036207.

238.   Zemella A, Thoring L, Hoffmeister C, Kubick S. Cell-Free Protein Synthesis: Pros and Cons of Prokaryotic and Eukaryotic Systems. *Chembiochem.* Nov 2015;16(17):2420-2431. doi: 10.1002/cbic.201500340.

239.   Carlson ED, Gan R, Hodgman CE, Jewett MC. Cell-free protein synthesis: applications come of age. *Biotechnol Adv.* Sep-Oct 2012;30(5):1185-1194. doi: 10.1016/j.biotechadv.2011.09.016.

References

240.   Nirenberg MW, Matthaei JH. The dependence of cell-free protein synthesis in E. coli upon naturally occurring or synthetic polyribonucleotides. *Proc Natl Acad Sci U S A.* Oct 15 1961;47:1588-1602.

241.   Vilkhovoy M, Horvath N, Shih CH, et al. Sequence Specific Modeling of E. coli Cell-Free Protein Synthesis. *ACS Synth Biol.* Aug 17 2018;7(8):1844-1857. doi: 10.1021/acssynbio.7b00465.

242.   Krinsky N, Kaduri M, Shainsky-Roitman J, et al. A Simple and Rapid Method for Preparing a Cell-Free Bacterial Lysate for Protein Synthesis. *PLoS One.* 2016;11(10):e0165137. doi: 10.1371/journal.pone.0165137.

243.   Whittaker JW. Cell-free protein synthesis: the state of the art. *Biotechnol Lett.* Feb 2013;35(2):143-152. doi: 10.1007/s10529-012-1075-4.

244.   Thoring L, Wustenhagen DA, Borowiak M, Stech M, Sonnabend A, Kubick S. Cell-Free Systems Based on CHO Cell Lysates: Optimization Strategies, Synthesis of "Difficult-to-Express" Proteins and Future Perspectives. *PLoS One.* 2016;11(9):e0163670. doi: 10.1371/journal.pone.0163670.

245.   Ritchie TK, Grinkova YV, Bayburt TH, et al. Chapter 11 - Reconstitution of membrane proteins in phospholipid bilayer nanodiscs. *Methods Enzymol.* 2009;464:211-231. doi: 10.1016/s0076-6879(09)64011-8.

246.   Quast RB, Kortt O, Henkel J, et al. Automated production of functional membrane proteins using eukaryotic cell-free translation systems. *J Biotechnol.* Jun 10 2015;203:45-53. doi: 10.1016/j.jbiotec.2015.03.015.

247.   Zawada JF, Yin G, Steiner AR, et al. Microscale to manufacturing scale-up of cell-free cytokine production--a new approach for shortening protein production development timelines. *Biotechnol Bioeng.* Jul 2011;108(7):1570-1578. doi: 10.1002/bit.23103.

248.   Endoh T, Kanai T, Sato YT, et al. Cell-free protein synthesis at high temperatures using the lysate of a hyperthermophile. *J Biotechnol.* Nov 1 2006;126(2):186-195. doi: 10.1016/j.jbiotec.2006.04.010.

249.   Hodgman CE, Jewett MC. Characterizing IGR IRES-mediated translation initiation for use in yeast cell-free protein synthesis. *N Biotechnol.* Sep 25 2014;31(5):499-505. doi: 10.1016/j.nbt.2014.07.001.

250.   Roberts BE, Paterson BM. Efficient translation of tobacco mosaic virus RNA and rabbit globin 9S RNA in a cell-free system from commercial wheat germ. *Proc Natl Acad Sci U S A.* Aug 1973;70(8):2330-2334.

251.   Buntru M, Vogel S, Stoff K, Spiegel H, Schillberg S. A versatile coupled cell-free transcription-translation system based on tobacco BY-2 cell lysates. *Biotechnol Bioeng.* May 2015;112(5):867-878. doi: 10.1002/bit.25502.

252.   Stech M, Brodel AK, Quast RB, Sachse R, Kubick S. Cell-free systems: functional modules for synthetic and chemical biology. *Adv Biochem Eng Biotechnol.* 2013;137:67-102. doi: 10.1007/10_2013_185.

253.   Anastasina M, Terenin I, Butcher SJ, Kainov DE. A technique to increase protein yield in a rabbit reticulocyte lysate translation system. *Biotechniques.* Jan 2014;56(1):36-39. doi: 10.2144/000114125.

254.   Johnston WA, Alexandrov K. Production of eukaryotic cell-free lysate from Leishmania tarentolae. *Methods Mol Biol.* 2014;1118:1-15. doi: 10.1007/978-1-62703-782-2_1.

255.   Brodel AK, Sonnabend A, Kubick S. Cell-free protein expression based on extracts from CHO cells. *Biotechnol Bioeng.* Jan 2014;111(1):25-36. doi: 10.1002/bit.25013.

256.   Bradrick SS, Nagyal S, Novatt H. A miRNA-responsive cell-free translation system facilitates isolation of hepatitis C virus miRNP complexes. *RNA.* Aug 2013;19(8):1159-1169. doi: 10.1261/rna.038810.113.

257.   Weber LA, Feman ER, Baglioni C. A cell free system from HeLa cells active in initiation of protein synthesis. *Biochemistry.* Dec 2 1975;14(24):5315-5321.

258.   Basile G, Peticca M. Recombinant protein expression in Leishmania tarentolae. *Mol Biotechnol.* Nov 2009;43(3):273-278. doi: 10.1007/s12033-009-9213-5.

259.   Spirin AS. How does a scanning ribosomal particle move along the 5'-untranslated region of eukaryotic mRNA? Brownian Ratchet model. *Biochemistry.* Nov 17 2009;48(45):10688-10692. doi: 10.1021/bi901379a.

260.   Mureev S, Kovtun O, Nguyen UT, Alexandrov K. Species-independent translational leaders facilitate cell-free expression. *Nat Biotechnol.* Aug 2009;27(8):747-752. doi: 10.1038/nbt.1556.

261.   Kovtun O, Mureev S, Johnston W, Alexandrov K. Towards the construction of expressed proteomes using a Leishmania tarentolae based cell-free expression system. *PLoS One.* Dec 21 2010;5(12):e14388. doi: 10.1371/journal.pone.0014388.

262.   Wang Z, Abubucker S, Martin J, Wilson RK, Hawdon J, Mitreva M. Characterizing Ancylostoma caninum transcriptome and exploring nematode parasitic adaptation. *BMC Genomics.* May 14 2010;11:307. doi: 10.1186/1471-2164-11-307.

263.   Schwarz EM, Hu Y, Antoshechkin I, Miller MM, Sternberg PW, Aroian RV. The genome and transcriptome of the zoonotic hookworm Ancylostoma ceylanicum identify infection-specific gene families. *Nat Genet.* Apr 2015;47(4):416-422. doi: 10.1038/ng.3237.

264.   Cantacessi C, Mitreva M, Jex AR, et al. Massively parallel sequencing and analysis of the Necator americanus transcriptome. *PLoS Negl Trop Dis.* May 11 2010;4(5):e684. doi: 10.1371/journal.pntd.0000684.

265.   Datu BJ, Gasser RB, Nagaraj SH, et al. Transcriptional changes in the hookworm, Ancylostoma caninum, during the transition from a free-living to a parasitic larva. *PLoS Negl Trop Dis.* Jan 9 2008;2(1):e130. doi: 10.1371/journal.pntd.0000130.

266.   Boratyn GM, Schaffer AA, Agarwala R, Altschul SF, Lipman DJ, Madden TL. Domain enhanced lookup time accelerated BLAST. *Biol Direct.* Apr 17 2012;7:12. doi: 10.1186/1745-6150-7-12.

267.   Mitchell AL, Attwood TK, Babbitt PC, et al. InterPro in 2019: improving coverage, classification and access to protein sequence annotations. *Nucleic Acids Res.* Jan 8 2019;47(D1):D351-d360. doi: 10.1093/nar/gky1100.

268.   Gotz S, Garcia-Gomez JM, Terol J, et al. High-throughput functional annotation and data mining with the Blast2GO suite. *Nucleic Acids Res.* Jun 2008;36(10):3420-3435. doi: 10.1093/nar/gkn176.

269.   Hawdon JM, Jones BF, Hoffman DR, Hotez PJ. Cloning and characterization of Ancylostoma-secreted protein. A novel protein associated with the transition to parasitism by infective hookworm larvae. *J Biol Chem.* Mar 22 1996;271(12):6672-6678.

270.   Hawdon JM, Narasimhan S, Hotez PJ. Ancylostoma secreted protein 2: cloning and characterization of a second member of a family of nematode

secreted proteins from Ancylostoma caninum. *Mol Biochem Parasitol.* Apr 30 1999;99(2):149-165.

271.   Williamson AL, Lustigman S, Oksov Y, et al. Ancylostoma caninum MTP-1, an astacin-like metalloprotease secreted by infective hookworm larvae, is involved in tissue migration. *Infect Immun.* Feb 2006;74(2):961-967. doi: 10.1128/iai.74.2.961-967.2006.

272.   Zhan B, Hotez PJ, Wang Y, Hawdon JM. A developmentally regulated metalloprotease secreted by host-stimulated Ancylostoma caninum third-stage infective larvae is a member of the astacin family of proteases. *Mol Biochem Parasitol.* Apr 9 2002;120(2):291-296.

273.   Robinson JT, Thorvaldsdottir H, Winckler W, et al. Integrative genomics viewer. *Nat Biotechnol.* Jan 2011;29(1):24-26. doi: 10.1038/nbt.1754.

274.   Chakrabarti S, Jahandideh F, Wu J. Food-derived bioactive peptides on inflammation and oxidative stress. *Biomed Res Int.* 2014;2014:608979. doi: 10.1155/2014/608979.

275.   Sotillo J, Ferreira I, Potriquet J, et al. Changes in protein expression after treatment with Ancylostoma caninum excretory/secretory products in a mouse model of colitis. *Sci Rep.* Feb 13 2017;7:41883. doi: 10.1038/srep41883.

276.   Vaiopoulou A, Gazouli M, Papadopoulou A, et al. Serum protein profiling of adults and children with Crohn disease. *J Pediatr Gastroenterol Nutr.* Jan 2015;60(1):42-47. doi: 10.1097/mpg.0000000000000579.

277.   Sandahl TD, Kelsen J, Dige A, et al. The lectin pathway of the complement system is downregulated in Crohn's disease patients who respond to anti-TNF-alpha therapy. *J Crohns Colitis.* Jun 2014;8(6):521-528. doi: 10.1016/j.crohns.2013.11.007.

278.   Carroll IM, Maharshak N. Enteric bacterial proteases in inflammatory bowel disease- pathophysiology and clinical implications. *World J Gastroenterol.* 2013;19(43):7531-7543. doi: 10.3748/wjg.v19.i43.7531.

279.   Hunter S, Jones P, Mitchell A, et al. InterPro in 2011: new developments in the family and domain prediction database. *Nucleic Acids Res.* Jan 2012;40(Database issue):D306-312. doi: 10.1093/nar/gkr948.

280.   Magrini V, Gao X, Rosa BA, et al. Improving eukaryotic genome annotation using single molecule mRNA sequencing. *BMC Genomics.* Mar 1 2018;19(1):172. doi: 10.1186/s12864-018-4555-7.

281.   Dobin A, Gingeras TR. Mapping RNA-seq Reads with STAR. *Curr Protoc Bioinformatics.* Sep 3 2015;51:11.14.11-19. doi: 10.1002/0471250953.bi1114s51.

282.   Cantacessi C, Hofmann A, Young ND, et al. Insights into SCP/TAPS proteins of liver flukes based on large-scale bioinformatic analyses of sequence datasets. *PLoS One.* 2012;7(2):e31164. doi: 10.1371/journal.pone.0031164.

283.   Cantacessi C, Campbell BE, Visser A, et al. A portrait of the "SCP/TAPS" proteins of eukaryotes--developing a framework for fundamental research and biotechnological outcomes. *Biotechnol Adv.* Jul-Aug 2009;27(4):376-388. doi: 10.1016/j.biotechadv.2009.02.005.

284.   Dennis RD, Schubert U, Bauer C. Angiogenesis and parasitic helminth-associated neovascularization. *Parasitology.* Apr 2011;138(4):426-439. doi: 10.1017/s0031182010001642.

285.   Ghosh K, Hotez PJ. Antibody-dependent reductions in mouse hookworm burden after vaccination with Ancylostoma caninum secreted protein 1. *J Infect Dis.* Nov 1999;180(5):1674-1681. doi: 10.1086/315059.

286.	Sen L, Ghosh K, Bin Z, et al. Hookworm burden reductions in BALB/c mice vaccinated with recombinant Ancylostoma secreted proteins (ASPs) from Ancylostoma duodenale, Ancylostoma caninum and Necator americanus. *Vaccine.* Jan 6 2000;18(11-12):1096-1102.

287.	Zhan B, Liu Y, Badamchian M, et al. Molecular characterisation of the Ancylostoma-secreted protein family from the adult stage of Ancylostoma caninum. *Int J Parasitol.* Aug 2003;33(9):897-907.

288.	Hunt VL, Tsai IJ, Coghlan A, et al. The genomic basis of parasitism in the Strongyloides clade of nematodes. *Nat Genet.* Mar 2016;48(3):299-307. doi: 10.1038/ng.3495.

289.	Jiang N, Moyle M, Soule HR, Rote WE, Chopp M. Neutrophil inhibitory factor is neuroprotective after focal ischemia in rats. *Ann Neurol.* Dec 1995;38(6):935-942. doi: 10.1002/ana.410380615.

290.	Krams M, Lees KR, Hacke W, Grieve AP, Orgogozo JM, Ford GA. Acute Stroke Therapy by Inhibition of Neutrophils (ASTIN): an adaptive dose-response study of UK-279,276 in acute ischemic stroke. *Stroke.* Nov 2003;34(11):2543-2548. doi: 10.1161/01.Str.0000092527.33910.89.

291.	O'Rourke D, Baban D, Demidova M, Mott R, Hodgkin J. Genomic clusters, putative pathogen recognition molecules, and antimicrobial genes are induced by infection of C. elegans with M. nematophilum. *Genome Res.* Aug 2006;16(8):1005-1016. doi: 10.1101/gr.50823006.

292.	Wang J, Kim SK. Global analysis of dauer gene expression in Caenorhabditis elegans. *Development.* Apr 2003;130(8):1621-1634.

293.	Ookuma S, Fukuda M, Nishida E. Identification of a DAF-16 transcriptional target gene, scl-1, that regulates longevity and stress resistance in Caenorhabditis elegans. *Curr Biol.* Mar 4 2003;13(5):427-431.

294.	Cantacessi C, Gasser RB. SCP/TAPS proteins in helminths--where to from now? *Mol Cell Probes.* Feb 2012;26(1):54-59. doi: 10.1016/j.mcp.2011.10.001.

295.	Ragland SA, Criss AK. From bacterial killing to immune modulation: Recent insights into the functions of lysozyme. *PLoS Pathog.* Sep 2017;13(9):e1006512. doi: 10.1371/journal.ppat.1006512.

296.	Mihelic M, Vlahovicek-Kahlina K, Renko M, et al. The mechanism behind the selection of two different cleavage sites in NAG-NAM polymers. *IUCrJ.* Mar 1 2017;4(Pt 2):185-198. doi: 10.1107/s2052252517000367.

297.	Jakaitis BM, Denning PW. Human breast milk and the gastrointestinal innate immune system. *Clin Perinatol.* Jun 2014;41(2):423-435. doi: 10.1016/j.clp.2014.02.011.

298.	Thompson A, Bhandari V. Pulmonary Biomarkers of Bronchopulmonary Dysplasia. *Biomark Insights.* Jul 2 2008;3:361-373.

299.	Lee D, Albenberg L, Compher C, et al. Diet in the pathogenesis and treatment of inflammatory bowel diseases. *Gastroenterology.* May 2015;148(6):1087-1106. doi: 10.1053/j.gastro.2015.01.007.

300.	Sonnhammer EL, Durbin R. Analysis of protein domain families in Caenorhabditis elegans. *Genomics.* Dec 1 1997;46(2):200-216. doi: 10.1006/geno.1997.4989.

301.	Wang T, Van Steendam K, Dhaenens M, et al. Proteomic analysis of the excretory-secretory products from larval stages of Ascaris suum reveals high abundance of glycosyl hydrolases. *PLoS Negl Trop Dis.* 2013;7(10):e2467. doi: 10.1371/journal.pntd.0002467.

References

302.   Tzelos T, Matthews JB, Buck AH, et al. A preliminary proteomic characterisation of extracellular vesicles released by the ovine parasitic nematode, Teladorsagia circumcincta. *Vet Parasitol.* May 15 2016;221:84-92. doi: 10.1016/j.vetpar.2016.03.008.

303.   Hewitson JP, Harcus Y, Murray J, et al. Proteomic analysis of secretory products from the model gastrointestinal nematode Heligmosomoides polygyrus reveals dominance of venom allergen-like (VAL) proteins. *J Proteomics.* Aug 24 2011;74(9):1573-1594. doi: 10.1016/j.jprot.2011.06.002.

304.   Sotillo J, Sanchez-Flores A, Cantacessi C, et al. Secreted proteomes of different developmental stages of the gastrointestinal nematode Nippostrongylus brasiliensis. *Mol Cell Proteomics.* Oct 2014;13(10):2736-2751. doi: 10.1074/mcp.M114.038950.

305.   Kennedy MW, Allen JE, Wright AS, McCruden AB, Cooper A. The gp15/400 polyprotein antigen of Brugia malayi binds fatty acids and retinoids. *Mol Biochem Parasitol.* Apr 1995;71(1):41-50.

306.   Hewitson JP, Harcus YM, Curwen RS, et al. The secretome of the filarial parasite, Brugia malayi: proteomic profile of adult excretory-secretory products. *Mol Biochem Parasitol.* Jul 2008;160(1):8-21. doi: 10.1016/j.molbiopara.2008.02.007.

307.   McDermott L, Kennedy MW, McManus DP, Bradley JE, Cooper A, Storch J. How helminth lipid-binding proteins offload their ligands to membranes: differential mechanisms of fatty acid transfer by the ABA-1 polyprotein allergen and Ov-FAR-1 proteins of nematodes and Sj-FABPc of schistosomes. *Biochemistry.* May 28 2002;41(21):6706-6713.

308.   Mondal M, Kundu JK, Misra KK. Variation in lipid and fatty acid uptake among nematode and cestode parasites and their host, domestic fowl: host-parasite interaction. *J Parasit Dis.* Dec 2016;40(4):1494-1518. doi: 10.1007/s12639-015-0718-5.

309.   Franchini GR, Porfido JL, Ibanez Shimabukuro M, et al. The unusual lipid binding proteins of parasitic helminths and their potential roles in parasitism and as therapeutic targets. *Prostaglandins Leukot Essent Fatty Acids.* Feb 2015;93:31-36. doi: 10.1016/j.plefa.2014.08.003.

310.   Murphy G. Tissue inhibitors of metalloproteinases. *Genome Biol.* Nov 11 2011;12(11):233. doi: 10.1186/gb-2011-12-11-233.

311.   Cantacessi C, Hofmann A, Pickering D, Navarro S, Mitreva M, Loukas A. TIMPs of parasitic helminths – a large-scale analysis of high-throughput sequence datasets. *Parasites & Vectors.* 2013;6(1). doi: 10.1186/1756-3305-6-156.

312.   Kucera K, Harrison LM, Cappello M, Modis Y. Ancylostoma ceylanicum excretory-secretory protein 2 adopts a netrin-like fold and defines a novel family of nematode proteins. *J Mol Biol.* Apr 22 2011;408(1):9-17. doi: 10.1016/j.jmb.2011.02.033.

313.   DeVoss J, Diehl L. Murine models of inflammatory bowel disease (IBD): challenges of modeling human disease. *Toxicol Pathol.* Jan 2014;42(1):99-110. doi: 10.1177/0192623313509729.

314.   Gadaleta RM, Garcia-Irigoyen O, Moschetta A. Exploration of Inflammatory Bowel Disease in Mice: Chemically Induced Murine Models of Inflammatory Bowel Disease (IBD). *Curr Protoc Mouse Biol.* Mar 2 2017;7(1):13-28. doi: 10.1002/cpmo.20.

315.   Isik F, Tunali Akbay T, Yarat A, et al. Protective effects of black cumin (Nigella sativa) oil on TNBS-induced experimental colitis in rats. *Dig Dis Sci.* Mar 2011;56(3):721-730. doi: 10.1007/s10620-010-1333-z.

316.   Randhawa PK, Singh K, Singh N, Jaggi AS. A review on chemical-induced inflammatory bowel disease models in rodents. *Korean J Physiol Pharmacol.* Aug 2014;18(4):279-288. doi: 10.4196/kjpp.2014.18.4.279.

317.   Wirtz S, Popp V, Kindermann M, et al. Chemically induced mouse models of acute and chronic intestinal inflammation. *Nat Protoc.* Jul 2017;12(7):1295-1309. doi: 10.1038/nprot.2017.044.

318.   Erben U, Loddenkemper C, Doerfel K, et al. A guide to histomorphological evaluation of intestinal inflammation in mouse models. *Int J Clin Exp Pathol.* 2014;7(8):4557-4576.

319.   R Core Team. R: A language and environment for statistical computing. website. http://www.R-project.org/. Published 2013.

320.   Benjamini Y, Hochberg Y. Controlling the False Discovery Rate: A Practical and Powerful Approach to Multiple Testing. *Journal of the Royal Statistical Society Series B (Methodological).* 1995;57(1):289-300.

321.   Pourhoseingholi MA, Vahedi M, Rahimzadeh M. Sample size calculation in medical studies. *Gastroenterol Hepatol Bed Bench.* Winter 2013;6(1):14-17.

322.   de Almeida AB, Sanchez-Hidalgo M, Martin AR, et al. Anti-inflammatory intestinal activity of Arctium lappa L. (Asteraceae) in TNBS colitis model. *J Ethnopharmacol.* Mar 7 2013;146(1):300-310. doi: 10.1016/j.jep.2012.12.048.

323.   Tribolet L, Cantacessi C, Pickering DA, et al. Probing of a human proteome microarray with a recombinant pathogen protein reveals a novel mechanism by which hookworms suppress B-cell receptor signaling. *J Infect Dis.* Feb 1 2015;211(3):416-425. doi: 10.1093/infdis/jiu451.

324.   Muchowski PJ, Zhang L, Chang ER, Soule HR, Plow EF, Moyle M. Functional interaction between the integrin antagonist neutrophil inhibitory factor and the I domain of CD11b/CD18. *J Biol Chem.* Oct 21 1994;269(42):26419-26423.

325.   Dotti I, Mora-Buch R, Ferrer-Picon E, et al. Alterations in the epithelial stem cell compartment could contribute to permanent changes in the mucosa of patients with ulcerative colitis. *Gut.* Dec 2017;66(12):2069-2079. doi: 10.1136/gutjnl-2016-312609.

326.   Schmitt M, Schewe M, Sacchetti A, et al. Paneth Cells Respond to Inflammation and Contribute to Tissue Regeneration by Acquiring Stem-like Features through SCF/c-Kit Signaling. *Cell Rep.* Aug 28 2018;24(9):2312-2328.e2317. doi: 10.1016/j.celrep.2018.07.085.

327.   Lee M, Kovacs-Nolan J, Yang C, Archbold T, Fan MZ, Mine Y. Hen egg lysozyme attenuates inflammation and modulates local gene expression in a porcine model of dextran sodium sulfate (DSS)-induced colitis. *J Agric Food Chem.* Mar 25 2009;57(6):2233-2240. doi: 10.1021/jf803133b.

328.   Obita T, Ueda T, Imoto T. Solution structure and activity of mouse lysozyme M. *Cell Mol Life Sci.* Jan 2003;60(1):176-184.

329.   Noy N. Vitamin A Transport and Cell Signaling by the Retinol-Binding Protein Receptor STRA6. *Subcell Biochem.* 2016;81:77-93. doi: 10.1007/978-94-024-0945-1_3.

330. Schmidt A, Eriksson M, Shang MM, Weyd H, Tegner J. Comparative Analysis of Protocols to Induce Human CD4+Foxp3+ Regulatory T Cells by Combinations of IL-2, TGF-beta, Retinoic Acid, Rapamycin and Butyrate. *PLoS One.* 2016;11(2):e0148474. doi: 10.1371/journal.pone.0148474.

331. Osman A, Wang CK, Winter A, et al. Hookworm SCP/TAPS protein structure--A key to understanding host-parasite interactions and developing new interventions. *Biotechnol Adv.* May-Jun 2012;30(3):652-657. doi: 10.1016/j.biotechadv.2011.11.002.

332. Asojo OA, Goud G, Dhar K, et al. X-ray structure of Na-ASP-2, a pathogenesis-related-1 protein from the nematode parasite, Necator americanus, and a vaccine antigen for human hookworm infection. *J Mol Biol.* Feb 25 2005;346(3):801-814. doi: 10.1016/j.jmb.2004.12.023.

333. Mason L, Tribolet L, Simon A, et al. Probing the equatorial groove of the hookworm protein and vaccine candidate antigen, Na-ASP-2. *Int J Biochem Cell Biol.* May 2014;50:146-155. doi: 10.1016/j.biocel.2014.03.003.

334. Yang J, Yan R, Roy A, Xu D, Poisson J, Zhang Y. The I-TASSER Suite: protein structure and function prediction. *Nat Methods.* Jan 2015;12(1):7-8. doi: 10.1038/nmeth.3213.

335. Low BE, Wiles MV. A Humanized Mouse Model to Study Human Albumin and Albumin Conjugates Pharmacokinetics. *Methods Mol Biol.* 2016;1438:115-122. doi: 10.1007/978-1-4939-3661-8_7.

336. Storek and Monack. Bacterial recognition pathways that lead to inflam. 2015.

337. Koradi R, Billeter M, Wuthrich K. MOLMOL: a program for display and analysis of macromolecular structures. *J Mol Graph.* Feb 1996;14(1):51-55, 29-32.

338. Maxwell JR, Zhang Y, Brown WA, et al. Differential Roles for Interleukin-23 and Interleukin-17 in Intestinal Immunoregulation. *Immunity.* Oct 20 2015;43(4):739-750. doi: 10.1016/j.immuni.2015.08.019.

339. Jahic M, Veide A, Charoenrat T, Teeri T, Enfors SO. Process technology for production and recovery of heterologous proteins with Pichia pastoris. *Biotechnol Prog.* Nov-Dec 2006;22(6):1465-1473. doi: 10.1021/bp060171t.

340. Baghban R, Farajnia S, Ghasemi Y, Mortazavi M, Zarghami N, Samadi N. New Developments in Pichia pastoris Expression System, Review and Update. *Curr Pharm Biotechnol.* 2018;19(6):451-467. doi: 10.2174/1389201019666180718093037.

341. Bialkowska AB, Ghaleb AM, Nandan MO, Yang VW. Improved Swiss-rolling Technique for Intestinal Tissue Preparation for Immunohistochemical and Immunofluorescent Analyses. *J Vis Exp.* Jul 13 2016(113). doi: 10.3791/54161.

342. Howie D, Ten Bokum A, Necula AS, Cobbold SP, Waldmann H. The Role of Lipid Metabolism in T Lymphocyte Differentiation and Survival. *Front Immunol.* 2017;8:1949. doi: 10.3389/fimmu.2017.01949.

343. Bamias G, Arseneau KO, Cominelli F. Mouse models of inflammatory bowel disease for investigating mucosal immunity in the intestine. *Curr Opin Gastroenterol.* Nov 2017;33(6):411-416. doi: 10.1097/mog.0000000000000402.

344. Laroux FS, Norris HH, Houghton J, et al. Regulation of chronic colitis in athymic nu/nu (nude) mice. *Int Immunol.* Jan 2004;16(1):77-89.

345.	Araki R, Fujimori A, Hamatani K, et al. Nonsense mutation at Tyr-4046 in the DNA-dependent protein kinase catalytic subunit of severe combined immune deficiency mice. *Proc Natl Acad Sci U S A.* Mar 18 1997;94(6):2438-2443.

346.	Kotloff DB, Bosma MJ, Ruetsch NR. V(D)J recombination in peritoneal B cells of leaky scid mice. *J Exp Med.* Dec 1 1993;178(6):1981-1994.

347.	Lieber MR. The mechanism of double-strand DNA break repair by the nonhomologous DNA end-joining pathway. *Annu Rev Biochem.* 2010;79:181-211. doi: 10.1146/annurev.biochem.052308.093131.

348.	Robinson AM, Rahman AA, Carbone SE, et al. Alterations of colonic function in the Winnie mouse model of spontaneous chronic colitis. *Am J Physiol Gastrointest Liver Physiol.* Jan 1 2017;312(1):G85-g102. doi: 10.1152/ajpgi.00210.2016.

349.	Bouma G, Strober W. The immunological and genetic basis of inflammatory bowel disease. *Nat Rev Immunol.* Jul 2003;3(7):521-533. doi: 10.1038/nri1132.

350.	Huang Y, Chen Z. Inflammatory bowel disease related innate immunity and adaptive immunity. *Am J Transl Res.* 2016;8(6):2490-2497.

351.	Chen L, Deng H, Cui H, et al. Inflammatory responses and inflammation-associated diseases in organs. *Oncotarget.* Jan 23 2018;9(6):7204-7218. doi: 10.18632/oncotarget.23208.

352.	Hsu PS, Lai CL, Hu M, et al. IL-2 Enhances Gut Homing Potential of Human Naive Regulatory T Cells Early in Life. *J Immunol.* Jun 15 2018;200(12):3970-3980. doi: 10.4049/jimmunol.1701533.

353.	Govender L, Wyss JC, Kumar R, Pascual M, Golshayan D. IL-2-Mediated In Vivo Expansion of Regulatory T Cells Combined with CD154-CD40 Co-Stimulation Blockade but Not CTLA-4 Ig Prolongs Allograft Survival in Naive and Sensitized Mice. *Front Immunol.* 2017;8:421. doi: 10.3389/fimmu.2017.00421.

354.	Ng SC, Shi HY, Hamidi N, et al. Worldwide incidence and prevalence of inflammatory bowel disease in the 21st century: a systematic review of population-based studies. *Lancet.* Dec 23 2018;390(10114):2769-2778. doi: 10.1016/s0140-6736(17)32448-0.

355.	Ananthakrishnan AN. Epidemiology and risk factors for IBD. *Nat Rev Gastroenterol Hepatol.* Apr 2015;12(4):205-217. doi: 10.1038/nrgastro.2015.34.

356.	Nkurunungi G, Lubyayi L, Versteeg SA, et al. Do helminth infections underpin urban-rural differences in risk factors for allergy-related outcomes? *Clin Exp Allergy.* Jan 11 2019. doi: 10.1111/cea.13335.

357.	Smallwood TB, Giacomin PR, Loukas A, Mulvenna JP, Clark RJ, Miles JJ. Helminth Immunomodulation in Autoimmune Disease. *Front Immunol.* 2017;8:453. doi: 10.3389/fimmu.2017.00453.

358.	Croese J, Giacomin P, Navarro S, et al. Experimental hookworm infection and gluten microchallenge promote tolerance in celiac disease. *J Allergy Clin Immunol.* Feb 2015;135(2):508-516. doi: 10.1016/j.jaci.2014.07.022.

359.	Ruyssers NE, De Winter BY, De Man JG, et al. Schistosoma mansoni proteins attenuate gastrointestinal motility disturbances during experimental colitis in mice. *World J Gastroenterol.* Feb 14 2010;16(6):703-712.

360. McInnes IB, Leung BP, Harnett M, Gracie JA, Liew FY, Harnett W. A novel therapeutic approach targeting articular inflammation using the filarial nematode-derived phosphorylcholine-containing glycoprotein ES-62. *J Immunol.* Aug 15 2003;171(4):2127-2133.

361. Morante T, Shepherd C, Constantinoiu C, Loukas A, Sotillo J. Revisiting the Ancylostoma Caninum Secretome Provides New Information on Hookworm-Host Interactions. *Proteomics.* Dec 2017;17(23-24). doi: 10.1002/pmic.201700186.

362. Logan J, Manda SS, Choi Y-J, et al. Comprehensive analysis of human hookworm secreted proteins using a proteogenomic approach. *bioRxiv.* 2018:406843. doi: 10.1101/406843.

363. Falcon C, Carranza F, Martinez FF, et al. Excretory-secretory products (ESP) from Fasciola hepatica induce tolerogenic properties in myeloid dendritic cells. *Vet Immunol Immunopathol.* Sep 15 2010;137(1-2):36-46. doi: 10.1016/j.vetimm.2010.04.007.

364. Robinson MW, Dalton JP, O'Brien BA, Donnelly S. Fasciola hepatica: the therapeutic potential of a worm secretome. *Int J Parasitol.* Mar 2013;43(3-4):283-291. doi: 10.1016/j.ijpara.2012.11.004.

365. Lund ME, Greer J, Dixit A, et al. A parasite-derived 68-mer peptide ameliorates autoimmune disease in murine models of Type 1 diabetes and multiple sclerosis. *Sci Rep.* Nov 24 2016;6:37789. doi: 10.1038/srep37789.

366. Whelan RA, Rausch S, Ebner F, et al. A transgenic probiotic secreting a parasite immunomodulator for site-directed treatment of gut inflammation. *Mol Ther.* Oct 2014;22(10):1730-1740. doi: 10.1038/mt.2014.125.

367. Maizels RM, Smits HH, McSorley HJ. Modulation of Host Immunity by Helminths: The Expanding Repertoire of Parasite Effector Molecules. *Immunity.* Nov 20 2018;49(5):801-818. doi: 10.1016/j.immuni.2018.10.016.

368. Lund ME, To J, O'Brien BA, Donnelly S. The choice of phorbol 12-myristate 13-acetate differentiation protocol influences the response of THP-1 macrophages to a pro-inflammatory stimulus. *J Immunol Methods.* Mar 2016;430:64-70. doi: 10.1016/j.jim.2016.01.012.

369. Graham ML, Prescott MJ. The multifactorial role of the 3Rs in shifting the harm-benefit analysis in animal models of disease. *Eur J Pharmacol.* Jul 15 2015;759:19-29. doi: 10.1016/j.ejphar.2015.03.040.

370. Krepp J, Gelmedin V, Hawdon JM. Characterisation of hookworm heat shock factor binding protein (HSB-1) during heat shock and larval activation. *Int J Parasitol.* Apr 2011;41(5):533-543. doi: 10.1016/j.ijpara.2010.12.001.

371. Scholte LLS, Pascoal-Xavier MA, Nahum LA. Helminths and Cancers From the Evolutionary Perspective. *Front Med (Lausanne).* 2018;5:90. doi: 10.3389/fmed.2018.00090.

372. Adegbola SO, Sahnan K, Warusavitarne J, Hart A, Tozer P. Anti-TNF Therapy in Crohn's Disease. *Int J Mol Sci.* Jul 31 2018;19(8). doi: 10.3390/ijms19082244.

373. Xu Z, Davis HM, Zhou H. Clinical impact of concomitant immunomodulators on biologic therapy: Pharmacokinetics, immunogenicity, efficacy and safety. *J Clin Pharmacol.* Mar 2015;55 Suppl 3:S60-74. doi: 10.1002/jcph.380.

374. Leroux LP, Nasr M, Valanparambil R, et al. Analysis of the Trichuris suis excretory/secretory proteins as a function of life cycle stage and their

immunomodulatory properties. *Sci Rep.* Oct 29 2018;8(1):15921. doi: 10.1038/s41598-018-34174-4.

375.   Eichenberger RM, Talukder MH, Field MA, et al. Characterization of Trichuris muris secreted proteins and extracellular vesicles provides new insights into host-parasite communication. *J Extracell Vesicles.* 2018;7(1):1428004. doi: 10.1080/20013078.2018.1428004.

376.   Roig J, Saiz ML, Galiano A, et al. Extracellular Vesicles From the Helminth Fasciola hepatica Prevent DSS-Induced Acute Ulcerative Colitis in a T-Lymphocyte Independent Mode. *Front Microbiol.* 2018;9:1036. doi: 10.3389/fmicb.2018.01036.

377.   Eichenberger RM, Ryan S, Jones L, et al. Hookworm Secreted Extracellular Vesicles Interact With Host Cells and Prevent Inducible Colitis in Mice. *Front Immunol.* 2018;9:850. doi: 10.3389/fimmu.2018.00850.

378.   Gaze S, Driguez P, Pearson MS, et al. An immunomics approach to schistosome antigen discovery: antibody signatures of naturally resistant and chronically infected individuals from endemic areas. *PLoS Pathog.* Mar 2014;10(3):e1004033. doi: 10.1371/journal.ppat.1004033.

379.   Rodgers DT, Pineda MA, Suckling CJ, Harnett W, Harnett MM. Drug-like analogues of the parasitic worm-derived immunomodulator ES-62 are therapeutic in the MRL/Lpr model of systemic lupus erythematosus. *Lupus.* Nov 2015;24(13):1437-1442. doi: 10.1177/0961203315591031.

380.   Tanaka A, Allam V, Simpson J, et al. The parasitic 68-mer peptide FhHDM-1 inhibits mixed granulocytic inflammation and airway hyperreactivity in experimental asthma. *J Allergy Clin Immunol.* Jun 2018;141(6):2316-2319. doi: 10.1016/j.jaci.2018.01.050.

381.   Wu Z, Wang L, Tang Y, Sun X. Parasite-Derived Proteins for the Treatment of Allergies and Autoimmune Diseases. *Front Microbiol.* 2017;8:2164. doi: 10.3389/fmicb.2017.02164.

382.   Alvarado R, O'Brien B, Tanaka A, Dalton JP, Donnelly S. A parasitic helminth-derived peptide that targets the macrophage lysosome is a novel therapeutic option for autoimmune disease. *Immunobiology.* Feb 2015;220(2):262-269. doi: 10.1016/j.imbio.2014.11.008.

383.   Bing SJ, Ha D, Ahn G, et al. Galectin isolated from parasite inhibits remission of experimental autoimmune encephalomyelitis by up-regulating autoantibody. *Clin Exp Immunol.* Jun 2015;180(3):419-431. doi: 10.1111/cei.12594.

384.   Dixit A, Tanaka A, Greer JM, Donnelly S. Novel Therapeutics for Multiple Sclerosis Designed by Parasitic Worms. *Int J Mol Sci.* Oct 13 2017;18(10). doi: 10.3390/ijms18102141.

385.   Alvarado R, To J, Lund ME, et al. The immune modulatory peptide FhHDM-1 secreted by the helminth Fasciola hepatica prevents NLRP3 inflammasome activation by inhibiting endolysosomal acidification in macrophages. *FASEB J.* Jan 2017;31(1):85-95. doi: 10.1096/fj.201500093R.

386.   Veenstra AA, Tang J, Kern TS. Antagonism of CD11b with neutrophil inhibitory factor (NIF) inhibits vascular lesions in diabetic retinopathy. *PLoS One.* 2013;8(10):e78405. doi: 10.1371/journal.pone.0078405.

387.   Karin N, Wildbaum G. The Role of Chemokines in Shaping the Balance Between CD4(+) T Cell Subsets and Its Therapeutic Implications in Autoimmune and Cancer Diseases. *Front Immunol.* 2015;6:609. doi: 10.3389/fimmu.2015.00609.

388.   Ridiandries A, Tan JTM, Bursill CA. The Role of Chemokines in Wound Healing. *Int J Mol Sci.* Oct 18 2018;19(10). doi: 10.3390/ijms19103217.

389.   Chan SN, Low END, Raja Ali RA, Mokhtar NM. Delineating inflammatory bowel disease through transcriptomic studies: current review of progress and evidence. *Intest Res.* Jul 2018;16(3):374-383. doi: 10.5217/ir.2018.16.3.374.

390.   Peters LA, Perrigoue J, Mortha A, et al. A functional genomics predictive network model identifies regulators of inflammatory bowel disease. *Nat Genet.* Oct 2017;49(10):1437-1449. doi: 10.1038/ng.3947.

391.   Holgersen K, Kutlu B, Fox B, et al. High-resolution gene expression profiling using RNA sequencing in patients with inflammatory bowel disease and in mouse models of colitis. *J Crohns Colitis.* Jun 2015;9(6):492-506. doi: 10.1093/ecco-jcc/jjv050.

392.   Gao M, Zhong A, Patel N, Alur C, Vyas D. High throughput RNA sequencing utility for diagnosis and prognosis in colon diseases. *World J Gastroenterol.* Apr 28 2017;23(16):2819-2825. doi: 10.3748/wjg.v23.i16.2819.

393.   Nair AB, Jacob S. A simple practice guide for dose conversion between animals and human. *J Basic Clin Pharm.* Mar 2016;7(2):27-31. doi: 10.4103/0976-0105.177703.

394.   Kotla NG, Rana S, Sivaraman G, et al. Bioresponsive drug delivery systems in intestinal inflammation: State-of-the-art and future perspectives. *Adv Drug Deliv Rev.* Jun 29 2018. doi: 10.1016/j.addr.2018.06.021.

395.   Smout MJ, Sotillo J, Laha T, et al. Carcinogenic Parasite Secretes Growth Factor That Accelerates Wound Healing and Potentially Promotes Neoplasia. *PLoS Pathog.* Oct 2015;11(10):e1005209. doi: 10.1371/journal.ppat.1005209.

396.   Smout MJ, Mulvenna JP, Jones MK, Loukas A. Expression, refolding and purification of Ov-GRN-1, a granulin-like growth factor from the carcinogenic liver fluke, that causes proliferation of mammalian host cells. *Protein Expr Purif.* Oct 2011;79(2):263-270. doi: 10.1016/j.pep.2011.06.018.

397.   Dastpeyman M, Bansal PS, Wilson D, et al. Structural Variants of a Liver Fluke Derived Granulin Peptide Potently Stimulate Wound Healing. *J Med Chem.* Oct 11 2018;61(19):8746-8753. doi: 10.1021/acs.jmedchem.8b00898.